PREFACE

We would like to introduce the report of the scientific activity of the Frank Laboratory of Neutron Physics for 1994. The first part is a brief review of the experimental and theoretical results of investigations in condensed matter physics, nuclear physics and applied research. The second part presents, in a greater detail, the investigations which characterize the main directions of research. An emphasis should be put on the initiation of high pressure experiments with the DN-12 diffractometer and experiments with the HRFD diffractometer to investigate internal stresses in industrial samples. The reader can receive a more complete picture of the research carried out in the Laboratory from the list of publications for 1994 following Part 2.

In 1994 the Laboratory Directorate paid special attention to the basic facilities. The IBR-2 reactor was shut down in March for a scheduled replacement of the movable reflector. The intense work of a large group of engineers and workers of the technical departments of the Laboratory was successful, and at present, the new PO-2RM reflector is under testing at its regular site near the reactor core. At the end of March 1995 is to resume its regular operation mode.

A considerable advance has been made in the realization of the project for a new source of resonance neutrons - IREN - which is to replace the IBR-30 booster currently in operation. The solution of the problems associated with the fulfillment of obligations for constructing the main parts of the accelerator by the Institute of Nuclear Physics, Siberian Branch, Russian Academy of Sciences and transferring fuel for producing the multiplying target by the Ministry of Atomic Energy of the

Russian Federation created the necessary conditions for successful execution of the Project in 1998.

Further development of the User policy continued, aimed at attracting a larger number of physicists, chemists, biologists, and specialists in materials science to carry out experiments at the IBR-2 reactor. User Committees were formed for the four research directions: diffraction, small-angle scattering, inelastic scattering, polarized neutrons (reflectometry and depolarization). To increase the organization efficiency of the experiments the specific structure of the condensed matter physics department was elaborated.

The financial situation in the Laboratory did not noticeably change in 1994. The basic facilities and the technical infrastructure were financed from the JINR budget as in previous years. Instrument upgrades and the scientific program were provided for mainly from financial contributions in the frame of JINR-FRG and JINR-Hungary agreements for cooperation, as well as from other programs and funds. It should be specifically noted that the Ministry of Science and Technical Policy of the Russian Federation established the new National Research Program "Neutron Investigations of Matter" in 1994. This Program will undoubtfully contribute to the development of neutron scattering investigations at the IBR-2 reactor, which is the best research neutron source in Russia at present.

By and large the Frank Laboratory of Neutron Physics is one of the leading neutron centers of Europe and continues to develop in spite of the difficulties its host country currently experiences.

V.L.Aksenov
Director

21 February 1995

1.1. CONDENSED MATTER PHYSICS

1.1.1. EXPERIMENTAL INVESTIGATIONS

In 1994, the complex of 10 neutron spectrometers at the IBR-2 reactor permitted almost complete execution of the year's program for scientific research, in spite of a reduced (by approximately two times) reactor operation time due to the scheduled replacement of the IBR-2 movable reflector. A number of new results were obtained in all four of the FLNP research directions: investigations of crystal structures (neutron diffraction), macro-inhomogeneities in a medium (small-angle neutron scattering), micro-magnetic properties of matter (polarized neutron optics), and the dynamics of atoms (inelastic neutron scattering).

Diffraction. As in recent years, considerable attention was paid to HTSC materials. A method of isotopic contrast was used in HTSC structural investigations. Studies of the structure of the Y123 system were continued and reliable data on the distribution of cations in the structure and the influence of copper substitution on fine details of the structural organization of the system were obtained. The experiments were performed with pure Y123 (together with IC RAS, Moscow), with Y123-Cu/^{57}Fe (together with LLB, Saclay), and with Y123-Cu/Zn, Y123-^{65}Cu/Zn (together with RRC KI, Moscow). Figure 1 shows how the intensities of some diffraction peaks change following the substitution of Cu by ^{65}Cu in Y123-Cu/Zn.

Investigations of the Y124 compound were carried out where the doping with 10% Ca led to an increase in T_c of about 10 K. To increase contrast a ^{44}Ca isotope was used whose scattering length is markedly different from the scattering lengths of Y and Ba. The experiment was conducted with the HRFD diffractometer in the temperature interval from 8 to 300 K. Structural anomaly at about 150 K was experimentally confirmed on the microscopic level. It was also demonstrated that Ca replaced Y with a probability of almost 100%.

For several years investigations of structure modulation and its relationship to the superconducting properties in different bismuth superconductors have been carried out on the DN-2 diffractometer (together with IP, Prague). At present, the results of these investigations are considered as the most complete and reliable. These results permit one to understand the mechanism of building extra oxygen into the structure and the formation of Bi_nO_{n+y} chains. To systematize the obtained results the investigations were continued with the $Bi_{2.13}Sr_{1.87}CuO_{6+y}$ and $Bi_{2.05}Sr_{1.54}La_{0.41}CuO_{6+y}$ compounds, and modulation vectors and coordinates of all atoms were determined.

The traditional DN-2 direction is the investigation (together with IC RAS) of the structure of superionic crystals with hydrogen bonds (superprotonics) discovered in the early 1980's. New types and families of superprotonics are constantly appearing, which demand the use of neutron diffraction to determine the positions of light atoms. In the reported year, two types of crystals, $Cs_5(NH_4)_3(SO_4)_4$ and $Cs_5H_3(SeO_4)_4$, were investigated. A series of $BaCe_{1-x}Y_xO_{3-x/2}$ compounds was also investigated with DN-2 to obtain information about the mechanism of ionic conductivity recently discovered in this system. Reliable data were obtained on a high concentration of oxygen vacancies, which lead to the appearance of ionic conductivity upon doping $BaCeO_3$ with three-valent cations.
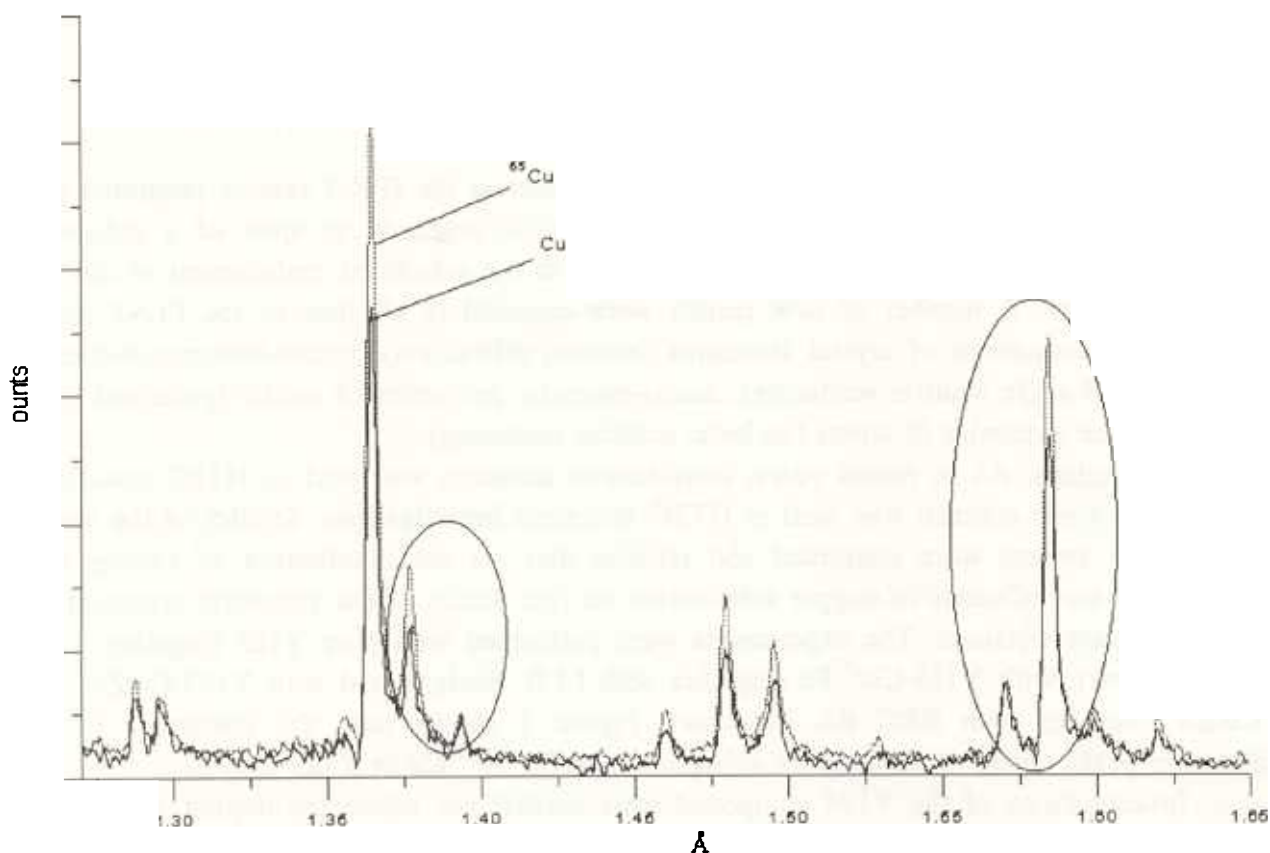
Fig.1. Part of diffraction spectrum of two samples of $YBa_2(Cu_{2.7}Zn_{0.3})O_{6+y}$, containing a natural mixture of copper isotopes and the ^{65}Cu isotope. The spectra were measured with HRFD.

Regular physical experiments on neutron diffraction at pressures up to 10 GPa and scattering at pressures up to 4 GPa were started on the DN-12 spectrometer constructed by FLNP together with RRC KI. To create the required pressures a technique of diamond and sapphire anvils was used. Though the physicists had a comparatively short time at their disposal for such experiments, a large volume of information was obtained on the orientational phase transition in hematite, on the structure and spectrum of vibrations in NH_4Cl, and on structure change in the Hg-1212 ($HgBa_2CaCu_2O_{6+y}$) high temperature superconductor. In NH_4Cl a decrease in the molecularity of the NH_4 ion following an increase in pressure was observed. This was demonstrated as a displacement of H towards Cl along an internal diagonal of the cube and a nearly linear increase in the frequency of the three observed vibrational modes: transverse optical, longitudinal acoustic, and librational (Fig. 2). In Hg-1212 the structure and partial compressibilities of lattice parameters and inter-atomic and inter-layer distances were determined for pressures up to 3.6 GPa (Fig. 3). At normal pressures the compound structure was in good agreement with known data, and at increased pressures a model of a structure with bridge oxygen disordered along diagonals in the (a,b) plane was in markedly better agreement with the measured and calculated diffraction spectra. The largest compressibility coefficient ($0.025\ GPa^{-1}$) was found for the distance between the Ba and oxygen layers which couple copper and hydrogen atoms. This investigation was performed in cooperation with the RRC Kurchatov Institute, Moscow State University, and the Laboratory of Crystallography in Grenoble.
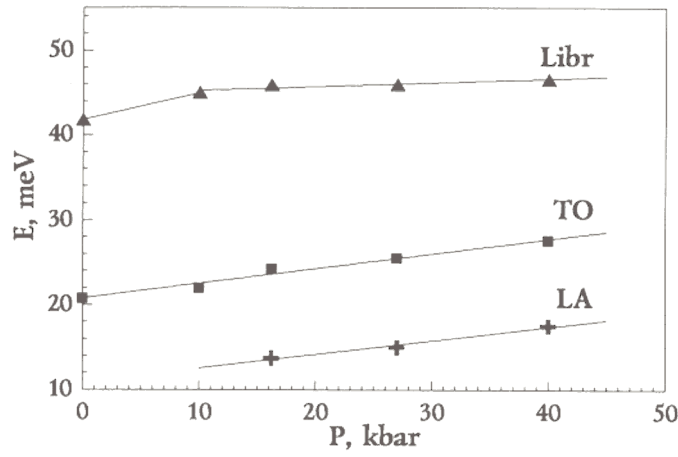
Fig.2. The pressure dependence of the characteristic energies of the librational (Libr), transverse optical (TO), and longitudinal acoustic (LA) vibrational modes of NH_4Cl as measured with the DN-12 spectrometer.
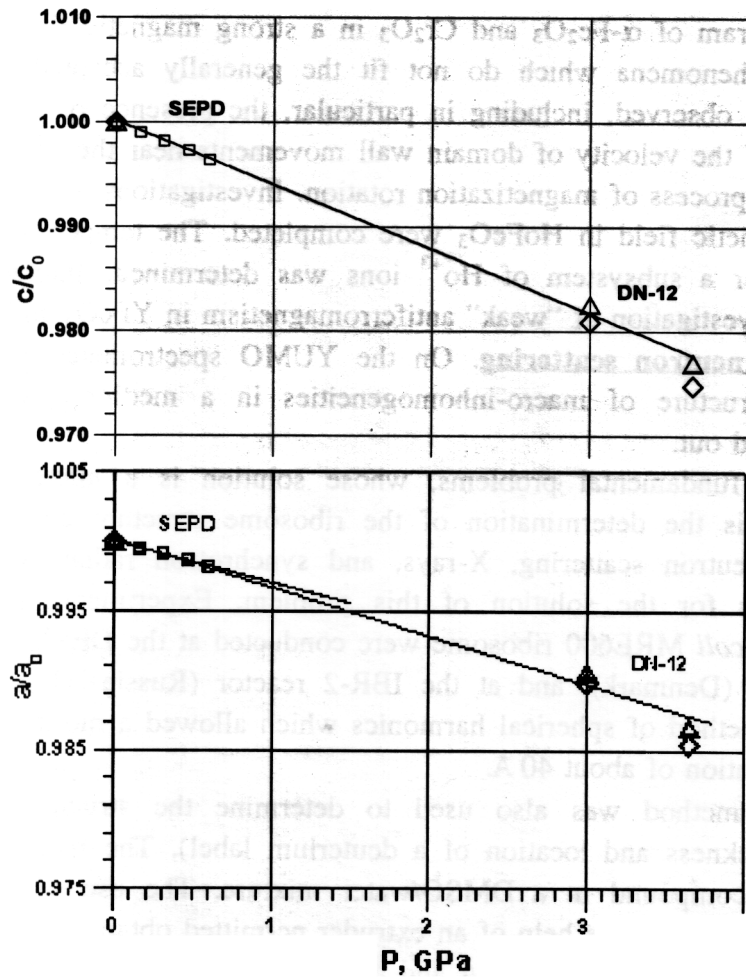

Fig.3. Relative changes in the lattice parameters of $HgBa_2CaCu_2O_{6.3}$, following an increase in pressure. The measurements were performed with the DN-12 diffractometer (IBR-2, Dubna) and the SEPD diffractometer (ANL, Argonne). For DN-12 two sets of points obtained by different methods of processing experimental spectra are shown.

11

Routine experiments to investigate texture formation processes in rocks continued on the NSVR diffractometer. Nine samples of quartzite, amphibolite, deformed calcite and tellutite were investigated in 1994. An essential influence of the phase transition in calcite on the texture transformation was discovered. In addition to experimental investigations, a large amount of work to optimize the process of measuring pole figures and improve procedures of data extraction from the measured diffraction spectra was carried out by the texture analysis group.

The SNIM-2 spectrometer is a unique facility providing a means for investigating the properties of crystals in strong pulsed magnetic fields (up to 150 kOe in the pulse). SNIM-2 is mainly used as a diffractometer, but an SNIM-2 operation mode with an energy analysis of scattered neutrons is also possible. Synchronization of magnetic field pulses with reactor power pulses permits carrying out effective investigations of the kinetics of transitional processes - first order magnetic phase transitions. The time resolution of the spectrometer can achieve a value of 4 μsec. The experimental data obtained with the SNIM-2 spectrometer are very difficult to interpret. Recently, however, we managed to carry out a series of experiments which provided the theoreticians with interesting results. In particular, detailed information was obtained about a spin-flip transition in antiferromagnetics with a rhombohedral structure, namely, the dynamic magnetic phase diagram of α-Fe_2O_3 and Cr_2O_3 in a strong magnetic field was investigated. A series of unusual phenomena which do not fit the generally accepted mechanism of phase reconstructions were observed, including in particular, the presence of a limit hysteresis loop, and the smallness of the velocity of domain wall movements near the critical field value which cause a delay in the process of magnetization rotation. Investigations of the AF-ordering induced by an external magnetic field in $HoFeO_3$ were completed. The temperature dependence of the AF susceptibility for a subsystem of Ho^{+3} ions was determined. Interaction constants were determined in the investigation of "weak" antiferromagnetism in $YFeO_3$ and $HoFeO_3$.

Small-angle neutron scattering. On the YUMO spectrometer a diverse program for investigating the structure of macro-inhomogeneities in a medium by small-angle neutron scattering was carried out.

One of the fundamental problems, whose solution is a matter of great interest in molecular biology, is the determination of the ribosome structure and its subparticles. The combined use of neutron scattering, X-rays, and synchrotron radiation is one of the most prospective methods for the solution of this problem. Experiments for studying the 50S subparticle of the *E.coli* MRE600 ribosome were conducted at the DESY synchrotron (FRG), at the reactor of Riso (Denmark), and at the IBR-2 reactor (Russia) (Fig. 4). The data were processed using a method of spherical harmonics which allowed a model of the structure to be derived with a resolution of about 40 Å.

The SANS method was also used to determine the structure parameters of lipid membranes (the thickness and location of a deuterium label). The measurements were carried out with a DPPC compound in a DMSO/water mixture. The use of a special method for preparing lipid vesicles with the help of an extruder permitted obtaining a homogeneous mixture of particles with a radius of about 800 Å and a prolonged linear part of the Guineir-curve. This provided the possibility of determining the parameters of the membrane with good accuracy. In addition, data on the dependence of the radius of gyration of membrane vesicles on the DMSO concentration in the water solution were obtained.
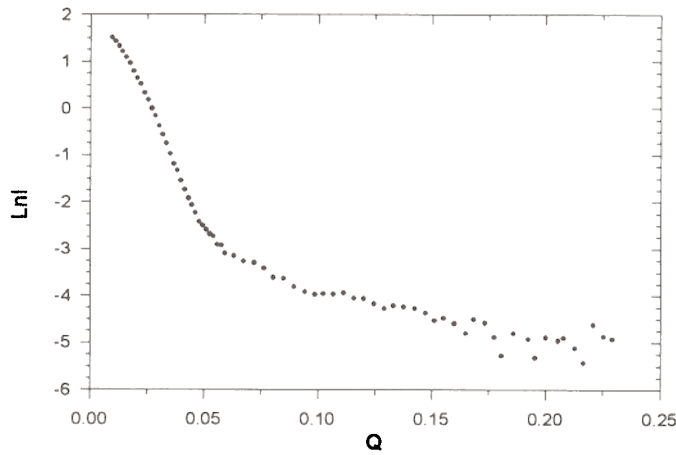
Fig.4. The dependence of the intensity, I, of the small-angle scattering of neutrons on the 50S subparticle of the *E.Coli* MRE600 ribosome on the Q (Å^{-1}) momentum transfer as measured with the YUMO spectrometer.

Work to study structures of tilacoid membrane chloroplasts participating in photosynthesis in plant cells was initiated in cooperation with MSU. The first small angle scattering curves were obtained and a number of structure parameters were estimated.

In a joint experiment with physicists of the Bayreuth University, FRG, the volume occupied by a water molecule in a microscopic size drop was determined by the SANS method for the first time. This volume appeared to be unexpectedly large (45 Å^3 instead of 30 Å^3).

The first measurements of self-organizing systems were carried out. These included investigation of the influence of a charge on the self-organization of a micellar system. This influence is demonstrated as a change in the shape of a micelle from cylindrical to spherical. The first results on the influence of pressures on self-organizing systems were also obtained.
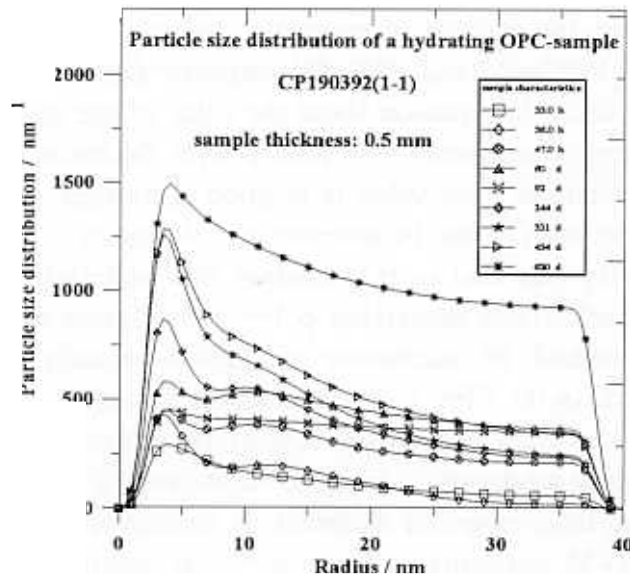

Fig.5. Changes in time of size distributions of Portland cement particles from 33 hours to 620 days following the moment of hydration. The data were obtained with the YUMO spectrometer.

13

Under the auspices of the FLNP and German institutes joint program for investigating materials having practical importance, a large volume of information on the processes of Portland cement solidification was obtained with the YUMO spectrometer. The SANS method permits one to trace the size distributions of particles formed in the process of cement solidification to a comparatively large depth (up to several mm). Figure 5 shows how these distributions change in time beginning from several hours to two years following the moment of hydration for one of the samples of industrial cement.

Investigations of some new surface-active substances (surfactants) were completed and information about the structure of their micellar aggregates was obtained. Work to study the effect of salts on the structure of non-ionogenic surfactant aggregates started in cooperation with the Kiev University (Kiev, the Ukraine)) and the Riso National Laboratory (Riso, Denmark).

Neutron optics with polarized neutrons. Investigations with polarized neutrons were carried out on the SPN-1 spectrometer which can be operated in two modes: depolarization and reflectometry. In the first case the depolarization of a primary polarized neutron beam transmitted through a sample is measured. In the second case, the intensity of neutrons reflected from the surface of a sample at small incidence angles is measured.

Systematic research of neutron depolarization in HTSC near the phase transition point in a wide range of external magnetic fields revealed previously unobserved anomalies revealing new properties of the mixed state of superconductors.

Investigations by a depolarization method were carried out with a Li-Zn-Ti-Fe, ferrite, a magnetite-based magnetic liquid, and a Y-123 superconductor. Indications of the existence of subregions with an induced magnetic moment were obtained. The H-T phase diagram of the behavior of a system of Abrikosov vortices near T_c was obtained for Y-123.

The first experiments to observe the effect of the Berri geometrical phase on the transmission of polarized neutrons through a medium with a collinear magnetic field were performed.

On the SPN-1 the reflectometry method has been used for several years in joint ILL (Grenoble) investigations on the analysis of magnetic interactions in multi-layer superthin films. In the reported year the Pd/Co/Pd and W/Fe/W magnetic films were investigated. The main attention was given to obtaining information about the value of the magnetic moments of Co and Fe atoms. So, for the magnetic moment of Fe with a layer thickness of only 6 Å at 300 K the value of $\mu=1.80$ μ_B was obtained. This value is in good agreement with theoretical predictions, allowing for a partial suppression of the Fe moment in a W matrix.

Neutron reflectometry was also used to analyze new materials on the basis of thin films alternating with layers of selectively deuterated polysterensulfonate and polyalamine. To obtain multilayer structures a method of successive absorption recently developed at the Meinz University (FRG) was used. In the SPN-1 experiments the assumed organization structure of the films was confirmed and the values of the main repetitiveness periods were obtained.

Inelastic scattering of neutrons. Inelastic scattering of neutrons, used to investigate the dynamics of atoms and their magnetic moments, is studied with three spectrometers at IBR-2: NERA-PR and KDSOG-M operating in the inverted geometry regime, and DIN-2PI in the direct geometry regime.

With the NERA-PR spectrometer, information about molecular dynamics and phase transitions in the $K_{1-x}(NH_4)_xSCN$, NH_4HSO_4, $(NH_4)_3H(SO_4)_2$ compounds was obtained for temperatures from 100 to 300 K and pressures up to 400 MPa. The ordering processes of NH_4^+

ions were observed and interpreted. In crystals of the camphor family ($C_{10}H_{16}O$) whose molecules have a nearly spherical form, phase transitions from the orientational disorder state at room temperature to the complete order state at $T < 200$ K were discovered. A large cycle of investigations with amino acid crystals was also conducted. Data on the main vibrational modes of L-leucine and L- and DL-valine were obtained.

A series of investigations of the contribution of hybridization to the crystal field in $ReCu_2Si_2$ (Re - rare earth) compounds were completed. Systematic studies of spin dynamics in the transition from a state with heavy fermions to a state with variable valency in $Ce_{1-x}YLa_xAl_3$ compounds were carried out. The obtained results are evidence of the existence of a specific s-f interaction in such systems and can be interpreted only in the frame of a hybridization model. The phonon density of states in the $La_2CuO_{4.1}$ superconductor was investigated. Indications of the nonphonon origin of the excessive density of low-frequency excitations were obtained. Work continued on the investigation of the interaction of hydrogen with p-elements in solid solutions of transitional metals. Data were obtained for the Ta-V-N-H, V-O-H, and Fe-Ni-H systems. An unusual behavior of hydrogen in the V-O-H system was observed.

Investigations of excitation spectra of liquid ^{4}He continued on DIN-2PI. Data on the three previously observed types of excitation whose demonstrations differed in dependence on temperature and wave vector were refined. Additional information was obtained about two characteristic regions of spectrum reconstruction: the temperature region - near the superfluid transition point, and the wave vector region - in the interval 0.5-0.65 $Å^{-1}$ following the transition from phonons to maxons. Investigations of liquid metals continued. In liquid potassium, collective excitation modes were observed up to $k \approx 1.25$ $Å^{-1}$. Investigations began of ionic and hydrophobic effects in liquid solutions. The first results were obtained for CsCl and $(CH_3)_4NCl$ solutions. Detailed data on the influence of nitrogen on the lattice dynamics of austenite alloys were also obtained.

1.1.2. METHODOLOGICAL WORK

In the course of the reported year methodological work on the development and upgrading of equipment for all diffractometers was carried out.

For the HRFD, the new Li-detector at the scattering angle of $90°$ was manufactured, assembled, and tuned. This detector will provide considerably better conditions for internal stress measurements than the $152°$ detector and will allow us to start experiments at high pressures with a gas cell for up to 15 kbar.

The DN-2 possibilities for conducting real time experiments were increased: 8 spectra for different scattering angles can be simultaneously measured. A two-dimensional multi-wire detector with a position resolution of 3 mm in both coordinates was prepared for operation.

At the DN-12, the second ring of 16 counters was prepared for operation. This ring will reduce the typical experimental time by 2 times.

For the NSVR, a "HUBER" automatic multi-axis goniometer was purchased and made ready to operate. This goniometer will permit us to start experiments for analyzing the relationship between the texture and internal stresses in industrial products and minerals.

On SNIM-2, work continued to put into operation a generator of rectangular pulses which would make the staging of experiments easier and clarify the interpretation of the performed investigations of transitional processes in magnetic crystals.

15
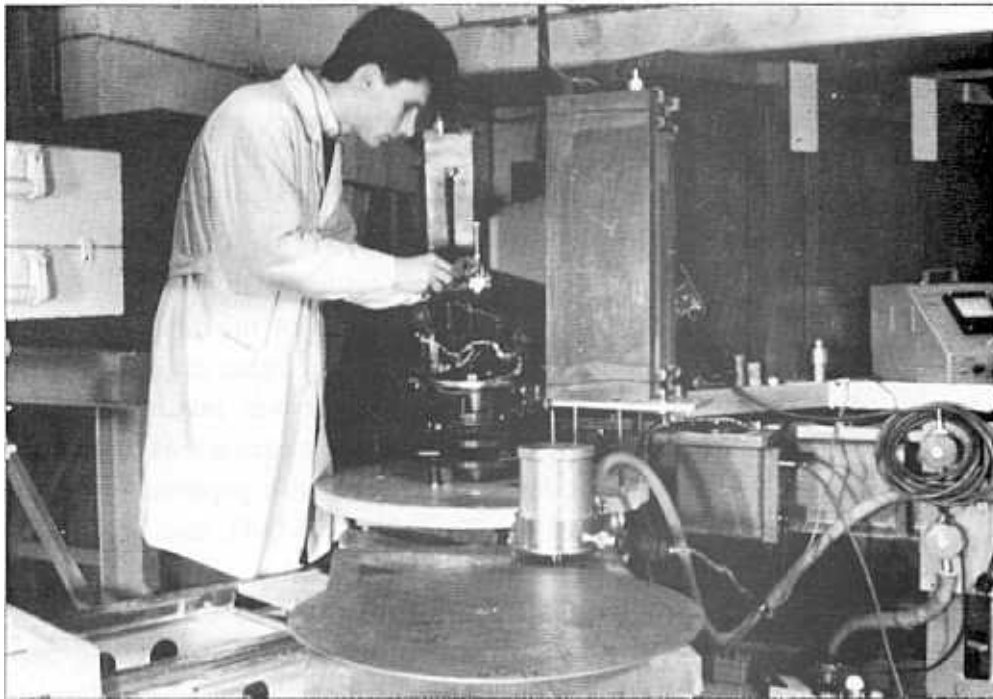
A complex for measuring internal mechanical stresses in industrial products and samples by the non-destructive method of neutron diffraction is being built for the HRFD Fourier diffractometer. G.D.Bokuchava is adjusting the new 90°-scattering neutron detector.
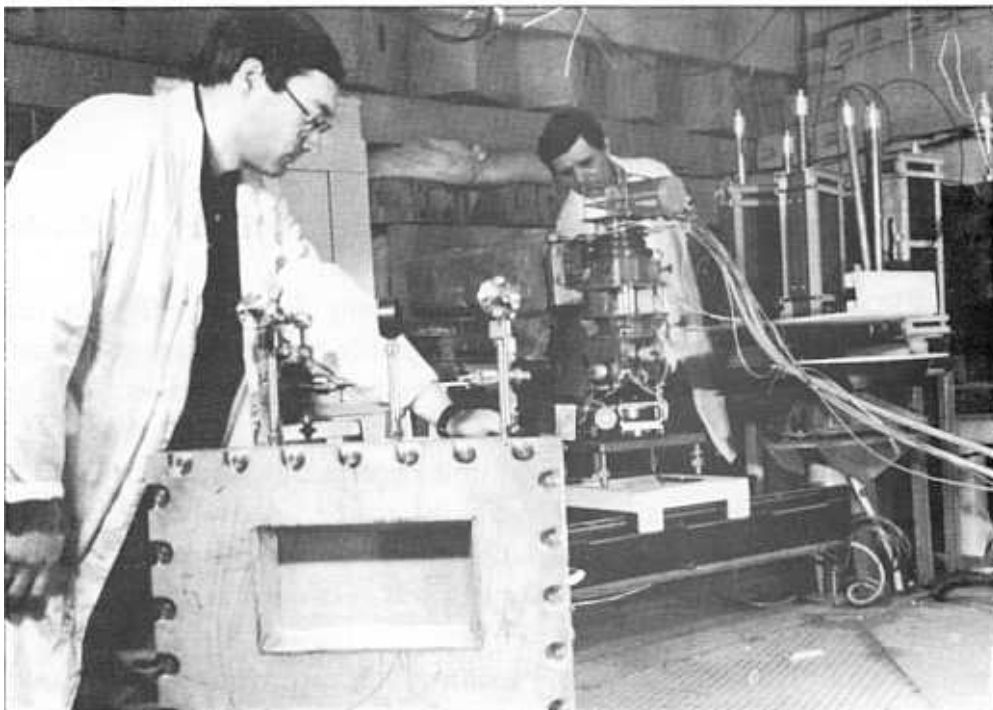
S.A.Kutuzov (left) and A.I.Beskrovnyi are preparing the two-dimensional detector and helium refrigerator to begin measurements with the DN-2 diffractometer.

16
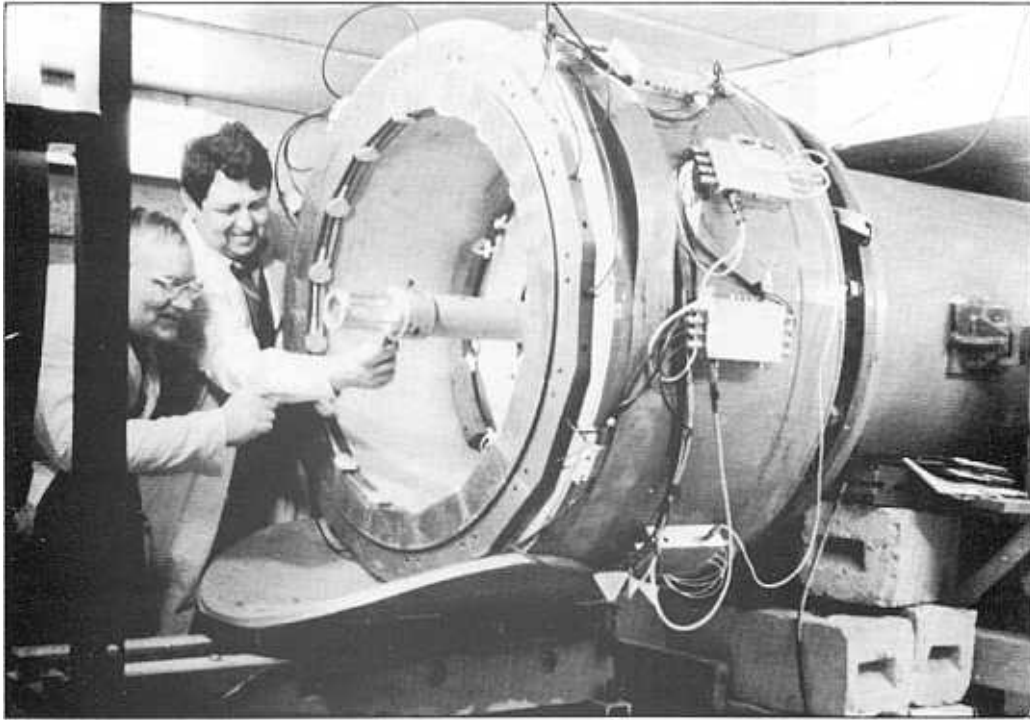
V.P.Glazkov and B.N.Savenko are tuning a high pressure cell with a sample on the DN-12 diffractometer.
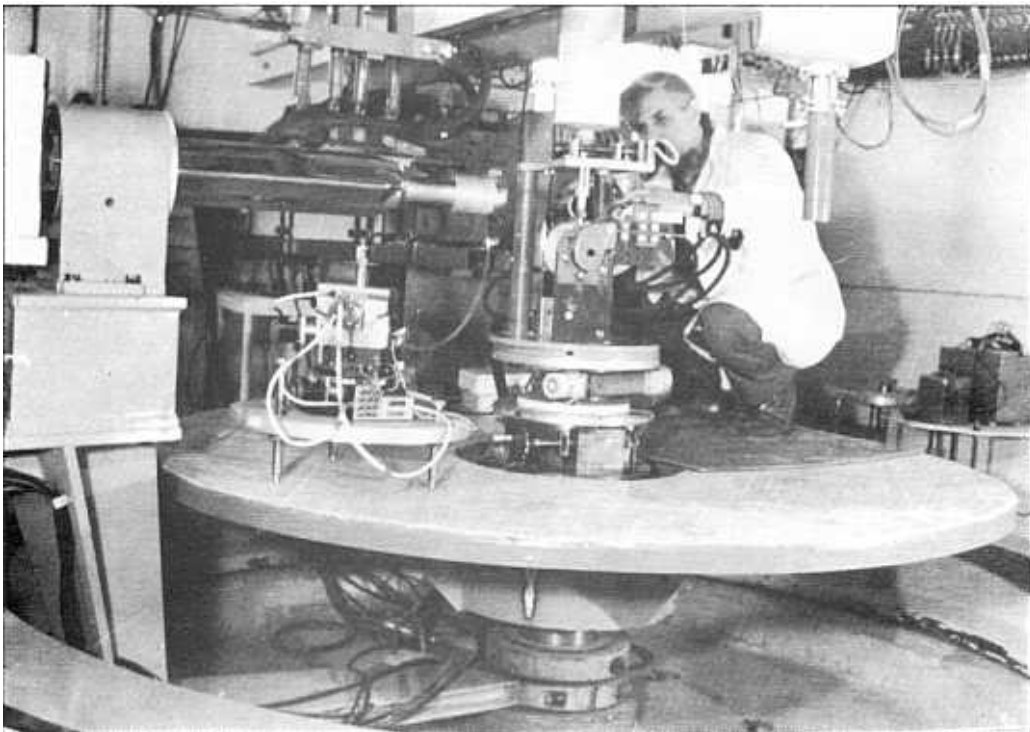
G.A.Varenik is adjusting a pulsed magnet for the SNIM-2 diffractometer.

K.Walther and N.N.Isakov are preparing the
HRNS diffractometer to start experiments.
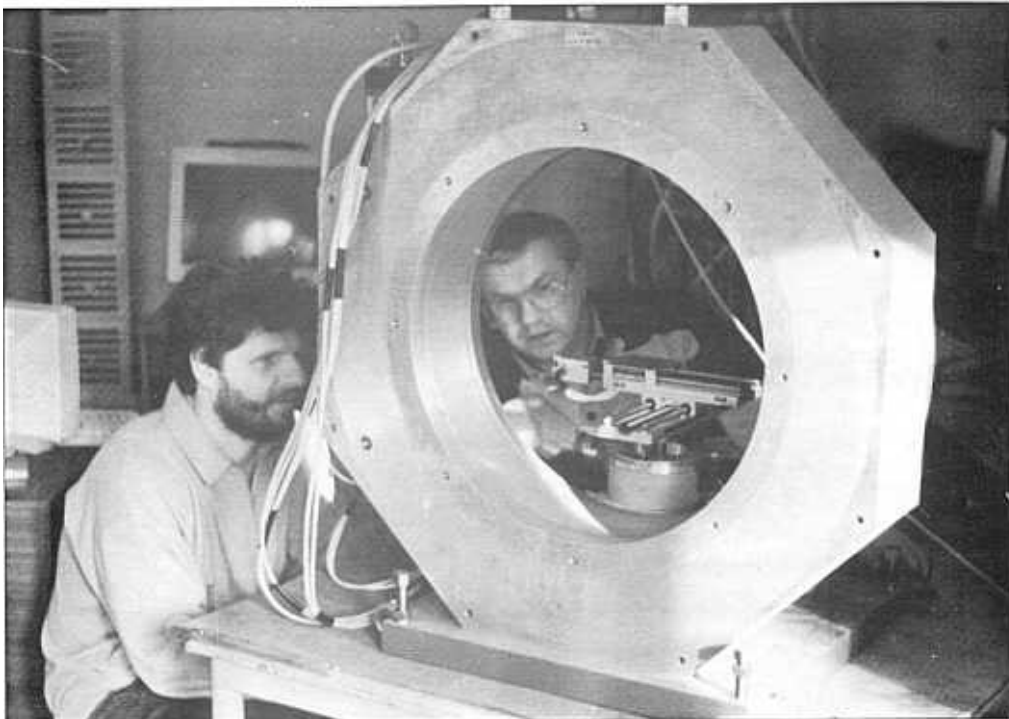
J.Heinitz and K.Walther are tuning the program for the new
multi-axis goniometer, a product of the HUBER firm, to be
used for measuring internal stresses in geomaterials.
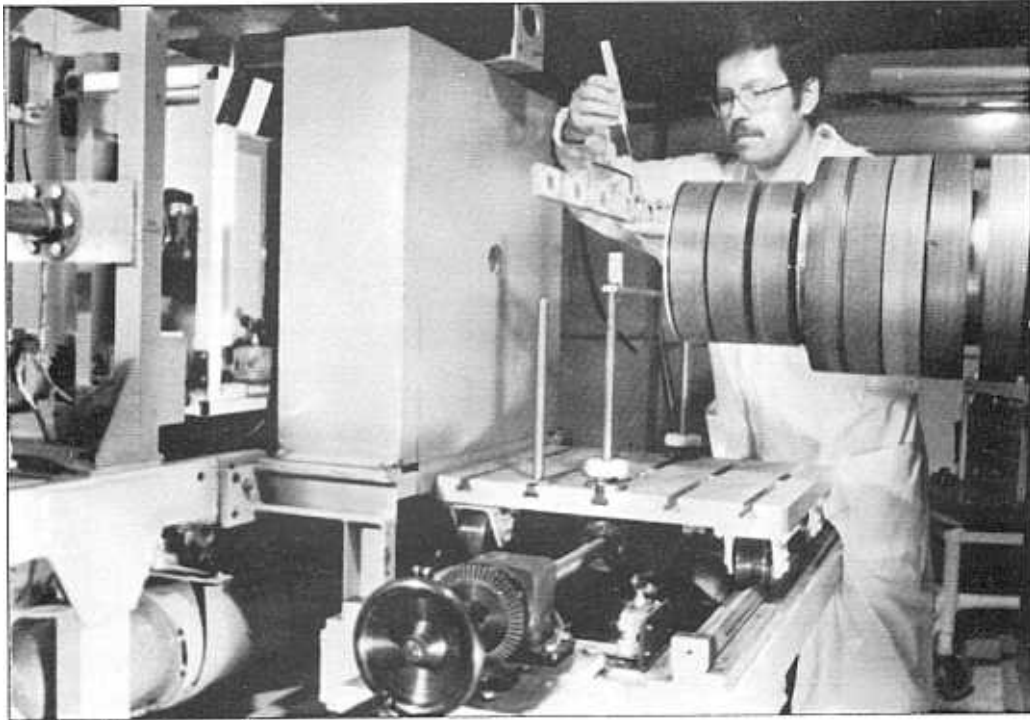
A.I.Kuklin is installing a cassette for changing samples
by remote-control on the YuMO spectrometer.
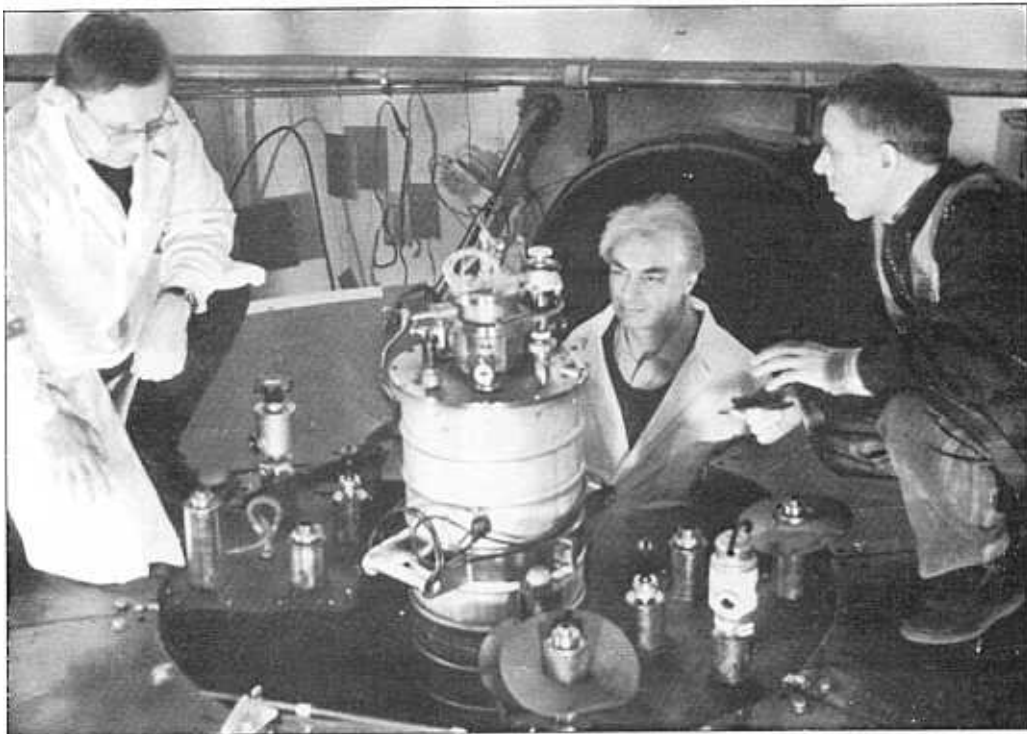
I.Natkaniec, L.S.Smirnov and S.I.Bragin are preparing experimental
equipment for measurements with the NERA-PR spectrometer.
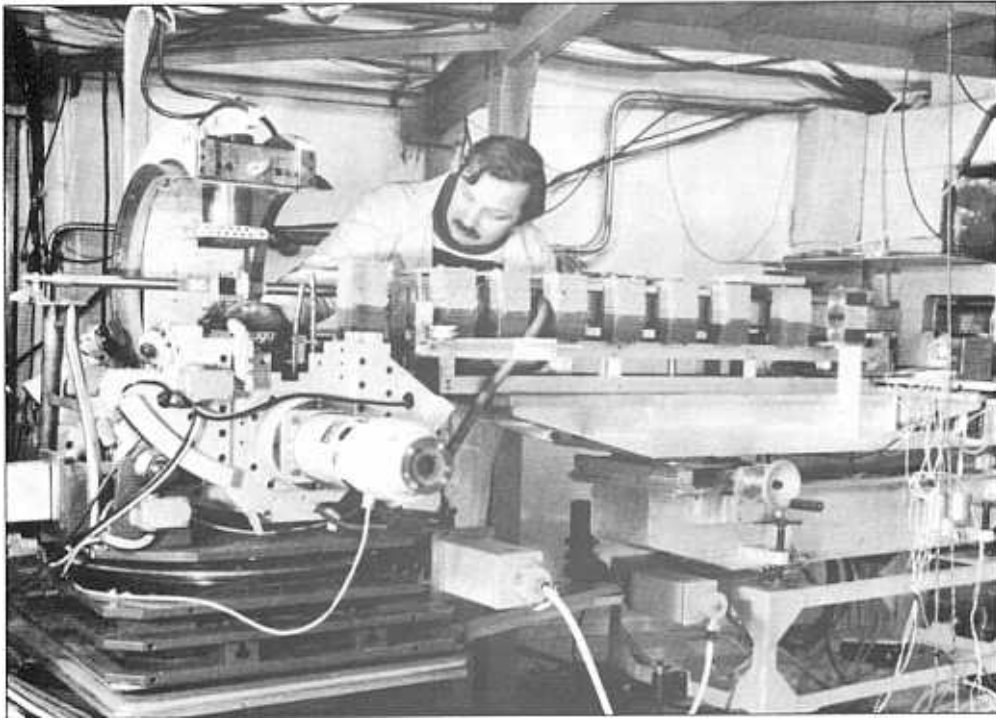
A.V.Petrenko is checking the precision of sample positioning at the SPN-1 spectrometer.

D.V.Lezhnev is assembling a cryostat at the REFLEX-1 facility.

For the YUMO spectrometer, a resistive anode-based ring PSD was manufactured and tuned.

The new background chopper was installed at KDSOG-M. This provided a several times increase in the effect to background ratio.

The new cryostat with a superconducting solenoid for the temperature range from 1.5 to 300 K and a furnace were prepared to operate with the SPN-1 spectrometer.

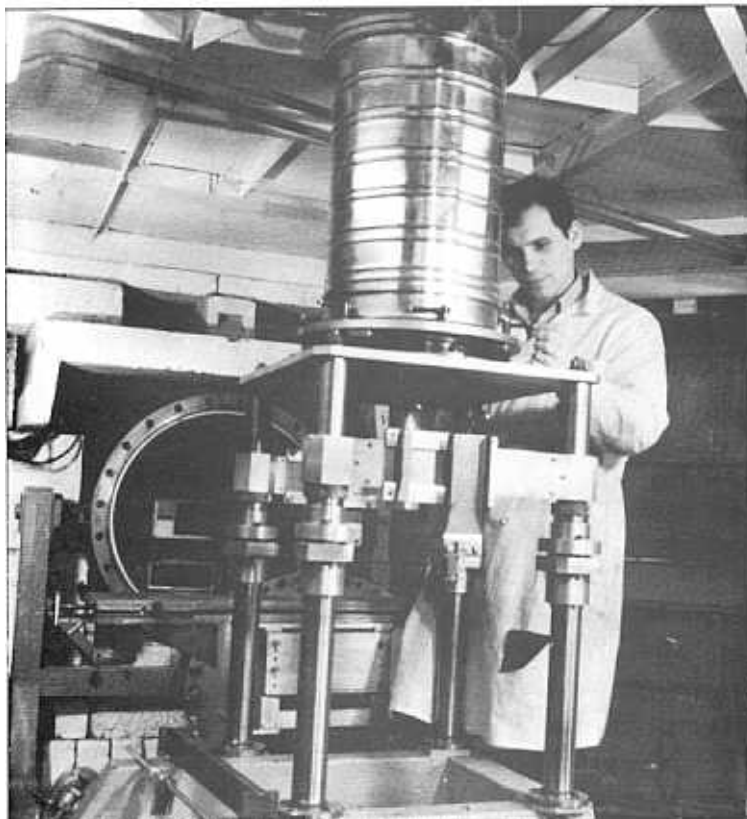At the REFLEX spectrometer for reflectometry experiments with both polarized and unpolarized beams of neutrons, the biological shielding and the assembly and adjustment of the main spectrometer block - the optical system - were completed. Its start-up is scheduled for the next year.

In the reported year, one of the important events was the test of the cryogenic methane moderator mounted on the side of channels N 4, 5 and 6 at the IBR-2 reactor (the YUMO, HRFD, DN-2, and SNIM-2 instruments). The most interesting results from the viewpoint of diffraction experiments were obtained with the DN-2 in investigating the kinetics of fast transitional processes studied in real time. A considerable increase in the cold neutron flux (by about 20 times for $\lambda = 8$ Å) permitted measuring diffraction spectra with good statistics for $d \geq 2$ Å during a time of about 1 min. The diffractometer's time-of-flight resolution of $\Delta t/t \approx 5 \cdot 10^{-3}$ over this region and a small number of diffraction peaks provide a means for reliable identification of crystal phases arising and vanishing in the process of the investigated reaction.

1.1.3. THEORY

High-temperature superconductivity. The discovery of high-T_c superconductivity stimulated a great number of theoretical works on this problem. The antiferromagnetic order observed in CuO_2 planes at small carrier concentrations indicates that the magnetic subsystem is of great importance to the formation of the superconducting state. Structural phase transitions, as well as a number of other experiments, give evidence of the important role of electron-phonon interactions. The reports concerning the direct observation of polarons in the dielectric phase upon carrier doping and small, but non-zero isotope effects lead to the same conclusion. It was shown that formation of a polaron in the 2D case within the model of local electron-phonon interaction is accompanied by the formation of a barrier attributed to a finite electronic bandwidth (lattice discreteness).

Yet, lattice discreteness has no influence on the qualitative picture of the formation of the self-localized state in 1D and 3D cases. The medium-size polarons are supposed to be formed in high-T_c superconductors.

The problem of the role of magnetic fluctuations on the appearance of the superconducting state in high-T_c superconductors has been discussed. In order to understand properly the microscopic nature of the superconducting state, experimental investigation of spin dynamics in the CuO_2 planes seems to be of great importance. In particular, the results of inelastic neutron scattering and nuclear magnetic resonance (NMR) experiments are of significance. The results of inelastic neutron scattering experiments on crystal field (CF) excitations in Tm substituted YBaCuO were analyzed and discussed in connection with the NMR results on ^{89}Y, ^{63}Cu and ^{17}O. It was shown that in the insulating state, the main contribution to the line broadening of the 4f transitions of Tm ions arises from the magnetic subsystem of Cu ions. The temperature dependence of the linewidth was described in terms of

linear spin-wave theory with a rather weak interaction of 4f levels with the magnetic moments in the CuO_2 planes. On the other hand, in superconducting compounds, due to the small coherence length of AF fluctuation, the direct contribution of AF fluctuations to the broadening of transitions is small. The temperature dependence of the linewidth is determined by the temperature dependence of the uniform static susceptibility.

Mid-infrared spectra have been obtained by exact calculations of the optical conductivity, $\sigma(\omega)$, of a finite size Holstein model. $\sigma(\omega)$ shows a number of peaks corresponding to the bound states of polarons with different numbers of phonons. It was found that for intermediate coupling, the $\sigma(\omega)$ peak is strongly asymmetric. The optical conductivity of the 2-site model in the presence of two electrons was studied. Numerical results show a shift of the $\sigma(\omega)$ peak to the low energy region with an increasing Hubbard U for strong electron-phonon interaction ($E_p > U$) whereas the peak moves to the high energy region for $U > E_p$. A new peak in the high energy region starts to develop at large U limit in the presence of phonons. The significance of these calculations for experimental observations of the mid-infrared spectra of high-T_c cuprates was discussed.

Neutron reflection. Studies of various kinds of multilayers have important practical applications in the construction of mirror walls for neutron guides. To increase the reflection coefficient from multilayer mirrors it is necessary to choose both layer materials and layer thicknesses properly. Recently, numerical calculations of the reflection of a plane wave from an equidistant set of delta-function potentials with two different strengths, u and v, which are the model parameters characterizing two sorts of materials, were performed. The sequence of potentials was chosen to form the so-called Fibonacci words. As the result of introducing disorder of a quasicrystal sort into the sequence of the neutron mirror material, the full reflection region may shift both into the small k-th and into the opposite values of momentum k.

Statistical mechanics. A lattice model having an exact solution in all dimensions was completely investigated. Partition functions of the model have been calculated by the Kirchhoff theorem. Universal behaviour of the thermodynamic functions were found in the limit of dense packing. A matrix procedure was developed for calculation of the correlation functions. The average number of atoms with given valences has been computed for the whole density range of polymers.

An exact enumeration of self-avoiding loops in a set of finite simple square lattices was performed. The partition function zeroes distribution was shown to be oval-like, in contrast to two intersecting circles, as in the case of the Ising model. An analysis of the partition function zeroes distribution showed the closeness of the critical point of the model to the ferromagnetic one of the Ising model.

Quantum mechanics. It is known that quantum systems with time-periodic hamiltonians have some general properties, depending on the fact that the hamiltonian is hermitian and time-periodic, but which do not depend on the details of the hamiltonian structure. An investigation of the general properties of quantum systems with time-periodic hamiltonians was continued. The scattering theory was constructed, the kinetic equation was introduced and the quasienergy spectrum transmutation was investigated.

1.2 NEUTRON NUCLEAR PHYSICS

1.2.1. EXPERIMENTAL INVESTIGATIONS

In the reported period, programs for investigations in the FLNP traditional research directions: experimental investigations of the fundamental properties of the neutron, studies of the processes of P-parity violation in different nuclear reactions induced by neutrons, investigations of high excited states of nuclei in reactions with resonance neutrons, etc., were continued.

The main part of these investigations were carried out on the neutron beams of the IBR-30 booster and the IBR-2 reactor. A number of works, however, were conducted in collaboration with nuclear centers of Russia, the Ukraine, Germany, Belgium, the USA, and China at the neutron sources of these centers.

Electromagnetic properties of the neutron. The n-e scattering amplitude is the critical parameter in determining the mean square charge radius of the neutron. The existing spread of experimental values leads to different sign assignments for this quantity.

The processing was completed of the data obtained in high precision measurements of total cross sections and scattering amplitudes with ^{206,207,208}Pb and Bi samples which were carried out by a Dubna-Garching-Riga collaboration. The n-e scattering length of $b_{ne} = (-1.32\pm0.03)\cdot10^{-3}$ fm as earlier measured in Garching was confirmed, which led to the conclusion that the sign of the mean square charge radius of the neutron was positive, in contradiction with the standard theory. A new value for the coefficient of the electric polarizability of the neutron, $\alpha_n = (0.0\pm0.5)\cdot10^{-3}$ fm, was also obtained. The planned experiment to investigate the scattering of slow neutrons on noble gases to prove the possibility of measuring the n-e scattering amplitude with an accuracy better than 5% by using the time-of-flight technique at the IBR-30 and IBR-2 facilities was modeled.

In the frame of the program for studying the electromagnetic properties of the neutron, measurements of the total neutron cross section of ^{208}Pb for three energy intervals were conducted to determine the polarizability of the neutron using resonance filters on the 70 m flight path of the IBR-30. The obtained results are being processed.

In cooperation with INI AS of the Ukraine, a measuring procedure was tested and a preliminary result was obtained on the value of the total cross section of ^{208}Pb for quasi-monochromatic neutrons with the energy of $\sim$ 24 keV, obtained with ^{56}Fe+Al+S filters at the VVR-M stationary reactor. In 1995, continued measurements with other filters will permit us to increase the accuracy of α_n coefficient determination.

The situation regarding experimental determination of the considered fundamental electromagnetic characteristics of the neutron remained rather uncertain. Hence, new methods and additional measurements are necessary, the preparation of which is actively being pursued in FLNP.

Parity violation in neutron reactions. The analysis was finished of S-parity violation effects in 25 p-wave neutron resonances measured with the ^{113}Cd enriched isotopic target by a FLNP (Dubna, Russia), LANL (Los-Alamos, USA) and IRMM (Geel, Belgium) collaboration. The resonance averaged value of the matrix element of weak interaction for nuclei with the mean atomic weight $M(^{113}Cd)=2.0^{+1.6}_{-0.9}$ was determined (fig.6). For the first time, the

dominance of the mechanism of compound-compound parity mixing was experimentally confirmed, and the first step towards investigating the mass dependence of M was also made, which is most important for theory.
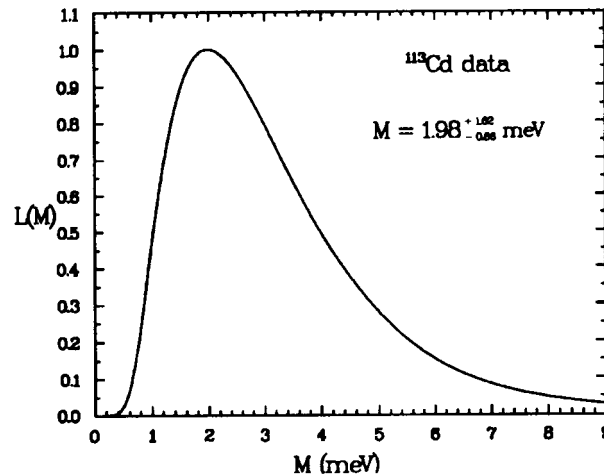

Fig.6. The credibility function, L(M), in dependence on the M matrix element of weak interaction for the ^{113}Cd target nucleus.

The new technique for measuring P-odd correlations with polarized thermal neutrons in reactions with the emission of charged particles was elaborated in cooperation with a PINP (Gatchina) group. The corresponding instrument for measuring P-odd correlation in the ^{10}B(n, α)^{7}Li*→γ reaction with γ-registration was constructed and tested in a beam of polarized neutrons with a flux of 10^9 n/s. For the final tuning of the equipment and conducting the main measurements a flux of 10^{10} n /sec is necessary, which is expected from the VVR-M reactor of PINP in 1995.

Neutron radioactive capture. Measurements of radioactive neutron capture provide valuable information about the structure and properties of the decay of excited states. During the past several years FLNP has collected a large volume of (n,2γ) reaction data for 18 spherical and deformed nuclei from ^{137}Ba to ^{198}Au which was used in a comparative analysis of the probability of excitation and decay of intermediate levels at neutron energies close to the neutron binding energy. It was shown that the observed experimental dependences were difficult to describe in the frame of generally accepted models of radioactive transition widths and energy dependencies of excitation level densities. This should stimulate further experimental and theoretical research in the given direction.

With the ROMASHKA multi-detector facility measurements of gamma-quanta multiplicities and the determination of the parameters of neutron resonances: spins, radioactive widths and neutron strength functions, and mean gamma-ray multiplicity, in separate resonances of the ^{177}Hf, ^{178}Hf, ^{119}Sn, ^{113}In, ^{115}In isotopes over the energy interval from 0.015 to 1.5 keV were conducted. The importance of these measurements was determined by the incomplete data on spins and radioactive widths and a practical lack of information about the gamma-spectra of neutron resonances of the mentioned nuclei. The radioactive neutron capture cross section of the Hf, Sn, and In, isotopes in the resonance neutron energy range is interesting from the point of view of understanding the process of nucleosynthesis. At the same time, these investigations have certain applied importance. Some of the above mentioned isotopes are used in reactor

building, where new and more exact and reliable data are now necessary in connection with the increasing precision of nuclear reactor calculations. A detailed study of the resonance parameters of, e.g., hafnium nuclei, is necessary for the determination of different reactor parameters, such as resonance integrals and Doppler reactivity coefficients. Data on the spectra of capture γ-rays are important for shielding calculations.

Reactions with the emission of charged particles. Investigations of the (n,α) and (n,p) reactions on slow neutrons were continued. Data processing on the ^{14}N(n,p)^{14}C reaction was completed and the results were published. Cross section measurements of the ^{35}Cl(n,p)^{35}S, ^{36}Cl(n,p)^{36}S, ^{36}Cl(n,α)^{33}P reactions on thermal neutrons were begun. Measurements of the ^{36}S(n,γ)^{37}S reaction, being of great importance to astrophysics, were carried out at the energy of 25 keV in collaboration with Karlsruhe.

In the field of investigations with fast neutrons, data processing on angular distributions and cross sections of the ^{58}Ni(n,α)^{55}Fe reaction at 5.1 MeV was completed in collaboration with the Beijing and Tsinghua Universities (Beijing). The ^{64}Zn(n,α)^{61}Ni reaction was measured for the neutron energies of 5 and 6.5 MeV. Data processing is being performed now. Work to systematize (n,α) and (n,p) reaction cross sections in the neutron energy interval from 2 to 16 MeV for the wide range of atomic weights A=19-197 was carried out. The dependence of cross sections on the (N-Z)/A parameter was obtained.

The first phase of the experiment to measure the energy dependence of the angular anisotropy of fragment emission following the fission of aligned ^{235}U nuclei induced by resonance neutrons was completed (fig.7). Although the statistics were low, the interference of s-resonances with different spins, predicted earlier by FLNP, was discovered. For qualitative analysis of the discovered effects, however, an essential increase in the statistics, as well as a number of technique and equipment improvements, in particular a replacement of the cryostat by an updated one, are necessary.
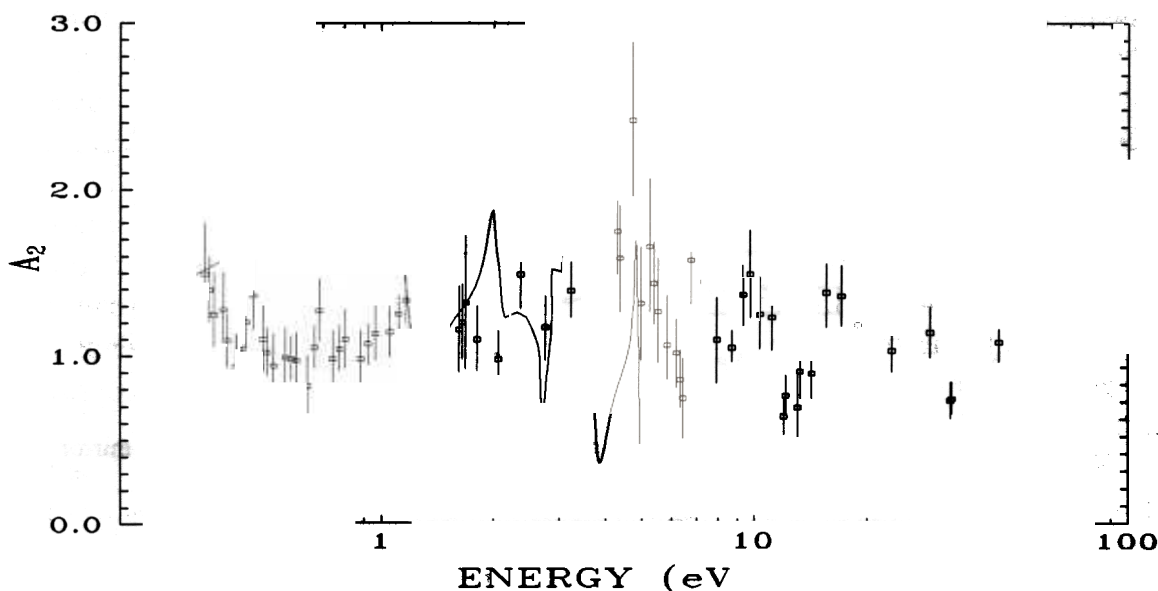

Fig.7. The energy dependence of the A_2 coefficient of the angular anisotropy of fragment emissions in the fission of aligned ^{235}U nuclei induced by resonance neutrons. The solid line is the result of the calculation without consideration of the interference of compound states with different spins.

25

1.2.2. METHODOLOGICAL DEVELOPMENTS

In 1994 construction of the UGRA facility for precision measurements of the angular distribution of resonance neutrons was continued. The large volume of work done allows us to schedule the on-beam assembly of the facility at IBR-30 for the first half of 1995.

The construction of the test prototype of the high density ultracold neutron source on the basis of the BIGR reactor (Arzamas-16) was completed (the ISPIN project). Full-scale tests of the facility were carried out. Transportation of the facility and assembly in Arzamas-16 are scheduled for the first half of 1995.

The modernization of the KOVSH facility for measuring the life-time of the neutron by the method of UCN storage was completed in collaboration with PINP (Gatchina). The new UCN trap with movable sides and a new cryogenic system were constructed, and the system for oxygen spraying was modernized. Measurements will begin at the UCN source of ILL (Grenoble) in the first half of 1995.

The new, more perfect cryostat for experiments studying the dependence of fission fragment emissions following the interaction of neutrons with aligned nuclei was installed on beam 5 of the IBR-30 booster. Its in-beam adjustment is in process now. The temperature of the sample surface in the beam is estimated to be ~ 0.15 K. First experiments with the new cryostat will be carried out at the beginning of 1995.

The ISOMER instrument for measuring delayed neutron yields and, additionally, for measuring prompt neutrons of isomeric fission had underwent radical improvements on beam 11 of the IBR-2 reactor (fig.8). The facility tests with ^{235}U and ^{233}U nuclei were conducted.
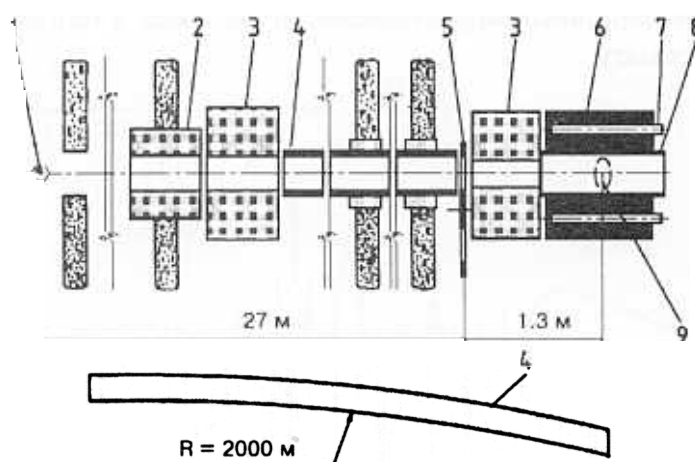
Fig. 8. Schematic of the IZOMER setup: 1 - reactor core, 2,3 - collimators, 4 - mirror neutron guide, 5 - chopper, 6 - moderator, 7 - neutron counters, 8 - Cd cylinder, 9 - sample.

Experiments to measure fission spectra of neptunium and coincidences with prompt fission gamma-quanta over the resonance neutron energy range from 3 to 500 eV were carried out with the new ionization fission chamber containing 1.5 g of high purity ^{237}Np (the portion of uranium and plutonium nuclei is ~10^{-6}). The measurements were carried out with the aim of studying gamma-quanta yield fluctuations in separate resonances. The data processing has been started.

The detector system of the ROMASHKA spectrometer was modernized. The HPGe detector was switched on in coincidence with the NaI scintillation detector and, as a result, the
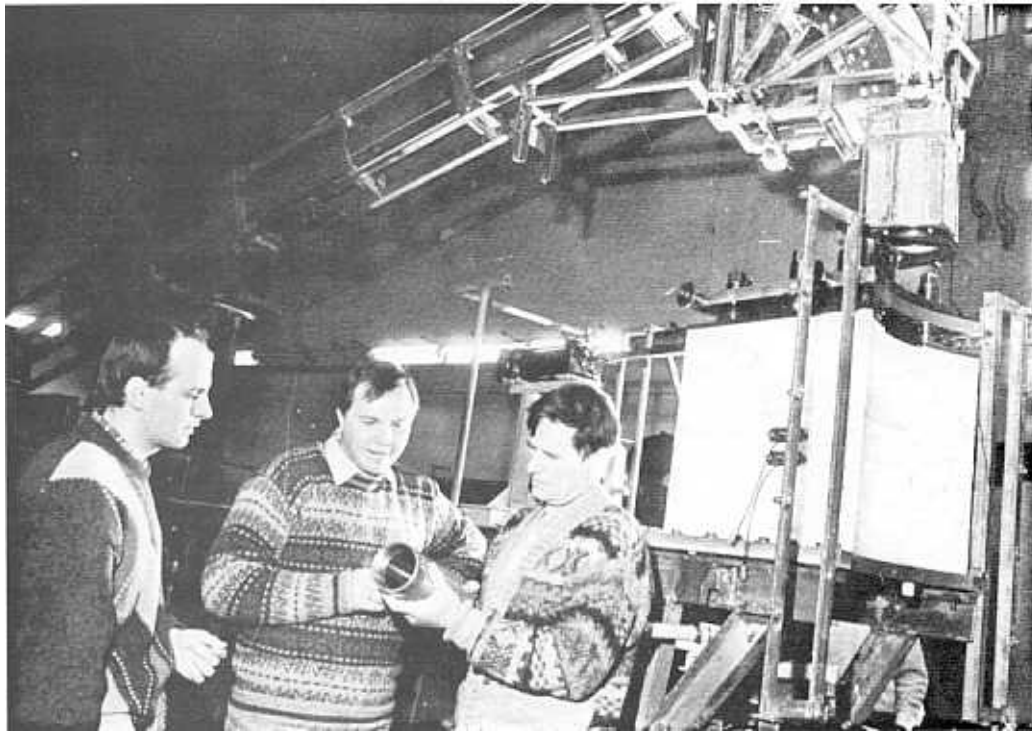
Assembling a pneumatic drive for the transport system of the ISPIN facility - UCN neutron source at the BIGR reactor (Arzamas-16).
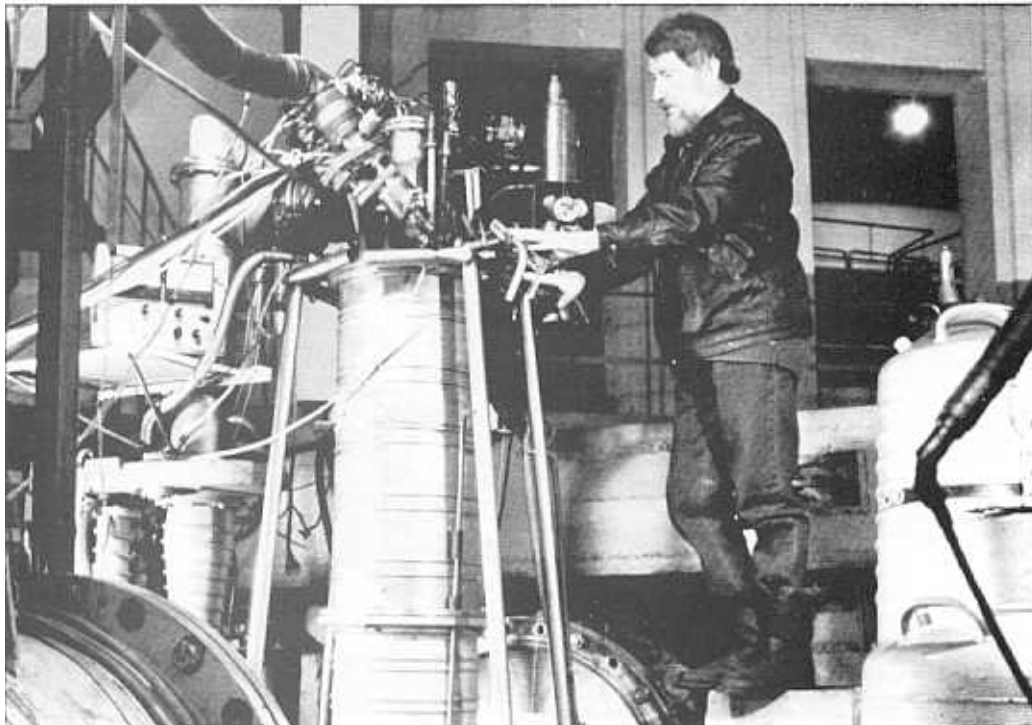
A.B.Popov is preparing a cryostat for the ^{235}U aligned nuclei target to perform measurements on beam 5 at the IBR-30 booster.

The POLYANA set-up on beam 4 of the IBR-30 booster.
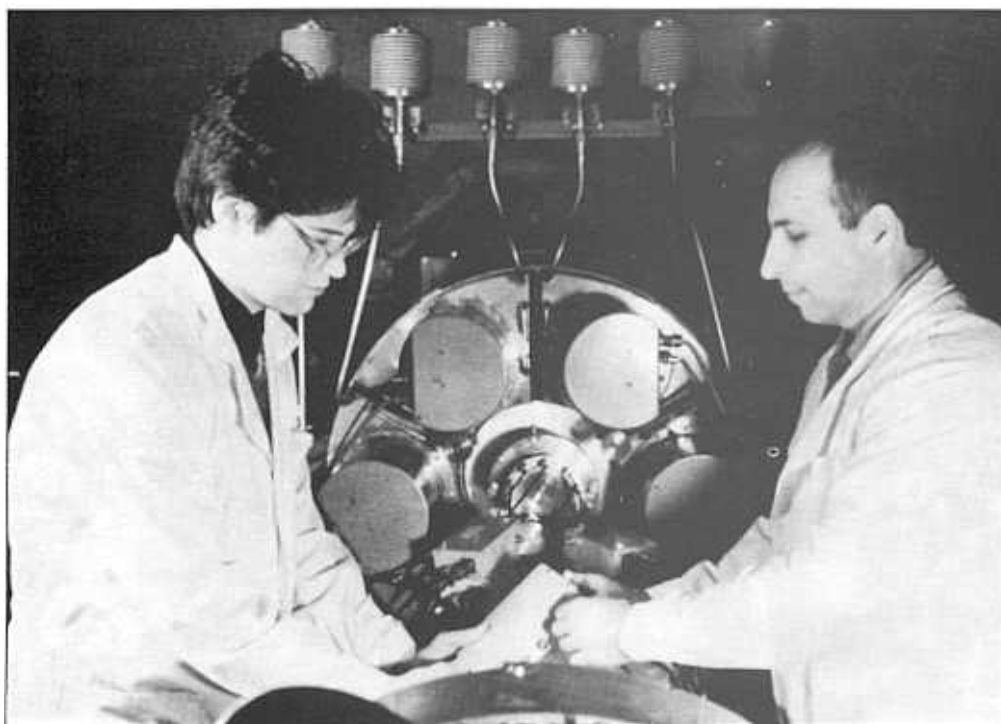
I.Ruskov and V.Konovalov, members of the nuclear fission group, are tuning equipment for carrying out measurements with a neptunium target.

parameters of the facility were essentially improved. Work to create a high pressure spectrometer for the registration of gamma-quanta from fission fragments was carried out on the basis of the HPGe spectrometer with BGO anti-Compton shielding.

Work on modeling a unique experiment for direct measurements of neutron-neutron scattering at the BIGR pulsed reactor was conducted with participation of specialists from LCTA, Dubna and VNIIEF, Arzamas-16.

In addition, much work has been done to improve experimental techniques and to create a new generation of measuring electronics. This work was orientated to conducting experiments at the new source of resonance neutrons, IREN, which is currently under construction. The characteristics of this source (an order of magnitude shorter pulse duration at a two times larger mean neutron flux) would permit carrying out experiments on shorter flight paths and permit a considerable increase in the electron tract loads in a majority of experiments.

1.2.3. THEORY

Cluster radioactivity. New possibilities of discovering the spontaneous cluster radioactivity of unstable heavy nuclei with consideration for the conditions of obtaining them in amounts necessary for measurements, were investigated. In 1994, the theoretical prediction of a new island of cluster radioactivity in the region of $A \cong 140$ was confirmed in the measurements by a German-Italian group in Darmstadt. The recent data are in good agreement with the corresponding investigations performed by LNR, JINR following the proposal made by FLNP theoreticians in 1993.

Fission. A new theory of nuclear fission induced by resonance neutrons was developed. The new and sufficiently natural interpretation of A.Bohr fission channels follows from this theory. The description on the same basis of both P-even and P-odd angular correlations of fission fragments has been gained. Part of the predicted new effects found confirmation in the works performed at FLNP.

π-meson gas. Investigations continued of the behavior of π-meson gas at high temperatures and densities which arise following collisions of high energy heavy ions. The pion spectrum, density, thermodynamical potential, entropy and other characteristics were calculated. The obtained results permitted, in particular, the temperature characteristic of the cyral condensate to be obtained.

UCN. It has been shown that a discrete energy spectrum in an UCN beam can arise not only at fast chopping of the beam (the quantum chopper) but also as a result of UCN diffraction on a fast moving grating. It was found that a quantum modulator can be used not only for coherent splitting of the initial monochromatic beam into a series of waves with different energies and wave numbers (quasienergies), but also for the inverse process. The use of a combination of quantum modulators permits the creation of a new type of device which is called the time interferometer. The theory of such a device was developed and a brief analysis of the possibilities of using it in fundamental investigations was made.

Work continued on the theoretical investigation of the dynamic reflection of neutrons, i.e., of the reflection of neutrons from an oscillating potential.

Attempts were made to explain the anomaly of ultracold neutrons by fundamental reasons. An assumption was made that the neutron can be described by a non-spreading wave packet and a reduction of the wave function takes place both in coordinate and momentum space. It has been also noticed that a particle and its wave function are a non-local object whose

coordinates and momentum demand exact mathematical determination and can be determined unambiguously and simultaneously without coming in contradiction with the uncertainty principle, which appears to have no relation to quantum mechanics. In the frame of the canonical approach, one fails to describe anomalous losses. In the frame of the de Broil representations, a singular wave packet can be ascribed to the neutron. In this case the anomaly can be explained by over-barrier leakage. As a result, the packet width is determined, the future of the neutron is predicted and the possibility of an experimental verification of this prediction is hoped for.

The use of the recurrent method developed in FLNP to solve the problem of the scattering of neutrons and X-rays on surface layers shows that contributions to the scattering intensity from the investigated layer and substrate can be divided analytically by introducing a narrow imaginary gap between them.

1.3 APPLIED RESEARCH

In the reported year, in addition to traditional FLNP nuclear methods, such as neutron activation analysis, scattering of charged particles, etc., the method of neutron diffraction and the depolarization of polarized neutron beams upon their transmission through the investigated sample were used to solve applied problems.

Neutron-activation analysis. The program for investigating the ecological situation in the Tver Region, in the region near Dubna, and in the Kola Peninsula (in regions close to the nickel smelting plant) and in some regions of Norway by using moss and pine needles as biomonitors was started in 1993 and continued in 1994. In ecological investigations in Franz Josef Land, indigenous lichens, samples of fresh snow, firn, melt water, and water from three lakes were used.

To activate these natural monitors, the irradiation channels of the IBR-2 reactor with cadmium and gadolinium screens were used. The possibility of reliable identification of several dozens of elements, including rare-earth elements (REE) was demonstrated. For example, 45 elements, including 10 REE were identified in the DK-1 moss. Important results were obtained which would allow us to follow changes in the ecological situation in the investigated areas and give recommendations on regulating the industrial activity.

The NAA method was used for nuclear, physical and chemical monitoring of water ecosystems. The investigations were carried out in the Oka River basin together with the Institute of the Lithosphere of the Earth, RAS. The results indicated the existence of geochemical and biochemical anomalies in the investigated region.

To determine the element composition and quantitative content of microadmixtures, an analysis of a number of samples of super-pure aluminum produced by the Voronezh plant was carried out. To solve the question of the degree of Al purification by zone melting, samples made from processed and raw aluminum were analyzed. It was established that pollution by aluminum is mainly caused by raw aluminum, because the element compositions of super-pure and raw aluminum are the same and differ in concentrations only.

Development continued of methods for dyeing topazes from different natural deposits in the mixed neutron and gamma-fields of the IBR-2 irradiation channels. Results were obtained in forming dyeing centers of different shades of blue.

Radiation investigations. In the frame of the ATLAS project (CERN) investigations continued of the radiation resistivity of S-detectors using the fast neutron beams at the IBR-2

reactor (together with LSHE). The results are used in developing equipment for high energy physics.

In the reported year, the previous year's experiment to check the radiation resistivity of AsGa electronics in fast neutron fields was repeated. The difference was in the fact that the repeated experiment was carried out at nitrogen temperatures with the IBR-30 booster, and the first was conducted at room temperature with the IBR-2. The results of both experiments coincided. The experiments were performed together with LSHE.

Neutron diffraction. The high resolution achieved at the HRFD Fourier diffractometer permitted the start of the program for determining internal mechanical stresses in materials, by the nondestructive testing method of neutron diffraction, in collaboration with the Saarbrucken Institute for Nondestructive Testing.

A series of experiments was performed to measure residual stresses in cold-rolled steel disks (500 mm in diameter and 2.5 mm thick) used in forming bottoms for high pressure gas tanks. The results were compared with the data obtained by magnetic and acoustic methods. It was concluded that the neutron diffraction method could provide good calibration for other, more express methods. Recommendations on the technology of preparing the disks for the forming process were given to the Manufacturer.

Polarized neutrons. In the reported year, the depolarization method was applied to perform nondestructive testing of industrial products for the first time. Fragments of the Ni-coating from the walls of an internal combustion engine cylinder, whose earlier investigation by acoustic methods pointed to the presence of inhomogeneities, were examined. The coating scan by a neutron beam measuring 2x4 mm² confirmed the presence of inhomogeneities (fig.9), and the analysis of the depolarization function led to the conclusion that these inhomogeneities were related to the character of internal stresses in the Ni layer.
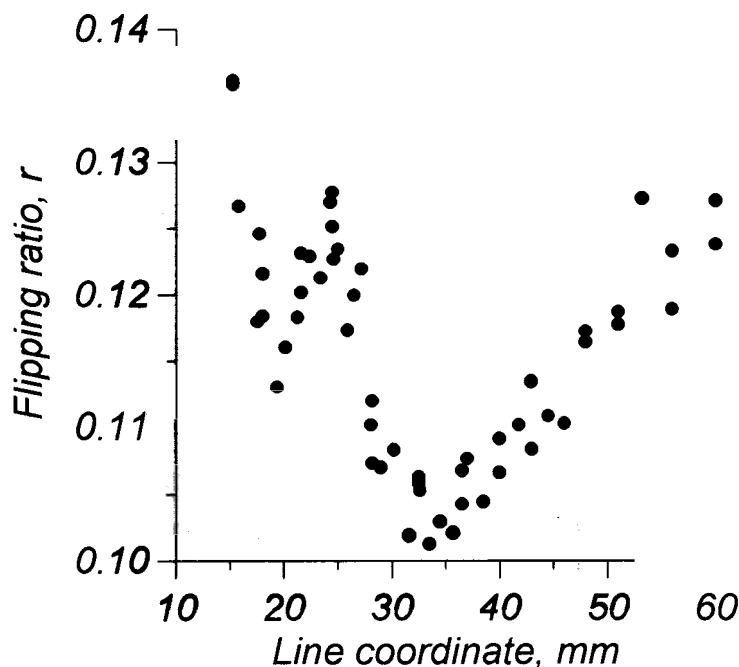

Fig.9. The effect of depolarization of a polarized neutron beam measured on the SPN-1 spectrometer. The beam scanned along one of the lines on the surface of the sample of Ni-coating from the walls of the combustion engine cylinder.

31

Charged particles. Investigations were carried out at the EG-5 electrostatic generator. FLNP, in cooperation with the Electrical and Technical Institute of the Slovak Academy of Sciences, continued investigations by RBS, PIXE, ERD and channeling methods of HTSC films on different substrates, as well as of films with buffer layers, with the aim of elaborating a technology for building buffer layers to enable conjunction of incompatible crystal structures of the film and substrate.

A method of energy analysis following the scattering of helium ions had appeared to be extremely productive in investigating multi-layered structures. The information about the thickness and composition of each layer could be obtained without destroying the investigated sample. Investigations of metallized coatings with enhanced adhesive properties deposited on glasses and ceramics by the IBAD method were conducted.

2.1. CONDENSED MATTER PHYSICS

CONTENTS

Low Resolution Model of Ribosomes and Their Subparticles. Structural Model of the 50S Subunit of *E.Coli* Ribosomes from Solution Scattering
D.I.Svergun, M.H.Koch, I.Skou Pedersen, I.N.Serdyuk

Inelastic Scattering
Neutron Scattering Studies of Pressure Induced Phase Transitions in NH_4HSO_4
L.Bobrowicz, I.Natkaniec, T.Sarga, S.I.Bragin

Investigations of the Liquid Helium-4 Excitations Spectrum Structure
I.V.Bogoyavlenskii, L.V.Karnatsevih, Zh.A.Kozlov, A.V.Puchkov

Neutron Scattering Studies of Orientational Disorder in Camphor-Like Plastic Crystals in the Temperature Range of 10-300 K
K.Holderna-Natkaniec, I.Natkaniec

The Temperature Dependence of the Phonon Density of States of Superconducting La_2CuO_4.
E.A.Goremychkin, I.L.Sashin, G.F.Syrykh, V.P.Glazkov

The Crystal Field Effects in the $YbCu_2Si_2$ Compound
E.A.Goremychkin, A.Yu.Muzychka

The Spectrum of the Inelastic Neutron Scattering from the Polymethylsilicate Acid Xerogel
V.D.Khavryuchenko, A.V.Khavryuchenko, A.Yu.Muzychka

Polarized Neutrons
Anomalous Dependence of Neutron Depolarization on Magnetic Field in $YBa_2Cu_3O_{6.9}$ Ceramics near T_c
V.L.Aksenov, E.B.Dokukin, V.K.Ignatovich, S.V.Kozhevnikov, E.I.Kornilov, Yu.V.Nikitenko, A.V.Petrenko, Yu.V.Bugoslavskij, A.A.Minakov

Time-of-Flight Neutron Depolarization for Nondestructive Testing
L.P.Chernenko, D.A.Korneev, J.Schreiber

Ground State Moment Reduction in an Ultra-Thin W(110)/Fe(110)/W(110) Film
V.Pasyuk, O.F.K.Mc Grath, H.J.Lauter, A.Petrenko, A.Lienard, D.Givord

Neutron diffraction study of the high-T_c superconductor HgBa$_2$CaCu$_2$O$_{6.3}$ under high pressure

V.L.Aksenov, A.M.Balagurov, B.N.Savenko, FLNP, JINR, Dubna, Russia
V.P.Glazkov, I.N.Goncharenko, V.A.Somenkov, RNC KI, Moscow, Russia
E.V.Antipov, S.N.Putilin, MSU, Moscow, Russia
J.-J.Capponi, Lab. of Crystallography, CNRS, Grenoble, France

In the recently discovered series of HgBa$_2$Ca$_{n-1}$Cu$_n$O$_{2n+2+x}$ compounds[1,2,3], as well as in other layered copper oxide high-temperature superconductors, a significant increase in the superconducting transition temperature is observed when high external pressure is applied[4,5]. For example, in the compound with n=3 (Hg-1223), T_c increases from 134 K at normal pressure to 150 K at P=11 Gpa[6]. High-pressure neutron diffraction experiments have previously been performed on mercury-based superconductors in[7], where all three representatives of the series were investigated: for compounds with n=1, 2, and 3, an experiment was performed under pressures up to 0.6 GPa; for the compound with n=3, additional measurements were carried out for P=4.0 and 9.2 GPa. One of the problems which has emerged in[7] in the diffraction data analysis was the presence of an appreciable quantity of impurities, such as BaCuO$_{2+x}$, CaO and Ba$_2$Cu$_3$O$_{5+x}$, in the samples of compounds with n=2 and 3. In principle, their influence could have biased the structural analysis results. It is this factor that the authors of[7] emphasize to explain unusual behavior of the interatomic distances in Hg-1223. Thus, more experiments are needed to confirm this data.

Our experiments were performed on the HgBa$_2$CaCu$_2$O$_{6+x}$ compound, the synthesis and properties of which are given in[8], with the DN-2 and DN-12 time-of-flight diffractometers. The experiment at the DN-2 diffractometer was performed in order to determine the degree of phase homogeneity of the sample (the available amount of sample was about 0.2 g) and to refine its oxygen content. Fig. 1 shows the measured diffraction spectrum after Rietveld refinement. It was found that two phases were present in the sample: Hg-1212 and traces of metallic Au. Evidently, the later fell into sample during extraction from the container. The DN-12 diffractometer is specifically intended for work with high-pressure cells based on sapphire anvils. The measurements at DN-12 were performed on a sample with a mass of about 1 mg under pressures of P=0, 3.0 and 3.6 GPa; the measurement time for each pressure value was about 50 hours. The diffraction spectra were processed by the Rietveld method with the help of the MRIA software.
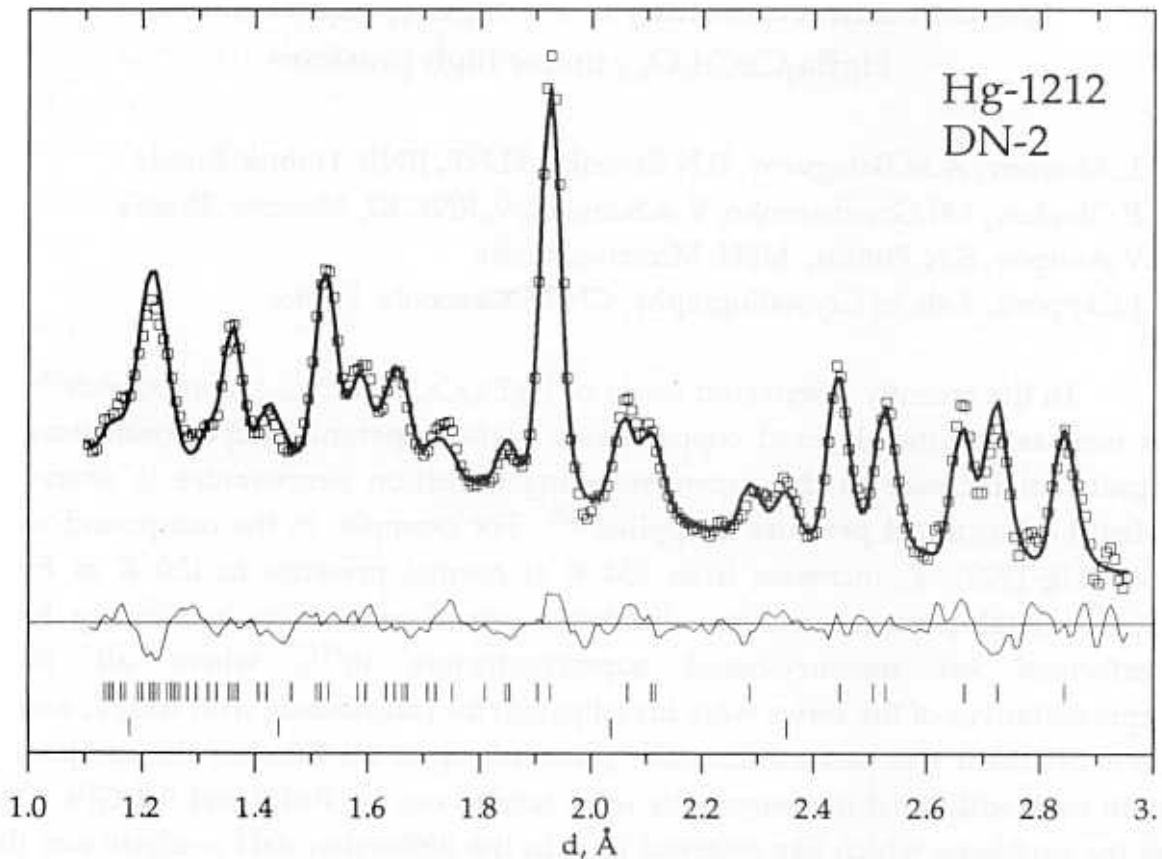
Fig.1. *Diffraction spectrum from HgBa₂CaCu₂O₆₊ₓ measured with the DN-2 diffractometer. Experimental points, calculated profile, and difference curve (experiment - calculations) are shown. The positions of the Bragg peaks for the main phase and metallic Au are also indicated.*

Data processing was performed in several stages. The spectrum measured at DN-2 was processed for the interval of $1.1 < d_{hkl} < 3.0$ Å which contained about 50 peaks from the tetragonal phase, space group P4/mmm. The data from[8] were used as the initial parameter values. The relatively low quality of the diffraction spectra (bad effect-to-background ratio and restricted possibilities of analyzing data in the region of small d_{hkl}) prevented the thermal atom parameters from being reliably evaluated. Therefore, we chose to fix them: B=0.5 Å² for Ba, Cu, and Ca; B=1.0 Å² for all oxygen atoms. Varying these parameters within the limits of 50% only slightly influenced the structural parameters of the atoms. While processing the spectra measured at DN-12, the thermal parameters, and the O3 oxygen content, n(O3)=0.3, were fixed. In addition, the lattice parameters at P=0, a=3.850 Å and c=12.629 Å, as determined by processing the data obtained at DN-2, were fixed as well. From the comparing measured and calculated profiles it follows that the spectrum fitting was quite good at zero pressure, but at higher pressures the fitting quality is definitely worse. Another conspicuous factor was the sharp shortening of the Hg-O2 bond length with the increase in pressure. That is why

we undertook several attempts in order to change the initial model of the structure. The best result was obtained for the model with disordered O2 oxygen. Realistic values for the bond lengths were obtained on the assumption that O2 is disordered along the diagonals in the (a,b) plane, i.e., its position is described by the (x,x,z) coordinates. The most easily evaluated and reliable results of our measurements are the dependencies of the Hg-1212 lattice parameters on pressure. They are shown in Fig.2 as normalized to P=0 together with the data from[7] obtained at the SEPD diffractometer. For our data, values are shown for the models with ordered and disordered O2. Lines, obtained with the help of the least square method, are drawn only for the second model. The least square line is also drawn for parameter a according to the SEPD data. For parameter c, this line is indistinguishable from ours. The compressibility values, determined as $\kappa_q = -(1/q)\delta q/\delta P$ $(10^{-3}/\text{GPa})$, where q is the parameter, calculated for the crystallographic axes and for the unit cell volume are given in Table 1. The compressibility values for the distances are also given in Table 1. For comparison, the data from[7] on Hg-1212 and Hg-1223 are presented in that table.

Table 1.

Compressibilities of the lattice constants and selected bonds of Hg-1212, measured with DN-12 (up to 3 GPa) and SEPD (up to 0.6 GPa), and Hg-1223, measured with HIPD (up to 9.2 Gpa).

Compressibilities	$1212_{\text{DN-12}}$	1212_{SEPD}	1223_{HIPD}
κ_a	3.48	2.94	2.28
κ_c	6.15	6.04	4.7
κ_v	13.0	11.9	9.1
$\kappa_{\text{Cu-O2}}$	7.9	14	2
$\kappa_{\text{Hg-O2}}$	19	0	14
$\kappa_{\text{Ba-O2}}$	25	50	10

Our results for the compressibility values of the Cu-O2 and Hg-O2 interatomic distances noticeably differ from the data in[7]: $\kappa_{\text{Cu-O2}}$ is two times smaller, $\kappa_{\text{Hg-O2}}$ is large. For Hg-O2 bound our result, in fact, correspond better to the result for Hg-1223. In[7], the data for Hg-1223 are regarded as unexpected and the assumption was made that the diffraction spectrum analysis results were distorted by the impurity phases in the sample. One can admit that a similar systematic error is present in our work, but it should be noted that these results were obtained on different samples and diffractometers. Another possible explanation could be in a change in the character of the dependence of these interatomic distances in Hg-1212 under pressures higher than 1 GPa. It is also

possible that the presence of O3 oxygen in any quantity noticeably affects the specific values of compressibility.

The greatest absolute values of compressibility were obtained for the distances between the Ba-O2 and Ba-Hg atom layers. Despite a relatively broad spread in specific values, the general tendency is beyond doubt. It was noted recently that the magnitude of the Coulomb splitting of the cation - anion layers is very sensitive to changes both in the compound content and in external conditions, when the ambience charge is asymmetrical (Ba and O2 layers in our case). The results of our experiment and the data in$^{/7/}$ confirm this conclusion. Defining more exactly the cause of the large compressibility values for these distances, one may say that they are due, to a great extent, to the motion of Ba atoms towards the Hg atom plane.

Fig.2. *Dependences of the Hg-1212 lattice parameters on pressure, normalized to the values at P=0. Points obtained on DN-12 and SEPD are shown. Lines are drawn by the least square method. The lines drawn for c through both sets of data are indistinguishable.*

References

1. S.N.Putilin, E.A.Antipov, O.Chmaissem and M.Marezio, Nature (London) 362 (1993) 226.
2. A.Schilling, M.Cantoni, J.D.Guo and H.R.Ott, Nature (London) 363 (1993) 56.
3. S.N.Putilin, E.A.Antipov and M.Marezio, Physica C 212 (1993) 266.
4. C.W.Chu, L.Gao, F.Chen, Z.J.Huang, R.L.Meng, and Y.Y. Xue, Nature (London), 365 (1993) 323.
5. M.Nunez-Regueiro, J.-L.Tholence, E.V.Antipov, J.-J. Capponi, and M.Marezio, Science, 262 (1993) 97.
6. H.Takahashi, A.Tokiwa-Yamamoto, N.Mori, S.Adachi, H.Yamauchi and S.Tanaka, Physica C 218 (1993) 1.
7. B.A.Hunter, J.D.Jorgensen, J.L.Wagner, P.G.Radaelli, D.G.Hinks, H.Shaked and R.L.Hitterman, Physica C 221 (1994) 1.
8. E.A.Antipov, J.-J.Capponi, C.Chaillout, O.Chmaissem, S.M.Loireiro, M.Marezio, S.N.Putilin, A.Santoro and J.L.Tholence, Physica C 218 (1993) 348.
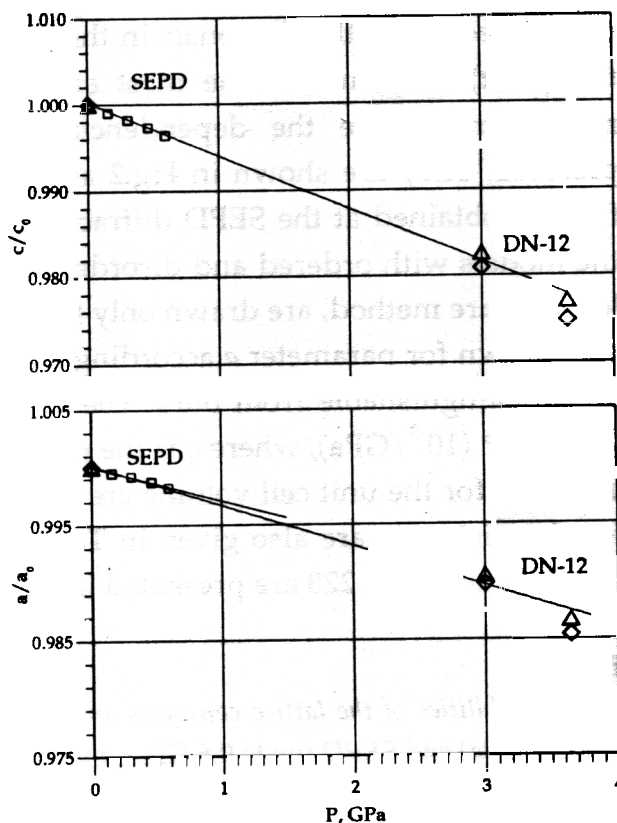
ESTIMATION OF RESIDUAL STRESS IN COLD ROLLED IRON-DISKS FROM STRAIN MEASUREMENTS ON THE HIGH RESOLUTION FOURIER DIFFRACTOMETER

V.L.Aksenov, A.M.Balagurov, G.D.Bokuchava*, J.Schreiber**, Yu.V.Taran

Frank Laboratory of Neutron Physics, JINR, Dubna, Russia
* Institute for Nuclear Research of RAS, Moscow, Russia
** Fraunhofer Institute for Nondestructive Testing, Dresden, Germany

INTRODUCTION

Forming process outcomes can be influenced by residual stress states in the formed material. For example, cold rolled steel disks used for forming small, gas pressure tanks can have inadmissible folds on their borders after the first forming step. Residual stresses might appear in the disks due to several reasons, one being the means of cutting the disk from rolled sheet metal. To have an effective forming process it is important to be able to check residual stress states, as well as the initial material texture by a quick and easy testing method. For this purpose, magnetic [1] and ultrasonic [2] nondestructive testing methods have been developed and utilised. These techniques have certain disadvantages, however. Magneto-elastic measurements do not permit direct testing of residual stresses and provide information on stress states in the near surface region only. The ultrasonic technique gives stress values averaged over the scanned path and the sound-wave beam cross-section. In both cases the rolled texture complicates the determination of stress states in sheet metal. Calibration of these techniques is therefore necessary for a reliable assessment of rolled plates used in forming processes. This calibration can be performed by neutron diffraction, a unique non-destructive reference method [3].

This paper presents and discusses the results of estimating residual stresses in cold rolled iron disks by measurements with the high resolution Fourier diffractometer (HRFD) at the IBR-2 pulsed reactor in Dubna [4]. A ^6Li - glass scintillation detector is installed at the scattering angle $2\theta=+152°$ on the HRFD. The neutron intensity on the sample is 10^7 $n/cm^2/s$ and the resolution achieved by the diffractometer is $\Delta d/d=10^{-3}$. This allows the measurement of strain in bulk metallic specimens with sufficiently high precision and within a reasonable measuring time.

To verify expectations for the possibility of strain measurements in steel components with HRFD, a relatively simple program has been started using the back scattering geometry of this spectrometer. Prospects of HRFD development will be discussed in the concluding section of this paper.

EXPERIMENTS

The tested objects were cold rolled steel disks of 2.5 mm thickness and diameter of about 500 mm (steel - C(0.127 %), Si(0.100 %), Mn(0.760 %), P(0.011 %), S(0.008 %), and AlS(0.043 %). The bulk elastic constants were: $E \cong 180$ kN/mm^2, and $\mu \cong 0.3$. The yield point $R_{p0.2}$ of this material was 276 MPa and the tensile strength R_m was 434 MPa. A first indication of the presence of residual stress states in the considered disk is disk unevenness (Fig. 1). The magnetic and ultrasonic measurements carried out at the Fraunhofer-Institute for Nondestructive Testing in Saarbrücken indicated characteristic changes in stress states across the disk. The magnetic testing method had a lateral resolution of about 20×20 mm^2, which was determined by the geometry of the magnetic sensors. The gauge volume for the neutron diffraction measurements was chosen accordingly. With the help of a boron nitride (BN) mask, the cross-section of the neutron beam was reduced to 2×20 mm^2 (Fig. 2).

To determine the strain tensor, ε, from neutron diffraction spectra, the scattering vector, Q, has to be oriented in different directions. Because stresses are averaged over the interior of the scattering volume, the internal stress components belonging to the normal direction to the disk plane should vanish. As a result, the determination of the main components of the local strain and stress states is reduced to a quasi two-dimensional problem. Extensive investigations were not possible due to the limited measuring time and, therefore, only four directions of the scattering vector Q were chosen: the radial direction ($\varphi'=0°$) of the disk, the tangential component ($\varphi'=90°$), and the $\varphi'=\pm45°$ directions in the (x',y') local coordinate system built by the radial and tangential components. At several points the normal component of the strain perpendicular to the disk-plane was also measured.

A survey of the changes in the internal strain and residual stresses was obtained for eight observation points on a track lying around the disk at a distance of ~55 mm from the border of the disk.
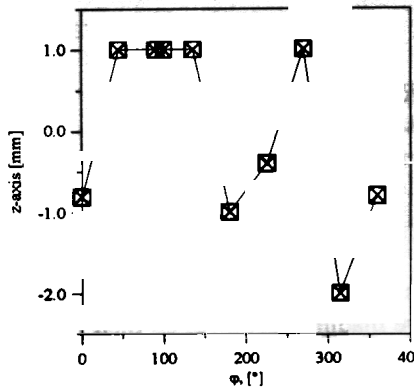
Fig. 1. Disk unevenness: off-plane deviations were measured at different angles φ around the disk at 50 mm from the disk border, the z-axis is perpendicular to the disk plane.
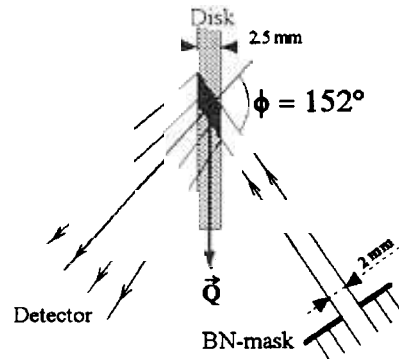
Fig. 2. The back scattering geometry for strain measurements in a cold rolled disk, Q - the scattering vector, ϕ - the scattering angle.

The lattice spacing in an unstrained state, d_0^{hkl}, was derived from the reverse time-of-flight (RTOF) spectrum for an annealed powder sample made from the disk material. The lattice strain is determined as a relative shift of the Bragg reflexes $\Delta^{hkl} = (d^{hkl} - d_0^{hkl})/d_0^{hkl}$, where d_0^{hkl} is the measured lattice spacing.

RESULTS

By analysing the positions of available Bragg reflexes the corresponding crystallite lattice plane spacing, d^{hkl}, was determined by the centre of gravity method, which takes into consideration the upper 50 % of the peak heights. The results are presented in Figs. 3-4.

A striking feature of all $\Delta^{hkl}(\varphi)$ is their correlation with disk unevenness. The obtained strain variations for different angles, φ, as well as for different local orientations (angle φ') of the scattering vector are rather strong. In addition, $\Delta^{hkl}(\varphi)$ shows a pronounced anisotropic effect.
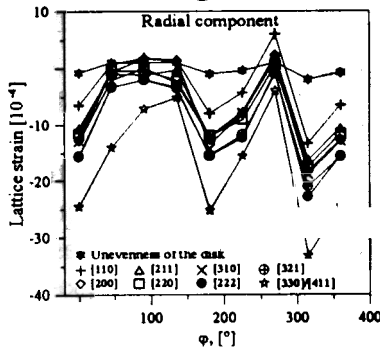
Fig. 3. The lattice strain, $\Delta^{hkl}(\varphi)$, for the scattering vector, Q, along the radial vector of the disk.
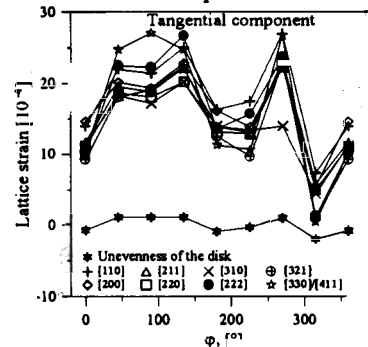
Fig. 4. The lattice strain, $\Delta^{hkl}(\varphi)$, for the scattering vector, Q, along the tangential vector of the disk.

In Fig. 5 the internal strain as a function of the anisotropy factor is presented. The irregular behaviour of $\Delta^{hkl}(\Gamma,\varphi)$, points to a strong influence of plastic anisotropy and large stresses due to grain interaction (microstresses - see [5], [6]), a linear dependence would have been caused by elastic anisotropy. Microstrains, which are related to the line widths of Bragg reflexes, do not show any significant dependence on the angle φ or on Γ. Only stochastic fluctuations seem to be present.

DISCUSSION

Actually, these results do not permit a quantitative analysis of stress [5]. Further investigations, i.e., measurements of the $\sin^2\psi$-dependence of $\Delta^{hkl}(\psi,\varphi)$ are necessary. To acquire experience
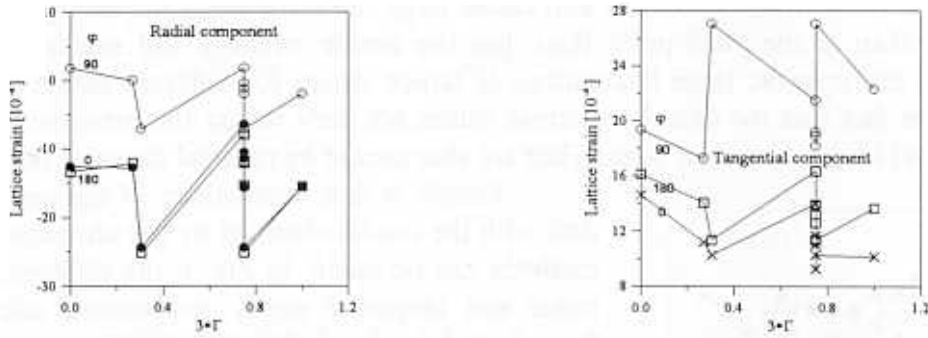
Fig.5. The dependence of the radial and tangential components of the internal strain on the anisotropy factor $\Gamma=(h^2l^2+h^2k^2+k^2l^2)/(h^2+k^2+l^2)^2$.

in analysing the measured strain data, the following evaluation procedure was performed. The least squares method was used to calculate components of the strain tensor: $\varepsilon^{hkl}=(\varepsilon^{hkl}(x', x'), \varepsilon^{hkl}(y', y'), \varepsilon^{hkl}(x', y'))^T$ where T means the transposed form. For this purpose, the measured $\Delta_i^{hkl}(\varphi)$ are collected to form a 4-dimensional vector: $\Delta^{hkl}=(\Delta_1^{hkl}(\varphi), \Delta_2^{hkl}(\varphi), \Delta_3^{hkl}(\varphi), \Delta_4^{hkl}(\varphi))^T$, where i denotes the different directions of Q in the (x',y') coordinate system: i=1 - $\varphi'=45°$, i=2 - $\varphi'=-45°$, i=3 - $\varphi'=0°$, i=4 - $\varphi'=90°$. Then, the strain tensor ε^{hkl} satisfies the equation: $\Delta^{hkl} = A*\varepsilon^{hkl}$. The line of the A matrix is defined as: $A_i=(m_i^2, n_i^2, n_i m_i)$, where $m_i=\cos(\varphi_i')$ and $n_i=\cos(90°-\varphi_i')$ are the direction cosines of Q. According to the least squares fit procedure, ε^{hkl} can be obtained by the formula:

$$\varepsilon^{hkl}=(A^T*A)^{-1}*A^T*\Delta^{hkl}.$$

The relative fitting error can be estimated by the following formula:

$$\delta\varepsilon_r^{hkl}=|(A*(A^T*A)^{-1}*A^T-I)*\Delta^{hkl}|/|\Delta^{hkl}|.$$

The principal strain, $\varepsilon^{D,hkl}$, and the principal strain axis can be determined by diagonalizing the strain tensor. Then, under the assumption of an elastic model, the components of the principal stress tensor are related as: $\sigma_{dd}^D=2 G^{hkl} \varepsilon_{dd}^{D,hkl} + \lambda^{hkl}\sum_{d=1}^{3} \varepsilon_{dd}^{D,hkl}$, where $G^{hkl}=E^{hkl}/2(1+\mu^{hkl})$ and $\lambda^{hkl}=\mu^{hkl}E^{hkl}/(1-2\mu^{hkl})(1+\mu^{hkl})$. The third component $\varepsilon_{33}^{D,hkl}$, which has not been considered so far, can be derived from the condition that $\sigma_{33}^D=0$. Unfortunately, the X-ray elastic constants are not known for the steel used to make disks. Because the investigated material is nearly isotropic in our case, the values of G^{hkl} and λ^{hkl} were estimated on the basis of those for bulk material which were determined by the manufacturer as G=70 GPa and λ=104 GPa.

Table 1 contains the results of a least squares fit for the [222]-reflex, i.e. the measured strain, Δ, the strain tensors ε, the principal strains ε^D, the relative error $\delta\varepsilon_r$ of the fit, and the principal stresses σ_{dd}^D along the principal strain axes rotated through the angle $\delta\varphi'$ in the local system (x',y'). The ε_{33}^D and $\varepsilon_{33}^{D,exp}$ quantities are the theoretical ($\sigma_{33}^D=0$) and measured normal strain components, respectively. The obtained results look quite reasonable, though the fitting errors are relatively large. The situation similar to that illustrated in Table 1 also takes place for other [hkl]-reflexes. It would be interesting to investigate whether the errors of the fit can be reduced by increasing the number of observation points. Repeat measurements with better statistics are planned.

Table 1

[222]-reflex of Fe	$\varphi=0°$	$\varphi=90°$	$\varphi=180°$
Δ [10^{-4}]	(-16.6, -13.4, -15.5, 10.1)	(-6.2, 8.0, -2.0, 22.3)	(-16.7, -3.2, -15.5, 13.6)
ε [10^{-4}]	(-21.6, 4.0, -1.6)	(-6.6, 17.7, -7.1)	(-20.0, 9.2, -6.8)
($\varepsilon_{11}^D, \varepsilon_{22}^D$) [$10^{-4}$]	(-21.8, 4.1)	(-8.5, 19.6)	(-21.5, 10.6)
$\delta\varepsilon_r$ [10^{-4}]	0.44	0.38	0.34
($\sigma_{11}^D, \sigma_{22}^D$) [MPa]	(-410, -48)	(-53, 340)	(-365, 84)
$\delta\varphi'$ [°]	-4	-15	-12
$\varepsilon_{33}^D/\varepsilon_{33}^{D,exp}$	7.5 / 2.3	-6.8 / -4.7	4.8 / not measured

43

The calculated stress values are also rather large. Stresses along the rolling direction are noticeably larger than at the yield point $R_{p0.2}$, but the tensile stress is still smaller than the tensile strength R_m. In our opinion, large fluctuations of lattice strains for different lattice planes nevertheless point to the fact that the calculated stress values not only reflect the existence of macroscopic residual stresses (1st kind residual stress), but are also caused by residual stress of the 2nd kind [6].
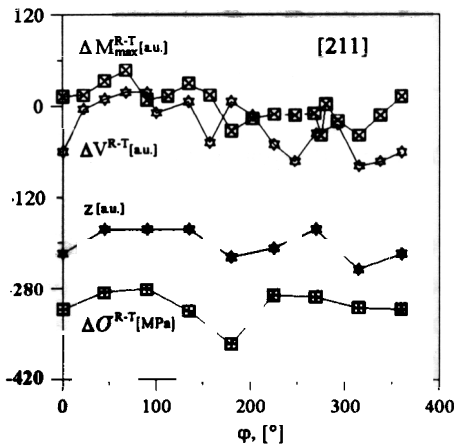
Finally, a first comparison of the neutron diffraction data with the results obtained by the ultrasonic and magnetic methods can be made. In Fig. 6 the difference between the radial and tangential stress components calculated by the formula $\Delta\sigma^{R-T}=\sigma^R-\sigma^T=2G(\Delta_R^{211}-\Delta_T^{211})$ is shown together with the corresponding change in the velocity of SH-waves Δv^{R-T} (the frequency is 800 kHz, the transmitter-to-receiver distance is 30 mm), and the Barkhausen noise amplitude, ΔM_{max}^{R-T}, measured in ac fields (50 Hz, 10 A/cm) over the frequency range of 10 - 30 kHz. The coercive field strength, H_{CM}, for the mentioned frequency region does not yield a significant φ-dependence, which is evidence of a weak texture influence in the considered disk.

Despite the fluctuations, a correlation of the estimated stress values with Δv^{R-T} and ΔM_{max}^{R-T} can be detected. Furthermore, angular dependencies of these quantities are connected in an obvious way with the disk unevenness, z. Hence, both residual stresses and disk unevenness influence the result of the forming process, i.e., folds should appear at the disk positions for which significant changes in these

Fig. 6. Comparison of the angular dependence of the residual stress, σ, determined from the [211]-reflex contained in the neutron diffraction data with the results on the ultrasonic velocity, v, of SH-waves and the Barkhausen noise amplitude, M_{max}. For all cases the difference between the radial and tangential components is drawn. The unevenness of the disk, z, is also shown.

quantities are observed. We do not know yet what the forming procedure will result in, but non-regular behaviour can be expected for the angles $\varphi = 180°$ and $270°$.

The existing deviations in the angular dependence of the three parameters $\Delta\sigma^{R-T}$, Δv^{R-T} and ΔM_{max}^{R-T}, could have several origins. First of all is inhomogenous microstructure. The averaging procedure over different measuring volumes might also be responsible for that. For instance, the inspection depth of the magnetic method is on the order of 0.3 - 0.5 mm only, and the magnetic results cannot be in correspondence with the bulk properties for any case.

1. Dobmann G., Höller P., Nondestructive Determination of Material Properties and Stresses, in: Proc. of the 10th Intern. Conf. on NDE in the Nuclear and Pressure Vessel Industries (Ohio: ASM International, 1990) p. 641.

2. Spies M., Schneider E., Nondestructive analysis of the deep-drawing behaviour of rolled sheets by ultrasonic techniques; in: Proc. of the 3rd Intern. Symp. on Nondestructive Characterisation of Materials, Eds. P. Höller, V. Hauk, G. Dobmann, C. Ruud, R. Green (Berlin: Springer-Verlag, 1989) p. 296.

3. Allen A.J., Calibration of portable NDE techniques for residual stress measurements (Dordrecht: Kluwer Academic Publishers and NATO Scientific Affairs Division, 1992) p. 559.

4. Aksenov V.L., Balagurov A.M., Simkin V.G., Taran Yu.V., Trounov V.A., Kudrjashev V.A., Bulkin A.P., Muratov V.G., Hiismaki P., Tiitta A., and Antson O., The new Fourier diffractometer at the IBR-2 reactor: Design and first results (Dubna: JINR Communication E13-92-456, 1992).

5. Hutchings M.T. and Krawitz A.D., Measurement of Residual and Applied Stress Using Neutron Diffraction (Dordrecht: Kluwer Academic Publishers and NATO Scientific Affairs Division, 1992).

6. Pintschovius L., Macrostresses, microstresses and stress tensors, ibid., p.115, and Grain interaction stresses, ibid., p. 189.

7. Popa N.C., Texture in Rietveld refinement, J. Appl. Cryst. 25 (1992) p. 611.

8. Balagurov A.M., Simkin V.G., and Taran Yu. V., Possible utilisation of high resolution Fourier diffractometer at the IBR-2 for strain measurements, in: Proc. of the 3rd Europ. Powder Diffraction Conf., Eds. R.Delhez, E.J.Mittemeijer (Trans Tech Publ., Switzeland, 1994) p.257.

EXPERIMENTAL STUDY OF THE VIBRATIONAL SPECTRUM AND STRUCTURE VARIATIONS IN NH₄Cl UNDER HIGH PRESSURE.

A.M.BALAGUROV and B.N.SAVENKO
FLNP, JINR,141980, Dubna, Russia

A.V.BORMAN, V.P.GLAZKOV, I.N.GONCHARENKO, V.A.SOMENKOV
and G.F.SYRYKH
RSC "Kurchatov Institute",123182, Moscow, Russia

Ammonium halides NH_4A, where A=Cl, Br or I, are rather simple, convenient and interesting objects for neutron scattering experiments. The strong influence of pressure on phase transitions in these systems has already been established by different methods, including neutron scattering. Under pressure the NaCl type cubic structure converts first into a CsCl type cubic structure with disordered and then with ordered ammonium ion arrangements, space group P43m, with the single parameter of a hydrogen atom centered at the threefold position.

Vibration frequencies of NH_4Cl have also been thoroughly studied. Together with intramolecular (175-400 meV range) and lattice vibrations (0-20 meV range), there is the libration mode (~42 meV) which is non-active in optical spectra and corresponds to the rotation of the NH_4^+ ion as a whole. It was established earlier that most part of the intramolecular frequencies decrease with pressure. As follows from the optical data a phase transition of unknown nature takes place for ammonium halides at high pressure, and the question arose about their stability if the density is high.

Recently, several studies of the atomic dynamics in these compounds by means of neutron inelastic scattering were performed under high pressure. For instance, NH_4Cl has been investigated/[1]/ at the IBR-2 pulsed reactor under pressures up to 10 kbar. The pressure of 25 kbar in the study of NH_4Br has been achieved/[2]/ at the pulsed source ISIS. Therefore, it is interesting to investigate the frequencies and structural parameters behavior of ammonium halides under pressure higher than before using sapphire anvils technique.

The neutron scattering experiments were performed at the IBR-2 pulsed reactor with the DN-12 diffractometer. The sample was placed between sapphire anvils, which were used to create the pressure. The sample volume was 2.5 mm³. A ring-shaped detector (16 independent ³He-counters) 800 mm in diameter was used to gather the scattered neutrons. The scattering angle was 90°; the diameter of the incident neutron beam was 2 mm.

For analysis of the neutron energy transfer, Be filters (a 120 mm thick Be layer, without cooling) were placed between the sample position and each counter. Inelastic scattering experiments were carried out under pressure of 0, 10, 16, 27 and 40 kbar at room temperature. Additionally, neutron diffraction patterns were measured at 0 and 25 kbar. Exposure time for the maximum pressure was ~50 hours for the inelastic and ~10 hours for the elastic scattering measurements. The background was measured with the high-pressure cell but without the sample.

The inelastic neutron scattering spectra were converted into generalized vibrational density of states G(E). After spectra processing the positions and widths of three low-frequency modes were obtained: libration, transverse optical and longitudinal acoustic. The values of the observed lattice and libration frequencies increase with increasing pressure, though with a different slope ($d\omega_{LA}/dP$ and $d\omega_{TO}/dP \approx 0.17$ meV/kbar; $d\omega_{Libr}/dP \approx 0.056$ meV/kbar).

To study the structure parameter variations with pressure the deuterated analog, ND_4Cl, was investigated. The neutron diffraction patterns of ND_4Cl at 0 and 25 kbar are shown in Figure 1. One can observe the sharp change in the set and intensity of the lines with pressure. After Rietveld refinement of the diffraction spectra at 0 and 25 kbar a definite result was obtained: position parameter u increases with pressure from 0.154 to 0.168 at 25 kbar while the unit cell volume decreases, with just the same slope as in[3]. The agreement of the calculated intensities to experimental ones may be considered as satisfactory, taking into account a low statistical precision. For zero pressure the u value agrees well with[4].

Contrary to the intramolecular vibrations, all the low-frequency vibrations obviously increase with pressure. The difference between the increasing rates of the lattice and libration frequencies indicates the possibility of frequency crossing. The point of intersection obtained by linear extrapolation is about 230 kbar. The increase of structural parameter u means that a reduction in the D-Cl bond length takes place with pressure (from 2.300 to 2.175 at 25 kbar) while the length of N-D bond remains nearly the same (1.038 Å at ambient pressure, 1.052 Å at 25 kbar). It is evident that as parameter u reaches the value of 0.25, either a collapse of molecular ND_4^+ ion or a change in its form or orientation towards the anion should be observed, because as $u=0.25$ the length of the N-D bond will be equal to the length of the D-Cl bond. The linear extrapolation of u to 0.25 gives a pressure value about 130 kbar for this transition. So, we may assume that the phase transition of unknown nature in ammonium halides is connected with the existence of a dynamics and structural critical point. It is also possible that the transition pressure is determined by the anion polarization ability and decreases with its growth (P =100 ±10 kbar for NH_4Cl, P =80 ±10 kbar for NH_4Br and P =54 ±4 kbar for NH_4I).

References

1. A.N.Ivanov, D.F.Litvin, Y.Mayer, I.Natkaniec and L.S.Smirnov, ITEP, Preprint 80-91, Moscow (1991).
2. M.A.Adams, European Workshop on Neutron Scattering at High Pressures, 19-21 March (1992) Abingdon, U.K.
3. G.K.Lewis, E.A.Perez-Albuerne and H.G.Drickamer, J. Chem. Phys., 45, 598 (1966).
4. H.A.Levy and W.Peterson, Phys. Rev., 86, 766 (1952).

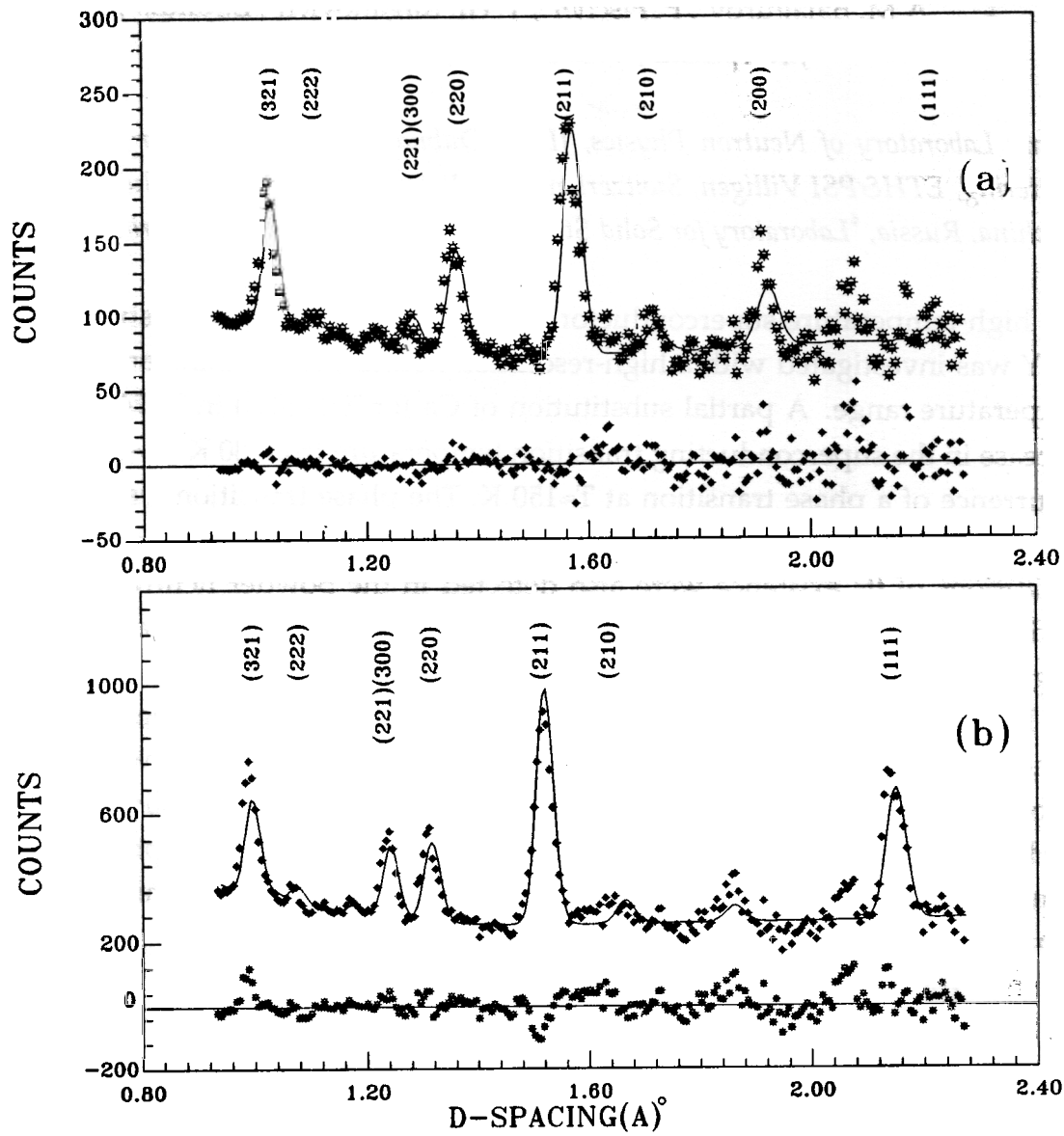**Figure 1** *Diffraction patterns of* ND_4Cl *at 0 (a) and 25 (b) kbar.*

Precision Neutron Diffraction Study of the High-Temperature Superconductor Y(^{44}Ca)Ba$_2$Cu$_4$O$_8$

A.M. Balagurov[1], P. Fischer[2], T.Yu. Kaganovich[3], E.Kaldis[4],
J.Karpinski[4], V.G. Simkin[1], V.A. Trounov[3]

[1]*Frank Laboratory of Neutron Physics, JINR, Dubna, Russia,* [2]*Laboratory for Neutron Scattering, ETH&PSI Villigen, Switzerland,* [3]*St. Petersburg Institute of Nuclear Physics, Gatchina, Russia,* [4]*Laboratory for Solid State Physics, ETH Zurich, Switzerland*

The high-temperature superconductor, YBa$_2$Cu$_4$O$_8$, with partial substitution of Ca for Y was investigated with a high-resolution neutron diffractometer over a wide temperature range. A partial substitution of Ca for Y (~10%) in Y124 leads to an increase in the superconducting transition temperature from 80 K to ~90 K and the occurrence of a phase transition at T$\approx$150 K. The phase transition was first found by means of elastic and specific heat measurements in a Ca doped compound[1]. Indications of its existence were also detected in the powder neutron diffraction study of Y(Ca)-124[2] and the X-ray structure analysis[3] of Y-124 and Y(Ca)-124 single crystals.

We have attempted to clear up the situation by carrying out an experiment on the same sample studied earlier in[2]. We performed our experiment with the high-resolution neutron Fourier diffractometer (HRFD) put into operation recently at the IBR-2 pulsed reactor in Dubna[4]. The resolution of HRFD is approximately 2.5 times better than that of the mini-SFINKS diffractometer in Gatchina where the results of Ref.[2] were obtained.

The neutron diffraction experiment was performed on powdered YBa$_2$Cu$_4$O$_8$ that had 10% of its Y replaced by ^{44}Ca. The coherent scattering length of the ^{44}Ca isotope (1.42 F) differs appreciably from that of Y and Ba (b$_Y$=7.75 F, b$_{Ba}$=5.07 F) thus facilitating the problem of identifying Ca atoms in the positions of Y or Ba. The X-ray phase analysis revealed the presence of small amounts of CuO and Y$_2$O$_3$ in the sample. The temperature of the superconducting phase transition was 87 K. The diffraction spectra were measured with good statistical accuracy at temperatures of 135, 165, and 293 K; structural analysis was then performed over these data. Additional measurements were performed at nine temperature points in the interval of 8 to 288 K. These data were used only for determining the temperature dependence of the lattice parameters. The spectra were measured with high resolution by the detector at a fixed mean scattering angle of 2θ=152° in the d-spacing range of 0.75 to 3.0 Å. The unit cell parameters were refined using the data from the interval of 1.35 Å $\leq d \leq$ 2.97 Å; Rietveld structural analysis was

performed on the interval from 0.73 Å $\leq d \leq$ 2.97 Å. Fig.1 shows portions of the spectrum with the experimental points, calculated profile, and the difference curve. The indication of the presence of a structural anomaly in the proximity of 150 K was obtained. It manifests itself by a change in the expansion coefficient along the b axis, irregular behavior of the orthorhombicity coefficient (Figs.2 and 3), and a noticeable change in bond lengths. The most distinct change is a contraction of the distance between the Cu2 copper atom and the apical O1 oxygen, as well as a change in the distance between the O2 and O3 atom chains in the CuO_2 layer.
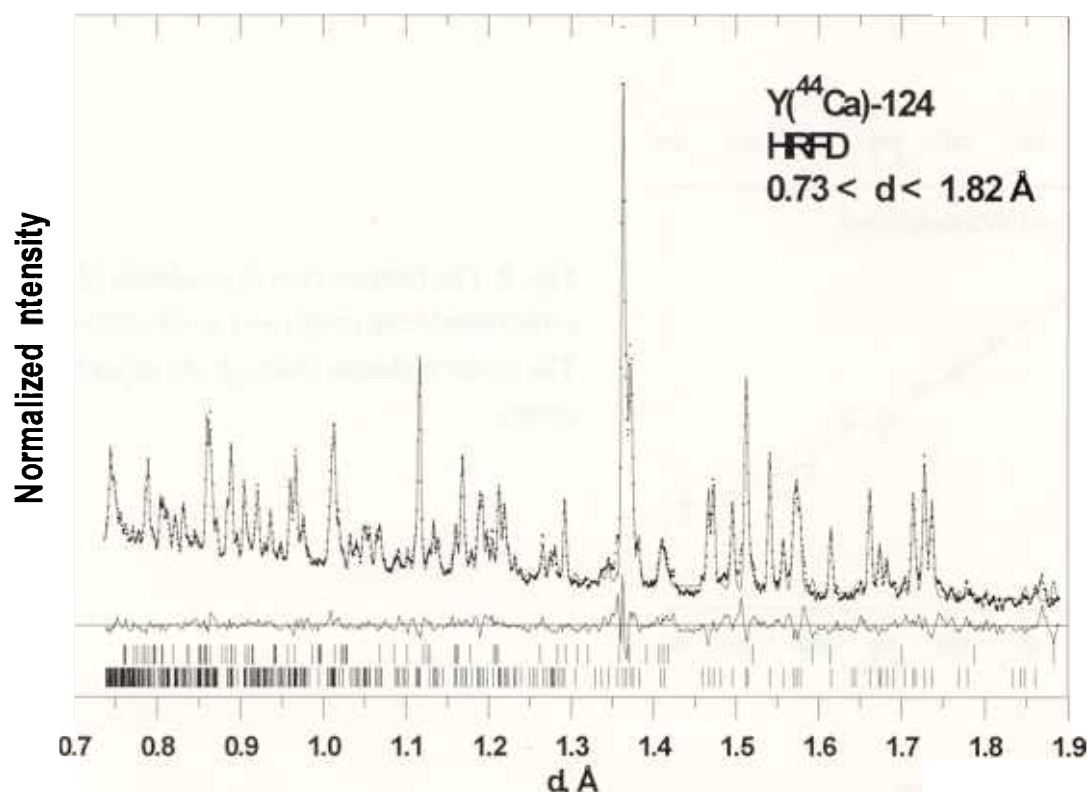
Fig. 1. *A portion of diffraction spectrum from the powdered $Y_{0.9}{}^{44}Ca_{0.1}Ba_2Cu_4O_8$ measured on the high-resolution Fourier diffractometer at the IBR-2 pulsed reactor showing the experimental points, profile calculated by the Rietveld method, and the difference curve.*

The population factor $n(Y)$ was found to be 0.889(5), which is practically equal to the nominal value of 0.9. The population factor of the Ba position coincides with the nominal value within the limits of error, which confirms the conclusion made earlier[2] that it is the Y position and not Ba that is replaced by Ca. This points to the main role in the substitution mechanism being played by the small ion radius

of Ca^{2+}, which practically coincides with the Y^{3+} radius, and not by its valency, which is equal to that of Ba.

To confirmed the results obtained a more detailed measurements as a function of temperature are planned on a new purer sample.
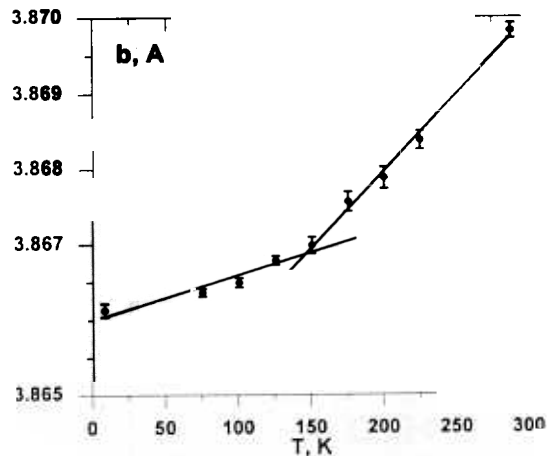
Fig. 2. The dependence of the unit cell parameter b of $Y(^{44}Ca)$-124 on temperature. Linear dependencies calculated by the least square method are drawn over separate temperature intervals.
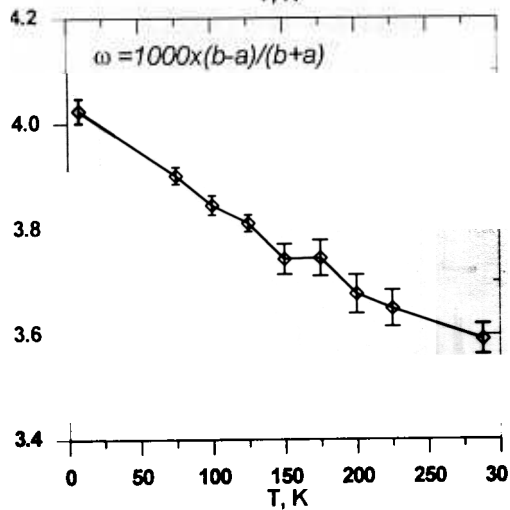
Fig. 3. The temperature dependence of the orthorhombicity coefficient $\omega=(b-a)/(b+a)$. The curve is drawn through the experimental points.

References

Wu Ting, O.-M.Nes, T.Suzuki, M.G.Karkut, K.Fossheim, Y.Yaegashi, H.Yamauchi, and S.Tanaka, Phys.Rev. B48 (1993) 607.

2. V.A.Trounov, T.Yu.Kaganovich, P.Fischer, E.Kaldis, J.Karpinski, and E.Jilek, Physica C 227 (1994) 285.

3. H.Schwer, J.Karpinski, and E.Kaldis, 4th Intern. Conf. M^2S-HTSC, Grenoble, July-1994, Abstracts, WD-PS 92, 139.

4. V.L.Aksenov, A.M.Balagurov, V.G.Simkin, Yu.V.Taran, V.A.Trounov, V.A.Kudrjashev, A.P.Bulkin, V.G.Muratov, P.Hiismäki, A.Tiitta, and O.Antson, Proceedings of ICANS-XII, 24-28 May 1993, Abingdon, U.K., vol.1, I-124.

THE CRYSTAL STRUCTURE OF THE IONIC
CONDUCTORS $BaCe_{(1-x)}Y_xO_{(3-x/2)}$

A.I.Beskrovnyi*, A.V.Strelkov**, I.G.Shelkova*

* Frank Laboratory of Neutron Physics, JINR, Dubna, Russia
** The Moscow State University, Department of Chemicals, Russia

The crystal structure of $BaCeO_3$ was examined by numerous authors [1, 2]. Atomic coordinates, **Pbmn** the space group, and the structural parameters a= 6.212(1)Å, b=6.235(1)Å, c=8.781Å were determined in [1]. It was noted, that the general regularity of the orthorhombic perovskite structures: $a \leq c\sqrt{2} < b$, was broken in $BaCeO_3$. In [2] the compound, $BaCeO_3$, was assumed to have the tetragonal structure with a=6.212(2)Å, c=8.804(4)Å.

Further, an interest in $BaCeO_3$, doped trivalent metals, arose due to the discovery of their high ionic conductivity [3, 4]. It was suggested, that the ionic conductivity, which appeared following the substitution of Ce^{4+} by trivalent cations was realised via oxygen vacancies. The protonic conductivity is the result of the action of water vapour on these materials.

In [5] the structural data, confirming the existence of oxygen vacancies in the amount of x/2 in a compound, doped with Y=0.1 and Gd=0.1, are given.

The examined samples were the $BaCe_{(1-x)}Y_xO_3$ (x=0.05, 0.10, 0.15, 0.20, 0.25, 0.30) compounds. No other phases were observed in the samples. Rietveld fiting was done under assumption, that the vacancies can occupy the positions O1 and O2 and their total number equals x/2. The diffraction patterns for x=0.05 and x=0.20 are shown in fig.1 and 2. Splitting of the diffraction peaks (110) and (002) (d=4.393Å) and their second orders (d=2.197Å) in a sample with Y=0.20 are illustrated on fig.2. A change in the lattice parameters following Y- doping is presented in fig.3. A very weak dependence on a,b and a high sensitivity c, to Y- doping attract attention. Another peculiarity of structural changes is the existence of the oxygen vacancies in four O2 positions only, which are in the apices of the octahedral basis. Two O1 are on a line parallel to c.

Obviously, the reason for a high ionic conductivity in $BaCeO_3$, which is doped with trivalent cations, is actually a high concentration of oxygen vacancies.

1. A.J.Jacobson, B.C.Tofield, B.E.F. Fender, Acta Cryst. 1972 b28, 956-61
2. V.Longo, F. Ricciardello, D.Minichelli, J. Mat. Sci., 1981, 16 3503-05
3. N.Bonanos, B. Ellis, K.S. Knight, M.N. Mahmood, Solid State Ionics, 1989,35
4. H.Iwahara, H. Uchida, K. Ono, J. Ogarki, J. Electrochem. Soc., 1988, 135
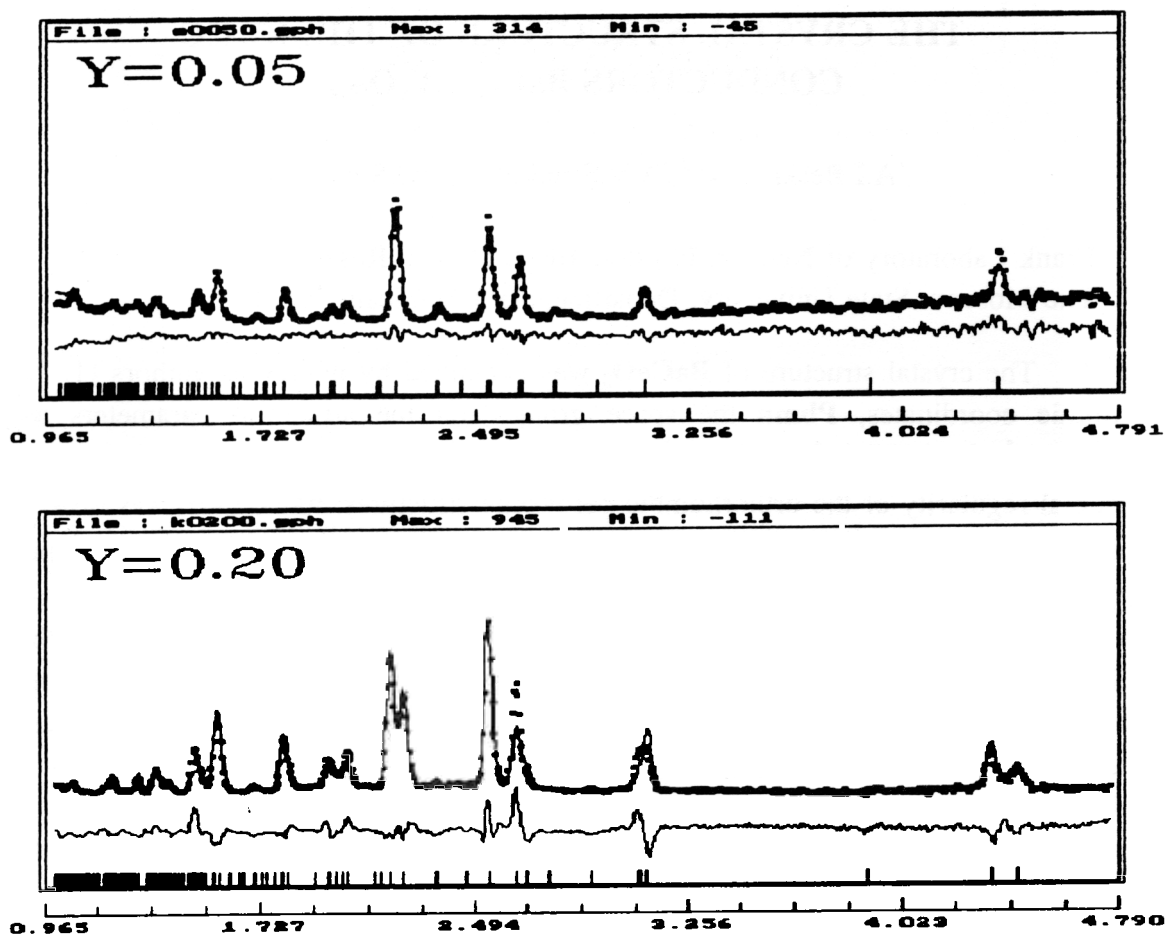5. N.Bonanos, M.Soar, Annual report ISIS, 1992, A56.
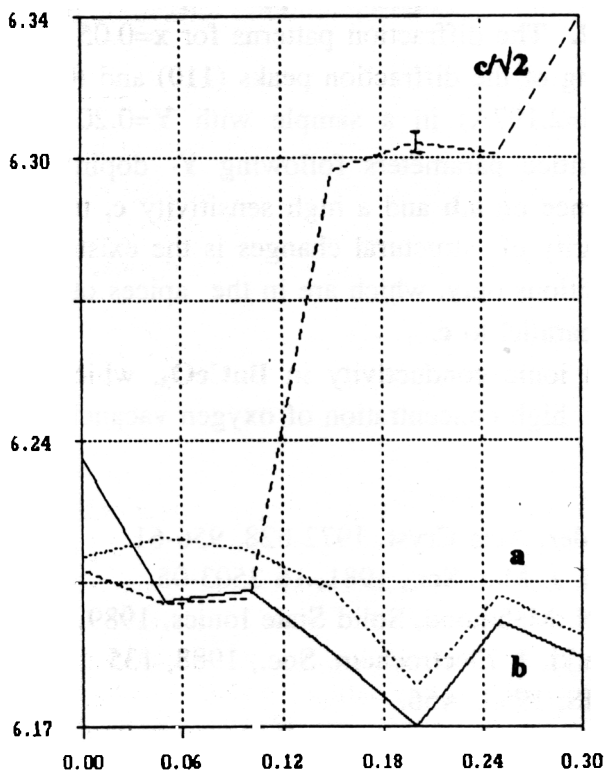
Fig.1,2 The diffraction patterns for x=0.05 and x=0.20

Fig.3 A change in the lattice parameters (sp.gr. Pbmn), following Y-doping; a, b, c for x=0.0 are taken from [1].

TEXTURE INVESTIGATIONS AT THE NSHR DIFFRACTOMETER: METHODICAL WORK

J. Heinitz, N. N. Isakov, V. Luzin, A.N. Nikitin, D.I. Nikolayev, K. Ullemeyer & K. Walther
Joint Institute of Nuclear Research, Dubna, Russia

Introduction

Beside the carrying out of pole figure (PF) measurements on geological samples by our group and external users, even methodical work is performed to rationalize PF measurements and to improve the extraction of pole density data from the recorded spectra. This research is based on the demands of structural geologists: to derive the development of geological structures from the textures of the rock forming minerals, generally many samples have to be measured. The reduction of measuring time for one sample without loss of texture information therefore is desirable. On the other hand, good counting statistics require long measuring times, and the determination of the lowest possible time is essential to avoid data falsification. One possible test to control the reduction of measuring time by means of data smoothing is reported.

Furthermore, some work has been initiated to improve PF extraction from time-of-flight (TOF)- spectra by means of peak profile analysis considering also the shape of the peaks. The fundamental concept is explained in this report.

Rationalization of pole density measurements

The required measuring time to obtain adequate texture information of one sample is determined by the number of sample positions [1,2], but also by the measuring time at one position. Since the quality of the recorded TOF- spectra depends on counting statistics (noise) and therefore on time, some expense is necessary to control the reduction of measuring time. This may be done by means of data smoothing.

The experimental PF $P_{h_i}(y)$ is considered to be the sum of some function and a superimposed noise δ, i.e. we usually get $P_{h_i}(y) + \delta$. It is assumed, that a long time measurement has a lower level of noise as a short time measurement and after smoothing better fits the real pole density distribution. Thus, the comparison of two smoothed data sets obtained with different measuring times will test the quality of the short time measurement. As an example, a carbonate mylonite was measured twice with 17 and 2 min exposure times, subsequently the extracted PFs were replaced by smoothed PFs $P_{h_i}^s(y)$ applying a Gaussian to determine the weights w_j [3]:

$$P_{h_i}^s(y) = \sum_{j=1}^{J} w_j P_{h_i}(y_j) \bigg/ \sum_{j=1}^{J} w_j \qquad\qquad w_j = \exp(-\omega_j^2 / \omega_0^2)$$

In Figure 1 the experimental and smoothed PFs of two overlapped Bragg reflections are given as an example, their differences are described by the statistical error parameter RP0 [4]. Rather good conformity even in detail is deduced from small RP0- values and from visual comparison, this is valid for experimental (RP0=3.6%) and smoothed (RP0=1.2%) PFs as well. In sections η = constant it becomes more obvious, but slight differences should also be noted (see Fig. 2). It seems, that for the considered PF an exposure time of 2 min is sufficient. On the other hand, we observed greater differences for weakly scattering peaks. As low intensity peaks determine the quality of quantitative texture analysis, a measuring time of 2 min to accumulate one spectrum is too short. We conclude, that the exposure time in principle may be reduced, but its lower limit must be determined carefully also considering the scattering behaviour of the present phases, sample volume and other parameters.

experimental | Dolomite (1 0 4) | smoothed
Calcite (0 0 6)

17 min

2.2 %

η

> 142.5
> 149.3
> 156.1
> 162.8

min: 117.4   3.6 %   max: 180.9   min: 126.5   1.2 %   max: 172.0

2 min

3.4 %

> 105.0
> 110.0
> 115.0
> 120.0

min: 79.8   max: 138.3   min: 94.1   max: 127.7
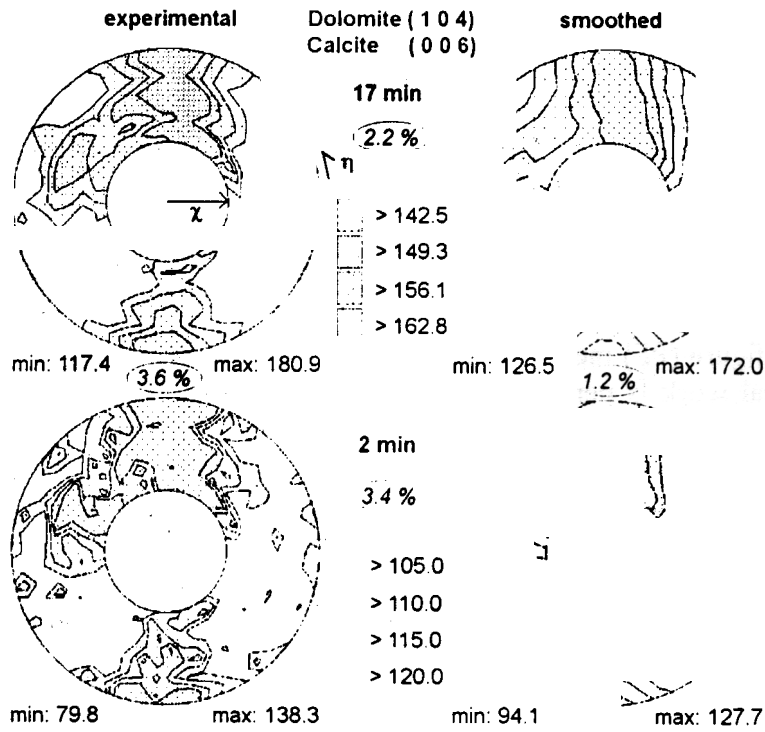
Fig. 1: Experimental and smoothed PFs of two overlapped Bragg reflections for exposure times of 17 and 2 min. RP0- values are given as percentages, the PF-angles χ and η are indicated.

Extraction of pole figures from TOF- spectra by means of peak profile analysis

To extract a PF one has to determine the integral intensity S^* of the associated Bragg reflection in dependence on a certain grid. The pole density $P_h(y)$ and S^* must be proportional to the scattering volume $V(h_i \| y)$:

$$P_h(y) \sim S \quad \frac{V(h_i \| y)}{}$$

Commonly a PF is considered as a normalized function $S(h_i,$

$$P_h(y) = \frac{S(h_i, y)}{\int S(h_i, y) dy}$$

Two different approaches in the processing of the experimental data and to obtain the estimate S may be realized - a parametric approach and a nonparametric one. Here, the parametric approach assumes a parametric model of the diffraction peak and not a parametric Poisson model of the countings in each channel. The approximating curve is composed of a limited set of parametric curves, which better match the experimental data. The area below the peak is obtained by integration over the intensities of that approximating curve, which is easy to calculate analytically. That property is desirable especially for texture analysis.

The parametric model overcomes several problems, but other problems arise. The most important one is the assumed peak shape. Accumulating all experience, the peak of the NSHR-instrument may be properly described by a composed function of the following type:

$$I(I) = \exp\left\{-\frac{(I-t_0)^2}{2\sigma_1^2}\right\}$$

$$I(t) = \exp\left\{-\frac{(t-t_0)^2}{2\sigma_1^2}\right\} \qquad\qquad t_0 \le t \le t_1$$

$$I(t) = \exp\left\{\frac{\gamma^2\sigma_2^2}{2}\right\}\exp\{-\gamma(-t_0)\},$$

where σ_1 and σ_2 are determining the width of the Gaussian regions at the left and right side of the peak and γ is the decay constant of the exponential region. The position $t_1 = t_0 + \gamma\sigma_2^2$ ensures a smooth transition between the regions.

Recently PFs obtained by means of the parametric model are compared with PFs obtained from the nonparametric model. First results show several advantages of the parametric model.
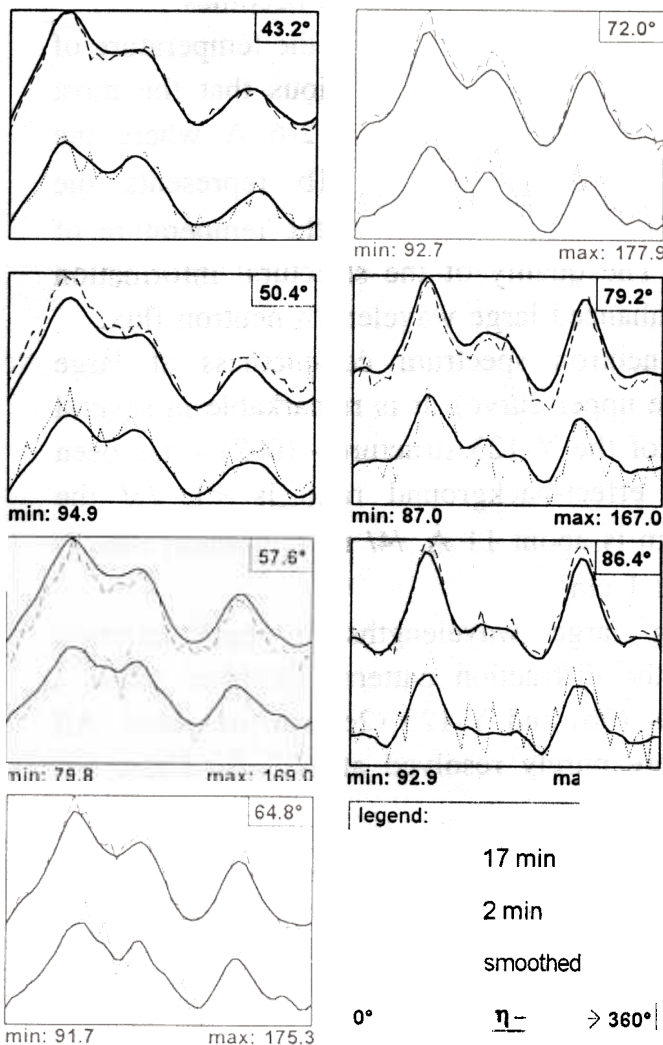
Fig. 2: Sections η = constant for the PFs. 'min' and 'max' give the intensity range, χ and η are defined in Figure 1.

References

[1] HELMING, K. (1992): Textures Microstruct. 19, 45-54.
[2] WILL, G.; SCHÄFER, W. & MERZ, P. (1989): Textures Microstruct. 10, 375-387.
[3] NIKOLAYEV, D. & ULLEMEYER, K. (1994): J. Appl. Cryst. 27, 517-520.
[4] MATTHIES, S.; WENK, H.-R. & VINEL, G. (1988): J. Appl. Cryst. 21, 285-304.

COLD MODERATOR AT THE IBR-2 REACTOR AS A BASIS FOR NEW POSSIBILITIES IN NEUTRON SCATTERING EXPERIMENTS

G.M.Mironova

Joint Institute for Nuclear Research, Frank Laboratory of Neutron Physics,
141980 Dubna, Russia

With the DN-2 difractometer (flight path 25 m) at the IBR-2 pulsed reactor the theoretically available range of neutron wavelengths is 1-30 Å, the lower limit being caused by the use of a bent neutron guide-tube and the upper is the recycle limit of the reactor. As the resolution $\Delta d/d \sim \Delta t/t$ for scattering angles near 180° and $\Delta t \sim 300$ μs, we obtain $\Delta d/d = 2 \cdot 10^{-2}$ ($\lambda = 2$ Å) - 10^{-3} ($\lambda = 30$ Å). So, the larger the available wavelength, the higher the resolution of the device becomes.

The diffraction pattern of a Y-123 ceramic sample measured at the temperature of the water moderator 300 K is presented in Fig.1a. It is obvious that the most useful information is located in the wavelength interval of 2-6 Å where the maximum available resolution is $\sim 6 \cdot 10^{-3}$ ($\lambda = 6$ Å). Fig.1b represents the diffraction pattern obtained under the same conditions, but at the temperature of the solid methane moderator, $T \sim 30$ K. The quality of the structural information significantly improved due to strongly enhanced large wavelength neutron flux.

Perhaps the brightest illustration of neutron spectrum completness at large wavelength and $T_{mod} = 30$ K is Fig.1c (the upper curve). It is remarkable in several aspects: /1/ one of the weakest reflexes of the Y-123 structure - (002) - has been measured at the 175° angle, /2/ the effect-background ratio is <1, /3/ the wavelength in this region of the spectrum is about 11 Å, /4/ measurement time is 1 minute, /5/ the sample volume is about 1 cm^3.

The practical consequences of using large wavelengths in backscattering diffraction are shown in fig.2, where the diffraction patterns of 'blue' phase - $Y_2Cu_2O_5$ (2a), 'green' phase - Y_2BaCuO_5 (2b) and Y-123 (2c) are presented. All the phases measured simultaneously were purely resolved at $\lambda > 6$ Å. There are two circumstances promoting this fact:

  1) the resolution $\Delta d/d$ is less than $5 \cdot 10^{-3}$ in this region;

  2) the natural rarefying of diffraction lines is significant.

  A resolution on the level of 10^{-4} would be necessary to solve the problem of quantitatively separating these phases at wavelengths less than 6 Å.

Taking into account the minute exposition being enough to have appropriate statistics in large wavelength range it is clear that quite new possibilities are offered in studying transient phenomena and chemical reactions in complex systems.

56
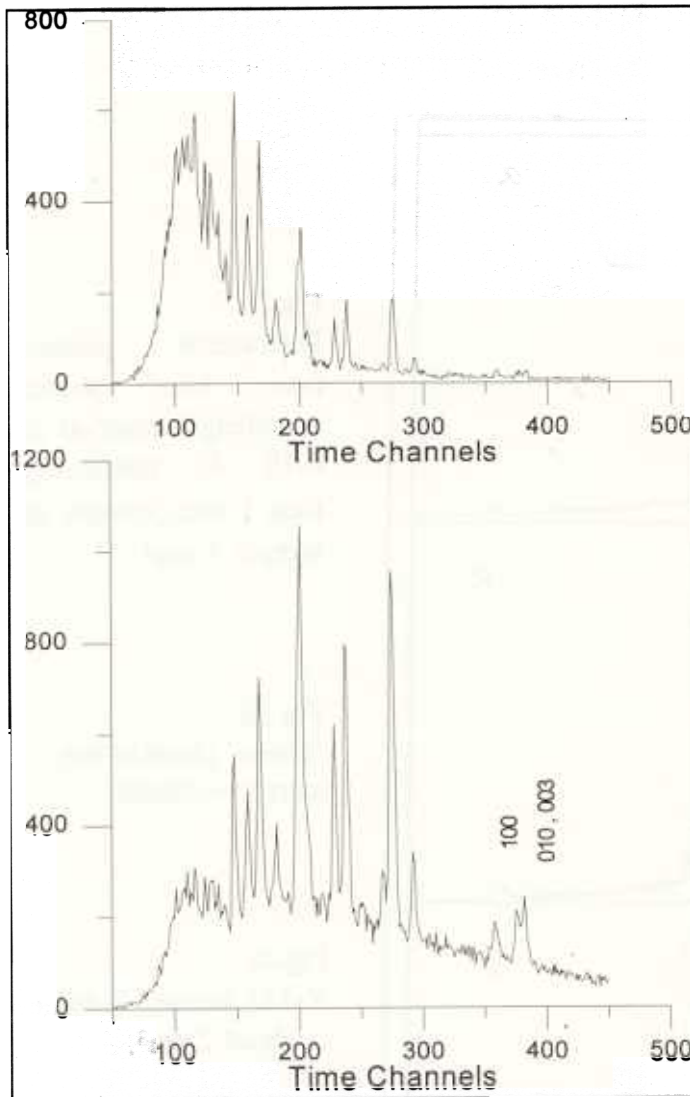
Fig.1a
The part of diffraction pattern measured for 1 min. from a 1 cm³ Y-123 ceramic sample for a channel width 128 microseconds, the range of wavelengths 1-9 Å and temperature of water moderator 300 K.

Fig.1b
All conditions are as in Fig.1a. The temperature of methane moderator 30 K.
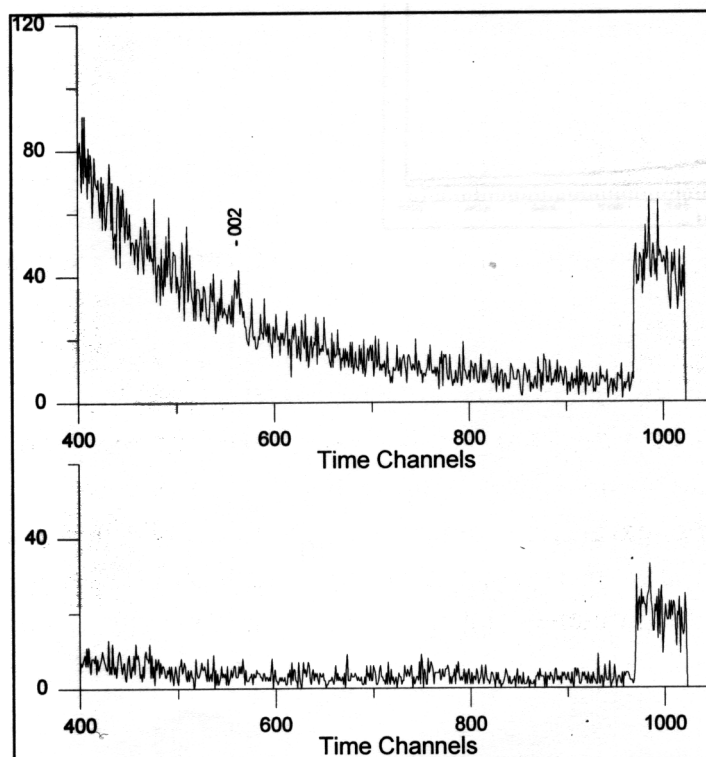
Fig.1c
Upper curve is the tail of the pattern presented in Fig.1b. In the range 970-1024 the channel width is 1024 microseconds. Wavelength interval ranges from 8 to 28Å. Lower curve is the tail of the spectrum in Fig.1a.
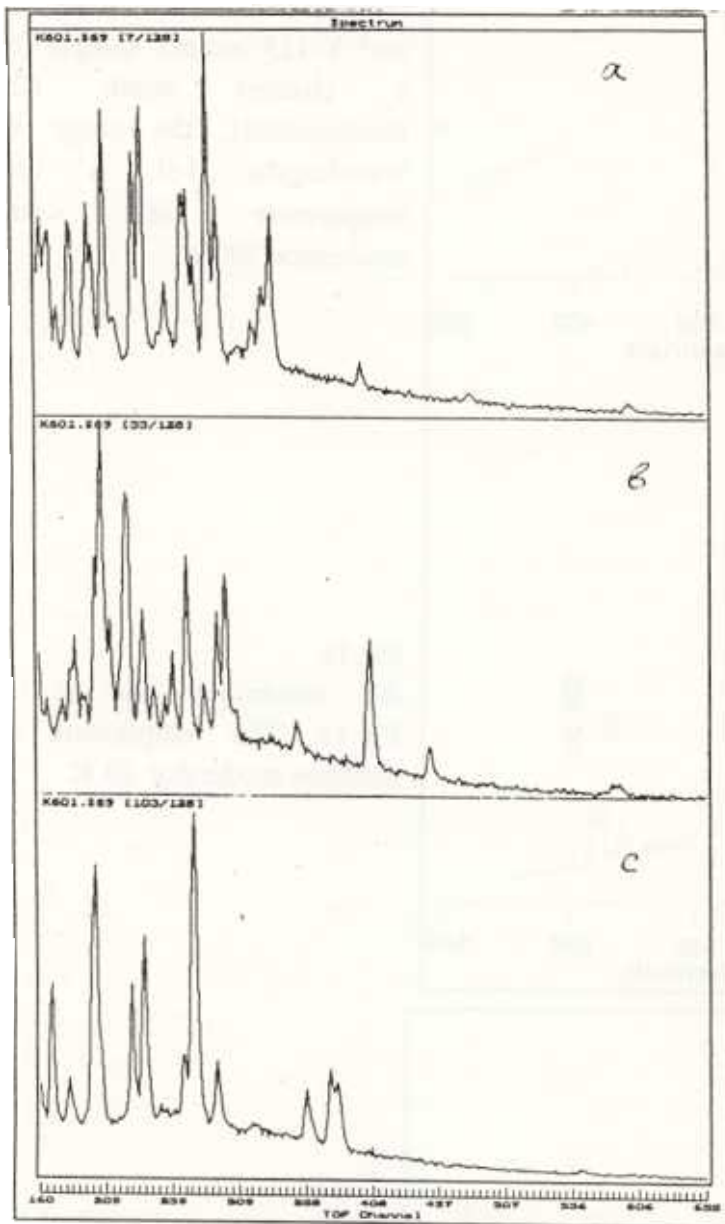
Fig.2a
Diffraction pattern from 'blue' phase: wavelength interval is 4-10 Å; measuring time 1 min.;volume of sample 1 cm^3.

Fig.2b
'Green' phase at the same conditions.

Fig.2c
Y-123 phase. Volume is about 2 cm^3.

Non-Ionic Surfactant Structures in Saline Water Solutions by SANS

L.A.Bulavin[1], V.M.Garamus[2], T.V.Karmazina[3]

1) Physical Department Kiev University, Kiev, Ukraine
2) Frank Laboratory of Neutron Physics, JINR
3) Institute of Colloidal Chemistry and Chemistry of Water, Kiev, Ukraine

The influence of salt on surfactant aggregates is a widely studied field in the case of ionic surfactants with a large electrical charge. Micelles formed by non-ionic surfactants contain a very small positive charge and the salt effects are considered negligible.

A set of experiments with two types of surfactants: ethoxylated di-isononylphenol (ODNP) and tetramethylbutylphenol ethylene oxide (Triton X-100) in NaCl and NaBr water mixtures with varying surfactant and salt/surfactant concentrations were performed on the "MURN" small-angle neutron scattering spectrometer. ODNP, recently synthesized, is an original two alkyl chain surfactant with specific properties which act on the oil-surfactant-water interface. The study of ODNP/water mixtures by SANS were performed earlier by our group [1]. Triton X-100 is a commonly used research subject because it has a well defined chemical structure [2].

In the case of dilute surfactant solutions (surfactant volume fraction is 0.01) the addition of salt gives rise to increases in the radius of gyration of the micelle. But direct use of the Guinier approximation is not valid because of interference effects in the scattering curves. The experimental results were modeled in two ways: monodisperse spheres with an adhesive potential, and ellipsoidal particles with a screened Coulomb potential. Both fit procedures gave consistent results: with the addition of salt the aggregation number and micellar repulsion decreased, and the radius of gyration increased. Micelles also became more non-spherical. The surface electric potential increased but the radius of the screened Coulomb potential decreased and effective micellar repulsion decreased, as well. The value of the surface potential was close to 1 mV (in the case of ionic surfactants, about 10-100 mV and decreasing with the addition of salt).

For analyzing data on concentrated surfactant solutions (surfactant volume fraction of 0.1) integrated parameters (Porod invariant, parameter $K = \int d\Sigma(q)/d\Omega q dq$) of the scattering curves were used. The average radius of the aggregates, Porod radius (V/S, where S is the total surface of aggregates and V is the aggregate volume) and their ratio versus NaBr concentration are represented in the table.

NaBr, g/cm^3	Average radius, $\overset{o}{A}$	Porod radius, $\overset{o}{A}$	Ratio
0	35.9	26.1	1.37
0.025	35.2	24.9	1.41
0.055	33.6	23.4	1.43

The ratio points to the slow increase of some non-spherical aggregate shapes with salt concentration.

The influence of salt on non-ionic surfactant solutions is somewhat different than for ionic surfactants, i.e., aggregate volume and aggregation number decrease, and the surface potential increases.
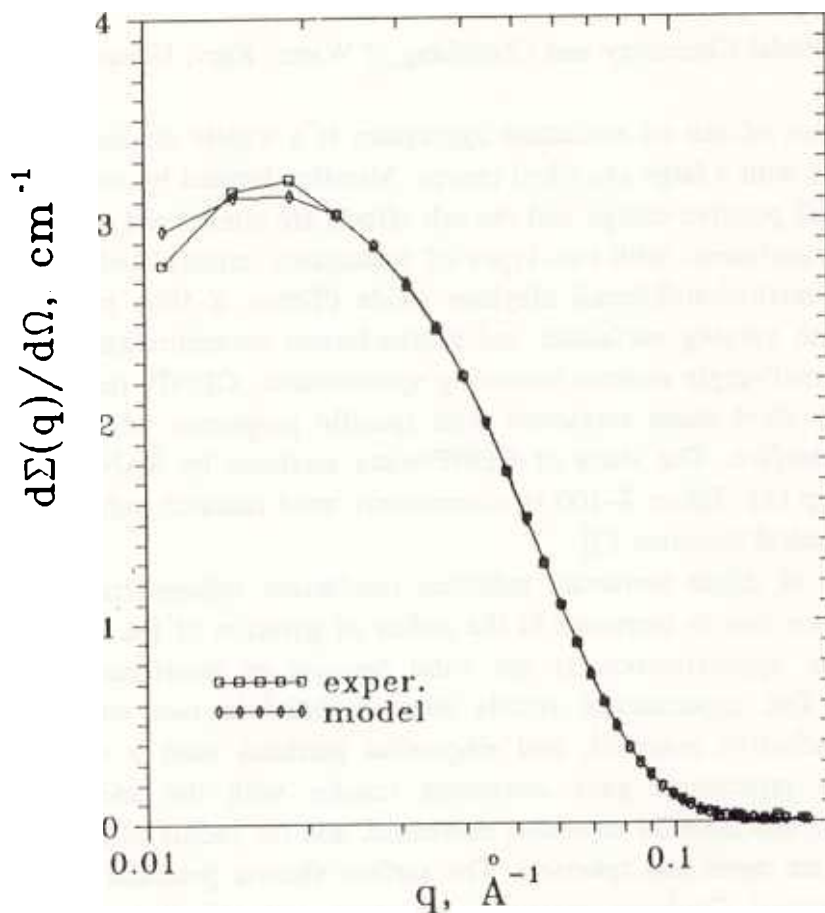
Fig.1. Experimental curve of neutron scattering of 8.11 mmol/l ODNP, 50 mmol/l NaCl and curve of the model for ellipsoidal particles with screened Coulomb potentials.

References:
1. L.A.Bulavin, V.M.Garamus, Yu.M.Ostanevich Colloids and Surfaces, accepted for publication #1654.
2. C.Monohar, V.K.Kelkar, B.K.Mishra, et al., Chem. Phys. Lett. v.171 p.451 1990.

60

Investigation of the structure and dynamics of lipid biological membranes via neutron and X-ray scattering

V.I.Gordeliy, M.A.Kiselev, A.I.Kuklin, V.G.Cherezov, S.P.Yaradaykin, A.H.Islamov,
A.D.Tougan-Baranovskaya*, A.V.Pole*, P.Balgavy[♦], V.A.Chupin[н], G.Klose[♠],
L.S.Yaguzhinskiy*

*–Moscow State University
[н]–Moscow Institute of Fine Chemical Technology
[♦]–University of Bratislava, Slovak
[♠]–University of Leipzig, Germany
+–Moscow Engineer-Physical Istitute

Investigations of membrane structure and the problem of membrane interactions were carried out at the YuMO spectrometer, DN-2 diffractometer and the DRON-4 X-ray diffractometer.

I. Small-angle neutron scattering.

1. The method developed in [н/] was used for measurements of membrane structural parameters (membrane thickness and positions of deuterium labels in it) by small angle neutron scattering. For this purpose it is important to have vesicles in the solvent with a radius larger than 500Å. This is necessary for a precise structure determination. This fact is demonstrated in Fig.1. A sample of one kind was taken (DPPC in a DMSO/water mixture with DMSO molar concentration 0.05), but two different methods for preparation of the vesicles have been used: the first - ultrasonically (in this case we have small vesicles with about 150Å radius) and the second - using an extruder (in this case the radius of the vesicles is determined by the radius of the nuclear membrane in the extruder, about 800Å)[2/]. The linear part of the curve for the sample prepared by extrusion is longer in the region of small q^2 - that giving the possibility to determine the membrane structure parameters with a higher accuracy relative to the sample prepared by ultrasonics.

2. A similar method was used to determine the membrane thickness and the location of surfactants in lipid unilamellar vesicles. The structure study of lipid membranes containing nonionic polyoxyethylene type surfactants has direct implications for a wide range of questions: for example, the origin of so-called hydration forces between lipid membranes, cell adhesion, cell fusion properties, etc. To determine the surfactant location in the lipid matrix, the following partially deuterated surfactants were used:

$C_{11}H_{23}CD_2O(CH_2CH_2O)_nH$ denoted by $C_{12}E_n-D_2$,

$C_{12}H_{25}O(CD_2CD_2O)_nH$ denoted by $C_{12}E_n-D_4$.

According to the results obtained from neutron diffraction, the polyoxyethylene groups of $C_{12}E_n$ are entirely incorporated in the polar part of the lipid matrix and the lipid/water interface increases. It was important to detect the location of the surfactant in the lipid matrix by SANS. The measurements carried out with contrasts of 100%, 50% and 25% D_2O showed that under the influence of the surfactant molecules, the membranes became asymmetric. To obtain the parameters of the asymmetry with sufficient accuracy, it is necessary to measure more points of

the contrast. This work was performed in collaboration with Prof.G.Klose, Germany, University of Leipzig.

3. The new direction of the SANS application to the study of biological membranes is the investigation of the thylakoid membranes of chloroplasts. These membranes play an important role in plant photosynthesis. The mechanism of photosynthesis and, in particular, the mechanism of proton transport through the membrane remains unknown. The purposes of the performed experiments were:

a) To properly extract single thylakoid membranes from the plants (spinach leaves) and to make clear whether it is possible to investigate these objects by means of small angle neutron scattering;

b) To measure the parameters of the thylakoid membranes.

Fig.2 represents the scattering curves at different contrasts in the D_2O/H_2O solution. These curves agree with the data in [5]. The scattering amplitude density calculated from the neutron experiments is $\rho = 0.0169 \cdot 10^{-12}$ cm/A^3. This value is in agreement with the theoretically estimated value of $0.0166 \cdot 10^{-12}$ cm/A^3. The measured membrane thickness was 53Å. This work provided a basis for futher accurate determinations of the structure parameters of thylakoid membranes under different conditions. The main aim of the planned experiments is to study the way of protons during the proton pumping. This study is being done in collaboration with Moscow State University, (Prof. L.S.Yaguzhinskiy).

II. Neutron and X-ray diffraction.

4. Up to now the mechanism of the huge repulsive forces acting at short distances between membranes, some biological molecules like DNA, collagen and colloids is unknown. A series of investigations have been done in order to understand the mechanism of the so-called hydration forces.

To understand the contribution of the out-of-plane fluctuations of lipid molecules to the balance of forces acting between membranes, the structure and hydration properties of membranes from a newly synthesized polymerizable lipid DTDPC (phosphatidylcholine with two conjugated diene groups on both ends of the hydrocarbon chains) were studied by X-ray diffraction and NMR.

Electron density profiles of polymerized bilayers and electron microphotographs show that polymerization occurs not only between adjacent lipids in the same monolayer but also between lipids from opposite monolayers which links these monolayers together. See Fig.3.

The "hydration" forces were measured in polymerized membranes by means of the osmotic stress method. It was found that the decay length of these forces has an anomalously low value ~ 0.7Å in polymerized membranes compared with nonpolymerizable analogs (~2Å). This can be attributed to restriction of the out-of-plane lipid motion caused by polymerization. Synthesis of DTDPC and the NMR experiments were done at the Moscow Institute of Fine Chemical Technology.

5. The second part of the membrane structure investigation was carried out at the DN-2 high-flux neutron diffractometer and was connected with the study of stacking disorder in model membranes via time-of-flight neutron diffraction. The stacking disorder in membrane systems has

an important implication for elucidating membrane structure and interactions. A knowledge of the nature of the disorder would allow the out-of-plane thermal fluctuations of lipid molecules to be determined correctly from neutron diffraction experiments. The latter is a "hot" problem concerned with Israelachvili's theory of entropic contribution to the "hydration" forces[4].

It is necessary to stress, however, that in traditional experimental set ups at steady state reactors and X-ray diffractometers, the reflection widths are largely determined by instrumental broadening, and it is practically impossible to remove this effect completely.

Time-of-flight neutron diffraction was used to extract the contribution due to intermembrane distance fluctuations from the diffraction peak width[5]. This method was also applied to investigate the second kind of disorder in model egg yolk lecithin membranes. The widths of several orders of diffraction at different hydrations were determined. Based on this data, conclusions concerning with the nature of the stacking disorder in model EYL membranes were drawn (Fig.4).

6. The membrane structure of a series of 1-palmitoyl-2-oleoyl-sn-glycero-3-phosphatidylcholine (POPC) modified by the nonionic surfactant $C_{12}H_{25}O(CH_2CH_2O)_nH$ $(C_{12}E_n)$ (n=2, 4 and 6) in a lipid/surfactant molar ratio of 2:1 and 1:1 have been investigated by X-ray and neutron diffraction at two relative humidities RH=85% and RH=97% (t=20°C, L_α phase). It was shown that the position of $C_{12}E_n$ in the lipid matrix depends on the osmotic pressure, molar ratio and length of the hydrophilic head of surfactant $(CH_2CH_2O)_n$. In some cases, with a decrease in the osmotic pressure, the hydrophilic head of the surfactant withdraws from the lipid matrix in the water layer. These data give important information for interpreting the results of measurements of the hydration forces between bilayers. The study has been performed in collaboration with University of Leipzig.

7. The mechanisms acting on the cells through biologically active molecules are being studied intensively now. In order to understand the role of the lipid bilayer in such phenomena, a study of the influence of local anesthetic on lipid membranes has been performed by X-ray diffraction[6]. A simple mathematical model explaining the quasi-parabolic dependence of the local anesthetic activity on the length of the hydrophobic substituent in the homologous series of tertiary amines (TA) has been proposed. It is suggested that the molecules of TA intercalate between the lipid molecules in bilayers. Due to the mismatch between the length of the lipid and TA hydrocarbon chains the intercalation results in a decrease in the bilayer thickness. The quasi-parabolic dependence is the result of the combination of partition equilibria and the geometrical parameters of interacting molecules in the bilayer. The model predicts that the TA chain length at which maximum activity is observed should depend on the lipid : aqueous phase volume ratio. The empirical parameters used in the model were obtained from X-ray diffraction on multilamellar egg yolk phosphatidylchoine (EYPC) dispersions with the monohydrochloride of the [2-(heptyloxy)-phenyl]-2-(1-piperidinylethyl) ester of carbamic acid and from the partition equilibria of its alkyloxy homologs with unilamellar EYPC liposomes. The results support the idea that one of the mechanisms of the influence of biologically active molecules on biological cells is the change in membrane thickness. This work has been performed in collaboration with the University of Bratislava (Dr. P.Balgavy).

8. Other kinds of work in the membrane field were started in 1993-1994 in collaboration with Leon Brillouin Laboratory, Saclay, France and the Institute of Biological Structure of KFA, Jülich, Technical University of Munich and BENSC HMI, Berlin, Germany. (See reports [8,9]).

References.

1. V.L.Gordeliy, L.V.Golubchikova, A.I.Kuklin, A.G.Syrykh, A.Watts:
   Progress in Colloid & Polymer Science, v.93, no.PI-38 (1993).

2. R.C.MacDonald, R.I.MacDonald, B.Ph.M.Menco, K.Takeshita, N.K.Subbarao, L.Hu:
   Bioch. Bioph. Acta, 1061, 297-303 (1991).

3. D.M.Sadler, D.Worcester: *J.Mol.Biol.* 159, 485-499 (1982).

4. J.N.Israelachvili, H.J.Wennerstrom: *J.Phys.Chem*, 96, p.520 (1992).

5. V.L.Gordeliy, A.Kh.Islamov, A.G.Syrykh: *Biologicheskie membrany*, v.9, num.2, pp.193-200 (1992) (in Russian).

6. D. Uhrikova, V. Cherezov, S. Yaradaikin, P. Balgavy: *J. Pharmazie*, 48, H.6, 446-450 (1993).

7. V.I.Gordeliy: Investigation of the structure liquid-crystalline lipid membranes via neutron diffraction. *Dissertation*, JINR, Dubna (1989).

8. L.G.Golubchicova, V.I.Gordeliy, M.A.Kiselev, J.Teixeira, S.P.Yaradaikin, V.G.Cherezov: *LLB Report*, Saclay, France (1993).

9. *BENSC Report*, Berlin, Germany (1994).

* vesicles prepared by extrusion from DPPC in $D_2O/DMSO_d$ mixture
+ vesicles prepared by sonication from DPPC in $D_2O/DMSO_d$ mixture
deuterium DMSO molar consentration 0.05
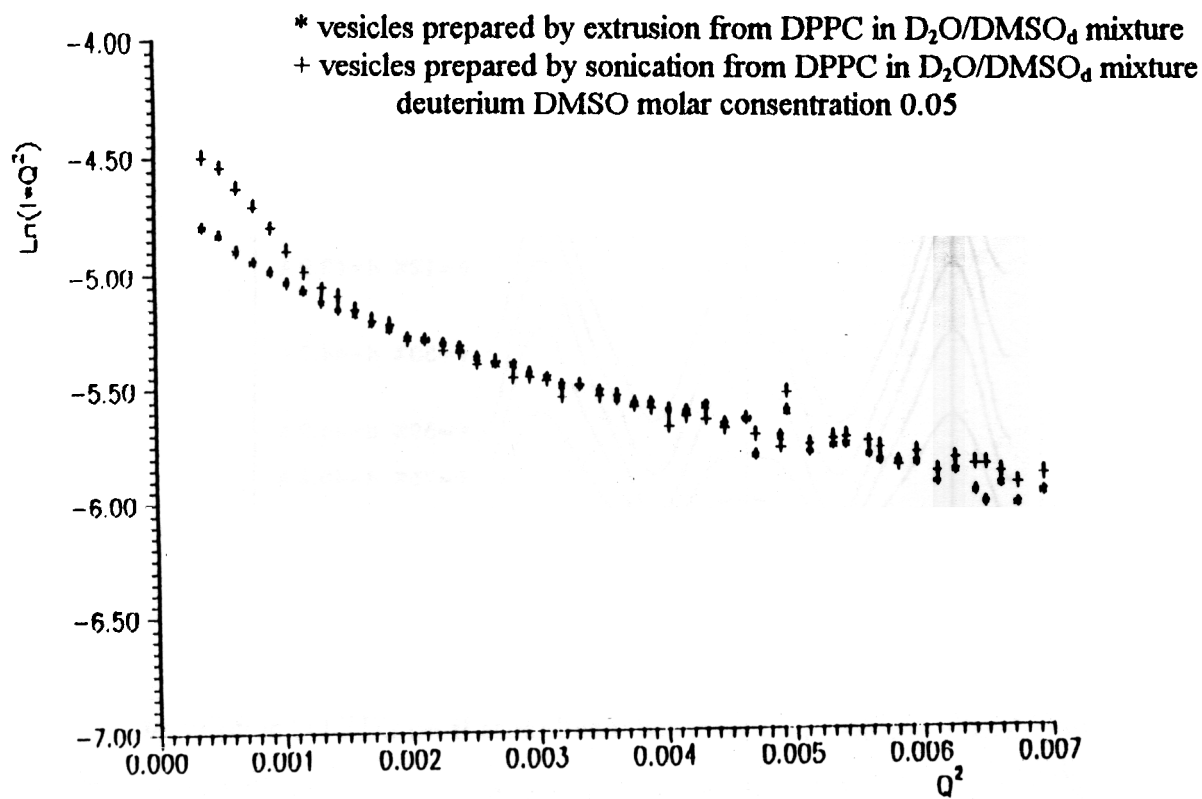
Fig.1. Guinier plot for two kinds of DPPC vesicle size distribution in $D_2O/DMSO_d$ mixture.
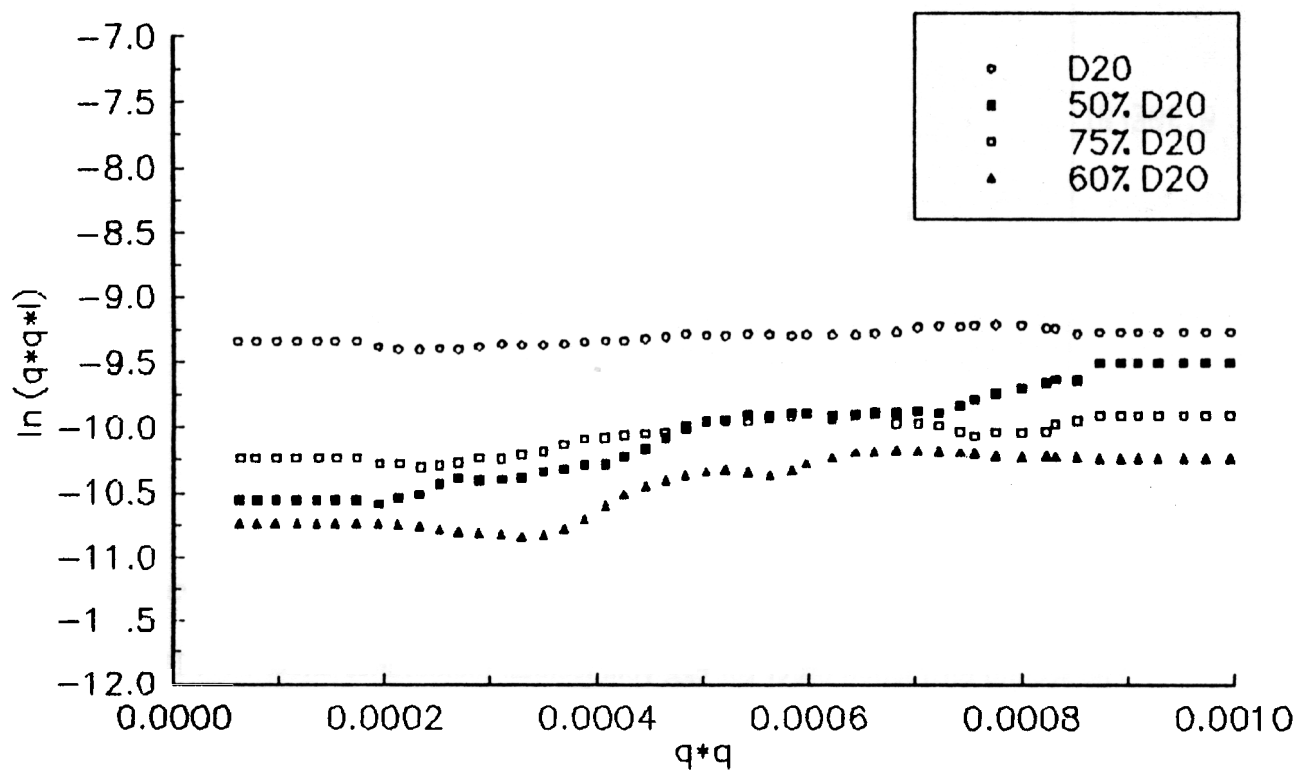
Fig.2. Guinier plot for thylakoid membranes at different H_2O/D_2O contrasts.
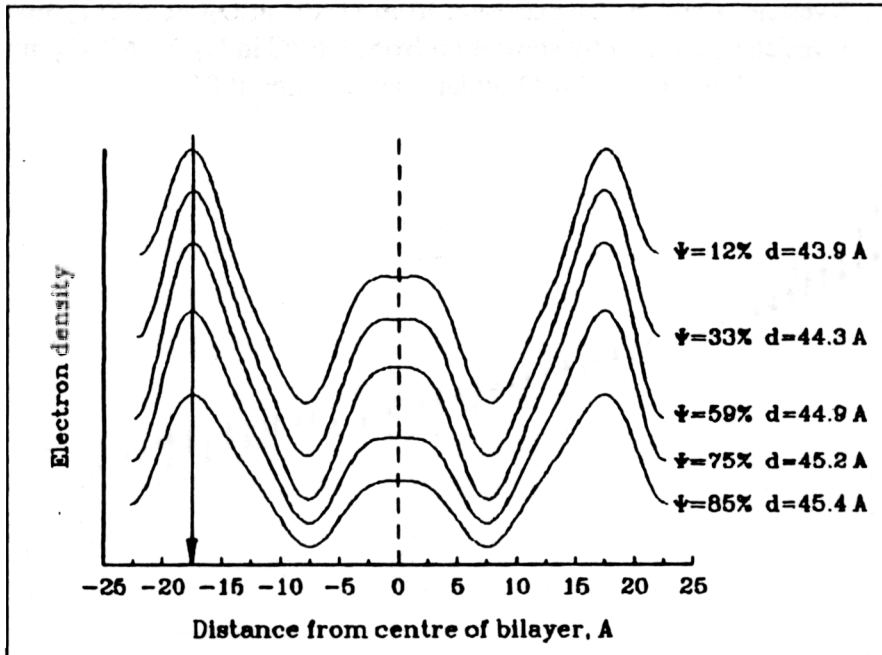
Fig.3. Electron density profiles of polymerised membranes from DTDPC at different humidities.
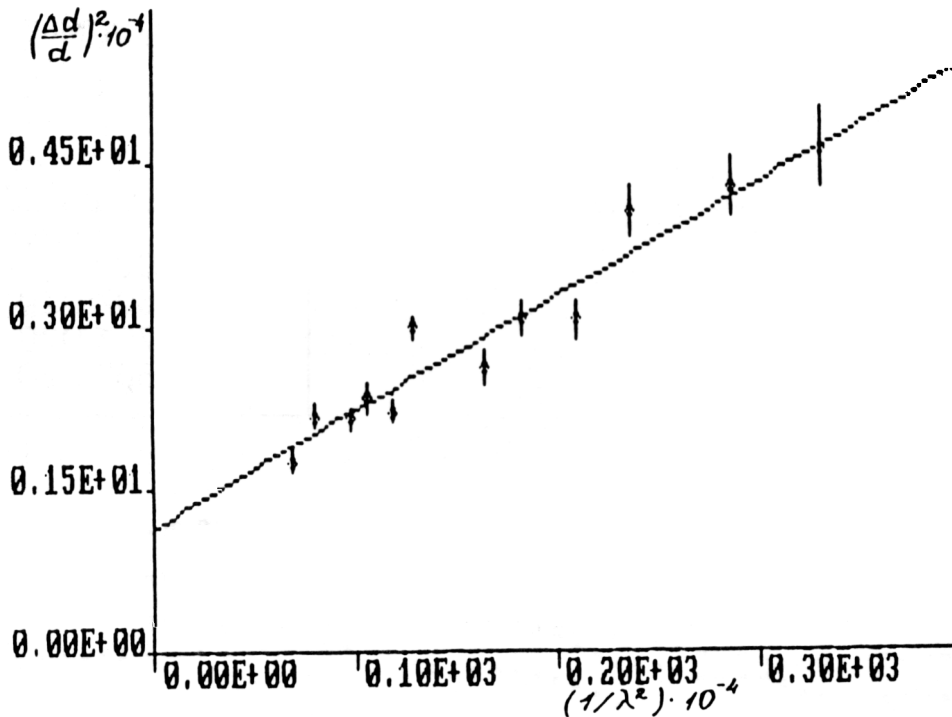
Fig.4. The diffraction peak width related to the repeat distance as a function of neutron wavelength: $(\Delta d/d)^2 = (\Delta d_s/d)^2 + tg\alpha/\lambda^2$.
The second diffraction order for egg yolk lecithin membranes under 97% D_2O humidity. The linear approximation gives the repeat distance fluctuation:

$$\Delta d_s/d = (1.08 \pm 0.04)\cdot 10^{-2}.$$

Material research on hydrating cement paste and solid state nuclear track detectors by SANS

M. Hempel[*], F. Häußler[*], F. Eichhorn[#], A. Hempel[#], H. Baumbach[+]

[*]Fraunhofer-Institut für zerstörungsfreie Prüfverfahren / EADQ Dresden, Germany
  present address: Frank Laboratory of Neutron Physics Dubna, Russia
[#] Forschungszentrum Rossendorf e. V. / IIM Dresden, Germany
[+]Fraunhofer-Institut für zerstörungsfreie Prüfverfahren Saarbrücken, Germany

Material research becomes more and more important today, especially with regard to the long time behaviour of the materials. In the case of hydrating cement paste it includes the unhydrated clinker minerals as well as the hydration products [1]. The SANS gives the opportunity to investigate cement samples with macroscopic thicknesses. In the case of the MURN facility of the IBR-2 the wavelength from (0.7 to 1.5) nm is used. Therefore SANS measurements on samples with thicknesses, which are relevant for building industry (up to some millimetres), are possible without any necessary corrections of multiple scattering effects. By means of different programs (SAS [2], FUMILI, ITP 92 [3]) the scattering data were used for the description of the development of the particle size distribution (Fig. 1) and of the time depending change of the interfaces (Fig. 2) [4]. By means of the inverse Fourier-transformation [3], it is possible to calculate the particle size distribution. Figure 1 shows the time depending change of the particle sizes (radius) in a 0.5 mm thick OPC (Ordinary Portland Cement) sample (not normalized). The SANS experiments were carried out during about 2 years (sample set CEMPAS). On the first hand it is visible that the size maximum position goes from about 5 nm up to 2.5 nm and during the hydration a second maximum will be observable (about 10 nm). The increasing of the integral about the probability shows that the number of scattering objects in the investigated size range becomes more and more. This facts are understandable when we assume that during the hydration the unhydrated clinker minerals will decompose and form new hydrated clusters partially.

The approximation of the scattering curve by a potential function gives the possibility to calculate an exponent A(2) of this function which can be associated with the dimension of mass or volume fractals d_m (A(2) = d_m) or surface fractals d_s(A(2) = 6-d_s) [4],[5]. The sketch of fractals is very useful for modelling of the inner structure which is important for description of the transport of liquids within the cement structure. The long-time behaviour of the exponent A(2) of the set CEMPAS is discussed in detail. With an increasing exponent the particle size distribution shows a translation of the first maximum to smaller sizes. After 92 and 434 days a distinct change both in the value of A(2) and in the size distribution was found. If the exponent decreases from 4 to 3 that means the inner structure becomes more and more fine [5],[6]. Other investigations are done on a set of 4 hydrating samples for the analysis of grain-size effects of the OPC particles. In this case a set of four samples of a hardened cement paste are prepared from ordinary Portland cement fractions of different grain sizes ((8-14)µm, > 45 µm) and water mixture (D_2O/water = 0.80) with a given water to cement ratio of 0.38. (sample set CPHYD) In the experiments an observation of the hydration progress within 378 days is done. Figure 2 shows the development of this exponent A(2) calculated by the fit procedure FUMILI.

In the observable size interval of the SANS instrument MURN (about 1 nm to 30 nm) [2] the cement structure can be described by means of volume fractals (in the first hours of hydration) and surface fractals. In figure 1 and 2 it is shown that not only in the first few days structural changes are visible, also after more than 200 days. Hereby the strong changes in the particle size distribution correlate with such in the exponent A(2). Experiments on single cement phases (Tricalciumsilicate) were carried out to complete these measurements. The continuation of these studies has to show the further evolution of the parameter A(2). In the case of A(2)= 4 the Porod law holds and the specific surface of the sample can be calculated in a straight forward way. It will be interesting to see whether the particle size distribution shows only one maximum.

In contrary of the hydrating cement paste the structure of irradiated and etched solid state nuclear track detectors (SSNTD) is more simple, but there are a lot of unsolved questions about the track formation, their shape and the spatial scattering length density distribution. The observable size interval of the spectrometer MURN is favourable to the investigation of the irradiation and etching process (etching time was up to 65 minutes). Figure 3 shows the Guinier-Plot of the scattering curve of irradiated and etched SSNTD. The radii of gyration R_g calculated from the slope of the scattering curve move within a range of about 5 nm to 15 nm for etched tracks. It shows a radius of the inhomogenieties of about 10 nm. The Guinier-plots of the etched samples show regions with different slopes, i.e. two R_g values. The R_g values measured by SANS were compared with the R_e values measured by a conductometric method. The dependence on the state of etching of the magnitudes of the R_g and R_e are different. SANS reflects structural changes of the neutron optical contrast. In contrary the conductometric method studies the electrical behaviour. The etching time varies and an increasing of the track radii is visible. Also only irradiated and non-etched SSNTD were investigated by SANS [7].

References:

[1] A. J. Allen, Time-resolved phenomena in cements, clays and porous rocks, J. Appl. Cryst. 24 (1991) pp. 624

[2] Yu. M. Ostanevich, Time-of-flight small-angle scattering spectrometers on pulsed neutron sources, Makromol. Chem., Macromol. Symp. 15 (1988) pp. 91

[3] O. Glatter, A New Method for the Evaluation of Small-Angle Scattering Data, J. Appl. Cryst. 10 (1977) pp. 415-421

[4] F.Häußler, F.Eichhorn, H.Baumbach, Description of the Structural Evolution of a Hydrating Portland Cement Paste by SANS, Physica Scripta 50 (1994) pp. 210-214

[5] P. W. Schmidt, Small-Angle Scattering of disordered, porous and fractal systems, J. Appl. Cryst., 24 (1991) pp. 414-435

[6] F. Häußler, M. Hempel, F. Eichhorn, A. Hempel, H. Baumbach, SANS Studies on Hydrating Cement Paste and SSNTD, Report of Activity 1992-93 of the FLNP, Dubna (Russia) 1994, pp. 158-162

[7] F. Häußler, M. Hempel, A. I. Kuklin, H. Baumbach, W. Birkholz, P. Yu.. Apel, M. Danziger, S. G. Stetsenko, SANS Studies of latent and etched ion tracks in PETP (poster), 17th International Conference on Nuclear Tracks in Solids, Dubna (Russia), 24-28 August 1994
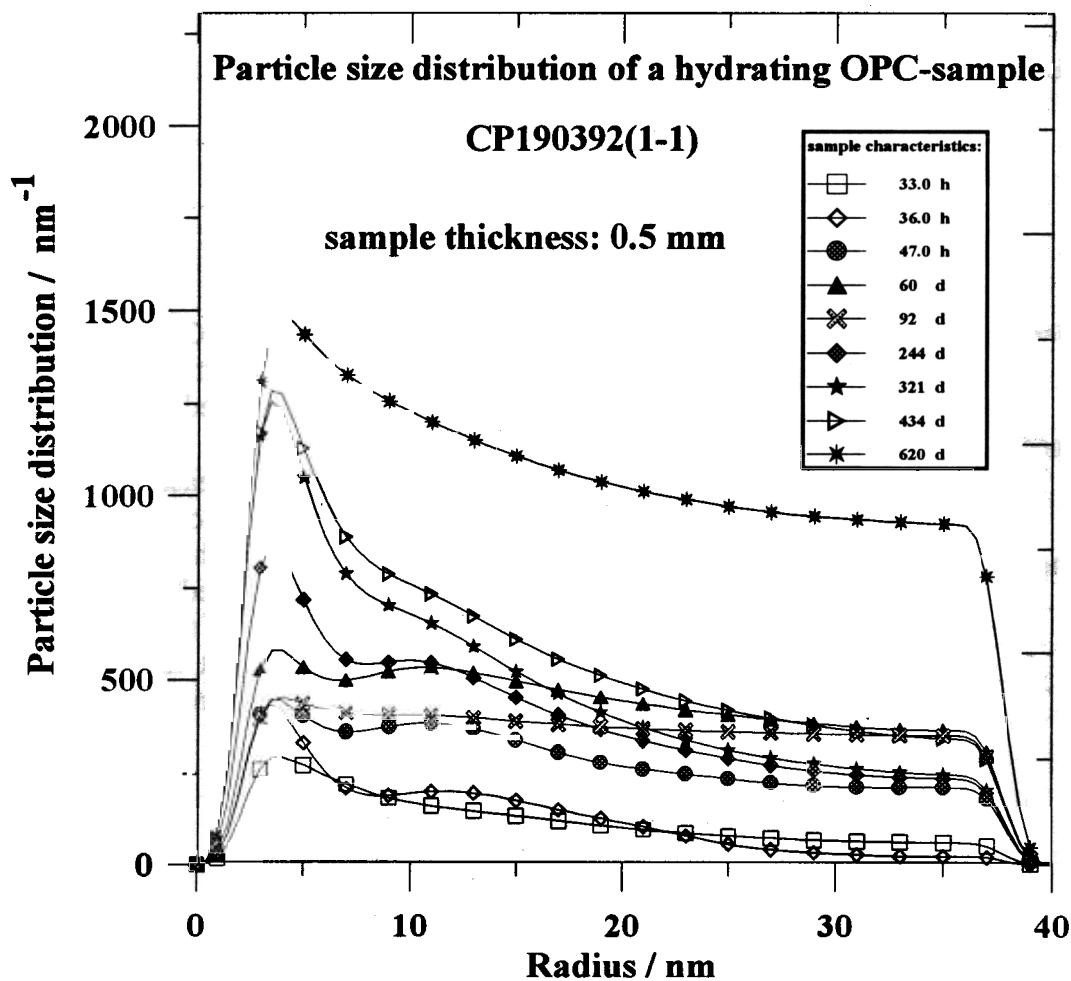
Fig. 1: Particle radius distribution of a hydrating OPC sample. The time-dependent evolution of this particle size distribution (PSD) is shown.
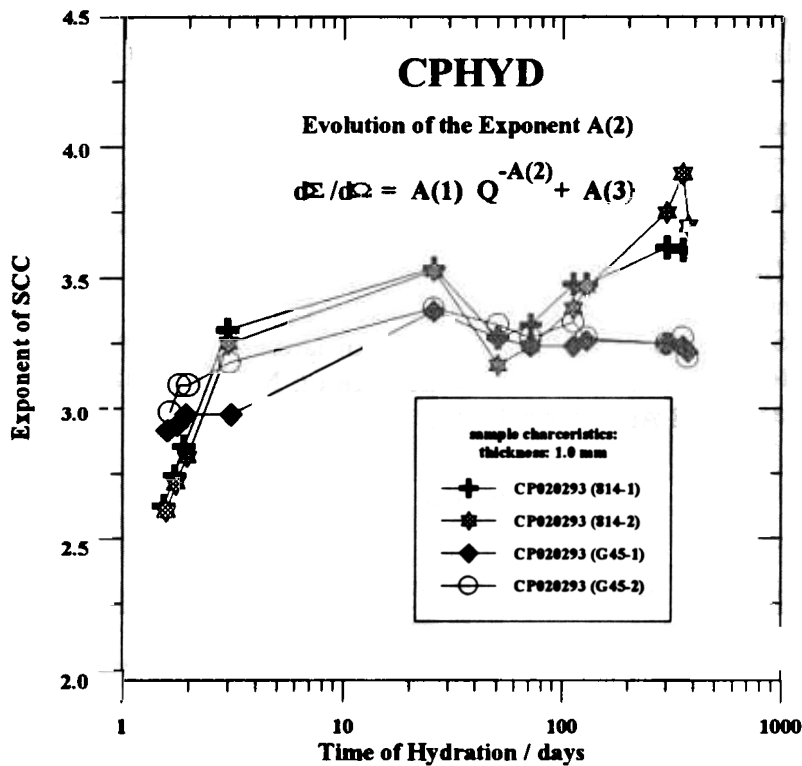
Fig. 2: The summary of the time-dependent behaviour of the exponent A(2). The dry clinker grains of OPC were separated into two classes ((8-14) μm, > 45 μm) The influence of the experimental parameter clinker grain size on the evolution is visible. The lines are drawn to connect the points.
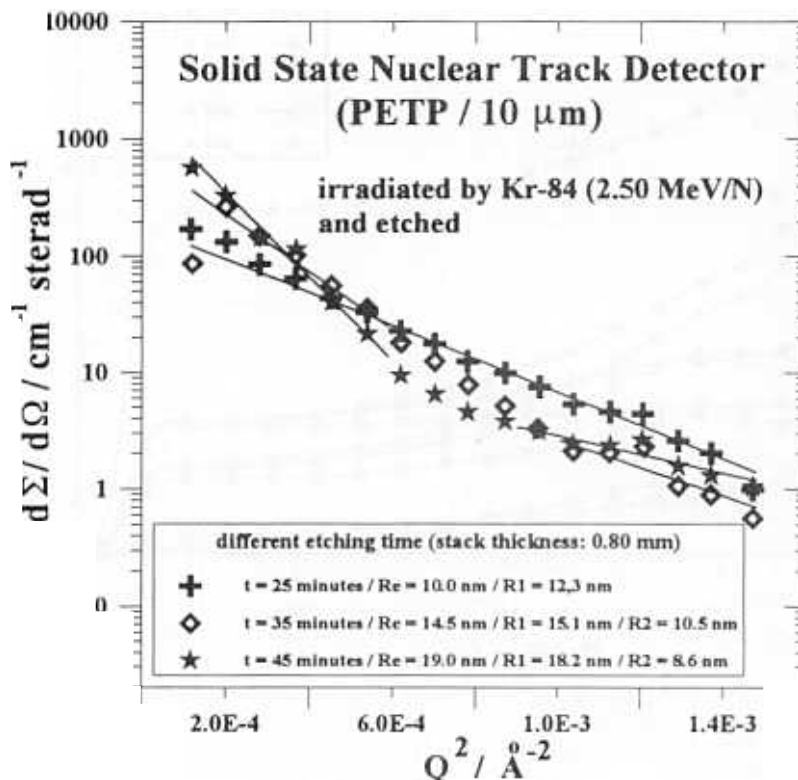
Fig. 3: Guinier plot of the scattering curve of irradiated and etched SSNDT. The radii R_e are measured by a conductometric method. The errors of the fit procedure for calculating the radii R (straight lines) are for about one per cent.

Low Resolution Model of Ribosomes and their Subparticles. Structural Model of the 50S Subunit of E.coli Ribosomes from Solution Scattering

D.I.Svergun, M.H.Koch

EMBL, Hamburg Outstation, Notkestrasse 85, D-22603 Hamburg, Germany;

I. Skou Pedersen

Department of Solid State Physics, Risø National Laboratory,

DK-4000 Roskilde, Denmark;

and I.N.Serdyuk

Frank Laboratory of Neutron Physics, Joint Institute
for Nuclear Research, 141980 Dubna, Moscow Region, Russia

Advances in crystallization of ribosomal particles have aroused hopes for their rapid decoding by X-ray analysis. However, a number of emerging problems have led many researchers to the conclusion that the decoding of the ribosome structure is, in all probability, a problem of the 21st century. Without disclaiming the possibility of obtaining electron density maps using powerful synchrotronic sources with a 5-10 Å resolution, we believe that new possibilities of small-angle scattering can today yield a 3-D resolution sufficient for constructing trustworthy models. The direct method of interpretation of scattering curves using spherical harmonics belongs to such possibilities [1-3]. In our work this method was applied to create a structural model of the large subunit of *E.coli* ribosomes.

The small-angle scattering intensity from monodisperse solution is proportional to the scattering from a single particle averaged over all orientations: $I(s) = <[F\{\rho(r)-\rho_o\}]^2>$, where $\rho(r)$ and ρ_o are the scattering length densities of the particle and the solvent, respectively, F denotes the Fourier transformation and s is the modulus of the scattering vector s, $s=(4\pi/\lambda)\sin\theta$, λ is the wavelength, and 2θ the scattering angle. The dependence of the scattering on the contrast $\bar{\rho} = \overline{\rho(r)}-\rho_o$, where $\overline{\rho(r)}$ is the average particle density, is given by (4)

$$I(s,\bar{\rho}) = \bar{\rho}^2 I_c(s) + \bar{\rho}I_{cs}(s) + I_s(s). \qquad (1)$$

$I_c(s)$ is the scattering of a uniform particle with the same shape ("shape scattering"), $I_s(s)$ that from inhomogeneities and $I_{cs}(s)$ is the cross

m. As the 50S subunit from *E.coli* is a two-component particle
ntaining 980 KDa RNA and 34 proteins with a total molecular mass of 460
)a, its scattering can also be represented as (5)

$$I(s,\overline{\rho}) = \overline{\rho}^2_{RNA}I_{RNA}(s) + \overline{\rho}_{RNA}\overline{\rho}_{pro}I_{Cross}(s) + \overline{\rho}^2_{pro}I_{pro}(s) \qquad (2)$$

ere $\overline{\rho}_{RNA}$, $\overline{\rho}_{pro}$ and $I_{RNA}(s)$, $I_{pro}(s)$ are the contrasts and the
attering intensities of the RNA and of the protein, respectively, and
$_{oss}(s)$ is again the cross-term. The scattering densities of the RNA
d proteins differ significantly from each other both for X-rays and
utrons so that contrast variation can provide valuable structural
ormation. Joint X-ray and neutron studies combine the advantages of
: high brilliance of synchrotron radiation and of the broader contrast
nge of neutrons.

50S ribosomal subunits of *E.coli* MRE600 bacteria were obtained by
: standard procedure [6]. The same batch of 50S ribosomal subunits was
:d as for X-ray and neutron experiments. In the X-ray experiments for
ntrast variation samples in buffers containing 0, 7, 14, 24, 32 and 38%
/w) sucrose were used. In the neutron experiments for contrast
riation samples in buffers containing 0, 14, 40, 67, 97% D_2O were used.

The X-ray scattering data were collected using X33 of EMBL on the
)rage ring DORIS III of DESY (Germany). The wavelength was $\lambda = 0.15$ nm
d the range of momentum transfer $[S_{min}, S_{max}] = [0.08, 1.53]$ nm^{-1}.

The neutron scattering experiments were performed at the Riso SANS
:ility using the cold source of the DR3 reactor. Two experimental
ttings were used: sample-detector distance 3 nm, average wavelength $\lambda =$
8 nm (setting 1 covering the range of momentum transfer $0.09 < s < 0.70$
n^{-1}) and sample-detector distance 1 m, average wavelength 0.6 nm
:tting 2, $0.4 < s < 2.0$ nm^{-1}). The neutrons were monochromatized by a
:chanical velocity selector giving a wavelength distribution with
ll-width-half- maximum $\Delta\lambda/\lambda = 0.18$.

The neutron scattering experiments were performed also at the IBR-2
actor using the YUMO instrument. Two experimental settings were used:
) sample-detector distance 10.52 m (detector-1 in this position covers
e range of momentum transfer from 0.07 to 1.2 nm^{-1}) and (2)
mple-detector distance 8.47 m (detector-2 in this position covers the
nge of momentum transfer from 0.5 to 2.5 nm^{-1}).

The scattering curves obtained are presented in Fig. 1 and Fig. 2.
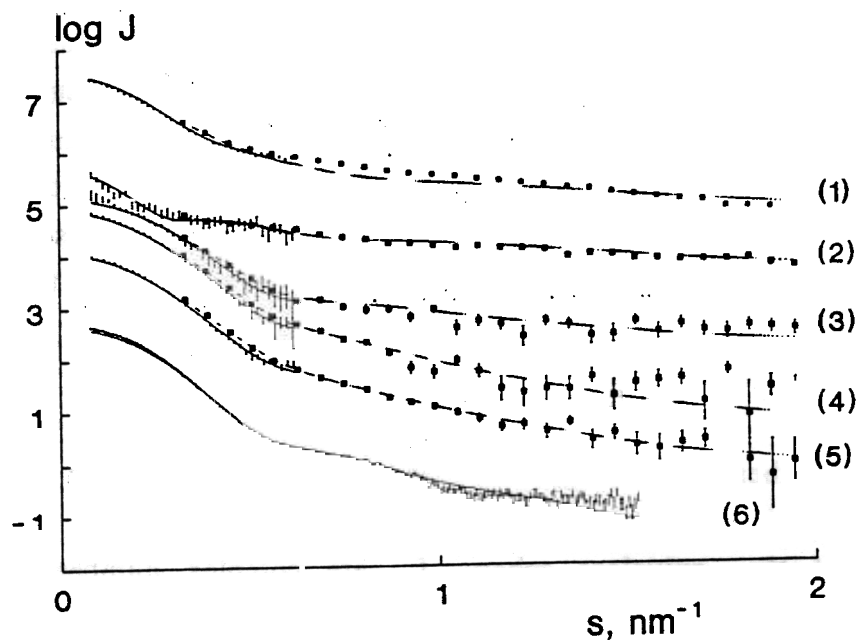
Fig. 1. Contrast variation data from the 50S ribosomal subunit. (1) to (5) neutron data in 0, 14, 40, 67 and 96% D_2O (Riso, Denmark). (6) X-ray scattering in H_2O (Desy, Hamburg). For clarity, successive curves are displaced down by one logarithmic unit.
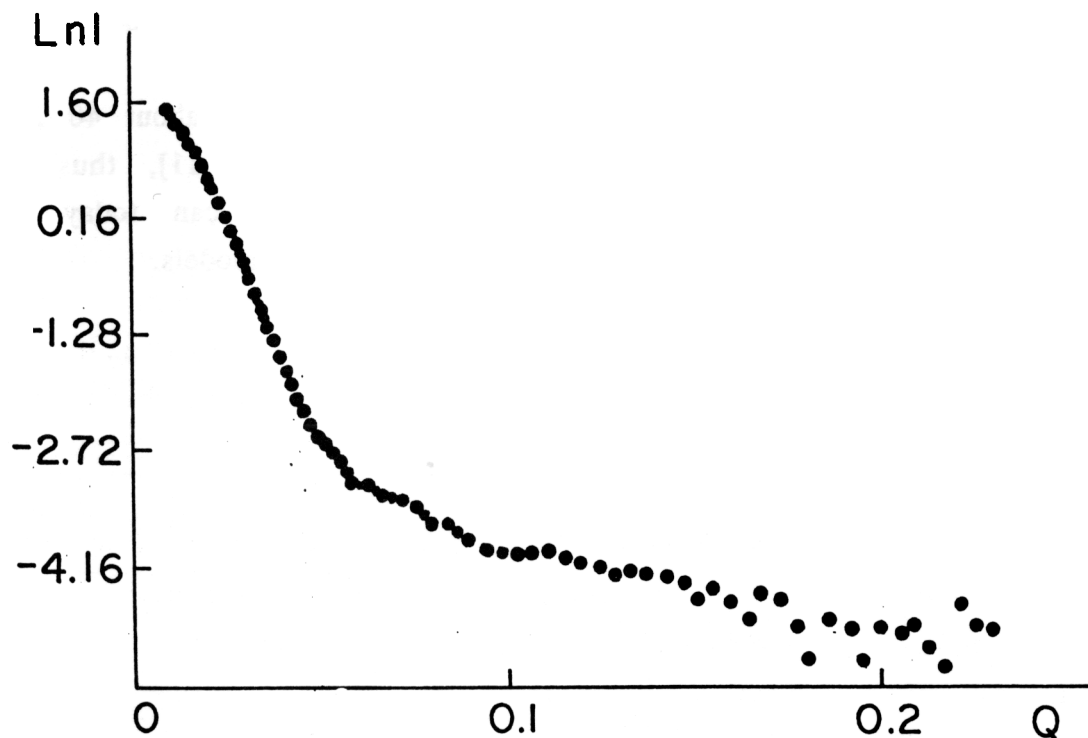
Fig. 2. Neutron scattering curve from the 50S ribosomal subunit in D_2O (IBR-2, Dubna).

73

Decomposition into the basic scattering functions according to Eq. 1 or Eq. 2 by the indirect transform program CGNOM (6) yielded the integral parameters. These are in good agreement with earlier results (7-9) and confirm that RNA forms a compact core surrounded by a protein shell.

At the next step the shapes of the 50S subunit and of the RNA were determined. The envelope of a globular particle can be described by the angular function $F(\omega)$ which is parametrized using the multipole expansion:

$$F(\omega) \simeq \sum_{l=0}^{L} \sum_{m=-l}^{l} f_{lm} Y_{lm}(\omega), \qquad (3)$$

where the highest value of L determines the resolution (the angular resolution is $\pi/(L+1)$ and spatial resolution is $R_o\pi/(L+1)$, where R_o is the radius of the equivalent sphere, f_{lm} are complex numbers, $Y_{lm}(\omega)$ are spherical harmonics and (r,ω) are spherical coordinates. The partial amplitudes $A_{lm}(s)$ in the corresponding scattering intensity

$$I(s) = 2\pi^2 \sum_{l=0}^{L} \sum_{m=-l}^{l} |A_{lm}(s)|^2, \qquad (4)$$

are expressed in terms of a power series with coefficients that are non-linear combinations of the shape coefficients f_{lm}. Using Eqs 2 and 3 for $I_c(s)$ and $I_{RNA}(s)$ the envelopes of the 50S and of the RNA were evaluated by a minimization procedure and presented in Fig. 2.

Our model for the 50S subunits (spatial resolution about 40 Å) is in good agreement with electron-microscopic models [10, 11], thus showing that the new possibilities of small-angle scattering can today yield a spatial resolution sufficient for constructing trustworthy models.
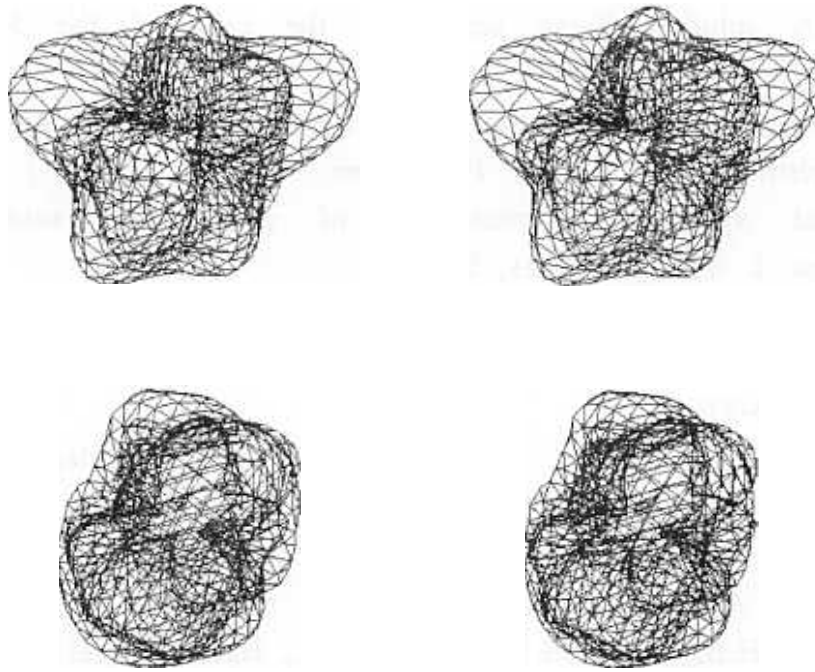
Fig. 3. Stereo pairs of the model of the 50S subunit (the particle envelope is shown in a red wireframe, the RNA-rich core in a blue wireframe). Crown view (top), kidney view (down). Bar length represents 50 Å.

REFERENCES

1. Stuhrmann H.B., Koch M.H.J., Parfait R., Haas J., Ibel K. and Crichton R.R. (1977). Shape of the 50S subunit of *Escherichia coli* ribosomes. Proc. Natl. Acad. Sci. USA 74, 2316-2320.

2. Svergun D.I. (1993) A direct indirect method of small-angle scattering data treatment. J. Appl. Crystallogr. 26, 258-267.

3. Svergun D.I. (1994) Solution scattering from biopolymers: advanced contrast variation data analysis. Acta Crystallogr., sect. A. 50, in the press.

4. Stuhrmann H.B. and Kirste R.G. (1965) Elimination der intrapartikularen Untergrundsteuung bei der Rontgenkleinwinkelstruung am kompakten Teilchen (Proteinen). Zeitschrift für Physikalische Chemie Neue Folge 46, 247-250.

5. Tardieu A. and Vachette P. (1982) Analysis of models of irregular shape by solution X-ray scattering: the case of the 50S ribosomal subunit from *E.coli*. EMBO J. 1, 35-40.

6. Gavrilova L.P., Kostiashkina O.E., Koteliansky V.E., Rutkevitch N.M. and Spirin A.S. (1976) Factor-free ("non-enzymatic") and factor-dependent system of translation of polyuridylic acid by *E.coli* ribosomes. J. Mol. Biol. 101, 537-552.

7. Serdyuk I.N., Smirnov N.I., Ptitsyn O.B. and Fedorov B.A. (1970) On the presence of a dense internal region in the 50S subparticle. FEBS Lett. 9, 324-326.

8. Serdyuk I.N. (1979) A method of joint use of electromagnetic and neutron scattering: a study of internal ribosomal structure. In: Methods in Enzymology (Moldave K. and Grossman L., eds.) vol. LIX, pp.750-775, Acad. Press, New York.

9. Stuhrmann H.B., Koch M.H.J., Parfait R., Haas J., Ibel K., De Wolf B. and Crichton R.R. (1976b) New low resolution model for 50S subunit of *E.coli* ribosomes. Proc. Natl. Acad. Sci. USA 73, 2379-2383.

10. Vasiliev V.D., Selivanova O.M. and Ryazantsev, S.N. (1983) Structure of the *E.coli* 50S ribosomal subunit. J. Mol. Biol. 1191, 561-569.

11. Redemacher M., Wagenknecht T., Verschoor A. and Frank J. (1987) Three-dimensional structure of the large ribosomal subunit from *E.coli*. EMBO J. 6, 1107-1114.

Neutron Scattering Studies of Pressure Induced Phase Transitions in NH$_4$HSO$_4$

L.Bobrowicz[1], I. Natkaniec[2], T.Sarga[2] and S.I. Bragin

Frank Laboratory of Neutron Physics, JINR, 141980 Dubna, Russia

Ammonium hydrogen sulphate (AHS), NH$_4$HSO$_4$, undergoes two solid phase transitions at atmospheric pressure. It was shown that in the temperature range of phase II, between 270 K and 154 K, AHS is ferroelectric [1]. Nuclear spin lattice relaxation time experiments [2] indicate a remarcable change in NH$_4$ motion at lower transition temperature, while no change is found at the upper phase transition. The ferroelectric properties of this crystal disappear with with increasing hydrostatic pressure [3] and proton superionic conductivity was observed at temperatures above 460K and pressures 500 MPa [4].

The results of neutron powder diffraction (NPD) and inelastic incoherent neutron scattering (IINS) investigations of the different AHS solid phases in the temperature range of 100 - 300 K under hydrostatic pressures up to 400 MPa are presented. The measurements were performed on the NERA inverted geometry spectrometer [5] of the IBR-2 pulse reactor at JINR in Dubna. The gas compressor made by UNIPRESS (Warsaw, Poland) was used as a high pressure source.

No change was found in the NPD and IINS spectra for the I - II second order phase transition at 270 K, while the II - III first order phase transition at 154 K was clearly seen .The latter phase transition is marked by a change in crystal structure and proton dynamics.
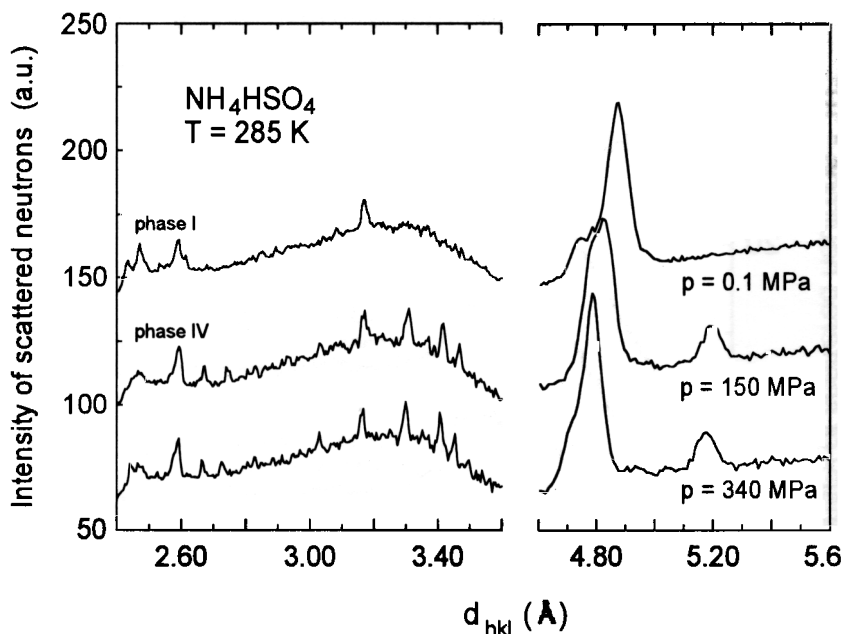
Fig.1. Pressure dependence of the neutron powder diffraction spectra of NH$_4$HSO$_4$.

1) On leave from the Institute of Physics, A.Mickiewicz University,
   60-780 Poznan, Poland.
2) On leave from the H.Niewodniczanski Institute of Nuclear Physics,
   31-342 Krakow, Poland

The latter phase transition is marked by a change in crystal structure and proton dynamics. In the low temperature phase III well resolved bands corresponding to the latice vibrations,translational and torsional vibrations of NH_4 ions, torsions of HSO_4 ions and internal vibrations of the SO_4 tetraedron are clearly seen.With increasing temperature these bands are smeared and look quite similar above ca 250 K in the both II and I phases [6].
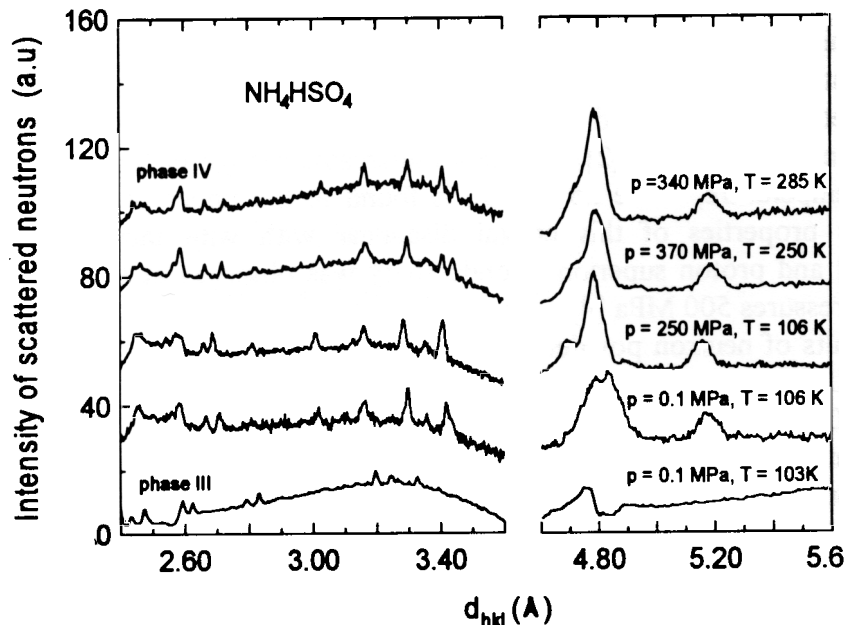
Fig.2. Neutron powder diffraction spectra of NH_4 HSO_4 at different pressures and temperatures.
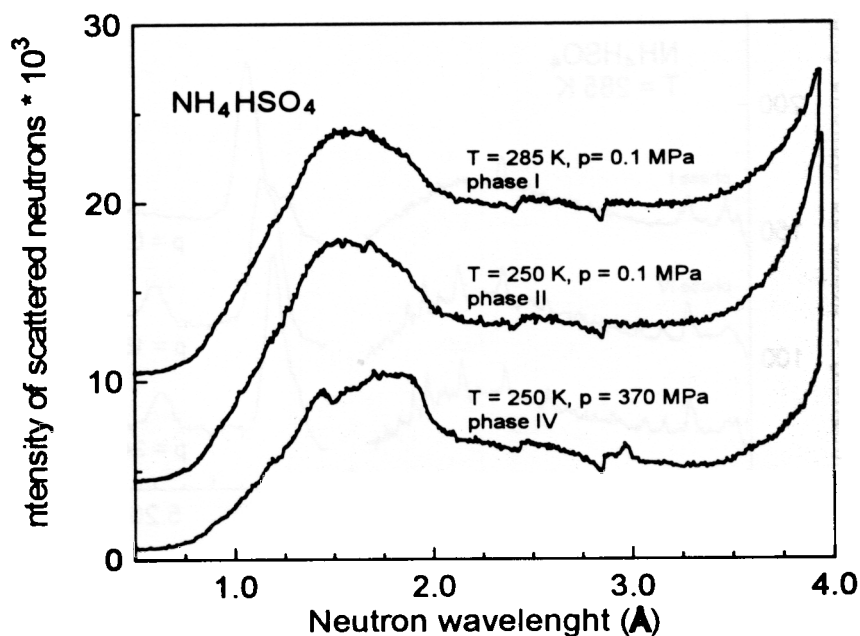
Fig.3. The IINS spectra of the phases I, II and IV of ammonium hydrogen sulphate.

With increasing hydrostatic pressure at the temperatures of 290 K (phaseI) and 250 K (phase II) we have observed the first order transition to phase IV (Fig.1 and 2).

Below ca. 250 K phase IV becomes matastable and can exist even in atmospheric pressure within temperature region of the phases II and III. With increasing temperature phase IV transforms directly to phase I at about 270 K. As it is shown in Fig.3 the IINS spectra of phases I, II and IV indicate on the stochastic character of hydrogen motion above the temperature of the II - III phase transitions. The quasielastic broadening caused by the fast reorientation of protons in the phase IV is smaller then in phases II and I. The diferences in vibrational spectra of phases III and IV (Fig.4) at low temperatures are caused by the ordering of NH_4^+ ions in two different crystal structures.
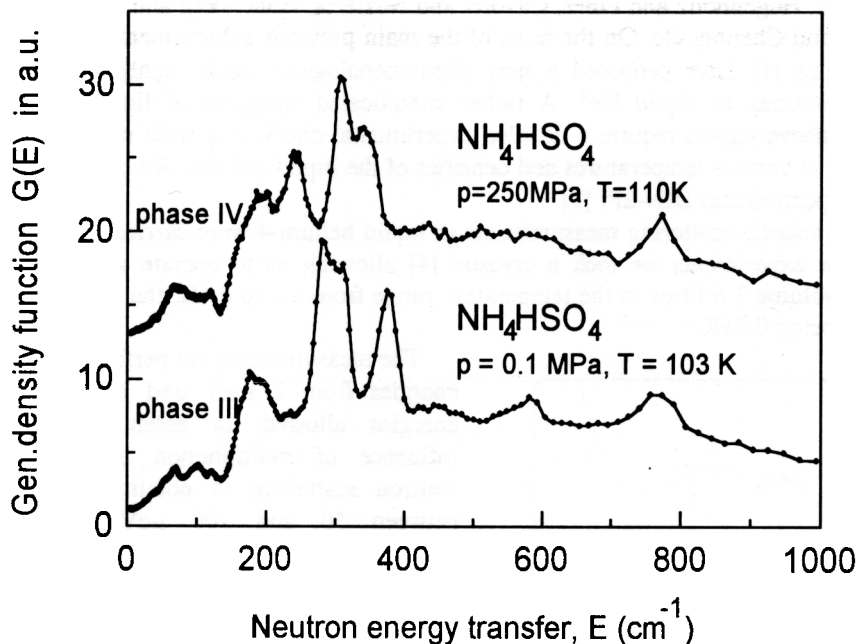
Fig.4. Generalized phonon density of states of the phases III and IV of NH_4 HSO_4.

References:

1. R. Pepinsky, K. Vedam, S. Hoshino, Y.Okaya, Phys. Rev., 111, 1508 (1958).
2. R. Miller, R. blinc, M. Brenman and J.S. Waugh, Phys. Rev., 126, 528 (1962).
3. I.N. Polandov, V.P. Mylov, B.A. Strukov, Fiz. Tverdovo Tela, 10, 2232 (1968).
4. A.N. Baranov, E.G. Ponyatovsky, V.V Sinitsyn, R.M. Fedosyuk, L.A. Shuvalov, Krystallografiya, 30, 1121 (1985).
5. I. Natkaniec, S.I. Bragin, J. Brankowski, J. Mayer, Proc. ICANS - XII, Abingdon 1993, RAL Raport 94-025, Vol.I. p.89-96.
6. L. Bobrowicz, K. Holderna- Natkaniec, M.Mroz, I. Natkaniec, W. Nawrocik, Ferroelectrics (1994) - submitted.

INVESTIGATIONS OF THE LIQUID HELIUM-4 EXCITATIONS SPECTRUM STRUCTURE

I.V.BOGOYAVLENSKII[a], L.V.KARNATSEVICH[a], Zh.A.KOZLOV[b], A.V.PUCHKOV[c]

[a]Institute of Physics and Technology, Kharkov, 310108, Ukraine
[b]Joint Institute for Nuclear Research, Dubna, 141980, Russia
[c]Institute of Physics and Power Engineering, Obninsk, 249020, Russia

The questions of fundamental physical reasons for the transformations of the excitation spectrum in liquid He^4 in the transition from the superfluid to normal phase is still open for discussion. Progress in understanding this behaviour was achieved due to the development of the microscopic theory of Bose-liquids by Belyaev, Hogenholtz and Pines, Gavoret and Nozieres, Hohenberg and Martin, Shepfaluzy and Kondor, Griffin and Cheung, etc. On the basis of the main previous achievements of the theory Griffin, Glyde and Stirling [1] have proposed a new phenomenological model qualitatively describing the spectrum of excitations in liquid He^4. A rather complicated spectrum of liquid helium excitations predicted in the above papers require a detailed experimental check in a wide range of wave vectors q from 0 to 3.5 Å^{-1} at various temperatures and densities of the liquid helium. We could start realizing this check on a new spectrometer DIN-2PI [2].

The neutron inelastic scattering measurements in liquid helium-4 were carried out using the DIN-2PI spectrometer. For experiments we took a cryostat [4] allowing us to operate with a sample of liquid helium-4 of the volume 3.6 litres in the temperature range from 4.2 to 0.4K, the accuracy in maintaining the temperature being 0.01K.
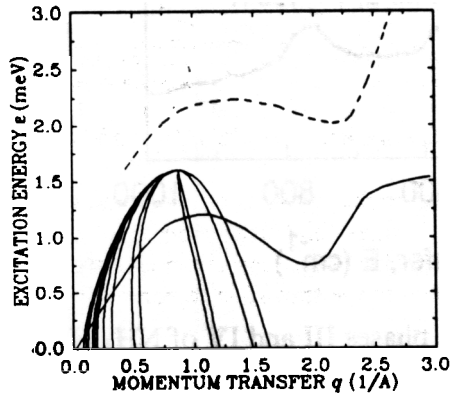
Fig. 1. The phonon-maxon-roton dispersion curve in superfluid helium-4 (solid line) and multiphonon excitations (dashed line). Set of kinematic laws at various angles scattering at incident neutron energy 1.6 meV is shown.

The measurements are performed at initial neutron energies from 2 meV and lower. The low initial energies allowed an essential reduction of the influence of multiphonon and multiple inelastic neutron scattering to obtain improved resolutions between 50 and 100 μeV, depending on the wavevector. Fig.1 illustrated this words and shows set of kinematic laws at initial neutron energy 1.6 meV. Themeasurements of the double differential cross section of the liquid helium were carried out at the initial neutron energies E_o=1.6; 2.08; 2.45; 3.5 meV and temperatures T=0.42; 0.45; 1.4; 1.45; 1.5; 1.72; 2.0; 2.05; 2.21; 2.25K in the range of the angle scattering from 5 to 135° (or wave vector from 0.08 to 2.5Å^{-1})[5].The main results of our analyse are shown in fig.2. The analyse was performed by the next way. The experimental double differential cross section of the liquid helium was transformed to the dynamic structure factor $S(q,\varepsilon)$. The shape of $S(q,\varepsilon)$-peaks were described by the various models. We could distinguish three characteristic regions of the wave vector q for which peaks are also different in shape. These are: the initial phonon part of the dispersion curve, when $q<0.5$Å^{-1}, the maxon-roton region of excitation, when $q>0.65$Å^{-1}, and the so-called transition region, when $0.5<q<0.65$Å^{-1}.

Below T$_\lambda$ in the maxon-roton region, a one-particle sharp peak of $S(q,\varepsilon)$ is ill described by a single Gaussian (G) or a single Lorentzian convoluted with a Gaussian (LG). A two-Gaussian model (G+G) and a two-convolution model (LG+LG) provides a better description of the sharp peak (in terms of χ^2, the correlation coefficients of the model parameters, and other statistical criteria of approximation). Two components of the scattering peak differ significantly in width, therefore, we will call one of them the narrow component (n) and mark it on the fig.2 by the solid circles; and the other, the wide component (w) and mark it by the open circles.

In the phonon region of the spectrum, these components are observed also. For the reason to be understood from a subsequent consideration, the narrow component here may be different in nature from the (n)-component and we will denote it by (zs) and mark it on the fig.2 by the triangles. The wide component is well seen in this region only about T_λ and at lower T its intensity decreases, thus making its separation difficult. In the transition region, the picture is the most complicated. Here, obviously, all
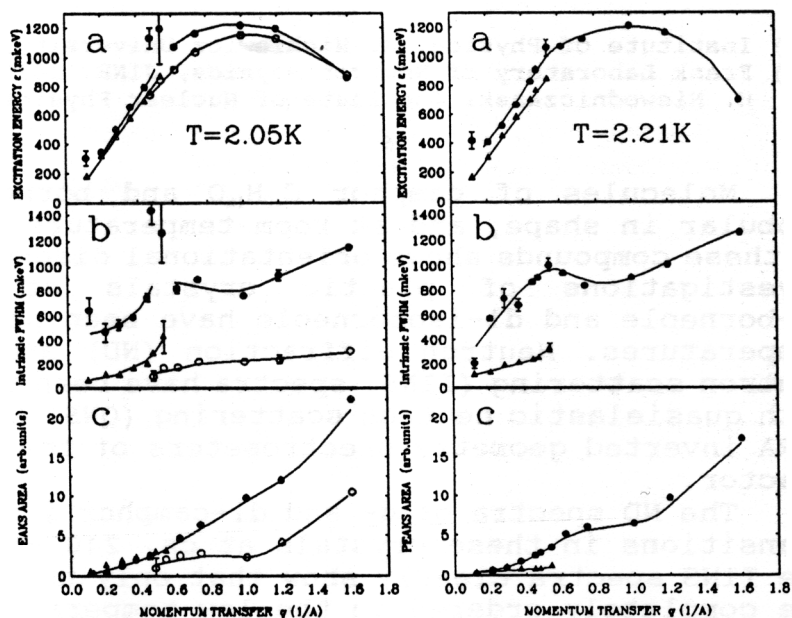
Fig. 2. The result of the description of experimental $S(q,\varepsilon)$ at various T by the (G+G) and (G)-model.

Above T_λ in the maxon-roton part of spectrum only wide peaks (w) are observed, and they are well described by one (G) or one (LG). In the phonon region, besides the broad component (w) a narrow component (zs) is seen. In the transition region, the latter component becomes rapidly attenuating and above $q \sim 0.65\text{Å}^{-1}$ it is not observed at all. The broad component in the transition region is ill defined. The narrow component (n) typical of He II is not observed above T_λ.

The modern experimental facilities of the spectrometer DIN-2 admit the detailed research of inelastic scattering in helium. The results were represent via the fit of the initial experimental data by the Gauss-Gauss and Gauss-Lorentz convolutions and it promoted us to follow the evolution of the peak of the scattering as a function of T and q. The origin of spectrum, in brief, is in accordance with the Griffin-Glyde theory. The (n)-component may be identified as the result of the quasiparticle excitations. In the normal state the narrow (zs) phonon branch may be explained as the zero-sound mode, and as the superposition of such a mode with phonon part of quasiparticle excitation in superfluid phase. The (w)-component may be understood as the collective excitations of phonon type, usual for the classical liquids. As to the mechanism of "interaction" among these three branches, the Griffin and Glyde's idea about the hybridisation of quasiparticles with the density fluctuations due to the presence of Bose-condensate to be adequate to the picture presented above.

References
[1] A.Griffin, Can.J.of Phys. 65 (1987) 1357; W.G.Stirling, H.R.Glyde, Phys.Rev. B41(1990) 4224; H.R.Glyde, A.Griffin, Phys.Rev.Lett. 65 (1990) 1454; H.R.Glyde, Phys.Rev. B45 (1992) 7321.
[2] N.M.Blagoveshchenskii et al., JETP Lett.,57(1993)428; N.M.Blagoveshchenskii et al., Physica B194-196 (1994) 545.
[3] A.V.Abramov et al., Atomnaya Energiya 66 (1989) 316, (in Russian).
[4] I.V.Bogoyavlenskii et al., Cryogenics 3 (1983) 498.
[5] N.M.Blagoveshchenskii et al., Phys.Rev., to be published.

NEUTRON SCATTERING STUDIES OF ORIENTATIONAL DISORDER IN CAMPHOR-LIKE PLASTIC CRYSTALS IN THE TEMPERATURE RANGE OF 10 - 300 K

K. Holderna-Natkaniec (1), I. Natkaniec (2)

(1) Institute of Physics, A. Mickiewicz University, 60-780 Poznan, Poland
(2) Frank Laboratory of Neutron Physics, JINR, 141980 Dubna, Russia
    H. Niewodniczanski Institute of Nuclear Physics, 31-342 Krakow, Poland

Molecules of camphor $C_{10}H_{16}O$ and borneole $C_{10}H_{18}O$ are nearly globular in shape, and at room temperature, the crystal structure of these compounds shows orientational disorder. Neutron scattering investigations of plastic crystals of d- and dl-camphor, dl-borneole and dl-isoborneole have been performed down to helium temperatures. Neutron diffraction (ND) and inelastic incoherent neutron scattering (IINS) spectra have been recorded simultaneously with quasielastic neutron scattering (QNS) spectra on the KDSOG and NERA inverted geometry spectrometers of the IBR-2 high flux pulsed reactor.

The ND spectra of d- and dl-camphor indicate structural phase transitions in these crystals at ca. 240 and 200 K, respectively. The IINS spectra clearly show that only the molecules of d-camphor are completely ordered in the low temperature phase. In addition, only six reflections in the ND spectra of dl-camphor and dl-isoborneole have been well observed down to 10 K. This relatively small number of reflections suggests the orientational disorder of molecules in the low temperature phase of tetragonal symmetry. Temperature dependence of the lattice spacing end intensity of these reflections evidently confirms the structural phase transition at 200K in dl-camphor and weakly indicates the transition at 290 K in dl-isoborneole within the tetragonal symmetry. The ND reflections of dl-borneole can be indexed in the cubic symmetry. Their temperature behaviour does not indicate any structural phase transition down to helium temperatures.

IINS spectra measured at low temperatures shows that internal molecular vibrations are well separated from crystal lattice vibrations. The differences in lattice and internal molecular vibrations of d- and dl- camphor are caused by intermolecular interactions related to various molecular packings in the crystals. Appropriate differences between the IINS spectra of dl-camphor and dl-isoborneole reflect the dynamics of slightly different molecules with the same crystal structure. Comparison of IINS spectra of dl-borneole and dl-isoborneole indicates the difference in the dynamics of similar molecules caused by various molecular conformation and crystal packing. The ND and IINS spectra of dl-borneole exhibits that the disorder characteristic of the plastic phase of camphor-like substances might be frozen down to helium temperatures. The QNS component in these substances is relatively weak and is caused mainly by stochastical jumps of methyl groups observed at temperatures above 100K.

$C_{10}H_{16}O$ $C_{10}H_{17}OH$

CAMPHOR   ISOBORNEOLE   BORNEOLE

$C_{10}H_{17}OH$
dl-izborneol

T=340K
T=290K
T=240K
T=200K
T=140K
T=80K
T=10K

$C_{10}H_{16}O$
dl-camphor

T=286K
T=240K
T=210K
T=190K
T=150K
T=100K
T=10K

IINS Intensity (a.u.)

Incident Neutron Wavelength in (A)
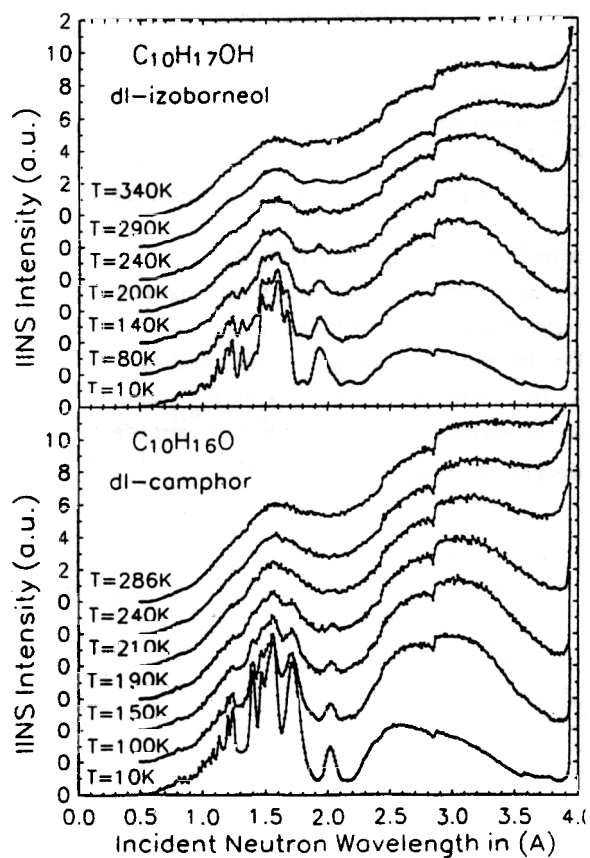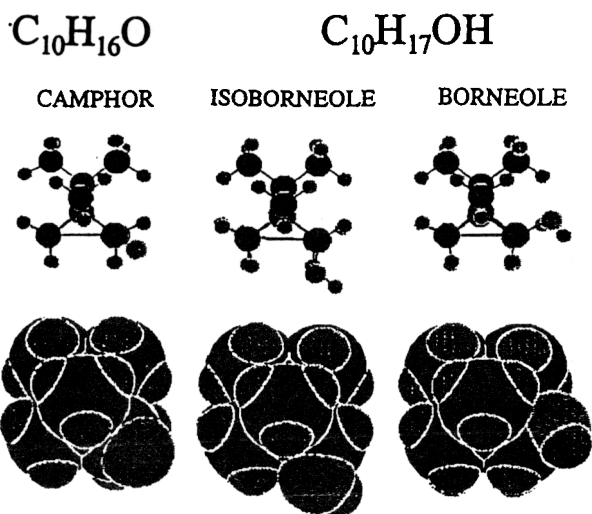
Temperature dependence of IINS spectra

$C_{10}H_{17}OH$
dl-borneol
d-borneol

G(E) (arbitrary units)

$C_{10}H_{17}OH$
dl-borneol
dl-izborneol

$C_{10}H_{16}O$
dl-camphor
d-camphor

Neutron Energy Transfer in cm^{-1}
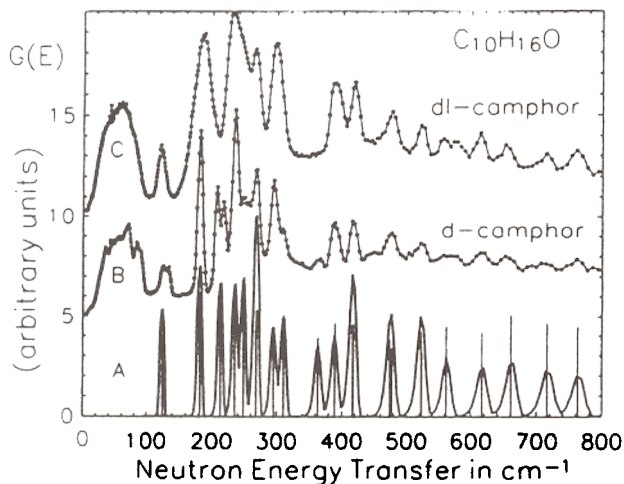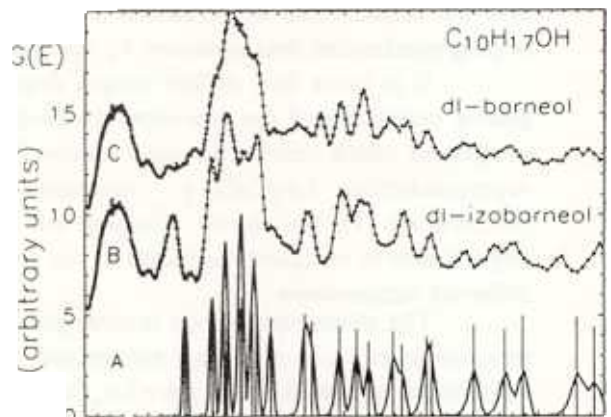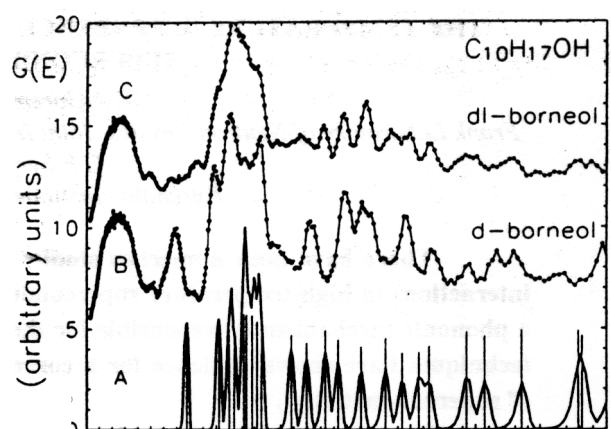
Vibrational spectra weighted to hydrogen atoms displacements:
A - calculated spectra of intra-molecular vibrations
B and C - experimental results at 10 K.

83

THE TEMPERATURE DEPENDENCE OF THE PHONON DENSITY OF STATES OF SUPERCONDUCTING $La_2CuO_{4.1}$

E.A.Goremychkin, I.L.Sashin.

Frank Laboratory of Neutron Physics, Joint Institute for Nuclear Research, Dubna, 141980, RUSSIA
G.F.Syrykh, V.P.Glazkov
Kurchatov Institute, 123182, Moscow, RUSSIA

There have been numerous studies indication the importance of the electron-phonon interactions in high-temperature superconducting ceramics, although it is not established that a phononic mechanism is responsible for the superconducting transition.Various spectroscopic techniques have shown evidence for a correlation between the lattice dynamics and the onset of superconductivity .

The compound La_2CuO_4 is a non-superconducting antiferromagnet but it was found that the introduction of interstitial oxygen by high pressure and other techniques provides a doping mechanism that produces T_c approaching 40K.

It is know that at low oxygen doping levels there is a miscibility gap with the two phases consisting of the non-superconducting parent compound and a metallic oxygen-rich compound which carries the supercurrent. Recent studies phonon density of states (PDOS) of superconducting $La_2CuO_{4.1}$, measured by inelastic neutron scattering, at the room temperature (1), has shown softening low energy part of the PDOS This provides a useful opportunity to compare the PDOS in the parent compound with the doped superconductor at different temperature

The measurements on inverse geometry spectrometer at KDSOG , Dubna, show an unusual dependence of the low energy part of the PDOS on different temperature and oxygen stoichiometry.The PDOS of pure La_2CuO_4 shows no temperature dependence . However, for $La_2CuO_{4.1}$ it was found substantial increasing PDOS in the low energy range with the decreasing temperature . The comparison of the PDOS for superconducting $La_2CuO_{4.1}$ and non-superconducting parent has shown excessive density of states for superconduction sample up to 15 meV (FIG.1) and increasing $\Delta G(\varepsilon)$ with the decreasing temperature .
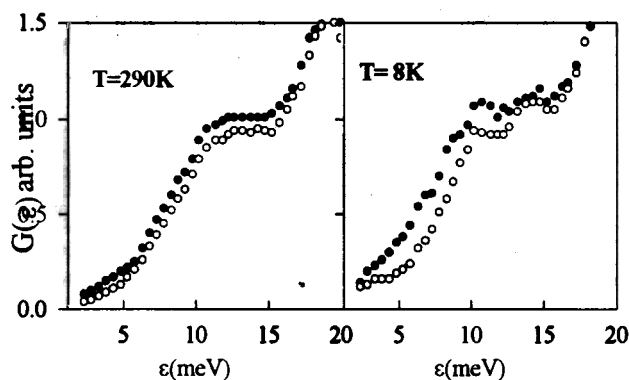
Fig.1. The PDOS of the La_2CuO_4(open circles) and $La_2CuO_{4+\delta}$ (closed circles) for T=290K and 8K

1. G.F.Syrykh et.al. "Superconductivity:physics, chemistry, technics", 1992, v.5, N11, p.2171.

THE CRYSTAL FIELD EFFECTS IN THE $YbCu_2Si_2$ COMPOUND

E.A. Goremychkin, A.Yu. Muzychka

I.M.Frank Laboratory of Neutron Physics, Joint Institute for Nuclear Research

The investigations of the dynamic magnetic susceptibility of the $YbCu_2Si_2$ compound, which is known as a compound with the intermediate valency (IV) of the rare earth ion, have been carried out with the help of the inelastic neutron scattering (INS). The greatest difficulty in the data processing was blending of the magnetic and phonon scattering.

Fig. 1 shows the scattering law at helium and room temperatures. An increase in $S(\varepsilon)$ with a decrease in temperature in the energy transfer region 20 to 40 meV points to a presence of a strong magnetic contribution to the neutron scattering in this region. On the other hand, the peculiarity in the region of small energy transfer values <5 meV is also of magnetic nature and it does not allow the magnetic scattering at >20 meV to be interpreted as the quasielastic one. It is just this peculiarity that is more likely to be a consequence of the quasielastic scattering. Thus, the magnetic response of the sample is a superposition of the quasielastic component with the line width of ~2.5 meV and the inelastic component, which is typical of the systems with heavy fermions (SHF) and not of the compounds with IV.

By means of the cosistent description of the spectra at T=10, 80, and 300 K, the magnetic response of the sample has been singled out (Fig. 2), on the basis of which the crystal field (CF) parameters have been obtained:

$$B_2^0 = -0.2; \quad B_4^0 = -0.21 \cdot 10^{-1}; \quad B_6^0 = -0.1 \cdot 10^{-4}; \quad B_4^4 = 0.46 \cdot 10^{-1}; \quad B_6^4 = 0.17 \cdot 10^{-2} \text{ (meV)}$$

The statistics deterioration with an increase in temperature seen in Fig. 2 is connected with the way of the data processing: the phonon component obtained by subtraction of the calculated magnetic one from the spectrum at T=10K was multiplied by the temperature occupancy factor and subtracted from the spectrum measured at the corresponding temperature.

The CF parameter analysis with the help of the superposition model [1], which has earlier been performed for the compounds with other rare earth elements [2,3], has allowed the internal parameters of the 4th and 6th orders for the Cu and Si coordination spheres to be determined:

$$A4(Si) = -0.06; \quad A4(Cu) = -5.5; \quad A6(Si) = 2.0; \quad A6(Cu) = 1.5 \text{ (meV)}$$

The comparison of these values with corresponding parameters of other rare earth elements gives one the grounds to make a conclusion that strong hybridization of the f-electrons and the Cu electrons takes place in this compound contrary to the $CeCu_2Si_2$ SHF, where the Si electrons participated in the hybridization with the f-electrons.
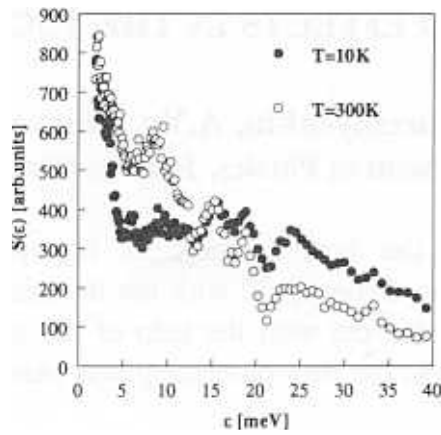
Fig. 1. The scattering law for YbCu2Si2 for different temperatures.
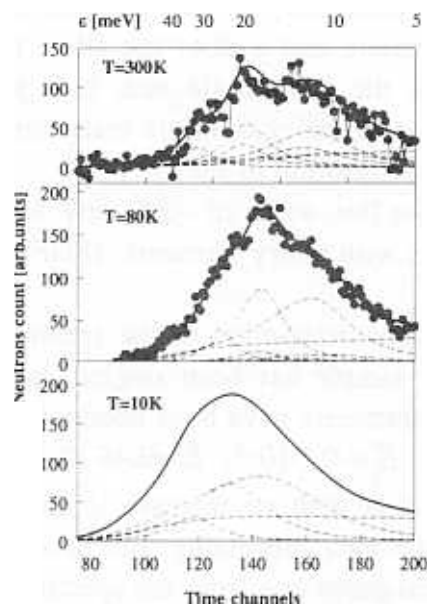
Fig. 2. Magnetic response at different temperatures:
   points represent the response extracted from the experimental spectrum;
   solid line represents the result of the calculation performed on the basis of the
obtained CF parameters;
   thin lines represent separate spectrum components.

1. D.J. Newman and B. Ng, Rep. Prog. Phys. **52** (1989), pp. 699-763
2. E.A. Goremychkin, A.Yu. Muzychka and R. Osborn, Pysica B **179**, 184 (1992)
3. E.A. Goremychkin, A.Yu. Muzychka, R. Osborn. Theses of the XXX workshop on the low temperatures. Dubna, 1994, v.2, p.224 (in Russian)

THE SPECTRUM OF THE INELASTIC NEUTRON SCATTERING FROM THE POLYMETHYLSILICATE ACID XEROGEL

V.D.Khavryuchenko, A.V.Khavryuchenko
Institute of Surface Chemistry, Ukrainian Academy of Sciences, Kiev

A.Yu.Muzychka
Frank Laboratory of Neutron Physics, JINR, Dubna, Russia

The polymethylsilicate acid xerogel is used in medical practice as a highly active enterosorbent, however, the mechanism of its action has not been investigated. The main obstacle consists in an uncertainty of its amorphous state structure. The only way to investigate the structure of such materials is the vibration spectroscopy, which includes both experimental methods (infrared spectroscopy and the inelastic neutron scattering spectroscopy) and the calculation methods in chemistry. To realize it, we have obtained with the help of the inelastic neutron scattering the amplitude-weighed spectrum of the vibration state density for an industrial sample of dried polymethylsilicate acid xerogel (Fig. 1).

According to performed calculations of the cluster models of the structure of this material, a preliminary description of the vibration spectrum may be done as follows:

- the region of 0 to 60 cm^{-1} corresponds to the torsional vibrations of the O_3SiCH_3 tetrahedra relative to the Si-O-Si bounds;

- the region of 180 cm^{-1} corresponds to the torsional vibrations of the methyl group;

- the region of 320 cm^{-1} corresponds to the deformation vibrations of the O-Si-C angles;

the region of 800 cm corresponds to the deformation vibrations of the Si-CH$_3$ angles.

Nature of peculiarities in the regions of 1500 cm^{-1} and 4000 cm^{-1} will be cleared up in further investigations.
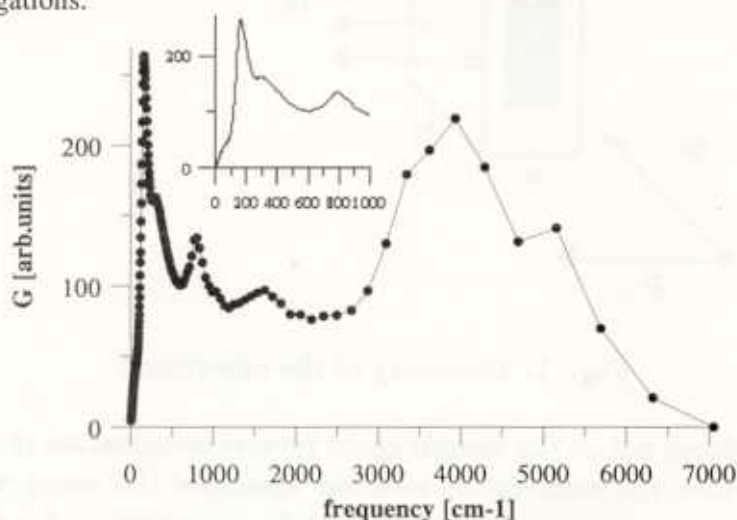
Fig. 1. Polymethylsilicate acid xerogel. The inelastic neutron scattering spectrum.

ANOMALOUS DEPENDENCE OF NEUTRON DEPOLARIZATION ON MAGNETIC FIELD IN YBa$_2$Cu$_3$O$_{6.9}$ CERAMICS NEAR T_c.

V.L.Aksenov, E.B.Dokukin, V.K.Ignatovich,
S.V.Kozhevnikov, E.I.Kornilov, Yu.V.Nikitenko, A.V.Petrenko
Frank Laboratory of Neutron Physics, Joint Institute for Nuclear Research, Dubna,
Russia

Yu.V.Bugoslavskij, A.A.Minakov,
Institute of Physics of the Russian Academy of Sciences, Moscow, Russia

This research is devoted to the investigation of magnetic field penetration inside the HTSC, YBa$_2$Cu$_3$O$_{6.9}$ and of the vortex system dependence on temperature and magnetic field strength. The method is based on neutron depolarization measurements as described in [1]. Former experiments [2-5] were performed in the temperature range of $T < 0.5T_c$. Here we report the results of measurements in the temperature range near T_c in a field up to 1 Tl where the HTSC exhibit new properties that were not previously observed.

The experiments were performed at the SPN-1 spectrometer of polarized neutrons of IBR-2. Neutrons were polarized and transmitted through the sample of YBa$_2$Cu$_3$O$_{6.9}$ as shown in fig.1. Dimensions of the sample and directions of the external magnetic field, neutron polarization and the beam are included. The sample had a transition temperature T_c=90.4 K with a transition region width of 1 K, and its density was $\rho = 4.9$ g/cm^3. It had a texture and the axis (001) of crystallites was oriented mainly along the "a"-direction of the parallelepiped, shown in fig.1.
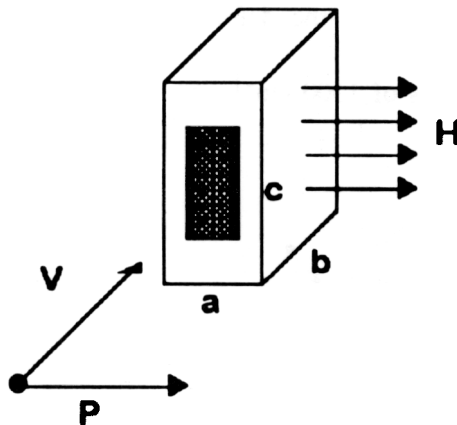
Fig. 1. Geometry of the experiment

A spin flipper placed before the sample could reverse polarization of the incident beam. A detector placed after the polarization analyzer measured the count rate $N^\pm(H,T,\lambda)$ of the transmitted beam in dependence on the field H, temperature T and the wave length of neutrons λ, with spin flipper switched off (+) and on (-) respectively, i.e., when the spin of the incident neutrons was directed along the field and against it.

Polarization of the transmitted beam, $P(H,T,\lambda)$, was determined as the ratio:

$$P(H,T,\lambda) = \frac{N^+(H,T,\lambda) - N^-(H,T,\lambda)}{N^+(H,T,\lambda) + N^-(H,T,\lambda)}. \tag{1}$$

The ranges of variables were: $0.5 < \lambda < 15\text{Å}$, $0 < H < 10$ kOe, $77 \le T \le 94$ K, respectively.

Information about processes inside the sample was extracted from the ratio

$$P(\lambda) = \frac{P(H,T,\lambda)}{P_0(T_0,\lambda)}, \qquad (2)$$

where index 0 is related to measurements at the temperature $T = T_0 = 250$ K, high above T_c, where $YBa_2Cu_3O_{6.9}$ is nonmagnetic and $P(T_0,\lambda)$ does not depend on the magnetic field.

Besides the spectral polarization $P(\lambda)$ (1) the integral polarization P was also used. It was defined with the help of relation (1), where $N^{\pm}(H,T,\lambda)$ was replaced with $N^{\pm}(H,T)$:

$$N^{\pm}(H,T) = \int N^{\pm}(H,T,\lambda)\,d\lambda.$$
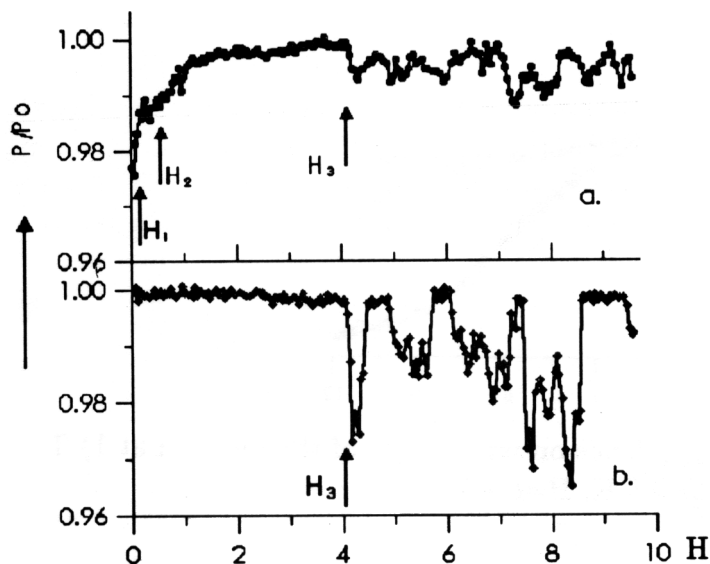
Fig. 2. Polarization in dependence on magnetic field. a) at an increase and, b) at a decrease of the field.

Fig. 2 shows the dependence of integral polarization P/P_0 at the temperature $T = 86$ K on the magnetic field: (a) when the field increases, (b) when the field decreases. It can be seen that besides the minima at $H = H_1$ and $H = H_2$, which were discussed in [1], there is a range of field strengths from $H_3 = 4.1$ kOe up to maximum 10 kOe, achieved here, where the polarization curve $P(H,T)$ has an irregular behavior.

We interpret the point H_3, which has an approximately linear dependence on temperature, as the transition point from the region $H < H_3$, where the Abrikosov vortexes are rectilinear and parallel to the external field, to the region $H > H_3$, where the Abrikosov vortexes acquire bending excitations.

Fig. 3 shows three curves for polarization in dependence on neutron wavelength, λ. Curve 1 shows $P_0(\lambda)$; curve 2 shows $P(\lambda)$ corresponding to the maximum point $H_{max} = 9$ kOe of curve (b) in fig. 2; and curve 3 shows $P(\lambda)$ corresponding to the minimum point $H_{min} = 8.4$ kOe of the curve (b) in fig. 2. Curve 3 in fig. 3 is where an anomaly is seen: the change in sign and an increase in polarization at long wave lengths, which can

89

be explained by inelastic scattering with a spin flip and the energy transfer from neutron to vortex lattice.

Such a scattering should enhance the intensity at long wave lengths when the spin flipper is switched on, or majority of neutrons are polarized against the external field. The enhancement was observed.

Comparison of neutron spectra transmitted by the sample at temperatures high above T_c and below T_c at the minimum polarization in the region of irregularities shows that the energy transfer should be ≈ 20 meV. Simple geometrical considerations show that the inelastic scattering creates bending excitations of the vortexes perpendicular to the field and to the direction of the beam.

The irregular behavior has a quasi-periodic character in dependence on the external field that may be connected with the period of the vortex lattice and the fluctuations appearing close to the lattice melting point [6,7].
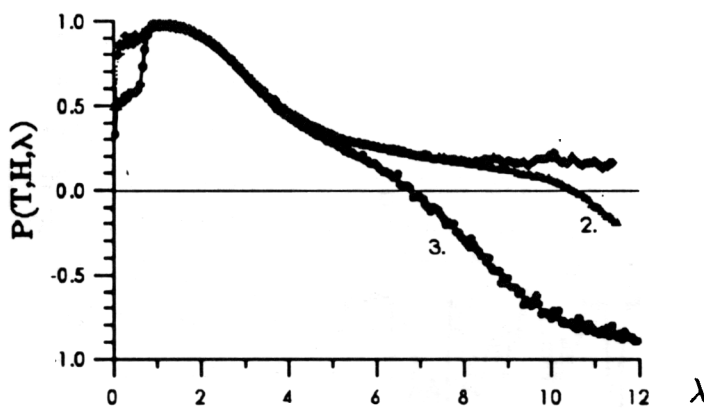
Fig. 3. Polarization in dependence on wavelength of the neutron at 1) T=250 K, 2) T=86 K, H=9 kOe, 3) T=86 K, H=8.4 kOe.

References

[1] V.L.Aksenov, E.B.Dokukin, Yu.V.Nikitenko et al., Physica Scripta **T49**, 650 (1993).

[2] R.J.Papoular, G.Collin. Phys.Rev. **B38**, 768 (1988).

[3] M.N.Volkov, R.P.Dmitriev, N.K.Zhuchenko et al., Pis'ma ZhETF **59**, v. 6, 186 (1988).

[4] R.P.Dmitriev, R.Z.Jagood, N.K.Zhuchenko et al., Z.Phys. **B83**, 155 (1991) (In Russian).

[5] W.Roest, M.Th.Rekveldt, Phys. Rev. **B48**, 6420 (1993).

[6] E.H.Brandt, J. Supercond. **6**, 201 (1993).

[7] G.Blatter, M.V.Feigel'man, V.B.Geshkenbein et al., Preprint ETH-TH/93-9, (1993).

Time-of-flight neutron depolarization for nondestructive testing

L.P.Chernenko, D.A.Korneev
Frank Laboratory of neutron Physics, JINR,
141980 Dubna, Moscow region, Russia

J.Schreiber
Fraunhofer-Institute for Nondestructive Testing,
Dresden, Germany

The run of 184 hr was carried on March 1994 to demonstrate the reliability of SPN installation for characterization of industrial sample like the car motor cylinder wall fragment. We performed a nondestructive study of the sample, which was tested previously by acoustic methods. The acoustic methods showed the existance of inhomogeneity in the ferromagnetic Ni coated layer of the sample area. According to the potential of the neutron depolarization method, it was interesting to search for the micromagnetic properties of the sample and make an evaluation of the important information for wear resistance study purposes. The first aim was to prove the existance of the acoustic methods pointing. We adopted the SPN set-up for a simple area scan along the right line marked on the sample. Fig. 1 shows the sketch of the experimental set-up. For the mode of data collection been the quickest we measure the flipping ratio (Fig. 2), which reveals the area inhomogeneiteis in correlation with the acoustic data. The series of measurements was made at three positions on the sample scan with coordinates equal to 25, 35 and 59 mm to compare the time-of-flight data of those positions. As seen from Fig. 3 there are remarkable differences in the behaviour of the depolarization functions at those positions. Analysis of the peculariteis of the depolarization function gives the conclusion about the character of stress condition in the Ni layer. This is the essential benefit of the time-of-flight information, which permits to develope the procedure of residual stress testing.
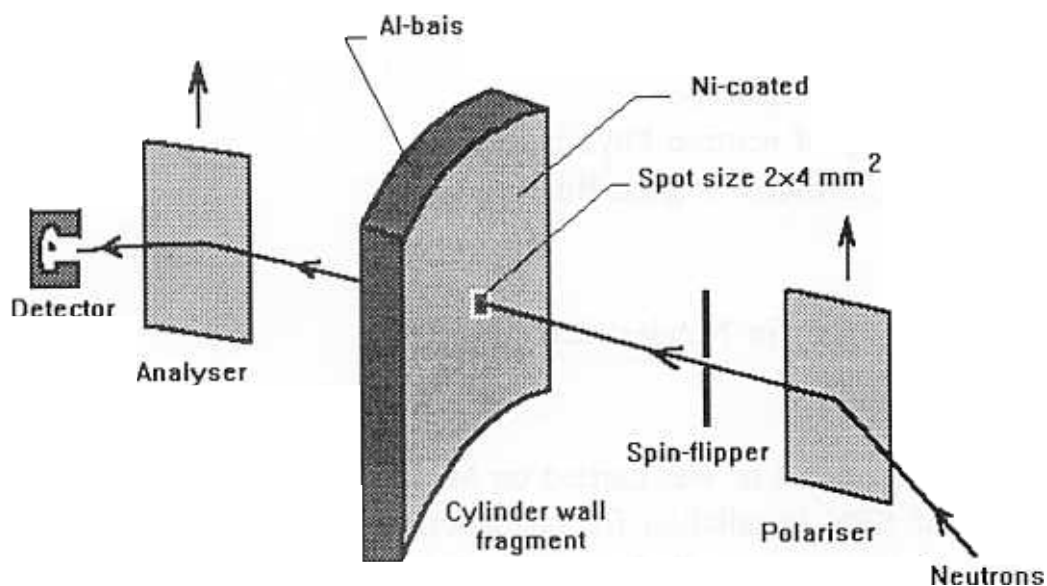
Fig. 1 Sketch of the experimental set-up
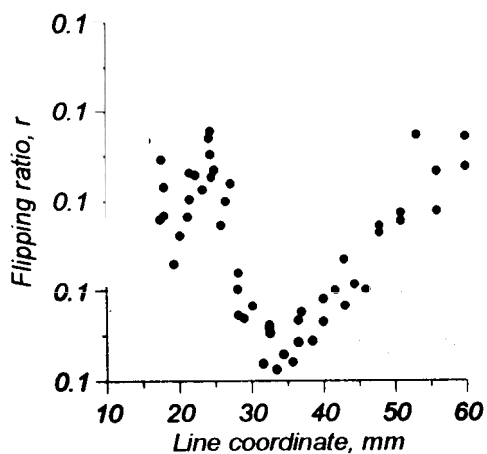
Fig. 2 The scan data curve clearly shows the inhomogeneous profile along the chosen marked right line of the sample area.
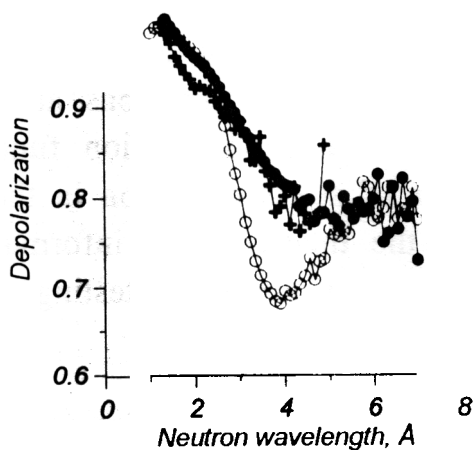
Fig. 3 Depolarization functions measured in an external magnetic field of 3.0 Oe at coordinates of 25 mm (crosses), 35 mm (full circles) and 59 mm (open circles).

92

Ground state moment reduction in an ultra-thin W(110) / Fe (110) / W (110) film.

V. Pasyuk[a,c], O. F. K. Mc Grath[a], H. J. Lauter[b], A. Petrenko[c,] A. Liénard[a], and D. Givord[a]

[a] Laboratoire Louis Néel, CNRS, BP 166, 38042 Grenoble Cedex, France.
[b] ILL, B.P.156, 38042 Grenoble Cedex 9, France.
[c] Frank Laboratory of Neutron Physics, JINR, 141980 Dubna, Russia.

Despite the large body of theoretical work devoted to the evaluation of the ground state moment in reduced dimensional magnetic systems, there exists very little experimental evaluation of the absolute value of the moment in ultra-thin films. Only one exact determination of the moment in ultra-thin Fe films has been previously reported [1], where the average moment in a monolayer and two-layer thick Fe film was deduced from magnetisation measurements and quartz microbalance thickness measurements.

In this paper we present an account of an experimental determination of the average moment in a three layer Fe (110) film.

A buffer layer of W (nominal thickness = 500Å) was initially deposited on Al_2O_3 (11$\bar{2}$0) by pulsed laser deposition, as reported elsewhere [2]. A detailed structural analysis of the growth of Fe on W was performed by means of in-situ RHEED and Auger and ex-situ by means of grazing incidence X-ray diffraction and specular reflection and will be reported elsewhere [3]. RHEED and grazing incidence diffraction analysis showed the Fe to grow epitaxially directly onto the W ; all crystallographic axes of Fe being parallel to the axes of W of the same index. The first monolayer of Fe is found to adopt the lattice parameter of bulk W, the film then relaxes as the thickness (d) increases. The relaxation follows an approximate 1 / d behavior. The film nucleates through the formation of in-plane isotropic crystallites which are greater then 50Å with a misorientation which is less than 1.8°. As the film thickness increases the crystallite size increases and the misorientation decreases. The film was subsequently protected by a

deposition of W (nominal quartz thickness 100 Å) at a rate of 0.5 Å.min^{-1} at 300 K. The W was found to grow epitaxially directly on the Fe.

The film thicknesses were determined by specular x-ray reflectivity, by fitting the experimental specular X-ray reflectivity profile. The obtained thickness of Fe (110) is 7 +/- 2Å . A 5Å roughness is found on either side of the Fe layer, the origin and the nature of this roughness was determined by the neutron reflection experiment and is discussed later in the text.

The polarised neutron reflectivities of the film were measured with the SPN spectrometer at the IBR-2 reactor. The $R^{+(-)}$ reflectivities were measured at 300K by applying an in-plane field (500 Oe) along the easy axis with the neutron beam polarised parallel (anti-parallel) to the magnetisation. The R^+ and R^- data, corrected for the imperfect polarisation of the neutron beam is shown in figure 1a and 1b respectively. The fitted reflectivities yield layer thicknesses and interface roughnesses which are in agreement with the x-ray data. The obtained thicknesses are: W(110)100+/-5Å/Fe(110)6+/-1Å/W(110)550+/-5Å. The neutron scattering length density profile normal to the film surface that was obtained after the fit is shown in figure 2. The origin of the 5Å roughness on the Fe/W interfaces determined by X-rays was studied more precisely by means of neutrons. A 5Å non-magnetic layer is found on either side of the Fe layer which contains approximately 20% Fe and 80% W. From the RHEED pattern during the growing of the Fe layer on W and then of the W layer on Fe one sees that the structure was not influenced by the small amount of the interdiffusion of Fe and W. So, basically, we had a system which was close to a model system.

The flipping ratio (R^+/R^-) (figure 1c) enables the magnetic interaction to be seen more clearly. The best fit yields an average magnetic moment of 1.80 +/- 0.05 μ_B in the Fe film. No magnetic moment, to within experimental error (0.05 μ_B) is detected in the intermixed layer either side of the Fe film.

In order to compare the above results with theoretical calculations one must extrapolate the 300 K value to 0 K. The thermal variation of the film magnetisation was
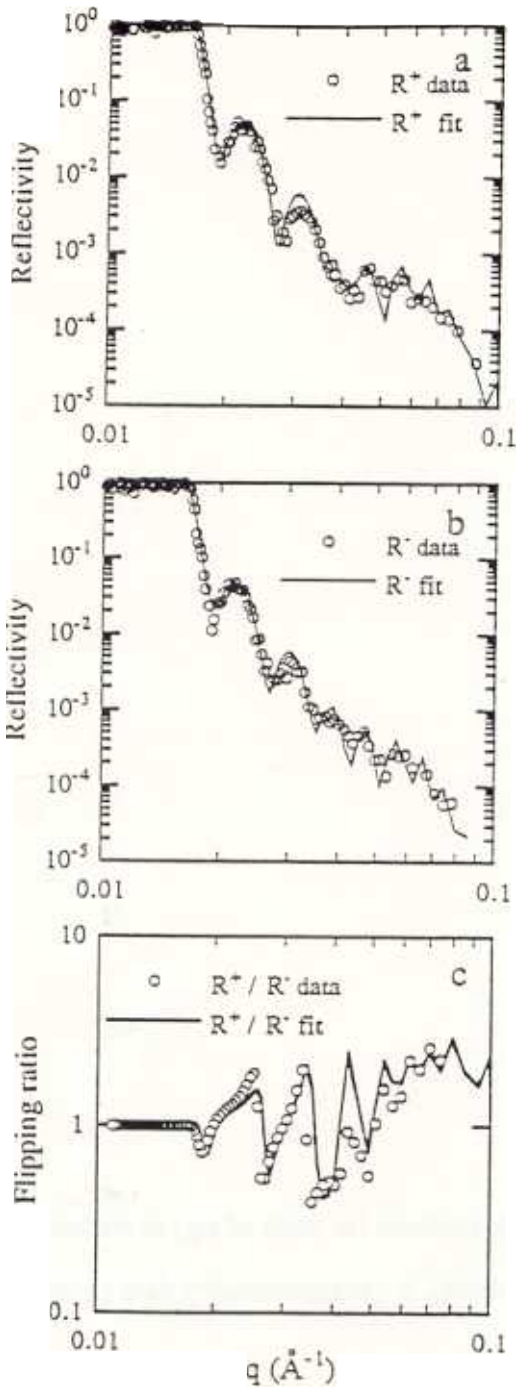
Figure 1. Specular neutron reflectivity data and fits for : a - neutrons polarised parallel to the magnetisation (R+), b - neutrons polarised anti-parallel (R-) and c - flipping ratio (R+/R-).
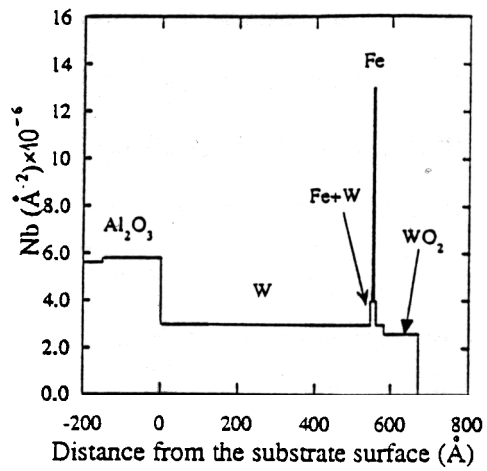
Figure 2. Neutron scattering length density profile as a function of the distance of the substrate surface.
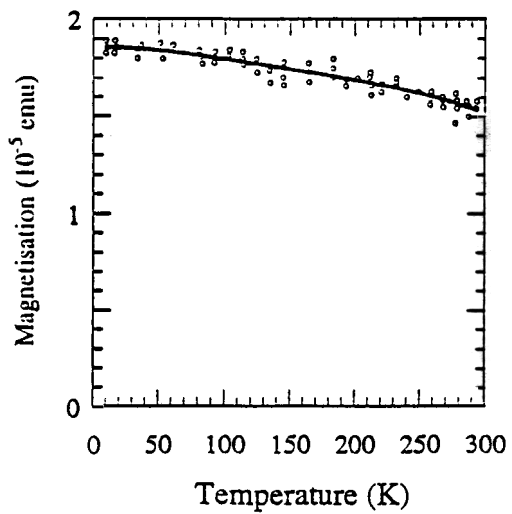
Figure 3. Thermal variation of the magneti-sation with an applied field of 1 kOe.
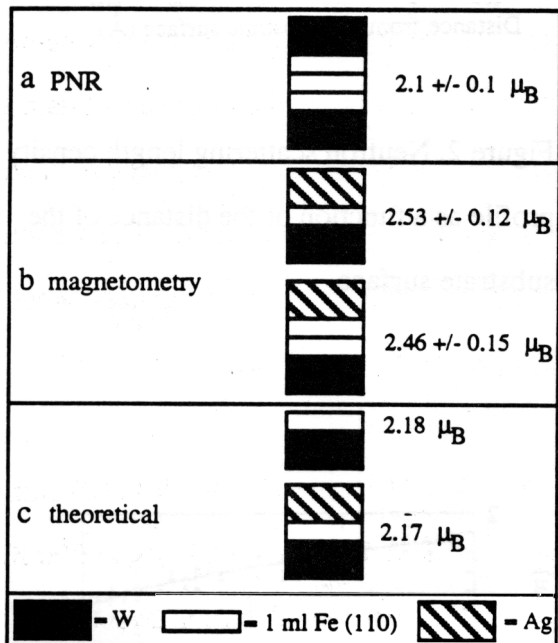
Figure 4. Schematic representation of the ground state moment (in units of μ_B) in various ultra-thin Fe films; a - polarised neutron data (this work), b - magnetometry data (from [1]), and c - theoretical calculations (from [5]).

measured by means of a SQUID magnetometer. The film was oriented onto the sample holder with the easy axis to within $0.5°$ of the field direction. A constant field of 1 kOe was applied and the magnetisation was measured at each temperature step (10 K) from 4.2 K to 300 K (fig. 3). The magnetisation is found to decrease from $1.85 +/- 0.05 \times 10^{-5}$ emu at 4.2 K to $1.57 +/- 0.05 \times 10^{-5}$ emu at 300 K. Assuming that the thermal decrease from 0 K to 4.2 K is negligible then the 300K moment, as determined by neutrons $(1.80 +/- 0.05 \ \mu B)$ can be extrapolated to $2.1 +/- 0.1 \ \mu B$ at 0K.

The above data is compared with the magnetometry / quartz data [1] and band structure calculations [5] in figure 4. Although a direct comparison between the three sets of data is not possible, the theoretical prediction that W leads to a reduction in the magnetic moment at an Fe interface appears to be verified by the above neutron data. Theoretical calculations for the symmetrical W / Fe / W system, including interface roughness, would enable a better comparison between theory and experiment to be made.

In conclusion, the average magnetic moment in a W (110) / Fe (110) / W (110) film, where the Fe thickness is three layers, has been measured as $1.80 +/- 0.05 \ \mu_B$ at 300 K. The value extrapolated to 0 K is $2.1 +/- 0.1 \ \mu_B$ which agrees with theoretical predictions that W leads to a reduction in the Fe moment at an interface compared with a free surface.

References

[1]   H. J. Elmers, G. Liu and U. Gradmann, Phys. Rev. Lett., 63 (1989) 566.

[2]   O. F. K. Mc Grath, F. Robaut, N. Cherief, A. Liénard, M. Brunel and D. Givord, Surf. Sci. Lett - to be published (1994).

[3]   O.F.K. Mc Grath, A. Liénard and D. Givord, to be published

[4]   G.P. Felcher, R.O. Hilleke, R.K. Crawford, J. Haumann, R. Kleb, and G.Ostrowski, Rev. Sci. Instrum. 58 (4) (1987) 609

[5]   C. L. Fu and A. J. Freeman, J. Magn. Magn. Mat., 69 (1987) L1

2.2. NEUTRON NUCLEAR PHYSICS

CONTENTS

Comparative Measurements of Independent Yields of ^{239}Pu Fission Fragments Induced by Thermal and Resonance Neutrons

N.Gundorin, Yu.Kopach, S.Telegnikov

An Improved Experimental Facility for Studying Delayed Neutrons and Preliminary Results of Measuring the β_{eff} Value for ^{233}U Relative to ^{235}U

S.B.Borzakov, E.Dermendjiev, V.M.Nazarov, S.S.Pavlov, A.D.Rogov, I.Ruskov, Yu.S.Zamyatnin

Reactions with the Emission of Charged Particles

Study of Fast Neutron Induced Charged Particle Producing Reactions. 1. Measurement of Angular Distribution and Cross Section for the ^{58}Ni(n,α)^{55}Fe Reaction at 5.1 MeV

Yu.M.Gledenov, G.Khuukhenkhuu, M.V.Sedysheva, Tang Guoyou, Bai Xinhua, Shi Zhaomin, Chen Jinxiang

Study of Fast Neutron Induced Charged Particle Producing Reactions. 2. Systematics of the Fast Neutron Induced (n,p) Reaction Cross Sections

G.Khuukhenkhuu, Yu.M.Gledenov, M.V.Sedysheva, G.Unenbat

Nucleosynthesis of the Rare Isotope ^{36}S: Measurements of the ^{36}S(n,γ) Cross Section at kT=25 keV and the ^{35}Cl(n,p)^{35}S Cross Section for Thermal Neutrons

Yu.M.Gledenov, Yu.P.Popov, V.I.Salatski, P.V.Sedyshev, M.V.Sedysheva, H.Beer, F.Kappeler

ON THE NEUTRON MEAN SQUARE INTRINSIC CHARGE RADIUS

Yu.A.Alexandrov

Frank Laboratory of Neutron Physics, JINR, Dubna, Russia

In 1994, the physical community of the world continued discussing the issue of the value of the n-e scattering length, a_{ne}, and of the sign of the neutron mean square charge radius $<r^2_{in}>_N$. The latter is related to a_{ne} through the Foldy relationship (Foldy, 1952) which Foldy obtained by solving the generalized Dirac equation:

$$<r^2_{in}>_N = (3\hbar^2/Me^2)\ (a_{ne} - a_F),\qquad(1)$$

where $a_F = \mu_n(e^2/2Mc^2) = -1.468 \times 10^{-3}$ fm Foldy scattering length.

With respect to neutron experimental data processing results physicists can be divided into two groups [1]: those belonging to the first group believe that $<a_{ne}> = (-1.31\pm0.02)\times10^{-3}$ fm (Krohn, Ringo (1973), Koester et al. (1988)) and, consequently, $<r^2_{in}>_N > 0$ (see (1)), and the others who believe that $<a_{ne}> = (-1.58\pm0.03)\times10^{-3}$ fm (Melkonian et al. (1959), Alexandrov et al. (1975 and 1986)) and, consequently, $<r^2_{in}> < 0$.

Calculations performed in [2] on the basis of the S-matrix of neutron scattering which take into account the phenomenon of inter-resonance scattering (Wigner (1946), Fogt (1958)), yielded an analytical expression for the inter-resonance interference term. This term, e.g., for bismuth for the neutron energy on the order of 10 eV is 90 times less than the total neutron cross section. In [2], it has also been shown that far from resonances the interference term is practically independent of neutron energies and thus cannot influence the value of a_{ne} obtained in Dubna, especially, if this value is obtained in a diffraction experiment. It has moreover been shown that the sum effect of resonance effects and inter-resonance interference is almost equal to zero for even-even nuclei (for the isotope ^{208}Pb and the neutron energy of 1 eV the contribution of this sum effect to the total cross section is approximately $10^{-6}\times10^{-24}$ cm^2), what means that for an even-even nucleus the resonance scattering should not affect the value of a_{ne}.

Reasons for a discrepancy in the determination of the a_{ne} value from transmission experiments performed in Garching (Koester et al. (1988)) and in Dubna (Alexandrov et al. (1986)) were also considered in [2]. It has been shown that the most probable reason for this discrepancy is the calculation methods by which the influence of negative energy resonances is accounted for. The Dubna calculation method seems to be a more preferred method.

In [1,2,3], a comparison was carried out between experimental and calculated values for a_{ne} and $<r^2_{in}>_N$ on the basis of modern theoretical representations of the nucleon. It has been shown that the well-known theoretical ideas of the nucleon structure based on the old meson theory by Yukawa (Cloudy Bag Model (Thomas (1983), Skyrme model (Skyrme, 1962), Numbu-Jona-Lasinio model (1993), collective model (Bijker, Iachello, Leviatan (1994), etc.) disagree with the experimental value $<a_{ne}> = -1.31 \times 10^{-3}$ fm ($<r^2_{in}>_N > 0$), and agree with the value $<a_{ne}> = -1.58 \times 10^{-3}$ fm ($<r^2_{in}>_N < 0$). This point of view has recently received positive response at the XVIII International Nuclear Physics Symposium at Oaxtepec (Mexico) held on January 4-7, 1995. At present there exists no adequate idea of the nucleon structure which would explain the value $<a_{ne}> = -1.31 \times 10^{-3}$ fm.

Referencess

1. Yu.A.Alexandrov. Neutron News 5, No. 1 (1994) 20.
2. Y.A.Alexandrov. Phys.Rev. C49 (1994) R2297.
3. Yu.A.Alexandrov. Neutron News 5, No. 4 (1994) 17.

RECENT INVESTIGATIONS OF NEUTRON POLARIZABILITY

T.L.Enik, L.V.Mitsyna, V.G.Nikolenko, A.B.Popov, G.S.Samosvat
(Joint Institute for Nuclear Research, Dubna)
V.G.Krivenko, A.V.Murzin, P.N.Vorona
(Institute for Nuclear Research, Kiev)

The electric polarizability of the neutron reflects its internal charge structure. For the polarizability coefficient, different theoretical models predict very similar values [1]

$$\alpha_n \sim 1 \cdot 10^{-3} fm^3. \tag{1}$$

But the situation with the experimental value of α_n is not clear. At the first sight, the problem seemed to be solved by the result of ref.[2]

$$\alpha_n = (1.20 \pm 0.15 \pm 0.20) \cdot 10^{-3} fm^3,$$

obtained in Oak- Ridge from neutron total cross section σ_t measurements on ^{208}Pb in the wide energy range up to 50 keV. But the careful analysis presented in ref.[3] showed the authors conclusion (2) to be too optimistic and the systematic error was to be increased by several times. Finally, there is a new result α_n [4] obtained by the Dubna- Garching- Riga collaboration from σ_t on ^{208}Pb for five quasi- monochromatic neutron groups, 1.26, 5.19, 18.6, 128 and 1970 eV:

$$\alpha_n = \begin{cases} (-1.3 \pm 0.5) \cdot 10^{-3} fm^3 & \text{for} \quad b_{ne} = (-1.59 \pm 0.04) \cdot 10^{-3} fm, \\ (-0.3 \pm 0.5) \cdot 10^{-3} fm^3 & \text{for} \quad b_{ne} = (-1.32 \pm 0.04) \cdot 10^{-3} fm. \end{cases}$$

It conflicts both with the theory (1) and with the previous result (2), especially if we use n-e scattering length b_{ne}, which theoretically seems more acceptable.

A program of further α_n investigations was developed in 1994 at Dubna and Kiev reactors.

In Dubna at the IBR-30 booster, we have started to measure σ_t for ^{208}Pb by classic time-of-flight method with the Co, Br, W, Ag and Rh filters with black resonances being permanently present in the beam for the background isolation. The neutron detector is 20 cm long 10 atm $^3He-$ counter, the flight path is $70.8\,m$, the beam diameter is $11\,mm$, the sample thickness is $20.8\,mm$ ($0.06872\,b^{-1}$). The runs with a sample (15 min) and without a sample (10 min) were alternated and controlled by the PC-286. 10 energy intervals between 1.6 and $97\,eV$ have been

chosen for the σ_t calculation. The result of the first seven 24-hour long runs is shown in Fig.1 by open circles together with 4 Garching points (full circles). The new σ_t below $4\,eV$ seem to be systematicaly higher than the old ones by $10-20\,mb$. We do not know yet the real reason of such a significant difference in the σ_t values.
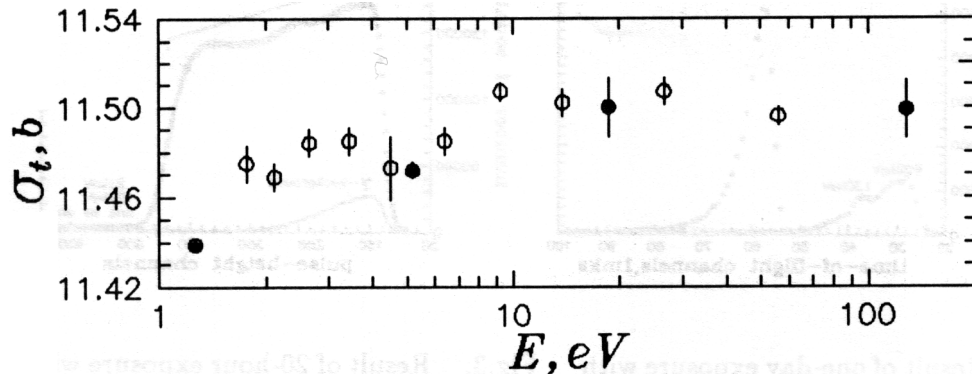
Fig.1. Total cross sections of enriched ^{208}Pb measured
in Garching (full circles) and in Dubna (open circles)

The most important aim of the investigations is to get σ_t at $E > 10\,keV$ because the α_n influence on σ_t is proportional to $E^{1/2}$ and the b_{ne} contribution at such energies is zero. $E = 24\,keV$ is chosen as the first step, which can be realized by transmission of the white spectrum neutrons through a thick layer of ^{56}Fe. In order to suppress the other neutron peaks, one uses additional filters such as Al and S.

The measurements with $24\,keV$ neutrons have been executed with the same technique as in the case of the eV neutrons, except filters, the flight path, and the $^3He-$counter, which were $24\,cm$ of natural Fe plus 10 or $20\,cm$ of Al, $74.4\,m$, and $50\,cm$, correspondingly. Fig.2 pictures the result of the one-day run including the time-of-flight spectrum without the sample and calculated transmission of the sample. The total result of 15 days is

$$\sigma_t \quad 11.047 \pm 0.019\,b. \tag{4}$$

The most essential result has been obtained in Kiev at the WWR-M reactor, in a beam of which the filters of $37\,cm$ of ^{56}Fe, $22\,cm$ of Al, and $10\,cm$ of S were placed. The 3 atm $22\,cm$ long H_2-counter was used as a neutron detector, the beam and the sample diameters were the same as in Dubna. The measurement
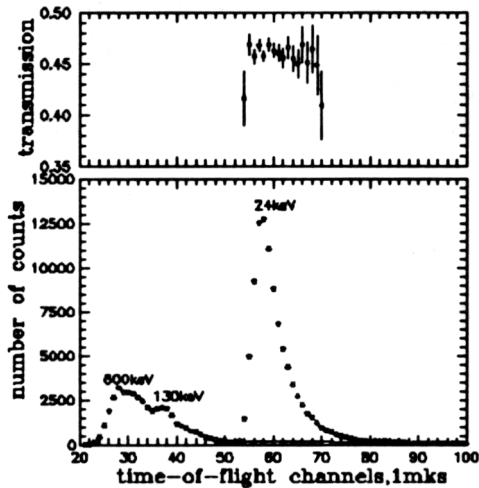
Fig.2. Result of one-day exposure with   Fig.3. Result of 20-hour exposure with
24 keV neutrons in Dubna.   24 keV neutrons in Kiev.

went on during 7 days by $2-3$ hours runs, with the 100 seconds exposure with and without the sample being alternated in each run. As an example, the spectrum of the 20-hour measurement with the sample is displayed in Fig.3. Some undulation of plateau is caused by the electronics nonlinearity. The underlayers of $\gamma-$background and peaks of the higher energies have been subtracted from the total spectrum to calculate the transmission. Processing about one third of data gives

$$\sigma_t = 11.009 \pm 0.003\,b. \tag{5}$$

Both (4) and (5) values , as well as the open circles in Fig.1, are rather preliminary results and they are to be confirmed in the future investigations.

REFERENCES

1. Petrun'kin V.A. Fiz. Elem. Chastits At. Yadra, 1981, v.12, p.692 [Sov. J. Part. Nucl., 1981, v.12, p.278].

2. Schmiedmayer J., Riehs P., Harvey J.A., Hill N.W. Phys. Rev. Lett., 1991 v.66, p.1015

3. Nikolenko V.G., Popov A.B. JINR E3-92-254, Dubna, 1992

4. L.Koester, W.Waschkowski, Yu.A.Alexandrov, L.V.Mitsyna, G.S.Samosvat, P.Prokofjevs, J.Tambergs (to be published).

104

Forward-backward asymmetry and p - resonances in the fission of ^{233}U and ^{235}U by neutrons

I.S. Guseva, G.A. Petrov, A.K. Petukhov, V.E. Sokolov

Peterbirg Nuclear Physics Institute of Russian Academy of Sciences, Gatchina, 188350, Russia

and

V.P. Alfimenkov, L.B. Pikelner, V.I. Furman

Frank Laboratory of Neutron Physics Joint Institute for Nuclear Research. Dubna 141980, Russia

The first parity violation effect is such reactions was observed by Abov et al. [1] in the asymmetric emission of γ - rays at the capture op polarized thermal neutrons. Later a similar asymmetry was observed in fragment emission during the fission of heavy nuclei [2]. The next step in this field was the discovery of parity nonconservation in p - wave neutron resonances [3]. The helicity dependence of the neutron cross section in such resonances amounts to ten percent.

Al of these effects were explained as being the result of mixing s - and p - resonances by weak interaction [4,5]. The values of these effects depends very strongly on the parameters of the resonances, which are well - known for s - resonances but are unknown for p - resonances. This is specially true for fissionable nuclei where information about p - resonances is totally absent, and is the reason why any new properties of the p - resonances is quite interesting.

One of the methods for discovering and studying p - resonances is the observation of various fission correlations. The angular distributions of fragments at the fission of nuclei by neutrons may be expressed as:

$$W(\theta) = 1 + \alpha_W (\vec{\sigma}_n \vec{p}_n) + \alpha_{LR} \vec{\sigma}_n [\vec{p}_f \times \vec{p}_n] + \alpha_{FB} (\vec{p}_f \vec{p}_n)$$

where $\vec{\sigma}_n$, $\vec{p}_n$ and $\vec{p}_f$ are unit vectors in directions of neutron polarization, neutron momentum and light fragment momentum, α_W is the coefficient of the P - odd correlation and α_{LR} and α_{FB} are the coefficients of P - even left - right and forward - backward correlations. All three coefficients are functions of the same parameters. Only α_W contains additional weak matrix element between the s - and p - levels.

The α coefficients are quite low, so the experimental results were only for thermal neutrons and not for resonance neutrons. Recently measurements of α_{FB} for ^{235}U were began in PNPI (Gatchina) and then continued on the IBR - 30 high intensive neutron source in Dubna.

Measurements were made with the ^{233}U and ^{235}U isotopes. For detection of fissed fragments a multisection ionization chamber was used. It gave the possibility of identifying both light and heavy

fragments escape: forward or backward relative to the neutron momentum. The chamber can rotate around the vertical axis and remain at $0°$ or $180°$ relative to neutron beam. This was necessary to remove apparatus asymmetry, which could distort the true value of α_{FB}.

Measurements were carried out by time - of -flight method on neutron beam No. 1 of the IBR - 30 at the flight path of 30 m. The asymmetry coefficient was determined from the relation:

$$\alpha_{FB} = \frac{N_+ - N_-}{N_+ + N_-}$$

where $N_\pm$ are the counts of the fission chamber at the detection of fragments of certain mass.

As a result of these measurements and calculations, the values of α_{FB} were carried out for ^{233}U and ^{235}U over wide energy interval 1 - 70 eV. Fig 1 shows the energy dependence of α_{FB} for ^{233}U (above) and the experimental fission count (below). It seems that the energy dependence of $\alpha_{FB}(E)$ has a complicated shape, which was expected because at a which was expected because at a many p - wave resonances. Analysis of the experimental data gave a set of parameters of the p-wave resonances which describe $\alpha_{FB}(E)$ quite well.
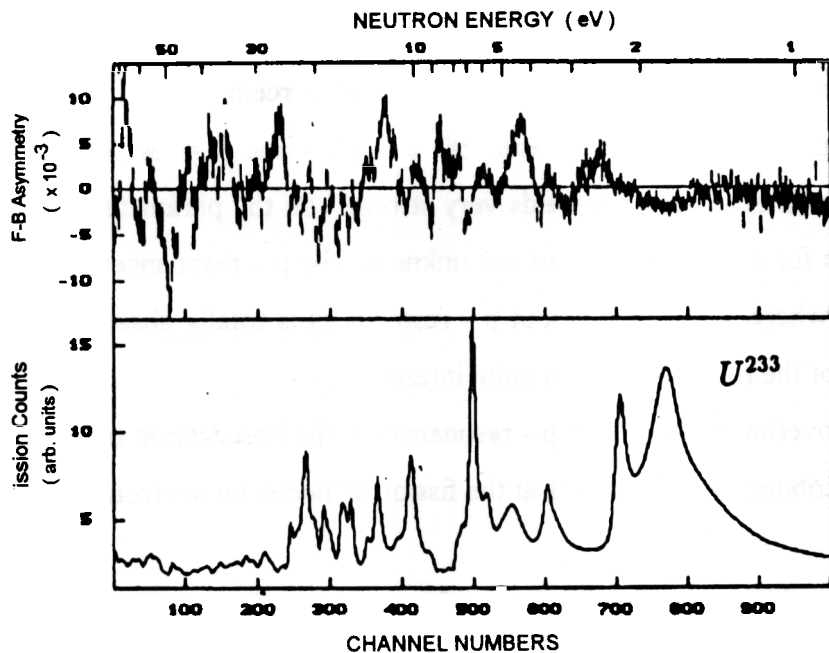
. Further development of such investigations will gave new information on the p -resonance, especially if the other correlation, $\alpha_{LR}(E)$, is also studied. Presently in FLNP JINR such an experiment is being prepared and should begin in 1995.

Figure

References

1. Yu.G.Abov et al. Phys. Lett., 1964, v.12, p.25

2. G.V. Danilian et al. JETP, Pis'ma 1977, v.26, p.197

3. V.P. Alfimenkov et al. Nucl. Phys., 1983, v.398, p.93

4. O.P. Sushkov, V.V. Flambaum JETP, Pis'ma 1980, v.32, p.377

5. V.E. Bunakov, V.P. Gudkov Ztschr. Phys., 1981 d303, p.285

6. A.M. Gadarski et al. JEPT. Pis'ma 1991, v.54 p.9

PARITY NONCONSERVATION IN NEUTRON CAPTURE ON ^{113}Cd

E.I. SHARAPOV, Yu.P. POPOV

Joint Institute for Nuclear Research, 141980 Dubna, Russia

S.J. SEESTROM, J.D. BOWMAN, C.M. FRANKLE, J.N. KNUDSON,
S. PENTILLA, P.E. KOEHLER, Y.F. YEN, V.W. YUAN

Los Alamos National Laboratory, Los Alamos, NC 87545 USA

D.G. HAASE, L.Y. LOWIE, G.E. MITCHELL, C.R. GOULD

Triangle University Nuclear Laboratory, Durham, NC 27708 USA,
North Carolina State University, Raleigh, NC 27965 USA

B.E. CRAWFORD, N.R. ROBERSON

Duke University, Durham, NC 27708 USA,
Triangle University Nuclear Laboratory, Durham, NC 27708 USA,

P.P.J. DELHEIJ

TRIUMF, Vancouver, British Columbia, V6T 2A3 Canada

H. POSTMA

Delft University of Technology, Delft, 2600 GA, the Netherlands

A. MASAIKE, Y. MATSUDA, M. IINUMA

Physics Department, Kyoto University, Kyoto 606-01, Japan

Y. MASUDA, H.M. SHIMIZU

National Laboratory of High Energy Physics, Tsukuba-shi 305, Japan

F. GUNSING, F. CORVI, K. ATHANASSOPULOS

Institute for Reference Materials and Measurements, Geel B-2440,
Belgium

Significant experimental progress has been achieved during the last years [1] in the study of parity nonconservation (PNC) in p-wave neutron resonances using longitudinally polarized beams of resonance neutrons and the time-of-flight methods of neutron spectroscopy. Parity-violating longi-

tudinal asymmetry of the cross section appears in those p-resonances which have large enough weak matrix elements M_{sp} to mix them with the s-wave resonances with the same spin J. Only the spin channel j=1/2 component of the total neutron width contributes to the experimental effect, therefore, spins and spin channel mixing ratios should be measured as well. The final parameter needed for the theory of weak interaction in compound nuclei is the root-mean-square value of matrix elements, M, or the corresponding spreading width Γ_w of the weak interaction

$$M = \sqrt{< M_{sp}^2 >}, \quad \Gamma_w = \frac{2\pi M^2}{D} \qquad (1)$$

which are independent of details of the wave functions of individual resonances (here, D is the average level spacing in the compound nuclei at given excitation energy).

If the spreading width Γ_w is essentially independent of the atomic mass number A, then the mass dependence of M should reflect the mass dependence of the level density D. On the other hand, a slightly different mass dependence of the kind [1]

$$M = 1.3 \times 10^{-8} \sqrt{Au_{eff}D} \qquad (2)$$

was argued in the work of Ref. [2] based on the mechanism of dynamical enhancement due to the virtual excitation of a giant 0^- resonance by the weak interaction. The mass dependence of the weak interaction matrix element has not been experimentally tested yet: only the work of Ref. [3] touched on this subject when analysing the early class of experiments with statistically inadequate data for single resonances in each nuclei. Therefore, after results for $A \simeq 235$ nuclei, the TRIPLE Collaboration started measurements of the PNC asymmetries in many resonances for nuclei around the 3p-maximum of the neutron strength function, $A \simeq 100$. The results for the target nucleous ^{113}Cd only are reported here.

The parity violation phenomenon in Cd was first discovered in 1964 at ITEP [4] as the asymmetry of γ-quanta decay of Cd after the capture of polarized thermal neutrons, and studied in 1991 at JINR [5] at a single resonance E_p=7.0 eV by a polarized neutron transmission technique. In a

---

[1] In this formula M, D and the effective excitation energy u_{eff} are in eV

given work, parity violation in 22 p-resonances found in Ref. [6] was investigated by measuring the total capture cross section of ^{113}Cd on the longitudinally polarized neutron beam at the LANSCE pulsed neutron source of the Los Alamos Meson Physics Facility. A 4π-capture detector based on BF_2 crystals was used. The sample was a highly enriched (93.35%) ^{113}Cd -metal disk. The spins of resonances were determined by measuring gamma-ray spectra from the individual resonances at the GELINA pulsed neutron source (IRMM, Geel) with the use of Ge-detectors and the same sample. The assignment of the spins was based on the population of low-lying states. A typical time-of-flight spectrum with the ^{113}Cd sample is shown in Figure 1 in logarithmic scale. The data were analyzed in the energy interval 7-495 ev. The results are listed in Table 1.

Four resonances showed non-zero parity violating asymmetries at the level equal or greater than 2.5 σ. From spin measurements it follows that only 10 resonances are liable to exibit parity violation, namely those with spins J = 0,1 but not J = 2. The statistical approach was applied to the analysis of the obtained data. The Dubna results of Ref. [7] on the neutron strength functions for j=1/2 and j=3/2 channels were effectively used instead of unknowm spin channel mixing parameters of resonances. The likelihood function of rms matrix element M was constructed and calculated giving for the first time the result

$$M(^{113}Cd) = 2.0 \, ^{+1.6}_{-0.9} \; meV.$$

This value is to be compared with the root-meam-square PNC matrix elemets obtained at LANSCE for ^{232}Th [8] and ^{238}U [9]:

$$M(^{232}Th) = 1.2 \, ^{+0.5}_{-0.4} \; meV$$

$$M(^{238}U) = 0.56 \, ^{+0.41}_{-0.20} \; meV.$$

The results indicate a smooth, if any, mass behavior of the weak matrix element.The statistical uncertainty of the above results do not allow to distinguish between different approaches to the mass dependence of M . PNC asymmetries measurements for more nuclei from the mass region of the 3p-maximum of the neutron strength function are necessary. They are under preparation as well as the spin assignment measurements on targets-candidates for parity violation study.

Table 1: PNC asymmetries and parameters of the p-wave resonances in ^{113}Cd

$E_n(eV)$	$P(\%)$	J	$g\Gamma_n(meV)$
7.00±0.01	−1.00±0.45	1	0.00031±0.00003
21.83±0.01	−0.05±0.28	2	0.0071 ±0.0002
43.38±0.03	−0.40±0.69	0	0.0047 ±0.0004
49.77±0.01	−0.06±0.27	1	0.0150 ±0.0005
56.23±0.01	+0.28±0.13	2	0.0403 ±0.0006
81.52±0.01	+0.70±1.42		0.0052 ±0.0006
·98.52±0.02	−0.41±0.26	2	0.042 ±0.001
102.30±0.02	+1.30±0.27	1	0.037 ±0.001
106.56±0.02	±		0.030 ±0.002
166.60±0.13	+2.49±1.22		0.020 ±0.002
196.15±0.04	−2.00±0.95		0.100 ±0.005
203.51±0.04	−0.63±0.43	1	0.067 ±0.003
211.88±0.05	±		0.078 ±0.003
237.87±0.05	+0.30±0.26	2	0.125 ±0.004
252.68±0.05	+0.32±0.31	2	0.140 ±0.004
271.50±0.06	±		0.26 ±0.01
289.64±0.09	+0.50±0.12	(1)	0.06 ±0.006
312.30±0.07	+0.20±0.19	2	0.491 ±0.007
343.79±0.07	−0.51±0.74	0	0.17 ±0.01
351.6± 0.2	−0.57±1.54	2	0.036 ±0.003
359.3± 0.1	−0.28±0.45	1	0.28 ±0.01
376.8± 0.1	−0.49±0.16	1	0.83 ±0.01
385.0± 0.1	−0.24±0.76		0.089 ±0.006
422.7± 0.1	±	2	1.00 ±0.02
489.9± 0.1	+0.05±0.28	1	0.72 ±0.02

References

[1] C.M. Frankle, S.J. Seestrom, Yu.P. Popov, E.I. Sharapov, N.R. Roberson, Fiz. Elem. Chastits i Atom. Yad. **24**, 939 (1993). [Sov. J. Phys. Part. Nucl. **24(4)**, 401 (1993)]

[2] S.G. Kadmenskii, V.P. Markushev, and V.I. Furman, Yad. Phys. **37**, 277 (1983).[Sov. J. Nucl. Phys. **37**, 345 (1983)].

[3] V.E. Bunakov, V.P. Gudkov, S.G. Kadmenskii, I.A. Lomachenkov and V.I. Furman, Yad. Fiz. **49**, 988 (1989) [Sov. J. Nucl. Phys. **49**, 613 (1989)].

[4] Yu.G. Abov, P.A. Krupchitsky, and Yu.A. Oratovsky, Phys. Lett. **12** 25 (1964).

[5] V.P. Alfimenkov, Yu.D. Mareev, L.B. Pikelner, V.R. Skoy, V.N. Shvetsov, Yad. Phys. **54**, 1489 (1991). [Sov. J. Nucl. Phys. **54**, 907 (1991)].

[6] C.M. Frankle, C.D. Bowman, J.D. Bowman, S.J. Seestrom, E.I. Sharapov, Yu.P. Popov, N.R. Roberson, Phys. Rev. **C45**, 2143 (1992).

[7] G.S. Samosvat, Fiz. Elem. Chastits i Atom. Yad. **17**, 713 (1986) [Sov. J. Part. Nucl. **17**,313 (1986)].

[8] C.M. Frankle, J.D. Bowman, J.E. Bush *et al.* (TRIPLE Collaboration) Phys. Rev. **C46**, 778 (1992).

[9] X. Zhu, J.D. Bowman, C.D. Bowman *et al.* (TRIPLE Collaboration), Phys. Rev. **C46**, 768 (1992).
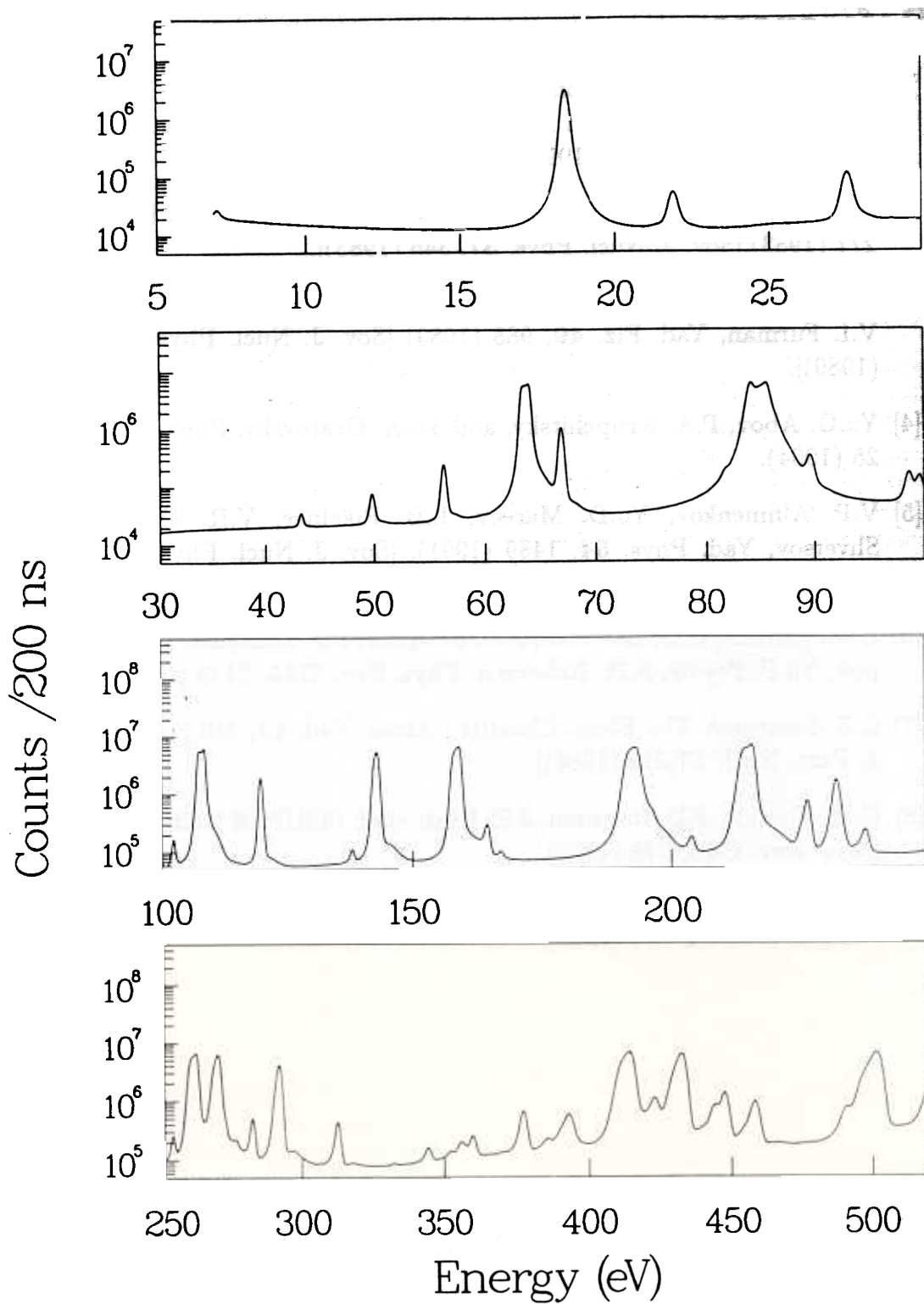
FIG.1 Neutron capture detector yield for [113]Cd in the energy range
E_n=7-530 eV as obtained at the 60 m flight path of the LANSCE
pulsed neutron source.

G.P.Georgiev[a]
Joint Institute for Nuclear
Research,
Dubna, 141980, Russia
7-095-924-39-14

Yu.V.Grigoriev
Physics-Power
Engineering Institute,
Obninsk, Russia

G.V.Muradyan
Kurchatov Research
Center,
Moscow, Russia

N.B.Janeva
Institute for Nuclear
Research and Nuclear
Energy, Sofia, Bulgaria

ABSTRACT

Neutron time-of-flight spectroscopy measurement was made on the sample enriched in ^{119}Sn at the pulsed neutron booster *IBR*-30 of the Joint Institute for Nuclear Research (JINR) in Dubna. The capture measurement was performed on the 502 *m* flight-path. The gamma-cascades from neutron resonances were measured with the *NaJ(Tl)* multisectional 4π-detector in order to obtain gamma-multiplicity spectra of resolved resonances in the energy range from 20 *eV* to 2000 *eV*. The Boron converter, positioned inside the detector, gave the opportunity for detecting of neutron scattering events by measuring monoenergy gamma-quanta from the $^{10}B(n,\alpha\gamma)$ reaction. The correlation between the multiplicity spectra and the spins of the resonances was investigated. Spins and radiative widths of resonances were determined.

I. INTRODUCTION

Studies of the radiative capture of neutrons are stimulated by the present-day physical picture and theoretical description of this process still remaining quite incomplete. Application of the method of multiplicity spectrometry of gamma-quanta[1] together with the time-of-flight (TOF) method yields extensive experimental information on radiative capture in the region of resonance neutron energies and on parameters of resonance levels. The data on the spins of the resonances of certain nuclei being fragmentary determines the interest in those characteristics of gamma cascades, which exhibit systematic dependence upon the spins of resonance levels.

In this work preliminary results are presented of an investigation of the radiative capture of resonance neutrons by ^{119}Sn isotope in the region of resolved resonances making use of the method of multiplicity spectrometry. The choice of the indicated isotope was due to the data on its spin and radiation width being incomplete[2] .The cross section of radiative capture by ^{119}Sn isotope in the region of resonance neutron energies is interesting from the point of view of understanding nucleosynthesis.

II. EXPERIMENT

A multisection 4π - "Daisy-type" scintillation detector located at the 502-meter-long TOF base of the *IBR*-30 pulsed neutron booster of the FLNP JINR[3,4], was used for measurements. The mean booster power and the resolution were 10 *kW* and 8 *ns/m* respectively. The detector consisted of 16 independent *NaJ(Tl)* crystal sections with a total volume of 36 litres and geometric efficiency of 80 %. A ^{119}Sn target[b] $5.97.10^{-4}$ nuclei/barn thick was used in the measurements. The sample of SnO_2 enriched in ^{119}Sn to 90.7 % abundance was positioned in the center of the detector in a thin *Al* container.

The neutron beam was monitored by two counters of *SNM* – 17 type and these were positioned at 60 *m* distance from the source. A B_4C (10 *mm*) filter was constantly in the beam to remove the recycling neutrons. The neutron TOF and the coincidence multiplicity of gamma-quanta were determined for each interaction event. In parallel with the gamma-quanta from radiative capture in the target, single 480 *keV*

gamma-quanta produced in the $^{10}B(n,\alpha\gamma)$ reaction, caused by neutrons scattered in the target and occurring in the Boron converter surrounding it, were detected. At the same time the converter screens the detector from scattering neutrons. The capture-event and the neutron scattering-event parameters are stored in the memory of the measuring module if the sum energy of the registered gamma-quanta is in the energy interval from 2 to $9\,MeV$ and from 0.35 to $0.50\,MeV$ respectively. Thus, the same detector registered events of radiative capture and of neutron scattering in the target simultaneously and in identical conditions. The high efficiency of the detector permits enhancement of the number of measurable resonances in neutron-scattering experiments by this method.

III. RESULTS

The experimental spectra were processed for determining the areas $S_\gamma(\kappa)$ under the resonance peaks in the time-of-flight spectra of differing multiplicities (κ) for detector sections fired simultaneously. Thus, the experimental gamma-quanta multiplicity spectrum $P(\kappa) = S_\gamma(\kappa)\big/\sum_\kappa S_\gamma(\kappa)$ for each resonance was obtained, and the mean gamma-quanta multiplicity $\langle\kappa\rangle = \sum_\kappa \kappa P(\kappa)$ determined. It turned out to be that for the even-odd ^{119}Sn isotope the $\langle\kappa\rangle$ values concentrated around two points: $\langle k\rangle = 2.50$ and $\langle k\rangle = 2.79$. Thus, in the range of energies up to $2000\,eV$, 9 spin 0^+ resonances and 13 spin 1^+ resonances were successfully identified for ^{119}Sn -Table 1.

For determining the parameters of the resonances a program was written which made possible computation of the expected TOF radiative capture and scattering spectra and fitting them to the respective measured spectra by varying the resonance parameters and fitting the parameters of the neutron spectrometer. The resolution function of the spectrometer and the detection efficiencies for various events were fitted for the whole set of resonances. The radiation width Γ_γ was fitted with the aid of the ratio of the partial areas A_γ and A_s under the respective resonance peak in the radiative capture and scattering spectra, of the known[2] neutron width Γ_n and of the distribution function obtained. The A_γ/A_s ratio is practically insensitive to the shape of the spectrum of incident neutrons and to details of the resolution function.

Table 1. Resonance parameters of ^{119}Sn

BNL-325			Present work		
E_0 eV	J^π	Γ_γ meV	E_0 eV	J^π	Γ_γ meV
-10	1^+	(87)			
6.22±0.06					
74.76±0.08			74.57±0.04	(0^+)	
114.8±0.2			114.83±0.07	1^+	
140.9±0.3			140.86±0.10	0^+	57±19
145.7±0.3			*not observed*		
222.6±0.4			222.64±0.18	1^+	68±30
261.6±0.5			261.15±0.23	0^+	
283.1±0.6			282.95±0.25	1^+	
330.0±0.7			c		
			408.1±0.5		
455.8±1.0			455.6±0.5	(1^+)	149±57
			657.2±1.0		
697±2			696.1±1.0	(1^+)	115±39
			738.6±1.1	1^+	
830±2			828.0±1.3	(1^+)	98±28
885.0±1.8			883.3±1.5	0^+	
948			941.1±1.6	(1^+)	
			1012±2	1^+	
			1026±2	1^+	
			1079±2		
1150			1144±2	0^+	
1258			1255±3	0^+	
			1310±3		
			1348±3	0^+	
			1393±3	0^+	
			1755±4	(1^+)	
			1797±4	1^+	
			1939±5	0^+	
			1987±5	1^+	

The energy limits of the calculated areas were chosen so as to reduce as much as possible the influence of adjacent resonances and of peculiarities of the incident

^{c} The Mn content in material of the vacuum neutron guide tube prevents the observation of this resonance.

114

neutron spectrum. In the fit, that value of Γ_γ was determined for which the computed A_γ/A_s ratio was in agreement with its experimental one. The radiative widths for five resonances were obtained - Table 1. Those data were used to extract the average value of Γ_γ for $^{119}Sn - \langle\Gamma_\gamma\rangle = 97\pm17\,meV$.

Besides the levels indicated in ref.[2], 13 new levels were observed for ^{119}Sn in the energy range up to $2000\,eV$ -Table 1. The neutron resonance energy values were determined by using those of ^{238}U as a standard[2]. The resonance energies are obtained practically without systematic errors because of the identical conditions of the measurements and data processing for ^{119}Sn and ^{238}U. The values of $D_0 = 62\pm21\,eV$ for ^{119}Sn was obtained in the energy range up to $1000\,eV$.

REFERENCES

1. G. V. Muradyan et al., "Multiplicity Spectrometer for Measurement of Neutron Cross Sections", *Nucl. Sci. Eng.*, **90**, 60 (1985).

2. S. F. Mughabghab, *Neutron Cross Section* 1, Part **B**, Academik Press, New York, (1984).

3. N. Janeva et al., "A Setup for Precise Measurement of Resonance Neutron Capture by Self-Indication", *Nuclear Instruments and Methods in Physics Research*, **A313**, 266 (1992).

4. G. P. Georgiev et al., "Determination of ^{147}Sm and ^{148}Sm Resonance Parameters", *Nuclear Physics A565, 643 (1993).*

NEUTRON RESONANCE SPECTROSCOPY
OF INDIUM-113 AND INDIUM-115

E.I. SHARAPOV, Yu.P. POPOV
Joint Institute for Nuclear Research, 141980 Dubna, Russia

S.J. SEESTROM, J.D. BOWMAN, C.M. FRANKLE, J.N. KNUDSON,
S.PENTILLA, Y.F. YEN, S.H. YOO, V.W. YUAN, X. ZHU
Los Alamos National Laboratory, Los Alamos, NC 87545 USA

C.R. GOULD, D.G. HAASE, G.E. MITCHELL, S.S. PATTERSON
Triangle University Nuclear Laboratory, Durham, NC 27708 USA,
North Carolina State University, Raleigh, NC 27965 USA

B.E. CRAWFORD, N.R. ROBERSON
Duke University, Durham, NC 27708 USA,
Triangle University Nuclear Laboratory, Durham, NC 27708 USA

P.P.J. DELHEIJ
TRIUMF, Vancouver, British Columbia, V6T 2A3 Canada

After the Dubna pioneer work on parity nonconservation (PNC) in neutron p-resonances [1] parity violation has been observed in a number of nuclei [2], [3], [4] and now appears as to be a general feature of compound states. A new approach to this phenomenon [5] treats the symmetry-breaking matrix elements as random variables and expresses their root-mean-square value M through the effective nucleon-nucleon weak coupling constants. Up to the last year the M-value was obtained only for Th^{232} and U^{238}. For further study of the mass dependence of M it is important to obtain more experimental data on p-wave resonances of nuclei-candidates for PNC measurements. In the given work this is done for indium which is near the maximum of the 3p peak in neutron strength function. The known data and simple statistical arguments suggested that the available sets of resonances in ^{113}In and ^{115}In were incomplete even in a low energy region up to several hundred eV, therefore new measurements were of interest.

The transmission time-of-flight measurements were made on the 56m

Table 1: ^{115}In p-wave resonance parameters

$E_n(eV)$	$g\Gamma_n(meV)$		$E_n(eV)$	$g\Gamma_n(meV)$	
29.67±0.05	0.0011	±0.0001	219.7±0.4*	0.014	±0.006
40.66±0.07*	0.0041	±0.0005	246.7±0.4	0.09	±0.003
58.70±0.10*	0.00014	±0.00002	264.5±0.5*	0.04	±0.02
66.40±0.12*	0.000040	±0.000002	275.0±0.5*	0.01	±0.01
73.04±0.13	0.011	±0.001	276.9±0.5*	0.04	±0.01
77.89±0.14*	0.0015	±0.0006	282.3±0.5	0.05	±0.02
85.50±0.15*	0.003	±0.001	285.1±0.5*	0.014	±0.006
86.32±0.15	0.017	±0.001	302.8±0.5	0.21	±0.07
88.40±0.16*	0.0017	±0.0005	304.1±0.5	0.16	±0.09
100.8±0.2	0.032	±0.002	308.2±0.5	0.06	±0.02
103.7±0.2*	0.0004	±0.0002	313.4±0.6*	0.11	±0.09
110.8±0.2	0.016	±0.002	317.0±0.6*	0.007	±0.005
114.3±0.2	0.072	±0.004	325.8±0.6*	0.29	±0.06
120.6±0.2	0.025	±0.003	329.5±0.6	0.18	±0.06
144.1±0.3	0.093	±0.007	333.5±0.6*	0.3	±0.1
145.7±0.3	0.036	±0.007	336.7±0.6	0.4	±0.1
146.9±0.3*	0.045	±0.008	344.7±0.6	0.11	±0.04
156.5±0.3*	0.008	±0.003	367.0±0.6	0.38	±0.05
158.6±0.3	0.052	±0.005	379.0±0.7	0.71	±0.04
162.2±0.3	0.11	±0.02	389.5±0.7*	0.06	±0.01
174.2±0.3	0.096	±0.005	394.7±0.7*	0.2	±0.1
190.9±0.3*	0.08	±0.04	398.2±0.7*	0.2	±0.1
192.4±0.3	0.37	±0.09	431.2±0.8	0.09	±0.05
194.5±0.3	0.05	±0.04	474.0±0.8	0.6	±0.2
198.7±0.3	0.034	±0.009	481.4±0.8*	0.2	±0.1
214.1±0.4	0.09	±0.01	488.1±0.9	0.16	±0.05

flight path at the LANSCE pulsed neutron source of the Los Alamos Meson Physics Facility. Neutrons were detected with a system of ^{10}B-loaded detectors. The details of the experimental set up are reviewed in Ref. [2]. A sample of natural indium had thickness 0.231 at/b. It was cooled with liquid nitrogen to reduce Doppler broadening. An additional, capture gamma-ray measurement, was performed with the 9.61 g of a highly enriched, 99.99%, ^{115}In sample shaped as a circular disk of area 20.8cm^2. This target was placed near a gamma detector consisted of two CsI (pure) crystals. The crystals were shielded from scattered neutrons by 5 cm of ^{6}Li-loaded polyethylene.

The data were analyzed in the energy interval 25-500 eV using the R matrix code SAMMY of the Oak Ridge National Laboratory. The new transmission data yield 43 new week resonances which are either s-wave resonances in the 4.28% abundant isotope ^{113}In or p-wave resonances in the dominant ^{115}In isotope. In the capture experiment with a highly enriched ^{115}In isotope 23 new resonances are observed, therefore identifying them as ^{115}In resonances. The new resonances which were not observed with the enriched ^{115}In sample were assigned to ^{113}In . The results for ^{115}In are listed in Table 1. Resonances labelled with an asterisk are new. The present results imply a total of 50 p-wave resonances between E_n=25 and 500 eV in ^{115}In which are suitable for study of parity violation pending the absence of information on their spin values.

References

[1] V.P. Alfimenkov, S.B. Borzakov, Vo Van Thuan, Yu.D. Mareev, L.B. Pikelner, A.S. Khrykin, E.I Sharapov, Nucl. Phys. **A398**, 93 (1983).

[2] C.M. Frankle, S.J. Seestrom, Yu.P. Popov, E.I. Sharapov, N.R. Roberson, Fiz. Elem. Chastits i Atom. Yad. **24**, 939 (1993).

[3] C.M. Frankle et al., Phys. Rev. **C46**, 778 (1992).

[4] X. Zhu et al.), Phys. Rev. **C46**, 768 (1992).

[5] M.B. Johnson, J.D. Bowman, S.H. Yoo, Phys. Rev. Lett. **67**, 310 (1991).

POSSIBLE EQUIDISTANCE OF THE EXCITATION ENERGIES OF THE INTERMEDIATE LEVELS OF THE MOST INTENSE γ-CASCADES

V.A. Khitrov, Yu.V. Kholnov, A.M. Sukhovoj,
E.V. Vasilieva, A.V. Vojnov

Frank Laboratory of Neutron Physics, Joint Institute for Nuclear Research, 141980, Dubna, Russia

The theoretical analysis developed, for instance, in the quasiparticle-phonon nuclear model (LTP JINR) shows that the structures of wave functions for rather high-lying ($E_{ex} > 2$ MeV) levels of compound nuclei contain a great number of similar magnitude components of various types. But this fact does not prevent the possibility that wave functions for some number of levels can contain the large components connected with simple excitation modes. For example, there can be vibration modes.

Presently, the only real possibility to experimentally observe such levels higher than 2 MeV, for example, in deformed even-even (and all the more so in odd) nuclei is the search for regularity in the spectra of the most intense cascade γ-transitions. Up to now such a regularity was observed most clearly in the intensity distribution of cascades between the compound-state and the first excited state of the ^{174}Yb nucleus. In the corresponding spectrum there are at least four groups of practically equidistant intense cascades. A similar equidistance can be revealed in all the cascade intensity distributions hitherto obtained for nuclei differing by such parameters as nuclear deformation or neutron number parity. It is very important to note that equidistant intervals can appear not only between the single levels but also between the multiplets of intermediate levels of intense cascades. This is a very strong argument in favour of the nonrandom nature of the observed equidistance of enhanced cascades.

A method for the search near equidistant spacings between "distinguished" intermediate cascade levels in the bulky mass of data values was developed for the first time in [1]. The functional connecting three tested cascade intensities, two spacings between their intermediate levels and the value of equidistant period searched for was suggested. It was assumed that average cascade intensities smoothly change with variations of their intermediate level energies. Unfortunately, this functional has not determined the solution in all cases which satisfy such limitations. In a real nucleus the experiment shows the presence of local variations of average cascade intensities at different nuclear excitation energies (it is a manifestation of nuclear structure effects). Such a situation noticeably decreases the possibility of solving the problem under study.

Nevertheless, the search for equidistance in a set of nuclei from ^{143}Nd up to ^{187}W shows the existance of equidistance periods whose values change rather regulary with variations of atomic mass of the examined nuclei. It is also possible that these values

differ for groups of nuclei with different ratios of reduced neutron widths of compound-states, Γ_n^o, to their average values. The same is possible for different multipolarities of cascade transitions.

The observed equidistance period varies over the range of 400-800 keV for the main part of the investigated nuclei and its value is comparable with typical quadrupole vibration energies both in spherical and deformed nuclei (corresponding 2^+ states energies). A qualitative explanation for thisf effect may be obtained if one suggests that a neutron captured by a nucleus does not pass on all of its energy to individual nuclons (it means that many-quasiparticle states are not excited or are poorly excited) but in some cases excites harmonic nuclear vibrations.

A preliminary conclusion about the possibility of observing a "cold" nucleus instead of a "hot" one after slow neutron capture was also made when analysing the density of levels excited by cascade transitions and radiative strength functions for primary low-energy transitions [2]. It is necessary to conclude that the experiment distinguishes the states differing by two phonons as a minimum. The remaining part of the energy inserted in to the nucleus by the neutron, is most probably concentrated on few-quasiparticle nuclear excitations. Accordingly, the primary and secondary transitions of a trio of equidistant cascades connect states differing by one to two phonons. The final proof or refutation of this hypotheses may be obtained only in the investigation of cascade γ-decays of the neutron resonances in different nuclei. Such an experiment is quite possible with the modern HPGe-detectors.

References

[1]. E.V.Vasilieva, et al., Izv RAN, ser. fiz., 57(10),1993,p.109

[2]. M.A.Ali, et al., JINR preprint E3-93-434, Dubna,1993.

PECULIARITIES OF HIGH-LYING LEVEL EXCITATION BY γ-CASCADES IN DIFFERENTLY SHAPED NUCLEI

V.A. Khitrov, Yu.V. Kholnov, A.M. Sukhovoj,
E.V. Vasilieva, A.V. Vojnov

Frank Laboratory of Neutron Physics, Joint Institute for Nuclear Research, 141980, Dubna, Russia

For a better understanding of the excitation and the depopulation mechanism for levels with different energies and structures, it is crucial to have information on the dipole radiative widths over a wide region of nuclear excitations. At present an unambiguous knowledge of this mechanism can be deduced only from investigations of two-step cascades. Such experiments [1] give indirect but very important information about level structures in the intermediate energy range from the ground-state up to neutron resonance. In particular, two-step cascade γ-decay spectra have been measured for many nuclei from the region of the $4S$-maximum of the neutron strength function - from ^{137}Ba up to ^{198}Au.

An important advantage of this method is the opportunity to detect all possible two-step cascades between the compound-state and several low-lying final levels and to extract useful information, even in cases when the spaces between decaying states are smaller than the resolution of the detector.

A very essential result was obtained earlier [1]: cascades from neutron resonances with large Γ_n^0 mainly excite few-quasiparticle low-lying final states. Those from states with small Γ_n^0 excite many-quasiparticle (collective) high-lying final states of rather complex structures. This result leads to a qualitative explanation [1] of cascade enhancements between compound-states with relatively large Γ_n^0 and final states with a pure single-particle nature. Such an explanation supposes the excitation of a system of intermediate levels that have reasonably few-quasiparticle components in their wave functions, as is the case for the decay of a compound state with a relatively large single-particle component in its wave function (the case of large Γ_n^0). It also supposes the excitation of a system of levels of a collective nature for cases of small single-particle components in the compound-state structure. The main part of the two-step cascade data for nuclei from the $4S$-resonance of the neutron strength function corresponds to the first case.

Information about the population probability of levels with different excitation energies was obtained from usual cascade intensity distributions decomposed into "primary" and "secondary" components using the γ-decay scheme constructed in the same experiment [1].

Figs.1-3 present the typical dependences of intensity distributions on the primary transition energy E_1 for spherical $(A \simeq 140)$, deformed $(A \simeq 160)$ and also spherical $(A \simeq 190)$ nuclei. The histogram shows the experimental data for two-step cascade

intensities summed in 500 keV energy bins. The problems which arise when deriving the data plotted in Figs.1-3 were discussed earlier [2,3]. It was shown that the possible systematic error in the determination of cascade intensity most probably did not exceed 50%.

The most noticable experimentally revealed feature of compound-state cascade depopulation is "nonstatistical" - the strongly structured shape of the intensity spectra (Figs.1-3). These structural effects regularly appear in different ways for various nuclei. For spherical nuclei, the most intense cascades are measured at primary transition energies $E_1 > 4 - 5$ MeV (Fig.1). Low-energy primary transition intensities in these nuclei are comparable to those calculated (or are less than the culculated intensities).
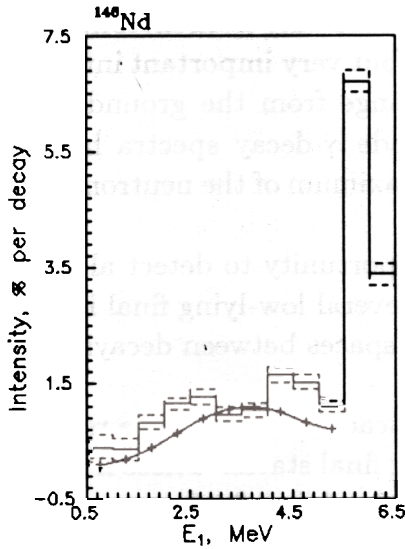
Fig.1. Distribution of total two-step cascade intensities (in % per decay) as a function of primary transition energy for the spherical ^{146}Nd nucleus.
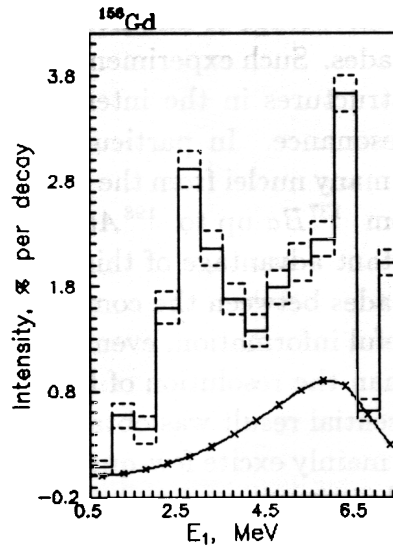
Fig.2. The same, as in Fig.1, for ^{156}Gd.

In strongly deformed nuclei from the begining of the $4S$-resonance of the neutron strength function, namely $^{156,158}Gd$ and ^{164}Dy, a second local maximum of the intensity distribution was revealed at the primary γ-quanta energy of $E_1 = 2 - 3$ MeV. This intensity enhancement is absent in the calculated intensities because the models commonly used predict a smooth energy dependence for level density as well as for the radiative strength functions.

In the middle of the $4S$-resonance region these two local intensity maxima probably create a joint peak, i.e., the greater part of the primary transition intensity falls in the excitation energy region of about $1/2B_n$.
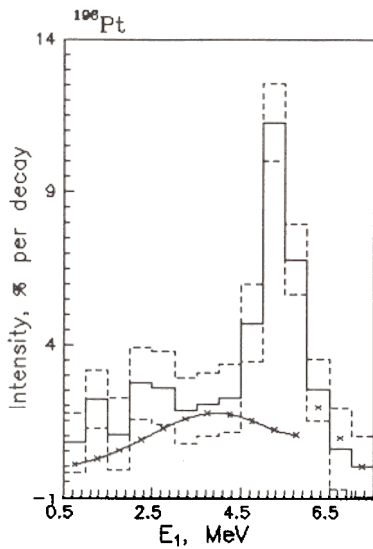
Fig.3. The same, as in Fig.1, for ^{196}Pt.

In nuclei from the end of the $4S$-resonance region, e.g., ^{196}Pt and ^{198}Au, this second local intensity maximum is not revealed. Probably, when increasing the mass number A and changing the shape of the nucleus, the cascade intensity distribution changes its shape as well.

Such a tendency permits the assumption that two-step cascade intensities depend on the shape of the nucleus. The coincidence between the intensity maxima for low-energy transitions and the calculated energies for the one-quasiparticle $3p_{1/2}$ and $3p_{3/2}$ neutron states for spherical nuclei, and the $K^\pi = 1/2^-$ and $3/2^-$ states for deformed nuclei, allows one to qualitatively explain this enhancement as a manifestation of one-particle transitions between the $4S$ and $3P$ states.

Finaly, one may conclude that two sets of nuclei, generally differing in shape, manifest different forms of cascade intensity distributions as a function of their primary transition energies.

References

[1]. S.T. Boneva, et al.: Sov. J. Part. Nucl. 22(2), 232 (1991)

[2]. S.T. Boneva, et al.: Z.Phys. A(330), (1988) 153

[3]. E.V. Vasilieva, et al.: Izv. RAN, ser. fiz. 57(10), (1993) 98

NEW RESULTS OF MEASUREMENT OF FISSION FRAGMENTS ANGULAR ANISOTROPY FROM RESONANCE NEUTRON INDUCED FISSION OF 235U ALIGNED TARGET

W.I.FURMAN[1], A.A.BOGDZEL[1], P.GELTENBORT[2], N.N.GONIN[3], M.A.GUSSEINOV[3], J.KLIMAN[4], Yu.N.KOPACH[1], L.K.KOZLOVSKY[3], L.V.MIKHAILOV[1], A.B.POPOV[1], H.POSTMA[5], N.S.RABOTNOV[3], D.I.TAMBOVTSEV[3]

[1]Frank Laboratory of Neutron Physics, JINR, Dubna, Russia
[2]Institute Laue-Langevin, Grenoble, France
[3]Institute of Physics and Power Engineering, Obninsk, Russia
[4]Institute of Physics, SAS, Bratislava, Slovakia
[5]Delft University of Technology, Delft, The Netherlands

1. Aims of investigation.

A long-standing problem of nuclear fission is the origin and nature of the so-called Bohr fission channels [1] including their interconnection and relation to fission modes recently considered in a clear and instructive manner in [2]. An investigation of epithermal neutron induced fission via largely isolated compound states, having a known spin J and parity π, gives a unique possibility, to get new insight into the problem.

It is appropriate to note that from a more general point of view this is an interesting example of the peculiar chaotic behaviour of a complex quantum system such as the heavy excited nucleus after neutron capture. In this case the complex excited nucleus (chaotic system I) goes via a very limited number of transitional states (Bohr's channels) of a highly deformed (and cold) nucleus to a nuclear system broken up into two fragments which have a wide distribution over mass and kinetic energy (chaotic system II) . These transitional states are relatively simple, but they are hidden between the two chaotic systems and therefore difficult to study. However, a better understanding of such states is of interest since they occur with nuclear matter in a rather unstable and excited condition.

The use of aligned target nuclei in the 235U(n,f)- reaction in the region of known s-wave neutron resonances [3] allows us to directly investigate [4] the dependence of partial fission amplitudes on the quantum number K, defined as a projection of spin J onto the deformation axis of a fissioning nucleus. In the experiment of Ref. [4] angular anisotropy coefficients have been measured for several s-wave resonances of the 236U compound nucleus. But, more valuable information can be extracted from the study of the energy dependence of this anisotropy. The differential cross-section of this reaction can be written in the following manner [5]:

$$\frac{d\sigma_{nf}}{d\Omega_{n_f}} = \frac{1}{4\pi}\left[\sigma_{nf}^0(E_n) + f_2\sigma_{nf}^2(E_n)P_2(\cos\theta)\right] \qquad (1)$$

The total fission cross-section $\sigma_{nf}^0(E_n)$ is expressed by

$$\sigma^0_{nf}(E_n) = \pi\lambda^2 \sum_J g_J \sum_K \left| S_J(0\tfrac{1}{2} \to Kf) \right|^2 \tag{2}$$

The energy dependent $S_J(lj \to Kf)$ is an element of the S-matrix describing the transition from the entrance channel $\{ljI\}$ (with an orbital momentum l, total spin j of the incident neutron and a target nucleus spin I) to the inclusive fission channel f with explicit quantum numbers JK energy dependent anisotropy is expressed by [5]:

$$\sigma^2_{nf} = \pi\lambda^2 \sum_{JJ'} \sqrt{g_J g_{J'}} \, U(\tfrac{1}{2}IJ2; JI) \sum_K C^{J'K}_{JK20} S^*_{J'}(0\tfrac{1}{2} \to Kf) S_J(0\tfrac{1}{2} \to Kf) \tag{3}$$

Here $g_J = (2J+1)(2(2I+1))^{-1}$, $U(\tfrac{1}{2}IJ2; JI)$ is a Racah coefficient and $C^{J'K}_{JK20}$ are Clebsch-Gordan coefficients providing the K-dependence of the anisotropy part of the cross-section in a different way compared to the total cross-section (2). A new and important point predicted by formula (3) is the presence of interference between s-wave resonances of different spins.

To obtain unambiguous partial fission amplitudes characterized by quantum numbers $J\pi K$ it is necessary to make a combined analysis on the basis of formulae (1)-(3) of the data on the spin separated total cross-sections [3] and the $\sigma^2_{nf}(E_n)$ value. This is the aim of this paper.

2. Experimental arrangements

The 235U target nuclei were aligned using the electric quadrupole hyperfine interaction in the uranyl group (UO_2) in a single crystal of rubidium uranyl nitrate (RUN), cooled to low temperature [4]. Two mosaic samples made from single crystal slabs of RUN having total areas of 20 cm^2 and 24 cm^2 were used. All slabs were properly oriented and attached to both sides of a copper target plate connected to the dilution chamber of a 3He/4He dilution refrigerator. The evaluation of the surface temperature under neutron irradiation from the angular anisotropy of the α- particles gives $0.15°K$. From this the nuclear alignment parameter $f_2 = -0.16$ is calculated for 235U.

The fission fragments from each sample were detected by three silicon surface barrier semiconductor detectors of rectangular form $((2\times5)cm^2$ active area each) mounted in the directions $0°$, $45°$ and $90°$ with respect to the C-axis of the single RUN crystals which were oriented along the neutron beam. In comparison with [4] the detectors at $45°$ were added to improve the investigation of fission fragment angular distributions. For monitoring the neutron flux an additional layer of a non-orientable 235U compound, about 0.5 mg/cm^2 thick, and a separate Si detector were placed in the neutron beam. All detectors were mounted onto the $1°K$ screen.

The data acquisition system with a PC on-line, plus a hard disk, allowed the accumulation of seven separate energy spectra (1024 channels each) of α- particles plus fission fragments and seven time-of-flight spectra (4096 channels each) of fission fragments.

The cryostat with an aligned 235U target was installed at beam No. 5 of the IBR-30 pulsed booster source on the flight path length of 29.4 m. with a neutron pulse width about 4 μs and a burst

frequency of 100 Hz. The time-dependent (neutron) background was measured at the "black resonances" of some beam filters.

A set of computer programs were developed for:

- calculation and extraction of neutron background from black filter files;

- correction for neutron background data files;

- calculation of real geometry experimental corrections using the Monte Carlo method;

-extraction of the coefficients A_2 and A_4 from data files.

3. Preliminary results

An example of a TOF-spectrum is shown in Fig.1. One can see that up to neutron energy $E_n \leq 30eV$ (channel numbers ≥ 500), the energy resolution is satisfactory.

In Fig.2, the experimental values $A_2(E_n)$ are shown as a ratio $\sigma_{nf}^2(E_n)/\sigma_{nf}^0(E_n)$ for the range of 0.2 - 70eV . This figure includes the results of a preliminary analysis of two initial runs. Due to low statistics, a summation over groups of 50 TOF channels was done. As seen in Fig.2 a prominent energy dependence of $A_2(E_n)$ exists. For the first 4^- resonance the present data reasonably resembled the old measurements [6]. The most interesting qualitative conclusion following from Fig.2 is a first indication of the presence of interference between s-wave resonances of different spins in the $A_2(E_n)$ on neutron energy. It can be seen immediately from a comparison of the measured A_2 with the calculated ones [7] obtained in a multilevel, two-channel approach neglecting, in formula (3), the terms with $J' \neq J$. But it is necessary to improve the statistics to obtain a more quantitative conclusion.

At this stage of the experiments, it becomes clear that some improvements of the method are necessary to achieve a desirable accuracy for measurements of the energy behaviour of the angular dependent part of the fission cross-section. The needed improvements are: quality of the sample surface, stability of the Si-detectors mainly against the γ-flash accompanying the neutron bursts, and the necessity to extend the measuring time at $0.15^\circ K$.

Now, a new dilution refrigerator with a "cold plate" to replace the $1^\circ K$ helium bath is under construction which will permit us to keep a low temperature during the full time of the run. A new type of implanted Si detectors are at the stage of development and testing. Uranium monosulphide is being investigated as a perspective replacement of the monocrystal sample, but this will require an external magnet.

Acknowledgment

126

References

[1] A.Bohr, Proc. Int. Conf. on Peaceful Uses of Atomic Energy, Geneva, 1955, v. 4,
   United Nations, N. Y., 1955, p.220

[2] U.Brosa et al., Phys. Reports, **197**,(1990) p.167

[3] M.S.Moore et al., Phys. Rev., **C18**, (1978),p.1328

[4] N.J.Pattenden and H.Postma, Nucl. Phys., **A167**, (1971),p.225

[5] A.Barabanov and W.Furman, Proc. of Int. Conf. on Nuclear Data for Science and Technology,
   Gatlinburg,1994, to be published

[6] H.Postma, Proc. Int. Symp. on Neutron Capture , Gamma-Ray Spectroscopy and Related Topics,
   Petten, 1974, p.619

[7] M.S.Moore et al., Nucl. Phys., **A502**,(1989), p. 443c
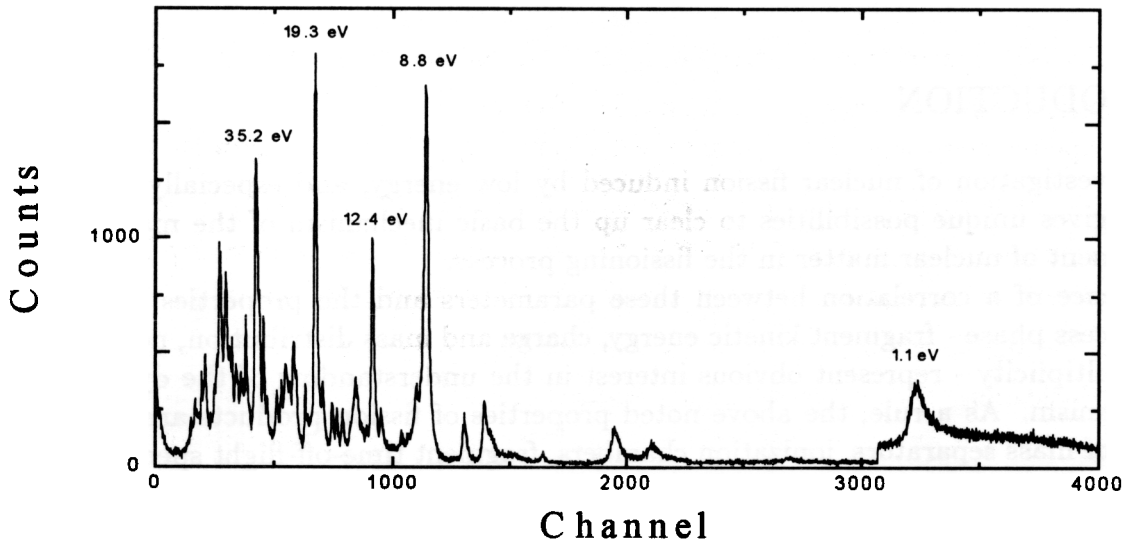
Fig.1 An example of a TOF spectrum for the 235U target, aligned in the RUN crystal at T=0.15°K measured at IBR-30. Experimental conditions are: t_n=4.0μs, L=29.4 m, initial delay 160μs. The time scale was split into 3072 channels of 0.5 μs and 1536 ones of 2.0 μs.
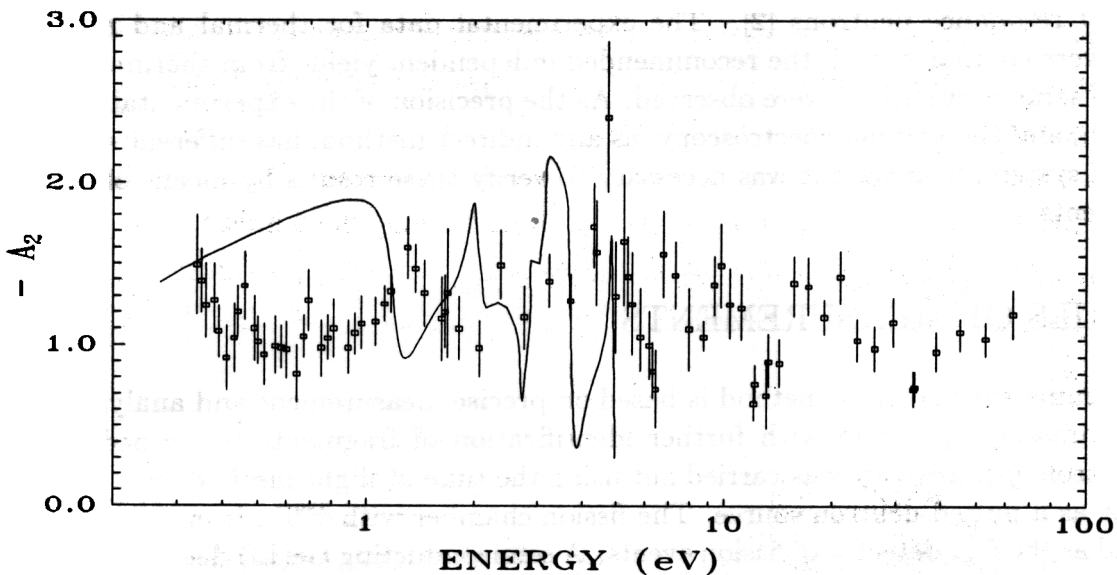
Fig.2 The dependence of $A_2(E_n)$ on neutron energy. The points are our results. The curve taken from ref. [7] is a result of calculations without accounting for the interference of the compound-states of different spins.

Comparative measurements of independent yields of ^{239}Pu fission fragments induced by thermal and resonance neutrons.

N.Gundorin, Yu.Kopach, S.Telegnikov

Frank Laboratory of Neutron Physics, Joint Institute for Nuclear Research,141980 Dubna, Moscow Region, Russia

1. INTRODUCTION

The investigation of nuclear fission induced by low energy, and especially resonance neutrons, gives unique possibilities to clear up the basic mechanism of the manyparticle rearrangement of nuclear matter in the fissioning process.
The existence of a correlation between these parameters and the properties of the end fission process phase - fragment kinetic energy, charge and mass distribution, neutron and gamma multiplicity - represent obvious interest in the understanding of the dynamic fission mechanism. As a rule, the above noted properties of fission products are measured by means of mass separators, ionization chambers, fragment time-off-flight spectrometers, and other arrangements with small amounts of fission materials in spectroscopic layer form. These arrangements have poor high-transmission and may be employed only in the intensive beam of high neutron flux sources. Another possibility, the use of gamma-ray spectroscopy methods to determine fission fragment yields, was first demonstrated during the investigation of spontaneous fission ^{252}Cf [1]. The greater high-transmission of this method was used in the investigation of gamma - rays from fission fragments of ^{239}Pu induced by resonance neutrons [2]. The experimental data for thermal and resonance neutrons were compared with the recommended independent yields from thermal neutron fission and some peculiarities were observed. As the precision of the experimental data was not enough, and the gamma-spectroscopy, as any indirect method, has different sources of possible of systematic errors, it was necessary to verify these results by means of the new measurements.

2. DETAILS OF MEASUREMENTS

The gamma-spectroscopy method is based on precise measurement and analysis of the fission gamma-ray spectrum with further identification of fragments by refined gamma lines. Neutron spectroscopy was carried out using the time-of-flight method with the IBR-30 reactor as a pulsed neutron source. The fission chamber with ^{239}Pu is employed as the target and as the fast detector of fission events. A semiconducting Ge(Li) detector was used

to measure the gamma-ray spectrum. To ensure the absence of systematic errors in the experimental data, fission yield fragments induced by thermal neutrons were measured. As the recycling energy for the pulse neutron spectrometer is 0.17 eV there is no possibility to use the time-of-flight method and a Cd-filter was used to separate out the thermal neutron fission. For the first measurement with the Cd-filter in the neutron beam, the integral yield of fragments for resonance neutron induced fission from the 0.4 to 230 eV energy region may be calculated by the formula:

$$Y_{fr}^{res} \quad Y_{\gamma}^{Cd}/k_{\gamma} \quad \frac{N_{\gamma}^{Cd} \cdot (1 + \alpha)}{k_{\gamma} \cdot \epsilon_{\gamma} \cdot N_{f}^{Cd}} \tag{1}$$

where Y_{fr}^{res} is the integral fragment yield per fission, Y_{γ}^{Cd} - the yield according the gamma line per fission through measurements with the Cd-filter in the neutron beam, k_{γ} - the number of gamma-rays per fragment, N_{γ}^{Cd} - the area of photo peak in gamma spectrum, α - the coefficient of intrinsic conversion of gamma-ray for this fragment, ϵ_{γ} - efficiency of the spectrometer, and N_{f}^{Cd} - the number of fission events during measurement with the filter. After the second measurement without the Cd-filter, the yield of fragments for thermal neutron induced fission, Y_{fr}^{th} may be calculated by the formula:

$$Y_{fr}^{th} \quad \frac{(N_{\gamma} \cdot N_{\gamma}^{Cd'}) \cdot (1 + \alpha)}{N_{f}^{Cd'}) \cdot k_{\gamma} \cdot \epsilon_{\gamma}} \tag{2}$$

where $N_{\gamma}^{Cd'}$, N_{γ}, $N_{f}^{Cd'}$, N_{f} are the areas of the photo peak and the numbers of fission events for the measurements with and without Cd-filter, respectively, normalized by the neutron flux. The average squared deviation for n experimental means from recommended data of fragment yields is characterized by parameter:

$$\chi^2/n \quad [\sum_{i=1}^{n}(Y_{th}^{exp} \quad Y_{th}^{rec})^2/(\Delta Y_{th})^2]/n \tag{3}$$

To increase the precision of comparative results the relative yields of fission fragments are compared by calculating the following ratio:

$$P_{th}^{res} \quad \frac{N_{\gamma}^{Cd} \cdot (N_{f} - N_{f}^{Cd'})}{N_{f}^{Cd} \cdot (N_{\gamma} - N_{\gamma}^{Cd'})} \tag{4}$$

The error of this ratio is connected mainly with the precision of the photo peak areas and it does not contain the error of specific gamma-spectrometer parameters.

3.RESULTS AND SPECTROMETER DEVELOPMENT

Partial results of comparative measurements are shown in Table 1. The independent yields of 15 even - even thermal neutron fission fragments of ^{239}Pu, measured in this experiment, are averaged with the few previous measurement results having different background conditions. This values are in column Y_{th}^{exp}. The recommended values Y_{th}^{rec}, the ratio between resonance and thermal neutron fission fragment yields P_{th}^{res} and the average squared

Table 1: The comparative measurement results

$_z\mathrm{Fr}^A$	Y_{th}^{exp} $\% \pm \Delta\%$	Y_{th}^{rec} [3] $\% \pm \Delta\%$	P_{th}^{res}
$_{36}\mathrm{Kr}^{88}$	0.83 ± 0.20	0.79 ± 0.03	1.08 ± 1.25
$_{36}\mathrm{Kr}^{90}$	1.14 ± 0.18	1.18 ± 0.05	2.50 ± 1.22
$_{38}\mathrm{Sr}^{94}$	2.79 ± 0.26	3.14 ± 0.16	0.77 ± 0.42
$_{38}\mathrm{Sr}^{98}$	2.85 ± 0.25	2.85 ± 0.14	0.54 ± 0.56
$_{40}\mathrm{Zr}^{100}$	4.72 ± 0.16	4.76 ± 0.24	1.03 ± 0.10
$_{40}\mathrm{Zr}^{102}$	1.45 ± 0.13	1.19 ± 0.12	1.14 ± 0.22
$_{42}\mathrm{Mo}^{104}$	4.50 ± 0.16	4.12 ± 0.21	0.98 ± 0.09
$_{42}\mathrm{Mo}^{106}$	2.09 ± 0.11	2.06 ± 0.10	1.71 ± 0.30
$_{52}\mathrm{Te}^{132}$	2.13 ± 0.23	2.36 ± 0.07	2.76 ± 1.31
$_{54}\mathrm{Xe}^{136}$	2.62 ± 0.28	3.02 ± 0.36	3.38 ± 3.43
$_{54}\mathrm{Xe}^{138}$	3.95 ± 0.23	4.08 ± 0.33	1.30 ± 0.37
$_{56}\mathrm{Ba}^{142}$	3.01 ± 0.17	3.27 ± 0.26	0.25 ± 0.25
$_{56}\mathrm{Ba}^{144}$	2.43 ± 0.12	2.05 ± 0.23	1.21 ± 0.19
$_{58}\mathrm{Ce}^{146}$	0.87 ± 0.12	0.95 ± 0.01	1.18 ± 0.45
$_{58}\mathrm{Ce}^{148}$	1.47 ± 0.11	1.09 ± 0.12	1.75 ± 0.27
χ^2/n	1.07		

deviation between the experimental data and recommended values are also shown in Table 1. The experimental results are in agreement with recommended data. The main differences of ratio P_{th}^{res} from unity for some fragments and the size of its experimental error are connected with the difficulties of γ-spectroscopy because of high background in fitting spectra and poor statistics for the measurement with the Cd-filter.

The main part of the experimental error is connected with the large continuous spectrum background due to the Compton scattered γ-rays. If the number of fission events during measurement are $3 \cdot 10^8$, the experimental errors of calculated yields are about 5 - 25%. It can be reduced by about one order of magnitude by means of "active" shielding of the Ge(Li) detector. The employment of a HPGe detector with high efficiency in the gamma-spectrometer and a reduction of electronic equipment deadtime are necessary to increase the number of identifiable fragments and the statistical provisions for measurements [4]. At the present time here is no possibility to measure the fission fragment yields of individual resonances for the range 40 - 230 eV due to insufficient neutron energy resolution on the IBR-30. It will increase after reconstruction of its neutron source according to the IREN project [5].

4. CONCLUSION

On the basis of the comparison of our results with the recommended data for thermal neutron induced fission, we can conclude that systematic error in the experimental data is absent. As a result of this comparative measurement we have not observed the peculiarities of integral yield fission fragments induced by resonance neutrons from 0.4 to 230 eV energy region within the experimental errors. For higher precision measurements of the yields of fission fragments by means of the gamma-spectroscopy method it is necessary to employ the Compton-suppression spectrometer with higher quality equipment. In this way, the number of identified fragments will be increased and independent yields of more than 1% could be measured to a precision of 1 - 3%. The measurements of the fission fragment yields from individual resonances for the energy region 40 - 230 eV will be possible after reconstruction of the IBR-30 reactor according the IREN project.

REFERENCES

[1] W. John et al, Phys. Rev. **C2**, 1451 (1970).

[2] A.A. Bogdzel et al, Proceedings of International Conference on Nuclear Data for Science and Technology, Jülich, May 13-17, 1991, pp. 150-152.

[3] A.C. Wahl, Atomic Data and Nuclear Data Tables, **39**, 118 (1988).

[4] N.A. Gundorin, International Workshop on Nuclear Fission, Obninsk, September 27-30, (1993).

[5] V.L. Aksenov et al, Communication of JINR, **E-3-92-110** Dubna, (1992).

An Improved Experimental Facility for Studying Delayed Neutrons and Preliminary Results of Measuring the β_{eff} value for ^{233}U relative to ^{235}U.

S.B. Borzakov, E. Dermendjiev, V.M. Nazarov, S.S. Pavlov, A.D. Rogov, I. Ruskov, Yu.S. Zamyatnin

Frank Laboratory of Neutron Physics,
Joint Institute for Nuclear Research
141980 Dubna, Russia

The effective fraction of delayed neutrons, $\beta_{eff} = \nu_{DN}/\nu$, is one of the principal reactor physics constants, important for nuclear reactor design, nuclear safeguards, etc. Here ν_{DN} is the total yield of delayed neutrons (DN) per fission, ν is the average number of fission neutrons per fission. The basic results on DN are described in [1].

Recently, Filip and D'Angelo [2] have shown that due to the continuous progress in nuclear reactor technology, measurements of enhanced accuracy are required of ν_{DN}-values for thermal neutron induced fission.

In order to perform investigations of delayed neutrons with high accuracy and to study short-time groups of DN, an improved experimental facility, using the method of periodic irradiation, was designed and tested. The facility utilizes the Dubna IBR-2 pulsed reactor (PR), a mirror neutron guide, a neutron chopper (NC), and a ^3He-filled multicounter neutron detector (ND).

The IBR-2 PR is used as a pulsed neutron source having a $200ms$ time interval between pulses. The bent mirror neutron guide considerably supresses the fast neutron background. The mean thermal neutron flux at a target is $2 \cdot 10^5$ n/sec·cm^2.

The NC consists of 2 mm thick Cd disk with two symmetric 20° slits. To get a better fixation of the termination of the neutron beam, the NC is mounted as close as possible to the ND after the mirror neutron guide. Rotation of the NC is synchronized with reactor bursts.

The ND consists of 12 ^3He-filled proportional counters placed in a polyethylene moderator. There is a hole in its centre for inserting samples. Monte-Carlo calculations show that the neutron detection efficiency for this setup is approximately 20%-30% in the 0.2 - 2.0 MeV range.

The measurement data are collected in the form of a time distribution (TD) of detected neutrons. All "start" pulses triggering the electronics are synchronized with the IBR-2 neutron bursts.

The TD of the detected neutrons consists of two different parts. The first part includes prompt fission neutrons (FN) detected during an exposure time Δt. The second part represents the time distribution of the detected DN in the time interval when the neutron beam is cut off.

If S_{FN} is the number of detected prompt fission neutrons and S_{DN} is the sum of DN detected in the time interval (t_1, t_2), $(t_1, t_2 < T)$, where t_1 and t_2 are counted after the exposure of the target is finished, then β_{eff} can be obtained from the equation:

$$\beta_{eff} = \frac{S_{DN}}{S_{FN}} \cdot \frac{\epsilon_{FN}}{\epsilon_{DN}} \cdot F(T, \Delta t, t_1, t_2) \tag{1}$$

where ϵ_{FN} and ϵ_{DN} are the detector efficiencies for prompt fission neutrons and delayed neutrons, respectively. One can readily obtain the value of $F(T, \Delta t, t_1, t_2)$ from the following expression, which takes into account the periodic exposure of the target and the existence of 6 DN groups, as suggested by Keepin [1]:

$$F(T, \Delta t, t_1, t_2) = \left[\sum_{i=1}^{6} \frac{A_i}{\lambda_i . \Delta t} \cdot \frac{1 - e^{-\lambda_i . \Delta t}}{1 - e^{-\lambda_i . T}} \cdot \left(e^{-\lambda_i . t_1} - e^{-\lambda_i . t_2} \right) \right]^{-1} \tag{2}$$

Here A_i is the relative yield ($\sum_{i=1}^{6} A_i = 1$) and λ_i is the decay constant for the i-th group of DN.

To test the facility, measurements with ^{235}U and ^{233}U targets were performed. The experimental TD of detected neutrons shown in Fig.1 and Fig.2 were measured with ^{235}U (0.3 g) and ^{233}U (0.1 g) targets, respectively. The background was measured with a 2 mm thick Cd filter in the neutron beam.
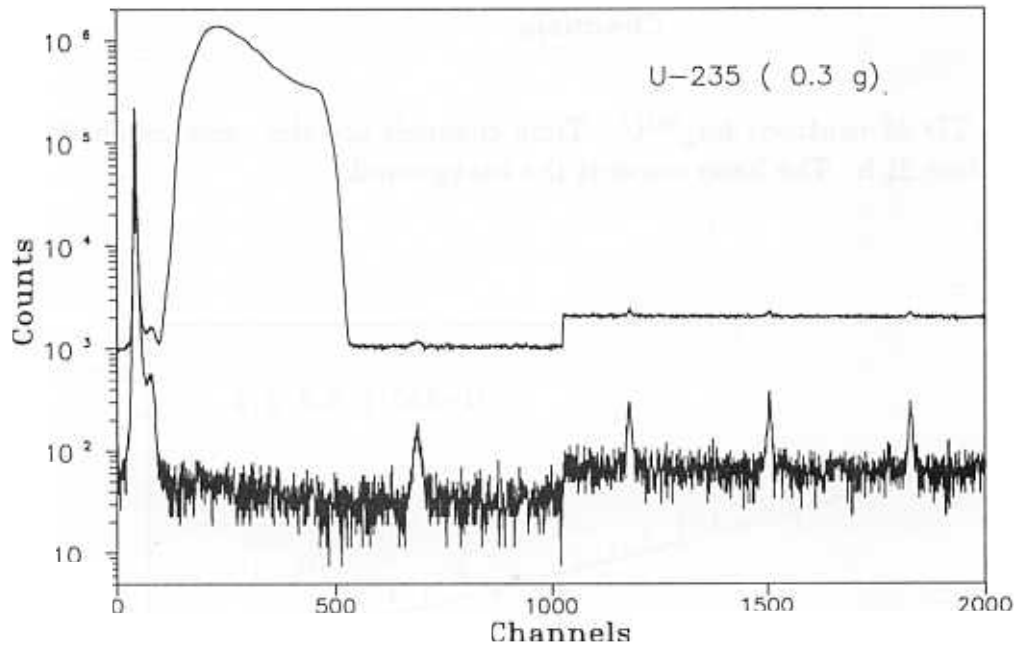
Fig. 1. A TD of neutrons for ^{235}U. Time channels $1024 \cdot 64\mu s + 1024 \cdot 128\mu s$, lower curve is the background. Measurement time 15 h.

By using the known values of $\beta_{eff}(^{235}U) = 0.0068 \pm 0.0002$ [4] we obtained the ratio of both neutron detector efficiencies for ^{235}U, which is in good agreement with the calculated value.

Calibrating our ^{233}U experimental data with the known data for ^{235}U, and making the assumption that the efficiency ratio for ^{233}U is the same as for ^{235}U, we have obtained the β_{eff} value for ^{233}U:

$$\beta_{eff}(^{233}U) = 0.0029 \pm 0.0002.$$

This value is in good accordance with the results in [3]. We must emphasize that the statistical error of the obtained values was several times less than system errors.
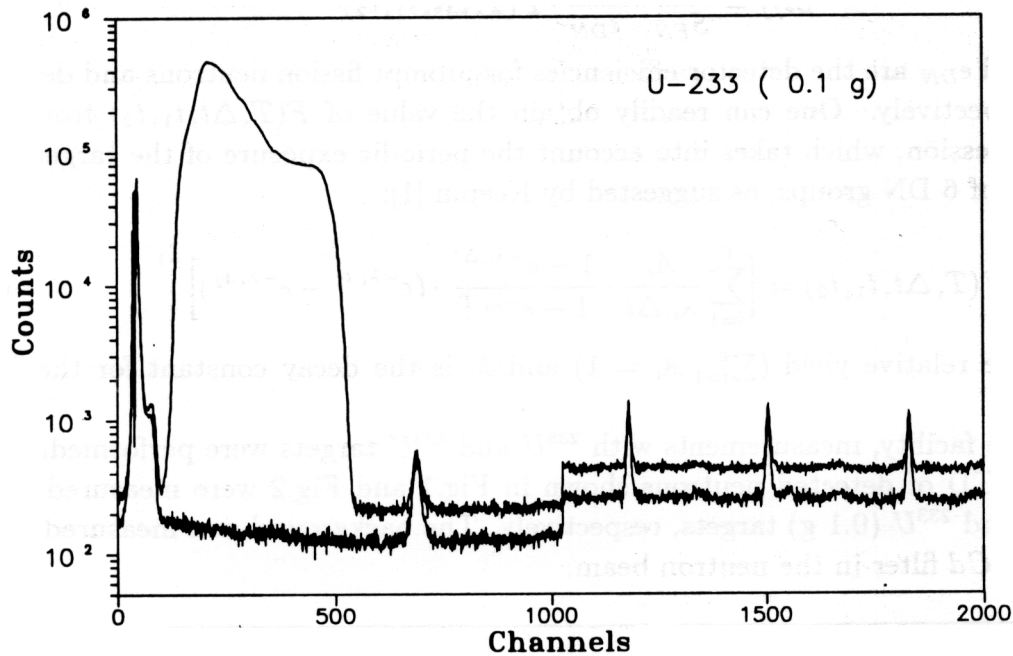
Fig. 2. A TD of neutrons for ^{233}U. Time channels are the same as on Fig. 1. Measurement time 21 h. The lower curve is the background.
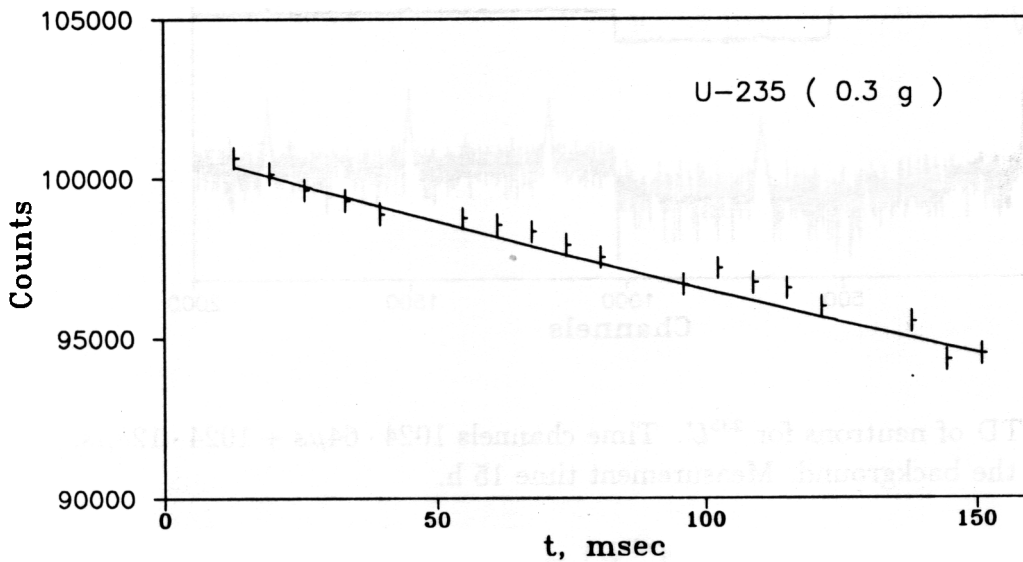
Fig. 3. Decay curve for ^{235}U. Every point is the sum of neutron counts in a 6.4 ms time interval.

The method of periodic irradiation allows the DN decay curve to be obtained from

our data (see fig.3). Our estimations for the possible existence of a 7-th group of DN with $\lambda_7 = 14$ sec^{-1} ($T_{1/2}= 50$ ms) show that $A_7 < 0.003$.

The facility for studying DN emission has been designed and tested. A method for periodic irradiation of a target by a pulsed reactor has been realized and the first measurements with good statistical accuracy and realistic results have been carried out.

The use of an extremely powerful pulsed neutron source, based on the IBR-2 pulsed reactor, gives the possibility of DN detection between neutron bursts starting a few "ms" after termination of the neutron beam by the NC. The facility gives the opportunity to estimate the contribution of short-lived groups to the DN emission.

We would also like to note that this is actually a multipurpose facility, which could be utilized in solving other problems relevant to nuclear fission, (n, γ)-reactions, etc. [5].

References

1. G.R.Keepin, Physics of Nuclear Kinetics, Addision Wesley, Reading Mass. (1965).

2. A. Filip, A. D'Angelo, "Nuclear data for Science and Technology", Proceedings, FRG, Juelich, 13-17 May 1991, p.946, Springer-Verlag, Berlin.

3. J.F. Conant, P.F. Palmedo, Nucl.Sci.Eng., 44, p.173 (1971).

4. J.Blachot, M.C. Brady, A. Filip, R.W. Mills, D.R. Weaver OECD-NEA Report, NEACRP-L-323 (1990), p.26.

5. E. Dermendjiev, W.I. Furman, Yu.S. Zamyatnin, Preprint JINR E3-93-7 (1993).

STUDY OF FAST NEUTRON INDUCED CHARGED PARTICLE PRODUCING REACTIONS

1. MEASUREMENT OF ANGULAR DISTRIBUTION AND CROSS SECTION FOR THE $^{58}Ni(n,\alpha)^{55}Fe$ REACTION AT 5.1 MeV

Yu.M.Gledenov, G.Khuukhenkhuu, M.V. Sedysheva
(*Frank Laboratory of Neutron Physics, JINR, Dubna, Russia*)
Tang Guoyou, Bai Xinhua, Shi Zhaomin, Chen Jinxiang
(*Institute of Heavy Ion Physics, Peking University, Beijing, P.R.China*)

Introduction

Investigation of charged particle emission reactions induced by fast neutrons is of interest for both nuclear energy applications and the understanding of basic nuclear physics problems. In particular the study of (n,α) reaction is important for estimating radiation damage due to helium production in the structural materials of fission and fusion reactors, as well as for testing nuclear reaction models.

Nickel is an important element of structural material. Natural nickel contains 68.27% ^{58}Ni. But experimental data of energy and angular distributions of alpha particle and cross section for the $^{58}Ni(n,\alpha)^{55}Fe$ reaction are very scarce in the energy range of several MeV. Because of this, was carried out measurement of energy spectra, angular distribution and cross section for the $^{58}Ni(n,\alpha)^{55}Fe$ reaction at 5.1 MeV [1].

Experimental method and results

Experiments were made in the D+D neutron beam of the Van de Graaf accelerator at the Institute of Heavy Ion Physics, Peking University, P.R.China. Emitted alpha particles were detected with a parallel-plate, gridded twin ionization chamber with a common cathode, which was made at the Frank Laboratory of Neutron Physics, JINR. The ionization chamber was filled with a mixture of 98.3% Kr and 1.7% CO_2 to 2.2 atm pressure. The first section of the twin ionization chamber contained studied target which is a metal disk of 99.9% enriched ^{58}Ni of 1.047 mg/cm^2 thickness. The target was backed on the aluminium cathode. The second section was empty and was used for background measurement. Neutron flux is monitored using a fission chamber with ^{238}U enriched to 99.997%. Two dimensional energy spectra of anode and cathode signals for emitted alpha particles were obtained with the help of measuring system based on the IBM PC AT-386 computer.

Cross section of the $^{58}Ni(n,\alpha)^{55}Fe$ reaction at 5.1 MeV was found to be 47.4 ± 5.0 mb. Angular distribution of alpha particles emitted in this reaction is nearly symmetrical with respect to $\theta=90°$ (Fig.1).

The comparison of the experimental results with the statistical model calculations shows [1] that the angular distribution and cross section for the $^{58}Ni(n,\alpha)^{55}Fe$ reaction at 5.1 MeV can be described by the compound nucleus model (Figs. 1 and 2).

References

1. Tang Guoyou et al. In: "Neutron Spectroscopy, Nuclear Structure, Related Topics". Proceedings of the II international Seminar on Interaction of Neutrons with Nuclei. 1994. Dubna. (In press)
2. S.M.Qaim et al. Nucl.Sci.Eng., vol.88, N2, (1984), P.143.
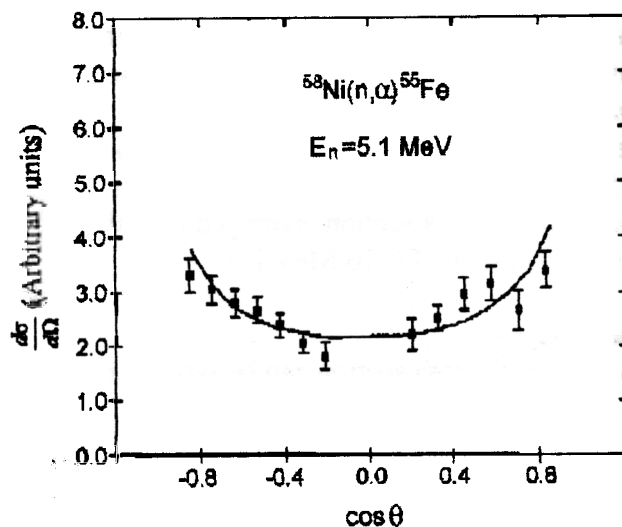
Figure 1.The angular distribution of alpha-particle emission in the $^{58}Ni(n,\alpha)^{55}Fe$ reaction at 5.1 MeV. Black points are our experimental data. Solid curve is the statistical model calculation.
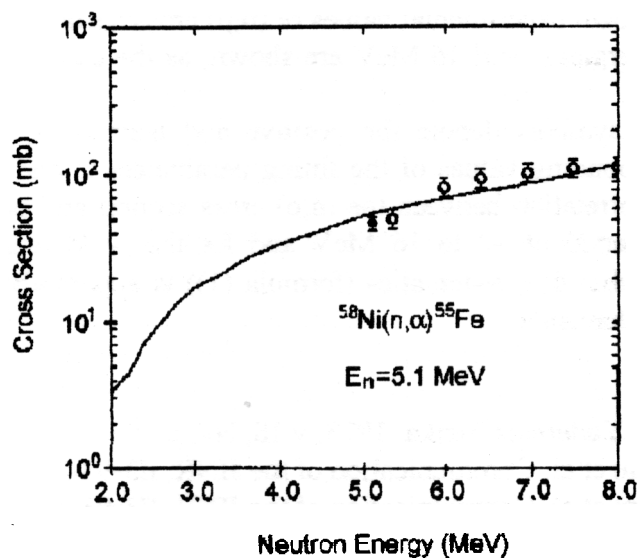
Figure 2. The excitation function of the $^{58}Ni(n,\alpha)^{55}Fe$ reaction.
Experimental points:O - ref.[2]; ● - present work. Solid curve is the statistical model calculation.

2. SYSTEMATICS OF THE FAST NEUTRON INDUCED (n,p) REACTION CROSS SECTIONS

G.Khuukhenkhuu, Yu.M.Gledenov, M.V.Sedysheva, G.Unenbat.

Introduction

In practice it is often necessary to evaluate the cross section of the nuclides, for which no experimental data are available. Therefore, it would be useful to derive some empirical law for governing neutron cross section variation. Besides, such empirical law is perhaps useful for the understanding of nuclear reaction mechanisms. Several formulae have bee suggested to describe the isotopic dependence of the (n,p) cross section around the neutron energy of 14.5 MeV only (see, for example, ref. [1]). Recently, we observed a similar dependence for the (n,p) cross section, averaged over the fission neutron spectrum of ^{235}U [2] and in the energy range of 6-16 MeV [3].

Formula and Data Analysis

For black target nucleus (n,p) cross section can be written as follows [4]:

$$\sigma_{np} = C\pi(R + \lambda)^2 \exp\left[-\frac{K(N-Z)}{A}\right] \qquad (1)$$

where $R = r_0 A^{1/3}$ is the radius of the target nucleus; λ is the wavelength of the incident neutrons divided by 2π; A, N and Z are the mass number, the number of neutrons and the charge of the target nucleus, respectively. The parameters K and C for different energies of neutrons can be determined from experimental data fitting, using formula (1).

Analysis of known experimental (n,p) cross sections depending on the relative neutron excess parameter $(N-Z)/A$ of the target nucleus showed that formula (1) satisfactorily describes all experimental (n,p) cross section data in the wide energy range of ~2 to 16 MeV [4]. The known experimental values of (n,p) cross sections and the line fitted by expression (1) at energies 6 and 16 MeV are shown, as the examples, in Figs. 1 and 2, respectively.

Plus and minus symbols denote the positive and negative Q-values of reactions, respectively. Corresponding values of the fitting parameters C and K are also given in these figures. The correlation between the (n,p) cross section and parameter (N-Z)/A in the wide energy interval of ~2 to 16 MeV and for the wide range of mass number A=19÷197 indicate that this systematics (formula (1)) is apparently independent on the nuclear reaction mechanisms.

References

1. V.N.Levkovsky. Yadernaja Fizika, 1973, v.18, N4, p.705.
2. G.Khuukhenkhuu et al. Communication of the JINR, E3-93-205, 1993, Dubna.
3. G.Khuukhenkhuu et al. Communication of the JINR, E3-93-466, 1993, Dubna.
4. G.Khuukhenkhuu et al. In: "Neutron Spectroscopy, Nuclear Structure, Related Topics". Proceedings of the II International Seminar on Interaction of Neutrons with Nuclei, 1994, Dubna. (in press)
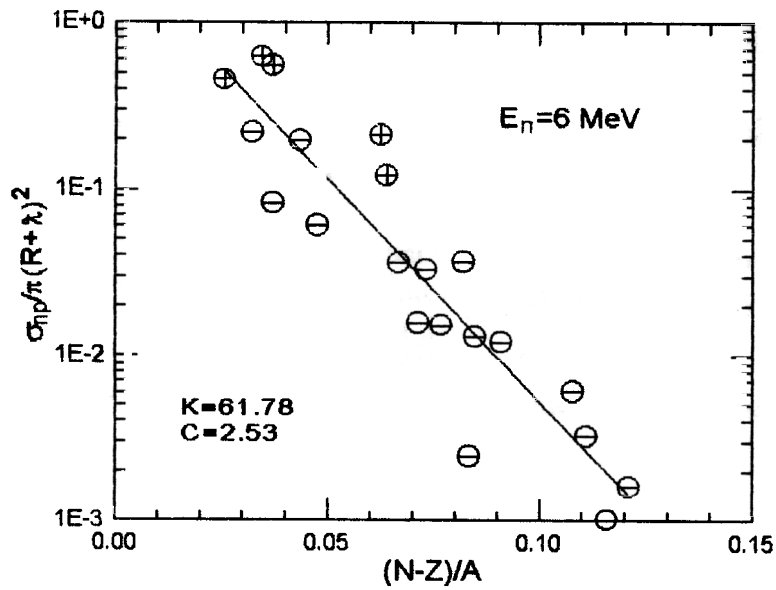
Figure 1. The dependence of reduced (n,p) cross section
upon the relative neutron excess parameter (N-Z)/A
of the target nucleus at E_n=6 MeV.
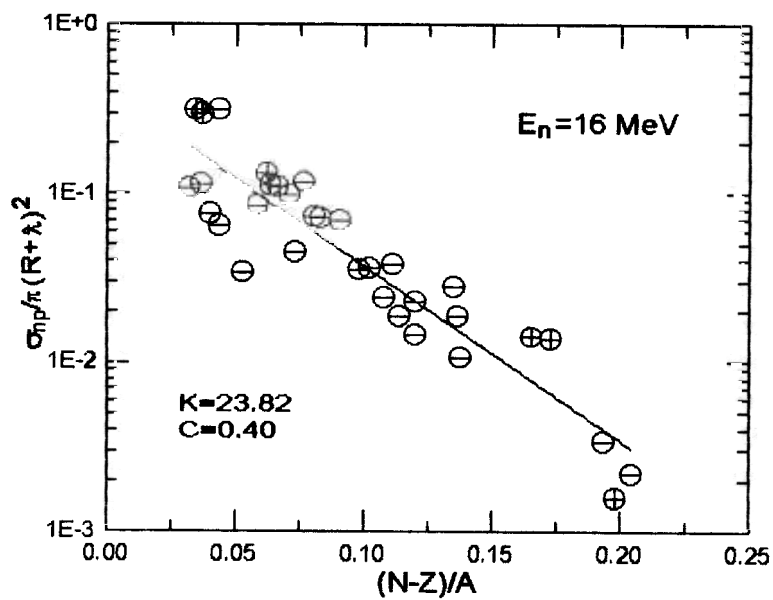
Figure 2. The same as in Fig. 1 at E_n=16 MeV.

NUCLEOSYNTHESIS OF THE RARE ISOTOPE ^{36}S: MEASUREMENTS OF THE ^{36}S(n,γ) CROSS SECTION AT kT=25 keV AND THE ^{35}Cl(n,p)^{35}S CROSS SECTION FOR THERMAL NEUTRONS

Yu.M.Gledenov, Yu.P.Popov, V.I.Salatski, P.V.Sedyshev, M.V.Sedysheva.
*Frank Laboratory of Neutron Physics, Joint Institute for Nuclear Research, 141980
Dubna, Russia.*
H.Beer, F.Kappeler.
*Kernforschungszentrum Karlsruhe, Institut fur Kernphysik III, P.O.Box 3640, D-76021
Karlsruhe, Germany.*

The synthesis of the rare nucleus ^{36}S is a long-standing problem in nuclear astrophysics. Most of the rare isotopes are thought to originate in explosive environments in stars [1]. Up to now, however, all explosive calculations appeared to overproduce ^{36}S. Recently, investigations of the s-process contribution to the abundance of nuclei from the S-Ca region have appeared [2]. One result of these calculations was that the s-process can account for most of the observed ^{36}S abundance. Both explosive nucleosynthesis and s-process calculations, however, have a significant uncertainty because the cross sections for the reactions that lead to ^{36}S or destroy it have not been measured and theoretical estimations are used instead. From this point of view, the ^{36}S(n,γ) reaction cross section at star temperatures is very important, as up to now there was only a theoretical estimation: 0.3 mb at 30 keV [3]. The ^{35}Cl isotope may also play a role in the nucleosynthesis of ^{36}S. This influence is introduced via branching, which determines the relative probability of the ^{36}S synthesis via the ^{35}Cl(n,γ)^{36}Cl(n,p)^{36}S and the ^{35}Cl(n,p)^{35}S(n,γ)^{36}S reaction sequences. It is clear that the Maxwellian average cross section (MACS) values at star temperatures (in the keV region) are needed in nucleosynthesis calculations. An accurate cross section value at thermal neutron energies is also very important. The thermal cross section has a direct impact on MACS-values, which may be significant, and this value is indeed to normalize cross section data at higher neutron energies. So, Koehler investigated the ^{35}Cl(n,p)^{35}S reaction from 25 meV up to 100 keV at the LANSCE facility, Los-Alamos (USA) [4] normalizing data to a thermal value of 489±14 mb from [5]. Wagemans, et al., repeated these measurements at the GELINA facility, Geel (Belgium) [6]. But they used the thermal value of 440±10 mb for normalization, which they also determined at the Grenoble reactor. Koehler's and Wagemans's MACS-values have a discrepancy factor of up to 1.5. In connection with this we carried out measurements of the ^{35}Cl(n,p)^{35}S reaction cross section for thermal neutrons.

The ^{36}S(n,γ)^{37}S (5.1 min) cross section was measured with neutrons at the pulsed 3.75 MV Van de Graaf accelerator of Kernforschungszentrum Karlsruhe (Germany). Using the special properties of the ^{7}Li(p,n) reaction near the reaction threshold a Maxwellian neutron spectrum with a thermal energy kT=25 keV was generated [7]. The cross section was determined by the fast cyclic activation technique which is described in detail in [7]. Samples of elemental sulphur enriched with ^{36}S by
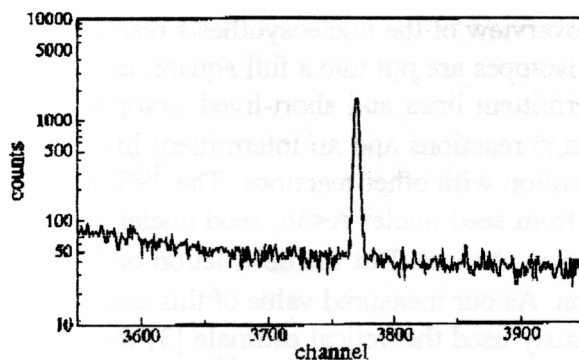
Fig. 1. The accumulated γ-ray intensity from a ^{36}S activation.

5.933% were irradiated, sandwiched between two gold foils which served as the capture standard. The γ-emission from the sulphur and gold was registered by a 175 cm^3 HPGe detector. In Fig.1 the accumulated 3103 keV γ-ray line from ^{36}S activation is shown. A preliminary MACS-value of 0.178 mb at kT=25 keV was obtained. The results were presented in [8].

Two runs of measurements of the ^{35}Cl(n,p)^{35}S reaction cross section for thermal neutrons were carried out on the neutron beam of the IBR-30 pulsed booster in Dubna. We used our facility based on the double grid ionization chamber and multiparameter data system acquisition [9,10]. The NaCl and LiF targets were prepared by vacuum evaporation and the ^{6}Li(n,t)^{4}He reaction served as a standard. In Fig.2 the amplitude spectrum of the ^{35}Cl(n,p)^{35}S reaction is shown. We have a preliminary result for this reaction at thermal neutrons: σ_{th}=540±40 mb. This result was presented in [11].
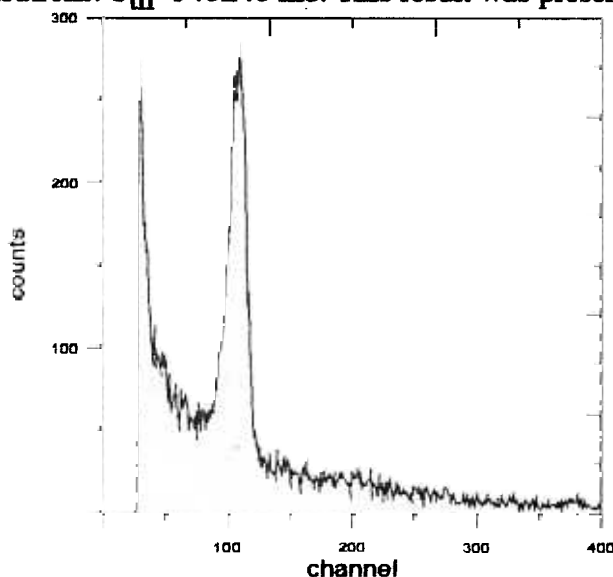
Fig. 2. Spectrum of the protons from the ^{35}Cl(n,p)^{35}S reaction at thermal neutrons.

Fig.3 gives an overview of the nucleosynthesis reaction sequences in the sulphur-calcium region. Stable isotopes are put into a full square, unstable but long-lived isotopes into a square with intermittent lines and short-lived isotopes are surrounded by a circle. Normal arrows mark (n,γ) reactions and an intermittent line means a less probable (n,γ) transition due to competition with other reactions. The ^{36}S production is mediated by the $^{36}Cl(n,p)^{36}S$ reaction from seed nuclei $A<36$, seed nuclei with $A>36$ can contribute via the $^{39}Ar(n,\alpha)^{36}S$ reaction channel. But the destruction of ^{36}S is only achieved through the $^{36}S(n,\gamma)^{37}S$ reaction. As our measured value of this cross section is by a factor of 1.8 smaller than the previously used theoretical estimate [3] the s-process production of ^{36}S will be enhanced by a factor 1.8. Concerning the $^{35}Cl(n,p)^{35}S$ reaction cross section, our value for thermal neutrons is 19% higher than the value used by Wagemans [6] and 9% higher than value used by Koehler [4,5]. It should be noticed, however, that our result is preliminary and we are planning to continue the measurements.
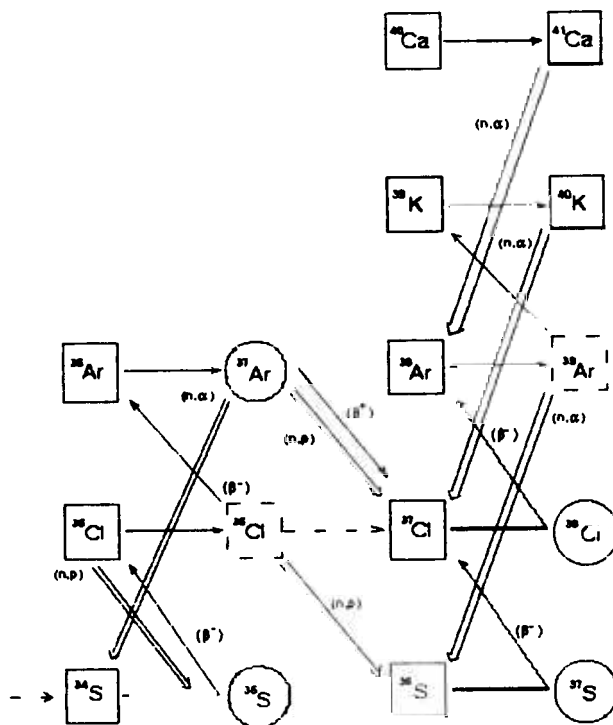
Fig. 3. Partial nucleosynthesis network in the S-Ca region.

References

1. W.M.Howard et al., Astrophys.J. 157 (1972), 201
2. H.Beer, R.-D.Penzhorn, Astron. Astrophys. 174 (1987), 323
3. S.E.Woosley et al., Atomic Data Nucl. Data Tables 22 (1978), 371
4. P.E.Koehler, Phys. Rev. C44(1991), 1675.
5. S.F.Mughabghab, M.Divadeenam, N.E.Holden, Neutron Cross Sections, vol.1 (Academic,New York, 1981), p.17-1.
6. S.Druyts et al., Nucl. Phys.A573 (1994), 291.
7. H.Beer et al., NIM A337 (1994), 492.

8. P.Sedyshev et al.,II International Seminar on Interaction of Neutrons with Nuclei (Abstracts), E3-94-113, Dubna(1994).

9. Yu.M.Gledenov et al., Prib. Tekh. Eksp., No3(1988), 55.

10. User Guide. Neutron Experimental Facilities at JINR. Compiled by A.V.Belushkin, LNP, JINR, Dubna, 1991, p.45-47.

11. Yu.M.Gledenov et al., III International Symposium "Nuclei in the Cosmos", (Abstract), Osservatorio Astronomico di Collurania, Teramo, Italy(1994).

3. PUBLICATIONS

CONDENSED MATTER PHYSICS

Diffraction

V.L.Aksenov, A.M.Balagurov, B.N.Savenko, V.P.Glazkov, I.N.Goncharenko, V.A.Somenkov, E.V.Antipov, S.N.Putilin, J.-J.Capponi. Neutron Diffraction Study of the High-T_c Superconductor $HgBa_2CaCu_2O_{6.3}$ under High Pressure. JINR, E14-94-467, Dubna, 1994 (subm. to High Press. Res.).

2. V.L.Aksenov, A.M.Balagurov, B.N.Savenko, V.P.Glazkov, I.N.Goncharenko, V.A.Somenkov, E.V.Antipov, S.N.Putilin, J.-J.Capponi. Neutron Diffraction Study of the High-T_c Superconductor $HgBa_2CaCu_2O_{6.3}$ under High Pressure., Int. Sem. Neutron Scattering at High Pressure, Dubna, 1994.

3. V.L.Aksenov, A.M.Balagurov, G.D.Bokuchava, J.Schreiber, Yu.V.Taran. Estimation of Residual Stress in Rolled Iron-Disc by Strain Measurements Using the High Resolution Fourier Diffractometer of Reactor IBR-2. ECM-15, Dresden, 1994.

4. V.L.Aksenov, A.M.Balagurov, S.L.Platonov, B.N.Savenko, V.P.Glazkov, I.V.Naumov, V.A.Somenkov, G.F.Syrykh. TOF Neutron Spectrometer for Microsamples Studies under High Pressure. JINR, P13-95-14, Dubna, 1995 (in Russian) (subm. to High Press. Res.).

5. V.L.Aksenov, A.M.Balagurov, S.L.Platonov, B.N.Savenko, V.P.Glazkov, I.V.Naumov, V.A.Somenkov, G.F.Syrykh. TOF Neutron Spectrometer for Microsamples Studies under High Pressure. Int. Sem. Neutron Scattering at High Pressure, Dubna, 1994.

6. A.M.Balagurov, F.Bouree, I.S.Lyubutin, I.Mirebeau. Atomic and Magnetic Structure of $YBa_2(Cu_{1-x}{}^{57}Fe_x)_3O_{6+y}$ Studied by Neutron Diffraction on Isotope Enriched Samples. Physica C, 1994, v.228, p.299.

7 A.M.Balagurov. High-Resolution and High-Intensity Neutron Diffraction at the IBR-2 Pulsed Reactor. PANS-II, Dubna, 1994.

8. A.M.Balagurov. Neutron Fourier Diffractometer for High Resolution Powder Work. ECM-15, Dresden, 1994.

9. A.M.Balagurov. Structural Aspects of High-T_c Superconductors from Neutron Diffraction Studies. Dubna, VI Trilateral Seminar, 1993.

10. A.M.Balagurov, A.A.Naberezhnov, N.M.Okuneva, B.N.Savenko, S.B.Vakhrushev. Modulation of a Crystal Lattice in the Sodium-Bismuth Titanate Crystal. 13th General Conference of the Condensed Matter Division European Physical Society, Regensburg, Germany, March 29 - April 2, 1993.

11. A.M.Balagurov, B.N.Savenko, A.V.Borman, V.P.Glazkov, I.N.Goncharenko, V.A.Somenkov, G.F.Syrykh. Study of the Vibration and Structural Changes of NH_4Cl under High Pressure. JINR, E14-95-1, Dubna, 1995 (subm. to High Press. Res.).

12. A.M.Balagurov, B.N.Savenko, A.V.Borman, V.P.Glazkov, I.N.Goncharenko, V.A.Somenkov, G.F.Syrykh. Study of the Vibration and Structural Changes of NH_4Cl under High Pressure. Int. Sem. Neutron Scattering at High Pressure, Dubna, 1994.

13. A.M.Balagurov, F.Bouree, I.S.Lyubutin, I.Mirebeau. Atomic and Magnetic Structure of $YBa_2(Cu_{1-x}{}^{57}Fe_x)_3O_{6+y}$ Studied by Neutron Diffraction on Isotope Enriched Samples. M^2S-HTSC IV, Grenoble, 1994.

14. A.M.Balagurov, P.Fischer, T.Yu.Kaganovich, E.Kaldis, J.Karpinski, V.G.Simkin, V.A.Trounov. Precision Fourier Neutron Diffraction Study of the High-Temperature Superconductor $Y({}^{44}Ca)Ba_2Cu_4O_8$. JINR, E14-94-415, Dubna, 1994.

15. A.M.Balagurov, V.G.Simkin. Possibilities of High Pressure Studies with the High-Resolution Neutron Fourier Diffractometer. High Pressure in Material Science & Geoscience, Brno, 1994.

16. A.M.Balagurov, V.P.Glazkov, I.N.Goncharenko, B.N.Savenko, V.A.Somenkov. Neutron Powder Diffraction at High Pressure in Diamond and Sapphire Anvils on Reactor IBR-2. Powder Diffraction and Crystal Chemistry, S.Petersburg, June 20-23, 1994.

17. A.M.Balagurov, Yu.V.Taran, I.S.Lyubutin, A.Ya.Shapiro. Atomic Structure of Y123-Cu/Fe in Oxygen-Saturated and Oxygen-Deficient States. Superconductivity, 1994, v.7, p.274.

18. A.M.Balagurov, Yu.V.Taran. Instrument for Stress Measurements on High Resolution Fourier Diffractometer at High Flux Pulsed Reactor IBR-2. Proc. of IV Int. Conf. on Residual Stresses, p.202, Baltimore, 1994.

19. A.I.Beskrovniy, S.Durdok, J.Hejtmanek, Z.Jirak, E.Pollert, I.G.Shelkova. Structural Modulation, Oxygen Content and Transport Properties in $Bi_{2.13}Sr_{1.87}CuO_{6+y}$ and $Bi_{2.05}Sr_{0.41}CuO_{6+y}$ Superconductors. Physica C, 1994, v.222, pp.375-385.

20. V.Yu.Bezzabotnov, V.V.Nietz, S.A.Oleynik. Non-Linear Periodical Waves and Solutions in the Antiferromagnet with Uniaxial Anisotropy at the Spin-Flop Transition. (Subm. to Journal of Magnetism and Magnetic Materials).

21. T.I.Bukharova, E.M.Ivanova, D.I.Nikolaev, T.I.Savjolova. Approximation of Orientation Distribution of Grains in Polycrystalline Samples by Means of Gaussians. Proceedings of the 10th International Conference on Textures of Materials, Editor H.-J.Bunge. Materials Science Forum, 1994, v.157/162, pp.323-326.

22. S.Buyko, D.Georgiev, K.Krezhov, V.Nietz, G.Passage. Induced Antiferromagnetism in $HoFeO_3$. JINR, P14-94-431, Dubna, 1994, (in Russian) (subm. to Journal of Magnetism and Magnetic Materials).

23. S.A.Buyko, D.G.Georgiev, V.V.Nietz, K.A.Krezhov, G.Passage. Measuring of the Antiferromagnetic Susceptibility of Ho^{+3} Ions in $HoFeO_3$ on SNIM-2 Spectrometer. XXX Conference on Low Temperature Physics, Dubna, 6-8 September 1994 (in Russian).

24. D.Georgiev, K.Krezhov, V.V.Nietz. Weak Antiferromagnetism in $YFeO_3$ and $HoFeO_3$. JINR, P14-94-430, Dubna. 1994 (in Russian) (subm. to Journal of Magnetism and Magnetic Materials).

25. D.Georgiev, V.V.Nietz, T.Petukhova, A.Sirotin, G.Varenik, A.Yakovlev. The Spectrometer for Neutron Studies of Condensed States with a Pulsed Magnetic Field. JINR, P10-94-434, Dubna, 1994 (in Russian) (subm. to Neutron Research).

26. D.Georgiev, V.V.Nietz. Observation of Hysteresis at the Spin-Flop Transition Induced by a Pulsed Magnetic Field. JINR, P14-94-429, Dubna, 1994, (in Russian) (subm. to Journal of Magnetism and Magnetic Materials).

27. D.G.Georgiev, V.V.Nietz. Investigation of Dynamic Phase Diagram of α-Fe_2O_3 in Pulsed Magnetic Field. XXX Conference on Low Temperature Physics, Dubna, September 6-8, 1994 (in Russian).

28. V.P.Glazkov, A.M.Balagurov, A.V.Borman, I.N.Goncharenko, B.N.Savenko, V.A.Somenkov, G.F.Syrykh. High Pressure Neutron Scattering Experiments with Diamond and Sapphire Anvils at the IBR-2 Reactor. XXXII Annual Meeting of the European High Pressure Research Group "High Pressure in Material Science and Geoscience", 1994.

29. J.Heinitz, Zen En Ken, N.N.Isakov, A.S.Kirilov, M.L.Korobchenko, A.I.Ostrovnoi, V.E.Rezaev, A.P.Sirotin. Data Acquisition and Control System at NSHR Spectrometer Based on VME Standard. JINR, P13-94-73, Dubna, 1994 (in Russian).

30. J.Heinitz, N.N.Isakov, A.N.Nikitin, W.A.Sukhoparov, K.Ullemeyer, K.Walther. High Pressure Device for In-Situ Measurements in a Neutron Beam. Proceedings of the 10th International Conference on Textures of Materials, Editor H.-J.Bunge. Materials Science Forum, 1994, v.157/162, pp.131-136.

31. K.Helming, R.A.Schwazer, B.Rauschenbach, St.Geier, B.Leiss, H.-R.Wenk, K.Ullemeyer, J.Heinitz. Texture Estimates by Means of Components. Z. Metallkunde, 1994, v.85, pp.545-553.

32. T.I.Ivakina, I.A.Kovalev, Ye.V.Kovaleva, A.N.Nikitin. Influence of Textural Transitions within an Inclusion on the Stressed State of an Elastic Medium. Physics of the Solid Earth, 1994, v.29, pp.545-552.

33. A.N.Ivanov, N.A.Nikolaev, B.N.Savenko, L.S.Smirnov. Ceramic High Pressure Cell with Profiled Anvils for Neutron Investigations up to 7 GPa. Int. Sem. Neutron Scattering at High Pressure, Dubna, 1994.

34. Z.Jirak, A.I.Beskrovnyi, J.Hejtmanek, E.Pollert. Structure and Transport Properties of $Bi_{2.13}Sr_{1.87}CuO_{6+y}$ and $Bi_{1.54}La_{0.41}CuO_{6+y}$ Superconductors. M^2S-HTSC IV, Grenoble, 1994.

35. A.I.Kolesnikov, A.M.Balagurov, I.O.Bashkin, A.V.Belushkin, E.G.Ponyatovsky, M.Prager. Neutron Scattering Studies of Ordered γ-ZrD. J.Phys.: Condens. Matter, 1994, v.6, p.8977-8988.

148

36. A.I.Kolesnikov, A.M.Balagurov, I.O.Bashkin, V.K.Fedotov, V.Yu.Malyshev, G.M.Mironova, E.G.Ponyatovsky. A Real-Time Neutron Diffraction Study of Phase Transitions in the Ti-D System after High-Pressure Treatment. J.Phys.: Condens. Matter, 1993, v.5, p.5045-5058.

37. A.I.Kolesnikov, V.E.Antonov, A.M.Balagurov, S.Bennington, M.Prager. Neutron Scattering Studies of the Structure and Dynamics of the PdCu-H Ordered Phase Produced under High Hydrogen Pressure. J.Phys.: Condens. Matter, 1994, v.6, pp.9001-9008.

38. Yu.A.Kumzerov, A.A.Nabereznov, B.N.Savenko, S.B.Vakhrushev. Freezing and Melting of Mercury in Porous Glass. JINR, E14-94-454, Dubna, 1994, p.6.

39. G.M.Mironova. A Cold Moderator at the IBR-2 as the Basis of the New Possibilities in Neutron Scattering Studies. PANS-II, Dubna, 1994.

40. G.M.Mironova. New Possibilities in Time-Resolved Neutron Scattering Studies by the Use of Cold Moderator at the IBR-2 Pulsed Reactor. PD-94, Powder Diffraction and Crystal Chemistry, St.-Petersburg, 1994.

41. E.A.Nenasheva, N.F.Kartenko, A.M.Balagurov, A.I.Beskrovnyi, L.S.Smirnov, O.A.Usov. Structure and Dielectric Properties of New Pyrochlor-Type Compounds with Stoichiometric Vacancies. ECM-15, Dresden, 1994.

42. V.V.Nietz. "Supercritical" Point on the Phase Diagram of Hematite in an External Magnetic Field. (subm. to Journal of Physics and Chemistry of Solids).

43. D.Nikolaev, K.Ullemeyer. A Note on Pre-processing of Diffraction Pole-Density Data. J. Appl. Cryst., 1994, v.27, pp.517-520.

44. D.I.Nikolaev. Numerical Optimization of the Series Method. Proceedings of the 10th International Conference on Textures of Materials, Editor Bunge H.-J. Materials Science Forum, 1994, v.157/162, pp. 393-400.

45. D.I.Nikolaev. Optimization Algorithm for the Bunge/Roe Method. Physics of the Solid Earth, 1994, v.29, pp.518-522.

46. D.I.Nikolaev, K.Walther. Absorption Correction for Non-Standard Geometry for Pole Figure Measurements. Proceedings of the 10th International Conference on Textures of Materials, Editor H.-J.Bunge. Materials Science Forum, 1994, v.157/162, pp.381-386.

47. D.I.Nikolaev, T.I.Savjolova. Approximation of the ODF by Gaussians for Sharp Textures. Proceedings of the 10th International Conference on Textures of Materials, Editor H.-J.Bunge. Materials Science Forum, 1994, v.157/162, pp.387-392.

48. F.Prokert, B.N.Savenko, A.M.Balagurov. The Observation of Phonons in TSCC by Pulsed Neutron Diffraction. Zeitschrift fur Kristallographie, Suppl., 1994, N8, p.309.

49. F.Prokert, B.N.Savenko, A.M.Balagurov. Thermal Diffuse Scattering in TOF Neutron Diffraction Studied on SBN Single Crystals. JINR, E14-94-99, Dubna, 1994 (subm. to Acta Cryst.).

50. V.A.Sarin, E.E.Rider, A.M.Balagurov, S.N.Barilo, A.I.Beskrovnyi, V.V.Bogatko, L.E.Fykin, D.Hohlwen, S.S.Negovelov, S.V.Shiryayev, Yu.N.Venevtsev. Neutron Structure Investigation of $BaBiO_3$-$KBiO_3$ Single Crystals. M^2S-HTSC IV, Grenoble, 1994.

51. B.N.Savenko. Neutron Diffraction on Ferroelastic Domain Structure. International Seminar Neutron Research with High Pressure, Poznan, 1994.

52. B.N.Savenko, A.N.Ivanov, B.Mroz, L.S.Smirnov, C.C.Wilson. Neutron Diffraction Studies of Low Temperature and Pressure-Induced Phase Transitions in $LiKSO_4$. 13th General Conference of the Condensed Matter Division, European Physical Society, Regensburg, Germany, 1993.

53. W.Skotzki, J.Dornbusch, F.Heinike, K.Ullemeyer. Formation of Oblique Shape and Lattice Preferred Orientation in a Quartz Band of a Gneissic Mylonite. Proceedings of the 10th International Conference on Textures of Materials, Editor: H.-J.Bunge. Materials Science Forum, 1994, v.157/162, pp.1481-1486.

54. K.Ullemeyer, K.Helming, S.Siegesmund. Quantitative Texture Analysis of Plagioclase. Textures of Geological Materials, Editors: H.-J.Bunge, S.Siegesmund, W.Skrotzki, K.Weber. DGM special publication, 1994, pp.93-108.

55. K.Ullemeyer, K.Weber. Correction of Phyllosilicate (002) X-ray Pole Figure Measurements. Textures of Geological Materials, Editors: H.-J.Bunge, S.Siegesmund, W.Skrotzki, K.Weber. DGM special publication, 1994, pp.83-92.

56. K.Ullemeyer, K.Weber. Preferred Orientation of Phyllosilicates in Mylonitic Rocks and Their Importance for Kinematic Interpretation. Physics of the Solid Earth, 1994, v.29, pp.553-561.

57. K.Walther, A.N.Nikitin, N.N.Isakov, K.Ullemeyer, J.Heinitz. Research on the Textured Structure of Geomaterials by the Diffraction Method Using a High-Resolution Neutron Spectrometer at the I.M.Frank Neutron Physics Laboratory of the Joint Nuclear Research Institute. Physics of the Solid Earth, 1994, v.29, pp.497-500.

58. K.Walther, A.N.Nikitin, T.D.Shermergor, V.B.Yakovlev. Determination of Effective Electroelastic Constants of Polycrystalline Textured Rocks. Physics of the Solid Earth, 1994, v.29, pp.533-538.

59. K.Walther, S.F.Kurtasov, A.N.Nikitin, Ye.G.Torina. Simulation of Deformation Textures in High-Temperature Quartz. Physics of the Solid Earth, 1994, v.29, pp.497-500.

60. V.B.Zlokazov. A Shape-Independent Reitveld-Analysis. American Crystallographic Association Annual Meeting (ACA-94), Atlanta, USA, 1994. Abstracts, s.2, v.22, p.155.

61. V.B.Zlokazov. AUTOX - a Program for Autoindexing Reflections from Multiphase Polycrystals. In Computer Physics Communications (accepted).

62. V.B.Zlokazov. The profile Analysis of the RTOF-Spectra. ECM-15, Dresden, 1994.

Small-Angle Scattering

1. A.V.Anikin, V.G.Cherezov, V.V.Chupin, V.I.Gordeliy. Polymerized Membranes: Structure and Hydration Properties. HERCULES, Grenoble, 1994.

2. L.A.Bulavin, V.M.Garamus, Yu.M.Ostanevich. Study of Micellar Solutions of Ethylxylated Di-isononylphenol by Small-Angle Neutron Scattering. (Subm. to Colloids and Surfaces).

3. V.I.Gordeliy, M.A.Kiselev. The Definition of Lipid Membranes Structural Parameters from Neutrongraphic Experiments with the Help of the Strip Function Model. (Subm. to Biophysical Journal).

4. N.Gorski. SANS-Investigation of Micelles Solutions at High Hydrostatic Pressures. Universitat Bayreuth, Physikalische, Deutchland, 1994.

5. N.Gorski, M.Gradzielski, H.Hoffmann. Mixtures of Non-ionic and Ionic Surfactants. The Effect of Countering Binding in Mixtures of Tetradecyldimethylamine Oxide and Tetradecyltrimethylammonium Bromide. Langmuir, 1994, v.10, pp.2594-2603.

6. N.Gorski, M.Gradzielski, H.Hoffmann. Mixtures of Non-Ionic and Ionic Tensiles. The Effect of Antiion Condensation. Hauptversamming der Kolloid-Gesellschaft, Julich, Deutschland, 1994 (in German).

7. N.Gorski, Yu.M.Ostanevich. Critical Micelle Concentration in $AOT-xH_2O-C_{10}D_{22}$ System as Determined by Small-Angle Neutron Scattering. Progress in Colloid and Polymer Science, 1993, v.84, p.235.

8. N.Gorski, Yu.M.Ostanevich. Small-Angle Neutron Scattering (SANS) Determination of the Volume Occupied by a Single Water Molecule in the Inverted Micellar Systems $AOT+x(H,D)_2O+C_{10}D_{22}$ by Internal Contrast Variation Technique. J. de Physique, 1993, v.3, pp.149-152.

9. F.Haussler, F.Eichhorn, H.Baumbach. Description of the Structural Evolution of a Hydrating Portland Cement Paste by SANS. Physica Scripta, 1994, v.50, pp.210-214.

10. F.Haussler, F.Eichhorn, H.Baumbach. Small-Angle Neutron Scattering on Hardened Cement Paste and Various Substances for Hydration. Cement and Concrete Research, 1994, v.24, pp.514-526.

11. A.Hempel, M.Hempel, F.Haussler, F.Eichhorn, H.Baumbach. Hydrating Cement Pastes as a Complex Disordered System. Euroconference, Stockholm, Sweden, 1994.

12. A.Hempel, M.Hempel, F.Haussler, F.Eichhorn, H.Baumbach. Investigation of Interfaces in Hydrating Cement Pastes by Small-Angle Neutron Scattering. 14th General Conference Condensed Matter Division, GCCMD-14, Madrid, 1994.

13. A.Hempel, M.Hempel, F.Haussler, F.Eichhorn, H.Baumbach. Microstructure of Hydrated Portland Cement Paste Investigated by Small-Angle Neutron Scattering. ECM-15, Dresden, 1994.

14. M.Hempel. Investigation of Latent and Short Etched Heavy Ion Tracks. 17th International Conference on Nuclear Tracks in Solids, Dubna, 1994.

15. M.Hempel, F.Haussler, H.Baumbach, A.I.Kuklin, W.Birkholz, P.Yu.Apel, M.Danziger, S.G.Stetsenko. SANS Studies of Latent and Etched Ion Tracks in PETP. 17th International Conference on Nuclear Tracks in Solids, Dubna, 1994.

16. Yu.V.Nikitenko. HTSC Investigation in Mixed State by Polarized Neutron Transmission. XXX Conference on Low Temperature Physics, Dubna, 1994 (in Russian).

17. J.Plestil, M.Ilavsky, H.Pospisil, D.Hlavata, Yu.M.Ostanevich, G.Degovics, M.Kriechbaum, P.Lagger. SAXS, SANS and Photoelasticity of Poly (N, N-Diethylacrylamide) Networks 1. Structure Changes after Temperature Jumps. Polymer, 1993, v.34, p.4846.

18. J.Plestil, M.Ilavsky, H.Pospisil. Small-Angle Neutron Scattering Study of Swollen Poly (N,N-Diethylacrylamide) Networks. 35 IUPAC International Symposium on Macromolecules, Prague, 1994, Book of Abstracts, p.84.

19. H.Pospisil, J.Plestil, Z.Tuzar. Small-Angle Neutron Scattering Study of Poly(Oxyethylene)-Block-Poly(Oxypropylene)-Block-Poly(Oxyethylene) in Aqueous Solutions. Collect. Czech. Chem. Commun., 1993, v.58, p.2428.

20. H.Pospisil, J.Plestil. Study of Micellar Behaviour of Triblock Copolymers by Means of SANS. Conference on "Experimental Technique in X-Ray and Neutron Structure Analysis", Ostrava, 1994, Proceedings, pp.255-258 (in Czech).

21. I.N.Serdyuk. Deuteration Biological Macromolecules for Neutron Scattering and NMR. Embo Workshop, Outrane, France, 1994.

22. I.N.Serdyuk. Small Angle Neutron Spectrometer YUMO (JINR DUBNA): Some Results and Perspectives. (Subm. to Physica B, 1994).

23. I.N.Serdyuk. Small-Angle Neutron Spectrometer "YUMO" (JINR Dubna): Some Results and Perspectives. In Abstracts of International Conference on Neutron Scattering, Sendai, Japan, 1994.

24. I.N.Serdyuk. The Triple Isotopic Substitution Method in SANS: Application to Some Problems of Structural Biology. International Conference on Neutron Scattering, Sendai, Japan, 1994.

25. I.N.Serdyuk, B.Zaccai, I.Rublevskaya, M.Pavlov. The Triple Isotopic Substitution Method in SANS: Application to Study of Ternary Complex EF-Tu-GTP-tRNK. J.Biophyis Chem, 1994 (accepted).

26. D.I.Svergun, M.M.Koch, I.N.Serdyuk. Structural Model of the 50S Subunit of E.Coli Ribosomes from Solution Scattering. (I) X-Ray Synchrotron Radiation Study. J. Mol. Biology, 1994, v.240, pp.66-77.

27. D.I.Svergun, M.M.Koch, J.S.Pedersen, I.N.Serdyuk. Solution Scattering from 50S Ribosomal Subunit Resolves Inconsistency between Electron Microscopy and Diffraction. Proc. Nat. Acad. of Science USA, 1994 (accepted).

28. D.I.Svergun, M.M.Koch, J.S.Pedersen, I.N.Serdyuk. Structural Model of the 50S Subunit of E.Coli Ribosomes from Solution Scattering. (II) Neutron Scattering Study. J. Mol. Biology, 1994, v.240, pp.78-86.

Inelastic Neutron Scattering

1. N.D.Afanasev, V.G.Gavrilyuk, S.P.Efimenko, G.G.Lishkevich, V.M.Nadutov, S.A.Danilkin, V.V.Sumin V.P.Minaev. Nitrogen and Carbon Effect on Crystal Lattice Dynamics in Austenitic Steels. III International Conference High Nitrogen Steels, Kiev, 1993.

2. N.B.Blagoveshchenskii, I.V.Bogoyavlenskii, L.V.Karnatsevich, Z.A.Kozlov, V.G.Koloborodov, A.V.Puchkov, A.N.Skomorokhov. On a Structure of Superfluid Helium-4 Elementary Excitations Spectrum. Physica B, 1994, v.194-196, p.545.

3. N.B.Blagoveshchenskii, I.V.Bogoyavlenskii, L.V.Karnatsevich, Z.A.Kozlov, V.G.Koloborodov, V.B.Priezzhev, A.V.Puchkov, A.N.Skomorokhov, V.S.Yarunin. Structure of Liquid He-4 Excitation Spectrum. JINR, P3-94-125, Dubna, 1994, p.22 (in Russian).

4. N.B.Blagoveshchenskii, I.V.Bogoyavlenskii, L.V.Karnatsevich, Z.A.Kozlov, V.G.Koloborodov, V.B.Priezzhev, A.V.Puchkov, A.N.Skomorokhov, V.S.Yarunin. Structure of Liquid He-4 Excitation Spectrum. (subm. to Phys.Rev., 1994).

5. L.Bobrowicz, K.Holderna-Natkaniec, M.Mroz, I.Natkaniec, W.Nawrocik. Neutron Scattering Studies of Phase Transitions in Protonated and Deuterated Ammonium Hydrogen Sulphates., 1994 (subm. to Ferroelectrics).

6. L.Bobrowicz, I.Natkaniec, K.Holderna-Natkaniec, M.Mroz, W.Nawrocik. Neutron Scattering Studies of Phase Transitions in Protonated and Deuterated Ammonium Hydrogen Sulphate. International Workshop on Neutron Research and Applications, Budapest, March 24-26, 1994.

7. L.Bobrowicz, S.I.Bragin, I.Natkaniec, T.Sarga. Neutron Scattering Studies of Pressure Induced Phase Transitions in NH_4HSO_4. International Seminar on Neutron Scattering at High Pressure (NSHP), Dubna, 1994.

8. I.V.Bogoyavlenskii, L.V.Karnatsevich, Z.A.Kozlov, V.G.Koloborodov, V.B.Priezzhev, A.V.Puchkov, A.N.Skomorokhov. Investigations of the Liquid Helium Excitations Spectrum by the Neutron Scattering Method. FNT, 1994, v.20.

9. I.V.Bogoyavlenskii, N.A.Ivanov, A.V.Puchkov. Cryostat for Neutron Investigations of a Large Volume of Liquid He between 5.2 and 1.2 K and Pressures up to 30 atm. (subm. to Cryogenics, 1994).

10. C.Cachet, A.Belushkin, I.Natkaniec, F.Fillaux, L.T.Yu. Characterization with Inelastic Neutron Scattering of Various Protonic Species in Manganese Dioxides. International Conference on Neutron Scattering, ICNS'94, Sendai, Japan, 1994.

11. S.A.Danilkin, A.I.Beskrovny. Nitrogen Effect on the Fe-18Cr-19Mn Alloy Lattice Dynamics. Preprint FEI-2372, Obninsk, 1994.

12. S.A.Danilkin, S.P.Efimenko, V.G.Gavriliuk, V.P.Minaev, V.V.Sumin. Slow Neutron Scattering Study of the Nitrogen Effect on the Fe-Cr-Mn-Ni Austenitic Steel Lattice Dynamics. International School and Symposium on Physics in Material Science, Jaszowiec, Poland, 1993.

13. S.A.Danilkin, V.P.Minaev, V.V.Sumin. Effect of Deformation on the Fe-18Cr-10Mn-15Ni Alloy Frequency Distribution. Preprint FEI-2371, Obninsk, 1994.

14. S.A.Danilkin, V.P.Minaev, V.V.Sumin. Inelastic Neutron Scattering Study of the Lattice Dynamics and Phase Composition of Ta-V-N Alloy. Preprint FEI-2349, Obninsk, 1994.

15. S.A.Danilkin, V.P.Minaev, V.V.Sumin. Investigation of Ta-V-N Alloy Dynamics and Phase Composition by Neutron Spectroscopy. Preprint FEI-2349, p.13, 1994, Obninsk.

16. T.Galbaatar, V.S.Shakhmatov, S.L.Dreksler. Phenomenological Theory of Phase Transitions in MeC_{60} (Me=K,Rb) Crystals. Proc. of XXX Symposium on Low Temp. Phys., Dubna, September 6-9, 1994 (in Russian).

17. V.G.Gavriluk, S.A.Danilkin, S.P.Efimenko, G.G.Lishkevich, G.G.Minaev, V.M.Nadutov, V.V.Sumin. Inelastic Neutron Scattering Study of the Nitrogen, Carbon and Metal Alloying Additions Effect on the Interatomic Interaction in Steels. (Subm. to Izvestiya Acad. of Sci. "Metally").

18. V.G.Gavriluk, V.M.Nadutov, S.A.Danilkin, V.P.Minaev, S.P.Efimenko, G.G.Lishkevich, V.V.Sumin. Study of the Nitrogen or Carbon and Metal Component Influence on the Interatomic Interactions in the Austenitic Steels by Inelastic Neutron Scattering.(Subm. to Mat. Sci. and Engineering).

19. V.G.Gavrilyuk, S.A.Sadikov, S.P.Efimenko, V.P.Minaev, V.V.Sumin. Investigation of the Interstitial Nitrogen Influence on Phonons Spectra of Austenite Steels by INS Method. Preprint FEI, № 2304, p.13, 1993, Obninsk.

20. E.A.Goremychkin, A.Yu.Muzychka, R.Osborn. Contribution of Mixing Interaction to the Crystal Field in $RECu_2Si_2$ (RE-rare earths). XXX Conference on Low Temperature Physics, Dubna, 1994 (in Russian).

21. E.A.Goremychkin, R.Osborn. Neutron Spectroscopy Study of the Heavy Fermion Compound $CeCu_6$. Phys.Rev.B, 1993, v.47, pp.14580-14584.

22. K.Holderna-Natkaniec, I.Natkaniec, I.Wasicki. Structural Phase Transitions and Molecular Dynamic in Bornyl Choride by Neutron Scattering and NMR Methods. 9th Symposium on Crystal Chemistry, Rydzyna, Poland, 1994.

23. K.Holderna-Natkaniec, I.Natkaniec, S.Habrylo, J.Mayer. Comparative Neutron Scattering Study of Molecular Ordering in d-Camphor and dl-Borneole. Physica B, 1994, v.194-196, pp.369-370.

24. K.Holderna-Natkaniec, I.Natkaniec. Neutron Scattering Studies of Disorder in Camphor-like Plastic Crystals in the Temperature Range of 10-300 K. Gordon Conference on Order/Disorder in Solids, New London, USA, 1994.

25. K.Holderna-Natkaniec, I.Natkaniec. Study of Internal Vibrations of dl-Camphene by IINS Method. Physica B, 1994, v.194-196, pp.371-372.

26. J.Kalus, M.Monkenbush, I.Natkaniec, M.Prager, J.Wolfrum, F.Worlen. Neutron and Raman Scattering Studies of the Lattice and Methyl Group Dynamics in Solid p-Xylene. 1994, (subm. to Liq.Cryst.Mol.Cryst.).

27. E.S.Klement'ev, P.A.Alekseev, V.N.Lazukov, I.P.Sadykov, A.Yu.Muzychka, I.L.Sachin. Definition of Condo-insulator CeNiSn Main State Forming Conditions. JETP, 1994, v.106, pp.1-18 (in Russian).

28. E.S.Klement'ev, P.A.Alekseev, V.N.Lazukov, I.P.Sadikov, A.Yu.Muzychka, W.Buehrer. Determination of Conditions of the Condo-insulator CeNiSn Ground State Formation. XXX Conference on Low Temperature Physics, Dubna, 1994 (in Russian).

29. A.I.Kolesnikov, V.V.Sinicyn, E.G.Ponyatovsky, I.Natkanec, L.S.Smirnov. Neutron Scattering Studies of Vibrational Spectrum of High Density Amorphous Ice in Comparison with Ice Ih and VI. J.Phys.: Condens.Matter, 1994, v.6, pp.375-382.

30. A.I.Kolesnikov, V.V.Sinicyn, E.G.Ponyatovsky, I.Natkaniec, L.S.Smirnov. Similarity of Vibrational Spectra of High Density Amorphous Ice and High Pressure Phase Ice VI. International Conference on Neutron Scattering, ICNS'94, Sendai, Japan, 1994.

31. A.I.Kolesnikov, V.V.Sinicyn, O.I.Barkalov, E.G.Ponyatovsky, V.K.Fedotov, A.M.Balagurov, G.M.Mironova, I.Natkaniec, L.S.Smirnov. Neutron Scattering Studies of Structural Transformations and Vibrational Spectra of Ice after High Pressure Treatment. International Seminar on Neutron Scattering at High Pressure (NSHP), Dubna, 1994.

32. I.Markichev, E.Sheka, I.Natkaniec, A.Muzychka, V.Khavryuchenko, Y.Wang, N.Herron. Density of Vibrational States of Thiol Capped CdS Particles. Inelastic Neutron Scattering. Physica B. 1994, v.1998, pp.197-199.

33. I.Markichev, E.Sheka, N.Goncharova, I.Natkaniec, A.Muzychka, V.Chukalin, V.Khavryuchenko, E.Nikitina. Density of Vibrational States of Silicon Nitride. Physica B, 1994, v.198, pp.200-202.

34. S.I.Morozov. Dynamics of Carbon in Interstitial Phase V-C. Fiz.Tverd.Tela, 1994, v.36, p.2763.

35. S.I.Morozov. Dynamics of Carbon in Interstitial Phase Nb-C. (Subm. to Fiz.Tverd.Tela, 1994).

36. S.I.Morozov. Interstitial Position and Vibrational Spectra of Hydrogen in A-V. (Subm. to Fiz.Tverd.Tela, 1994).

37. S.I.Morozov, V.V.Kazarnikov, V.V.Sumin. Vibrations of Interstitial N, H in Ta-N and Ta-N-H Solid Solution. Preprint FEI-2273, p.16, 1993, Obninsk.

38. S.I.Morozov, V.V.Kazarnikov. Investigation of the Nitrogen Atom Vibrations in a and b Phases Ta-N by Inelastic Slow Neutron Scattering. Fiz.Tverd.Tela, 1993, v.35, p.3145 (in Russian).

39. I.Natkaniec, A.V.Puchkov. Neutron Spectrometry at the IBR-2 Pulsed Reactor. Physics of/at Advanced Pulsed Neutron Sources, PANS-II, Dubna, June 14-16, 1994.

40. I.Natkaniec, E.S.Syrkin, S.B.Feodos'ev, B.K.Fedotov. Contribution of Copper Atoms to the Y-Ba-Cu-O Phonon Density of States. Localisation of Vibrations of the Cu_2 Atoms. XXX Conference on Low Temperature Physics, Dubna, 1994 (in Russian).

41. I.Natkaniec, L.S.Smirnov, A.I.Solov'ev. Ammonium Dynamics in Ordered and Disordered Phases of $K_{1-x}(NH_4)_xSCN$ Solid Solutions. International Conference on Neutron Scattering, ICNS'94, Sendai, Japan, 1994.

42. I.Natkaniec, L.S.Smirnov, A.I.Solov'ev. Ammonium Dynamics in Ordered and Disordered Phases of $K_{1-x}(NH_4)_xSCN$ Solid Solutions. Gordon Conference on Order/Disorder in Solids, New London, USA, 1994.

43. I.Natkaniec, L.S.Smirnov, A.I.Solov'ev. Ammonium Dynamics of Order and Disorder Phases of the $K_{1-x}(NH_4)_xSCN$ Solid Solution. XXX Conference on Low Temperature Physics, Dubna, 1994 (in Russian).

44. I.Natkaniec, S.I.Bragin, J.Brankowski, J.Mayer. Multicrystal Inverted Geometry Spectrometer NERA-PR at the IBR-2 Pulsed Reactor. ICANS-XII, Abingdon 1993, RAL Report 94-025, v.1, pp.89-95.

45. A.G.Novikov, M.N.Rodnikova, V.V.Savostin, O.V.Sobolev. The Investigations of Cs Diffusion in CsSl Solution by the Quasielastic Slow Neutron Scattering Method. Zhurnal Fiz.Chim., 1994, v.68, pp.1982-1986 (in Russian).

46. A.Pawlukojc. The INS Spectroscopy of Amino Acids. 9th Symposium on Crystal Chemistry, Rydzyna, Poland, 1994.

47. A.Pawlukojc, L.Bobrowicz, I.Natkaniec, J.Leciejewicz. The IINS Spectroscopy of Aminoacids: l- and dl-valine, 1994, (subm. to Spectrochimica Acta).

48. N.M.Plakida, V.S.Shakhmatov. Phenomenological Theory of Phase Transitions in $CsHSO_4$. (Subm. to Ferroelectrics, 1994).

49. I.L.Sashin. Crystalline Electric Field in Cubic Laves Phase Intermetallic Compounds $Y_{0.95}RE_{0.5}Ni_2$(RE=Pr, Nd, Tm, Er). International Conference of Magnetism, Warsaw, 1994.

50. I.L.Sashin. Phonon Density of States of the Superconducting $La_2CuO_{4.1}$. International Conference of Magnetism, Warsaw, 1994.

51. V.A.Semenov, V.S.Shakhmatov. Inelastic Scattering of Neutrons on Hematite. Preprint FEI-2376, Obninsk, 1994.

52. E.Sheka, V.Khavryutchenko, E.Nikitina, I.Natkaniec, I.Markichev, N.Goncharova, V.Chukalin. Surface Vibrations of Silicon Nitride: Inelastic Neutron Study and Computer Modeling. J.Electron Spectroscopy and Related Phenomena, 1994, v.67, pp.133-139.

53. E.F.Sheka, I.Natkaniec, V.D.Khavryutchenko, I.V.Markichev, I.V.Muzychka, N.Goncharova, V.Chukalin, E.Nikitina. Density of Vibrational States of Silicone Nitride. Physica B, 1994, v.198, pp.200-202.

54. L.S.Smirnov, I.Natkaniec, S.I.Bragin, J.Brankowski, A.I.Solov'ev, V.A.Goncharova, E.L.Gromnitskaya, G.G.Il'ina, O.V.Stal'gorova. The Neutron Powder Diffraction and Acoustic Investigations of NH_4SCN Phase Diagram. JINR, E14-94-266, Dubna, 1994.

55. L.S.Smirnov, I.Natkaniec, Yu.A.Shadrin, A.I.Solov'ev. Neutron Diffraction Studies of Lattice Parameters and the Phase Diagram of $K_{1-x}(NH_4)_xSCN$ Solid Solution. International Workshop on Neutron Research and Applications, Budapest, March 24-26, 1994.

56. L.S.Smirnov, V.A.Goncharova, E.L.Gromnitskaya, G.G.Il'ina, I.Natkaniec, A.I.Solov'ev, O.V.Stal'gorova. The Acoustic and Neutron Scattering Investigations of NH_4SCN Phase Diagram. High Pressure Research, 1994, v.13, pp. 65-70.

57. L.S.Smirnov, Yu.A.Shadrin. Thermal Properties of the NH_4SCN Monoclinic Phase (Neutron Diffraction Investigations). XII International Seminar on Intermolecular Interaction and Conformations of Molecules, Kharkov, Ukraine, 1994 (in Russian).

58. G.F.Syrych, V.P.Glazkov, I.L.Sashin, E.A.Goremychkin. Neutron Investigation of Temperature Dependence of HTSC $La_2CuO_{4.1}$. XXX Conference on Low Temperature Physics, Dubna, 1994 (in Russian).

59. M.Szafranski, A.Kartusiak. Phase Transitions and Competitive Interactions in Guanidinium Nitrate Crystals. 9th Symposium on Crystal Chemistry, Rydzyna, Poland, 1994.

60. A.A.Tumanov, V.I.Zarko. Influence of Pyrogenic Silica Hydration on Water Diffusion in Surface Layers. Reaction Kinetic and Catalysis Letters, 1993, v.50, p.189.

61. A.A.Tumanov, V.I.Zarko. Quasielastic Neutron Scattering from Adsorbed Water Molecules on Pyrolitic Silica Surface. Physica B, 1994, v.198. p.97.

62. M.B.Zaezzhev, A.G.Novikov, V.V.Savostin. The Isohoric Specific Heat and Anharmonic Effects in Liquid Potassium. Rasplavy, 1994, p.31.

63. M.V.Zaezzhev, M.N.Ivanovskii, A.G.Novikov, A.G.Savostin, A.L.Shimkevich. The Setup for Investigations of Impurities in Liquid Metals. Teplophisica visokih temperatur, 1994, v.32, pp.749-755 (in Russian).

64. M.V.Zaezzhev, M.N.Ivanovskii, A.G.Novikov, V.V.Savostin, A.L.Shimkevich. The Atomic Dynamics of Liquid Potassium at the Temperature Range 340-550 K. Zhurnal Fiz.Chim., 1994, pp.271-275 (in Russian).

Accelerated Ions

1. A.D.Bozhko, V.F.Dorfman, B.I.Pypkin, A.P.Kobzev, D.A.Korneev, L.P.Chernenko, D.M.Shirokov. Superconductivity of Carbon Tungsten Diamond-Like Films. XXX Conference on Low Temperature Physics, Dubna, 1994 (in Russian).

2. S.M.Duvanov, A.P.Kobzev, A.M.Tolopa, D.M.Shirokov. BS and ERD Analysis of the Metal-Glass Interfaces Produced by High Energy Metal Ion Beam Assisted Deposition. X International Conference on Ion Implantation Technology, Catania, Italy, 1994.

3. A.P.Kobzev, D.A.Korneev, L.P.Chernenko, D.M.Shirokov. Increase of Precision of Oxygen Depth Profiling of Thin Layer Samples. Poverkhnoct', 1994, v.6, pp.129-137.

4. R.Sandrik, V.Kliment, A.P.Kobzev, D.M.Shirokov. Applications of PIXE and RBS Methods in the Analysis of Thin Films of High-Tc Superconductors. Nucl. Instr. and Meth. in Phys. Res. B75, 1993, pp.392-396.

5. J.Semaniak, J.Braziewicz, M.Pajek, A.P.Kobzev, D.Trautmann. L-subshell Ionization of Heavy Elements by ^{3}He and ^{4}He Ions. Nuclear Instruments and Methods in Physics Research, 1993, v.875, pp.63-67.

6. J.Semaniak, J.Braziewicz, M.Pajek, T.Czyzewski, L.Glowacka, M.Jaskola, A.P.Kobzev, D.Trautmann. L-subshell Ionization of Heavy Elements by Protons and Deuterons. International Journal of PIXE, 1993, v.2, pp.241-246.

7. D.M.Shirokov, A.P.Kobzev, D.A.Korneev, L.P.Chernenko. Copper Transport Following Oxygen Annealing of a Superconducting Film Y-Ba-Cu-O. JINR, P3-93-242, Dubna, 1993 (in Russian).

Reflectometry, Polarized Neutrons

V.L.Aksenov, E.B.Dokukin, Yu.V.Nikitenko. Neutron Depolarization Investigations of High Temperature Superconductors in the Mixed State. Proceeding of the International Conference "Neutron Scattering", October 11-14, 1994, Sendai, Japan (to be publ. in Physica B).

2. V.L.Aksenov, Yu.V.Bugoslavskij, E.B.Dokukin, V.K.Ignatovich, S.V.Kozhevnikov, E.I.Kornilov, A.A.Minakov, Yu.V.Nikitenko, A.V.Petrenko. Anomalous Dependence of Neutron Depolarization on Magnetic Field in YBa$_2$Cu$_3$O$_{6.9}$ Ceramics near T$_c$. JINR, P4-94-476, Dubna, 1994 (in Russian), (subm. to JETP Lett.).

3. A.S.Borovik, A.A.Epifanov, A.P.Kobzev, D.A.Korneev, V.S.Malyshevski, S.N.Potapov. "Soft" Impact Effects on the Element Profiles and Superconducting Properties of Y-Ba-Cu-O Films. Proceeding of the XXIV National Meeting on the Physics of Charged Particle Interactions with Crystals, Moscow, May 30 - 1 June, 1994, Moscow.

4. A.D.Bozhko, V.F.Dorfman, B.I.Pypkin, A.P.Kobzev, D.A.Korneev, L.P.Chernenko, D.M.Shirokov. Superconductivity of a Tungsten-Containing Diamond-Like Films. Proc. of XXX Workshop on Low Temp. Phys., Dubna, 1994 (in Russian).

5. L.P.Chernenko, A.P.Kobzev, D.A.Korneev., D.M.Shirokov. Changes in Depth Profiles of Oxygen and Copper in Y-Ba-Cu-O Films under Annealing. 3rd European Workshop on Modern Developments and Applications in Microbeam Analysis, Rimini, Italy, May 9 - 13, 1993. Mikrochimica Acta, 1994, v.114-115, p.239-245.

6. L.P.Chernenko, A.P.Kobzev, D.A.Korneev, D.M.Shirokov. Damage in YBaCuO Films Produced by ^{4}He Ions. 3rd European Workshop on Modern Developments and Applications in Microbeam Analysis, Rimini, Italy, May 9 -13, 1993. Mikrochimica Acta, 1994, v.114-115, pp.247-254.

7. L.P.Chernenko, A.P.Kobzev, D.A.Korneev, D.M.Shirokov. Damage in Y-Ba-Cu-O Films Produced by 4He Ions. Russian-French Seminar on Current Topics of Condensed Matter Problems with Neutrons and Complementary Methods, Gatchina, 1993.

8. L.P.Chernenko, A.P.Kobzev, D.A.Korneev, D.M.Shirokov. On Mechanism of Damage Production in YBaCuO Films by ^{4}He Ions. VI Trilateral German-Russian-Ukrainian Seminar on HTSC, Dubna, 1993.

9. B.Chesca. An rf-SQUID Operating under Noise Influence. To be published as a contribution to the Proc. of the Eighth CIMTEC, Florence, July, 1994.

10. B.Chesca. Double SQUID Behavior in Superimposed rf and dc Magnetic Fields. To be published in World Scientific as a Contribution to the Proc. of the Conf. on Nonlinear Superconducting Devices & High Tc Materials, Capri, October, 1994.

11. B.Chesca. Sensitive Method for Studying the High Tc Superconducting Delicate Structures. Proc. of the XXX Conf. on Low Temp. Phys., Dubna, 1994 (in Russian).

12. E.B.Dokukin, S.V.Kozhevnikov, Yu.V.Nikitenko, A.V.Petrenko. Investigation of Fe_3O_4 Colloid Behaviour in a Magnetic Field by Polarized Neutron Transmission. JINR, E3-94-291, Dubna, 1994.

13. S.M.Duvanov, A.P.Kobzev, A.M.Tolopa, D.M.Shirokov. Investigation of the Element Depth Profiles in Layers of Glass Modified by Ion Beam Assisted Deposition. Nuclear Instruments and Methods in Physics Research. Beam Interaction with Materials and Atoms, B85, 1994, pp.264-267.

14. A.P.Kobzev, D.A.Korneev, L.P.Chernenko, D.M.Shirokov. An Influence of the Soft Action on the Element Profile and on the Superconducting Properties of the Y-Ba-Cu-O Films. Proc. of the XXIV International Meeting on Physics of the Charged Particle Interactions with Crystals, Moscow, 1994.

15. A.P.Kobzev, D.A.Korneev, L.P.Chernenko, D.M.Shirokov. Influence of the "Soft" Action on Elements Profile and Superconducting Properties of Y-Ba-Cu-O Films. Proc. of XXIV Intern. Workshop on Phys. of Charged Particle Interactions with Crystals, Moscow, 1994.

16. A.P.Kobzev, M.Maaza, D.M.Shirokov, D.A.Korneev. Characterization of Thin Film Multilayer Samples by MeV Ion Beam Techniques. International Symposium on Theoretical Physics "Kourovka-94": Magnetic Multilayers and Low Dimensional Magnetism, 1994, Ekaterinburg, Russia.

17. E.I.Litvinenko, Yu.V.Obukhov, A.N.Chernikov. SQUID-Susceptometer for Small Magnetic Moment Measurement. Proc. of 7th Intern. Symposium on Weak Superconductivity, June 6-10, 1994, Smolenice Castle, Slovakia, p.402.

18. V.V.Pasyuk, O.McGrath, H.J.Lauter, A.V.Petrenko, A.Leenard, D.Givord. Ground State Moment in an Ultra-Thin W(110)/Fe(110)/W(110) Film.(subm. to J. Mag. Mag. Mat.).

19. V.V.Pasyuk, O.McGrath, H.J.Lauter, D.Givord, A.V.Petrenko. Magnetism of W(110)/Fe(110)/W(110) Thin Films Studied by Polarised Neutron Reflection. Proc. of E-MRS on Magnetic Ultra-Thin Multilayers and Surfaces. Dusseldorf, Germany, 1994, v.1, p.429.

20. V.V.Pasyuk, H.J.Lauter, M.T.Johnson, F.J.A.den Broeder, E.Janssen, J.A.Bland, A.V.Petrenko. Magnetic Properties of Pd/Co/Pd Ultra-Thin Film Studied by Polarized Neutron Specular Reflection. Appl. Surface Science, 1993, v.65-66, p.118.

21. V.V.Pasyuk, H.J.Lauter, M.T.Johnson, F.J.A. den Broeder, E.Janssen, J.A.Bland, A.V.Petrenko, J.M.Gay. Interface Magnetisation in a Single Ultra-Thin Pd/Co/Pd Sandwich Structure. J. Mag. Mag. Mat., 1993, v.121, p.180.

Theory

1. V.L.Aksenov, V.V.Kabanov. Role of Antiferromagnetic Fluctuations in the Temperature Dependence of the Linewidth of the Transition between the Crystal-Field Levels in High-Tc Superconductors. Phys. Rev. B49, 1994, v.5, pp.3524-3527.

2. A.S.Alexandrov, V.V.Kabanov, D.K.Ray. From Electron to Small Polaron: an Exact Cluster Solution. Phys. Rev. B49, 1994, v.14, pp.9915-9923.

3. A.S.Alexandrov, V.V.Kabanov, D.K.Ray. Polaron Theory of Mid-Infrared Conductivity: a Numerical Cluster Solution. Physica C224, 1994, pp.247-255.

4. B.Chesca. On the Theory of an rf-SQUID Taking into Account the Noise Influence. Journal of Low Temp. Phys., 1994, v.94, pp.515-538.

5. B.Chesca. On the Theory of the Symmetrical Double SQUID. Physica C220, 1994, pp.249-257.

6. V.I.Dediu, V.V.Kabanov, A.S.Sidorenko. Dimensional Effects in V/Cu Superconducting Superlattices. Phys. Rev. B49, 1994, v.6, pp.4027-4032.

7. V.Gridin, S.Sergeenkov, R.Doyle, P. de Villers, M.Ausloos. Carrier Type Dependent Thermoelectric Response of the SNS Configuration in a C-Shaped Polycrystalline BiPbSrCaCuO. Phys. Rev. B47, 1993, pp.14591-14594.

8. V.V.Kabanov. Optical Conductivity in High-Tc Superconductors: Polaron Contribution. In: Book of Abstracts of the Conference on "Strongly Correlated Systems". Dubna, September 20-24, 1994. JINR, E17-94-304, Dubna, 1994, p.58.

9. V.V.Kabanov. Optical Conductivity in HTSC: Analysis of Polaron Contribution. XXX Conf. on Low Temperature Physics, Dubna, September 6-8, 1994. Abstract booklet. JINR, D14-94-268, Dubna, part 1, p.131-132 (in Russian).

10. V.V.Kabanov, D.K.Ray. Comment on the Paper of F.Marsiglio "Spectral Function of One-Dimensional Hostein Polaron". Phys. Lett. A, 1994, v.186, pp.438-440.

11. E.I.Kornilov. Calculation of Reflectivity from Fractal Multilayers. Physica B198, 1994, pp.38-39.

12. E.I.Kornilov, V.B.Priezzhev. An Exactly Solvable Lattice Model of Rooted Branched Polymers. Theor.Math.Phys., 1994, v.98, No.1, pp.90-105.

13. E.I.Kornilov, V.Yu.Pomjakushin. Strong Collision Approach to Calculation of Depolarization Function for Neutron Beam Passing through Ferromagnetic Bulk Domains. Solid State Communications, 1994, v.89, No.9, pp.767-770.

14. Yu.V.Obukhov. "Paramagnetic" Meissner Effect in Superconductors. JINR, E17-94-256, Dubna, 1994 (subm. to Physica C).

15. S.Sergeenkov. Ergodic Versus Nonergodic Behavior in Oxygen Deficient High-Tc Superconductors. Phys.Rev.B50, 1994, p.1.

16. S.Sergeenkov, M.Ausloos, M.Mehbod. On Back Bending of the Hall Number Density in YBCO High-Tc Superconductors. J. Phys.: Condensed Matter 1994, v.6, pp.L373-L376.

17. S.Sergeenkov, V.Gridin, P. de Villiers, M.Ausloos. Estimation of Effective Electronic Mass from the Magneto-Thermopower of the Polycrystalline $Bi_2Sr_2CaCu_2O_x$. Physica Scripta, 1994, v. 49, pp.637-641.

18. S.Sergeenkov, V.Gridin. Tunable Atomic Scale Josephson Effect in Dislocated High-Tc Superconductors. Phys.Rev.B50, 1994, pp.1293-1296.

19. A.A.Skoblin. Landau Quasienergy Spectrum Destruction for an Electron in Both a Magnetic Field and a Resonant Electromagnetic Wave. JINR, P4-94-176, Dubna, 1994 (in Russian).

20. A.A.Skoblin. Oscillator in Time-Dependent Periodic Strong Field. JINR, P4-94-93, Dubna, 1994 (in Russian).

21. A.A.Skoblin. Scattering Problem for Quantum System with Time-Dependent Periodic Hamiltonian. JINR, P4-94-63, Dubna, 1994 (in Russian).

22. A.A.Skoblin. The Kinetics of Quantum System with Time-Dependent Periodic Hamiltonian. JINR, P4-94-65, Dubna, 1994 (in Russian).

NEUTRON NUCLEAR PHYSICS

Experiment

A.A.Alekseev, A.A.Bergman, A.H.Volkov, M.V.Kazarnovsky, O.A.Langer, S.A.Novoselov, Yu.V.Ryabov, Yu.Ya.Stavissky, Yu.M.Gledenov, S.S.Parzhitski, Yu.P.Popov. High-Luminosity Lead Slowing-Down Neutron Spectrometer Driven by Linac of Moscow Meson Factory. In: Neutron Spectroscopy, Nuclear Structure, Related Topics. II Intern. Seminar on Inter. of Neutron with Nuclei. (Abstracts), JINR, E3-94-113, (1994), Dubna, p.9.

2. A.Aleksejevs, P.Prokofjevs, J.Tambergs, T.Krasta, S.Barkanova, W.Waschkowski, G.S.Samosvat. Neutron Electric Polarizability· Evaluation from Enriched ^{206,207,208}Pb Total Cross Sections Data. II International Seminar on Interaction of Neutrons with Nuclei, April 26-28, 1994, Dubna, Russia, JINR E3-94-113, Dubna, 1994, p.39.

3. Yu.Alexandrov. Intrinsic Charge Radius of the Neutron: Discrepancy Between the Garching and Dubna Results. Phys.Rev. C49, R2297 (1994).

4. Yu.Alexandrov. What is the Mean Square Charge Radius of the Neutron Actually Equal to? Part 1. Neutron News. 5, No 1, 20 (1994).

5. Yu.Alexandrov. Situation on Study of Electric Polarizability and Mean Square Charge Radius of the Neutron. JINR, E3-94-169, Dubna, 1994.

6. Yu.Alexandrov. On the Mean Square Intrinsic Charge Radius of the Neutron. Neutron News. 5, No 4, 17 (1994).

7. Yu.Alexandrov. What is the Mean Square Charge Radius of the Neutron Actually Equal to? Part 2. Proc. of the 8th Intern. Sympos. on Capture Gamma Ray Spectroscopy. World Scient., Singapore, New Jersy, London, Hong Kong. 1994, p.784.

8. Yu.Alexandrov, T.Enik, L.Mitsyna, V.Nikolenko, A.Popov, G.Samosvat, L.Koester, W.Waschkowski, V.Krivenko, A.Murzin, P.Prokofjev, J. Tambergs. Recent News of Neutron Polarizability Investigations. II Intern. Semin. on Interaction of Neutr. with Nuclei. Neutr. Spectroscopy, Nucl. Str., Related Topics. Abstracts, p.10, 1994, Dubna.

9. Yu.Alexandrov, A.Ioffe, P.Lukas, P.Mikula, M.Vrana, V.Zabiyakin. Measurement of the Neutron Scattering Length of Bi by Neutron Interferometry Method. Ibid. p.11, Dubna, 1994.

10. Yu.Alexandrov. The Neutron Mean Square Charge Radius and Electric Polarizability on the Basis of Data on Total Cross Sections. Report on Int. Workshop on Time Rev. Invar. and Parity Violation, May 4-7, 1993, Dubna.

11. Yu.Alexandrov. Does the Neutron-Electron Scattering Length Change with the Inter-Resonance Interference Taken into Account? JINR, E3-92-484, 1993, Dubna.

12. Yu.Alexandrov, A.Laptev, V.Nikolenko, G.Petrov, O.Sherbakov. Proceed. Intern. Conf. Nucl. Data for Sci. and Technology. Springer, 1992, p.160.

13. Yu.A.Alexandrov. On the Charge Radius of the Neutron Related to Its Inner Structure. In: Physics of Atomic Nucleus. Proceedings of the XXVII Winter School, PINP, St.Petersburg, 1993, p.43 (in Russian).

14. Yu.A.Alexandrov. Fundamental Properties of Neutron. Energoatomizdat, 3-rd edition., 1992 (in Russian).

15. M.A.Ali, V.A.Khitrov, Yu.V.Kholnov, O.D.Kjostarova, A.M.Sukhovoj, A.V.Voinov, E.V.Vasilieva. The ^{196}Pt Compound-State Gamma-Decay Cascades after Thermal Neutron Capture. JINR, E3-94-3, Dubna, 1994.

16. J.Andrzejevski, Yu.M.Gledenov, V.I.Salatski, P.V.Sedyshev, M.V.Sedysheva, V.A.Pshenichnyj. ^{14}N(n,p)^{14}C Reaction Cross Sections at Thermal, 24 keV, 54 keV and 144 keV Neutron Energy. In: Proceedings of the 8th International Symposium on Capture Gamma-Ray Spectroscopy, p.584-586. Fribourg 1993, editor J.Kern (1994).

17. J.Andrzejevski, Yu.M.Gledenov, V.I.Salatski, P.V.Sedyshev, M.V.Sedysheva, V.A.Pshenichnyj. Cross Sections of the ^{14}N(n,p)^{14}C Reaction at 24.5, 53.5 and 144 keV. Z.Phys. A348, 199-200 (1994).

18. J.Andrzejevski, Yu.M.Gledenov, Yu.P.Popov, V.I.Salatski, P.V.Sedyshev, V.A.Pshenichnyj. The Average Cross Section of the ^{7}Be(n,p)^{7}Li and ^{14}N(n,p)^{14}C Reactions at Stellar Energies. Annales Geophysicae, Suppl. III to vol. 10, p. 466, 1992.

19. A.L.Barabanov, E.I.Sharapov, V.R.Skoy, C.M.Frankle. Testing T-odd, P-even Interaction with Gamma-Rays from Neutron p-Wave Resonances. Phys.Rev.Lett., 70, 1216 (1993).

20. A.L.Barabanov, E.I.Sharapov, V.R.Skoy, C.M.Frankle. P-Even T-Violation from the Energy Shift in Nonpolarized (n,γ) Reaction. Time Reversal Invariance and Parity Violation in Neutron Reactions, Dubna, Russia, 4-7 May 1993, Editors C.R. Gould, J.D. Bowman, Yu.P. Popov, World Scientific, Singapore, 1994, p.175.

21. H.Beer, P.V.Sedyshev, Yu.P.Popov, F.Kappeler. Measurement of the ^{36}S(n,γ) Cross Section at kT=25 keV. In: Neutron Spectroscopy, Nuclear Structure, Related Topics. II Intern. Seminar on Inter. of Neutron with Nuclei. (Abstracts), JINR, E3-94-113, 1994, Dubna, p.30.

22. A.A.Bogdzel, N.A.Gundorin, A.Duka-Zoyomi, J.Kliman, Yu.G.Grigoriev. Fast Multilayer Fission Chamber with ^{239}Pu. Nuclear Instruments & Methods, A343 (1994), p.545.

23. A.A.Bogdzel, V.Polhorsky, J.Kliman, J.Kristiak, N.A.Gundorin, A.B.Popov, U.Gohs. Fission of ^{239}Pu by Resonance Neutrons. Nuclear Phys. 57 (1994), 57, 1198.

24. A.A.Bogdzel, W.I.Furman, P.Geltenbort, N.N.Gonin, M.A.Gusseinov, J.Kliman, Yu.N.Kopach, L.K.Kozlovsky, L.V.Mikhailov, A.B.Popov, H.Postma, N.S.Rabotnov, D.I.Tambovtsev. New Results of Measurement of Fission Fragments Angular Anisotropy from Resonance Neutron Induced Fission of ^{235}U Aligned Target. Proc. of the Workshop on Nuclear Fission and Fission Product Spectroscopy. Grenoble, May 2-4, 1994, pp. 197-201.

25. V.A.Bondarenko, I.L.Kuvaga, P.T.Prokofjev, A.M.Sukhovoj, V.A.Khitrov, Yu.P.Popov, S.Brant, V.Paar. Level of ^{137}Ba Studied with Neutron Induced Reactions. In: Capture Gamma-Ray Spectroscopy and Related Topics. Ed. J.Kern, Fribourg, 20-24 September 1993, p.372-374.

26. V.A.Bondarenko, I.L.Kuvaga, P.T.Prokofjev, A.M.Sukhovoj, V.A.Khitrov, Yu.P.Popov, V.Paar, S.Brandt, Lj.Simicic. Particle-Hole States in ^{138}Ba. In: Specialists' Meeting on Measurement, Calculation and Evaluation of Photon Production Data, Bologna, November 9-11, 1994, Booklet of Abstracts, p.22.

27. V.A.Bondarenko, I.L.Kuvaga, P.T.Prokofjev, A.M.Sukhovoj, V.A.Khitrov, Yu.P.Popov, V.Paar, S.Brandt. Levels of the ^{137}Ba Studied with Neutron Induced Reactions. Ibid., p.23.

28. V.A.Bondarenko, I.L.Kuvaga, P.T.Prokofjev, A.M.Sukhovoj, V.A.Khitrov, Yu.P.Popov, S.Brant, V.Paar, L.J.Simicic. Particle-Hole States in ^{138}Ba. In: Capture Gamma-Ray Spectroscopy and Related Topics. Ed. J.Kern, Fribourg, 20-24 September 1993, p.375-376.

29. S.Boneva, V.A.Khitrov, Yu.V.Kholnov, A.M.Sukhovoj, A.V.Voinov. Excitation Study of High-Lying States of Differently Shaped Heavy Nuclei by the Method of Two-Step Cascades. JINR, E3-94-403, Dubna, 1994.

30. S.B.Borzakov. The n-n-Interaction in the ^{1}S$_{0}$ State: a Virtual Level or a Dibaryon Resonance? Yad.Fiz., 1994, v.57, N3, p. 517-519 (in Russian).

31. S.B.Borzakov, E.Dermendjiev, Yu.S.Zamyatnin, V.M.Nazarov, S.S.Pavlov, A.D.Rogov, I.Ruskov. Setup for Investigating Delay Neutrons and Preliminary Results of Determination of the β_{eff} value for ^{233}U with respect to ^{235}U. JINR, P3-94-447, Dubna, 1994 (in Russian), (Submitted to "Atomnaya Energiya").

32. J.D.Bowman, E.I.Sharapov. Likelihood Analysis of Parity Violation in the Compound Nucleus. Time Reversal Invariance and Parity Violation in Neutron Reactions, Dubna, Russia, 4-7 May 1993, Editors C.R.Gould, J.D.Bowman, Yu.P.Popov, World Scientific, Singapore, 1994, p.69.

33. J.D.Bowman, C.M.Frankle, J.N.Knudson, S.I.Pentilla, S.J.Seestrom, J.J.Szymanski, Y.-F.Yen, S.H.Yoo, V.W.Yuan, B.E.Crawford, N.R.Roberson, X.Zhu, C.R.Gould, D.G.Haase, L.Lowie, G.E.Mitchell,

S.S.Patterson, P.P.J.Delheij, Yu.P.Popov, E.I.Sharapov, H.Postma, H.Shimizu, and Y.Masuda. Data on Parity Violation in the Compound Nucleus and its Interpretation. Ibid: p.8.

34. A.D.Budnik, Yu.N.Pokotilovski, A.D.Rogov, G.A.Ososkov, M.I.Kuvshinov, G.N.Maslov. Neutron-Neutron Scattering Experiment at the Pulse Reactor BIGR. Proc. Conf. "The Physics, Safety, and Applications of Pulse Reactors", ANS Winter Meeting, Nov. 13-17, 1994, p. 343.

35. Qu Decheng, Yu.M.Gledenov, G.Khuukhenkhuu, Yu.P.Popov, Bao Shanglian, Tang Guoyou, Cao Wentian, Chen Zemin, Chen Yingtang, Qi Huiquan. Study of the ^{40}Ca(n,α)^{37}Ar Reaction Induced by Fast Neutrons. JINR, E3-93-428, Dubna, 1993.

36. Qu Decheng, Yu.M.Gledenov, G.Khuukhenkhuu, Yu.P.Popov, Bao Shanglian, Tang Guoyou, Cao Wentian, Chen Zemin, Chen Yingtang, Qi Huiquan. Study of the ^{40}Ca(n,α)^{37}Ar Reaction at the Neutron Energy 4 and 5 MeV. In: Proceedings of the 8th International Symposium on Capture Gamma-Ray Spectroscopy. Fribourg 1993, editor J.Kern (1994) p.587-589.

37. Qu Decheng, Tang Guoyou, Zhong Wenguang, Cao Wentian, Bao Shanglian, Chen Zemin, Chen Yingtang, Qi Huiquan, Yu.M.Gledenov, G.Khuukhenkhuu. Angular Distribution and Cross Section Measurements for the Reaction ^{40}Ca(n,α)^{37}Ar, Using Gridded Ionization Chamber. Chinese Journal of Nuclear Techniques, v.17, No.3, p.129-133 (1994).

38. C.M.Frankle, J.D.Bowman, S.J.Seestrom, N.R.Roberson, E.I.Sharapov. Parity Violation Measurements Using the Neutron Capture Reactions. Time Reversal Invariance and Parity Violation in Neutron Reactions, Dubna, Russia, 4-7 May 1993, Editors C.R.Gould, J.D.Bowman, Yu.P.Popov, World Scientific, Singapore, 1994, p.204.

39. C.M.Frankle, S.J.Seestrom, Yu.P.Popov, E.I.Sharapov, N.R.Roberson. Recent Development in the Study of Parity Violation in Neutron p-Resonances. Fiz. Element. Chastits i At. Yadra, 24, 939 (1993). Phys. Part. Nucl., 24, 401 (1993).

40. C.M.Frankle, J.D.Bowman, B.E.Crawford, P.P.J.Delheij, C.R.Gould, D.G.Haase, J.N.Knudson, G.E.Mitchell, S.S.Patterson, S.I.Pentilla, Yu.P.Popov, N.R.Roberson, S.J.Seestrom, E.I.Sharapov, Y.-F.Yen, S.H.Yoo, V.W.Yuan, X.Zhu. Neutron Resonance Spectroscopy of ^{113}In and ^{115}In. Phys. Rev. C48, 1601 (1993).

41. C.M.Frankle, E.I.Sharapov, Yu.P.Popov, J.A.Harvey, N.W.Hill, and L.W.Weston. Neutron Resonance Spectroscopy on ^{113}Cd to E_n=15 keV. Phys. Rev. C50, 2601 (1994).

42. R.Georgii, T. von Egidy, J.Klora, H.Lindner, U.Mayerhofer, J.Ott, P. von Neuman-Cosel, A.Richter, C.Schlegel, R.Schulz, V.A.Khitrov, A.M.Sukhovoj, A.V.Vojnov, L.J.Simonova, P.T.Prokofjev. Complete Level Scheme of ^{124}Te up to 3.5 MeV Excitation Energy. In: Capture Gamma-Ray Spectroscopy and Related Topics. Ed. J.Kern, Fribourg, 20-24 September 1993, p.338-345.

43. G.P.Georgiev, Yu.V.Grigoriev, G.V.Muradyan, N.B.Janeva. Neutron Resonance Parameters of Sn. International Conference on Nuclear Data for Science and Technology, Gatlinburg, Tennessee, USA, May 9-13, 1994.

44. G.P.Georgiev, Yu.V.Grigorjev. Measurement of Gamma-Ray Multiplicity in Neutron Induced Reactions. NEA Specialists' Meeting on Measurement, Calculation and Evaluation of Photon Production Data, ENEA-Bologna, 9-11 November, 1994.

45. Yu.G.Georgiev, A.A.Kostina, A.I.Ostrovnoj, T.B.Petukhova, A.P.Sirotin, V.G.Tishin. Development of Spectrometric System for Automation of Multiparameter Measurements with Hardware Data Sorting "Romashka". JINR, P13-94-78, Dubna, 1994 (in Russian).

46. Yu.M.Gledenov, V.A.Vesna, I.S.Okunev, E.V.Shul'gina, S.Parzhitski, Yu.P.Popov. A Search for P-Odd Effects in the Reactions ^{10}B(n,α)^{7}Li, ^{6}Li(n,α)^{3}H. In: Weak and Electromagnetic Interactions in Nuclei (Proc. of III Intern. Symp., Dubna, 1992), Ed. Ts.D.Vylov, Word Scientific, Singapore-New Jersey-London-Hong Kong, p.419-422.

47. Yu.M.Gledenov, G.Khuukhenkhuu, M.V.Sedysheva, G.Unenbat. Systematical Analysis of the Fast Neutron Induced (n,p) Reaction Cross Sections. JINR, E3-93-466, Dubna, 1993.

48. Yu.M.Gledenov, P.E.Koehler, F.Kappeler, H.Schatz, Yu.P.Popov, J.A.Harvey, N.W.Hill, M.Wiescher, R.W.Kavanagh, R.B.Vogelaar. Recent Results in Explosive and s-Process Nucleosynthesis from Measurements on Radioactive and Stable Targets. In: Proceedings of the 8 International Symposium on Capture Gamma-Ray Spectroscopy, Fribourg, 1993, editor J.Kern (1994), p.714-723.

49. Yu.M.Gledenov, V.I.Salatski, P.V.Sedyshev. The ^{14}N(n,p)^{14}C Reaction Cross Section for Thermal Neutrons. Z.Phys. A346, 307-308 (1993).

50. Yu.M.Gledenov, G.Khuukhenkhuu, M.V.Sedysheva, G.Unenbat. Systematics of the Fast Neutron Induced (n,α) Reaction Cross Sections. JINR, E3-94-316, Dubna, 1994.

51. Yu.M.Gledenov, Tang Guoyou, Bai Xinhua, Shi Zhaomin, Chen Jinxiang, G.Khuukhenkhuu, Yu.P.Popov. Measurement of Angular Distributions and Cross Section for ^{58}Ni(n,α)^{55}Fe Reaction at 5.1 MeV. In: Neutron Spectroscopy, Nuclear Structure, Related Topics. II Intern. Seminar on Inter. of Neutron with Nuclei. (Abstracts), JINR, E3-94-113, Dubna, 1994, p.53.

52. Yu.M.Gledenov, I.S.Okunev, S.S.Parzhitski, E.V.Shul'gina, V.A.Vesna. Investigation of P-Odd Correlations in the Capture of Thermal Polarized Neutrons Involving Emission of Secondary Charged Particles. Nucl. Instr. and Meth. in Phys.Research A 350 (1994), p.517-524.

53. Yu.M.Gledenov, V.I.Salatski, P.V.Sedyshev, M.V.Sedysheva, P.E.Koehler, V.A.Vesna, I.S.Okunev. Recent Results of Measurements of the ^{14}N(n,p)^{14}C, ^{35}Cl(n,p)^{35}S, ^{36}Cl(n,p)^{36}S and ^{36}Cl(n,α)^{33}P Reaction Cross Sections. III International Symposium "Nuclei in the Cosmos" (Abstract booklet), Gran Sasso, Italy, July 8-13, 1994, Osservatorio Astronomico di Collurania, Teramo - Italy.

54. A.A.Goverdovsky, E.Dermendjiev, I.Ruskov, Yu.S.Zamyatnin. Resonance Areas and Fission Widths of Lowly-ing Fission Resonances of ^{237}Np. JINR, P3-93-283, Dubna, 1993. Yad.Fiz., 1994, v. 57, N8, p.1362 (in Russian).

55. A.A.Goverdovsky, E.Dermendjiev, I.Ruskov, Yu.S.Zamyatnin. ^{237}Np Fission Cross Section for the Neutron Energy up to $E_n \leq 500$ eV. JINR, P3-93-440, Dubna, 1993 (Submitted to Yad.Fiz.) (in Russian).

56. Yu.V.Grigorjev, V.V.Sinitsa, G.P.Georgiev, N.A.Gundorin. Measurements and Calculations of ^{235}U, ^{239}Pu, ^{232}Th Neutron Transmissions in Energy Range 2.15 eV - 14 MeV for Temperatures 77 and 293 K. International Conference on Nuclear Data for Science and Technology, Gatlinburg, USA, May 9-13, 1994.

57. N.A.Gundorin, Yu.N.Kopach, S.A.Telezhnikov. Comparative Measurements of Independent Yields of ^{239}Pu Fission Fragments, Induced by Thermal and Resonance Neutrons. Book of Abstracts of Int. Conf. on Nuclear Data for Science and Technology, May 9-13, 1994, Gatlinburg, USA.

58. N.A.Gundorin, A.B.Popov, W.I.Furman, J.Kliman. Advantages and Disadvantages of Gamma-Ray Spectroscopy in Investigation of Fission Fragment Characteristics. Workshop on Nuclear Fission and Fission Product Spectroscopy. Grenoble, May 2-4, 1994. Ibid. pp. 231-237.

59. N.A.Gundorin. On the Possibility of Improving the Fragment γ-Spectroscopy Method for Investigating the ^{239}Pu Nucleus Fission from Compound States. Yad.Fiz., 57 (1994), 1215 (in Russian).

60. N.A.Gundorin. Gamma Spectroscopy of Fragments to Investigate ^{239}Pu Fission Induced by Resonance Neutrons. JINR, P15-94-53, Dubna, 1994 (in Russian).

61. F.Gunsing, F.Corvi, K.Athanassopulos, H.Postma, Yu.P.Popov, E.I.Sharapov. Spin Assignment of Neutron p-Wave Resonances in ^{113}Cd. ISINN-2: II International Seminar on Interaction of Neutrons with Nuclei, Dubna, Russia, 26-28 April 1994. JINR, E3-94-113 Dubna, p.29.

62. Qi Huiquan, Tang Guoyou, Qu Decheng, Zhong Wenguang, Cao Wentian, Bao Shanglian, Chen Zemin, Chen Yingtang, Yu.M.Gledenov, G.Khuukhenkhuu. "Cross Section Measurements for ^{40}Ca(n,α)^{37}Ar Reaction". Chinese Journal of Nuclear Physics, v.15, No. 3, p.239-242 (1993).

161

63. A.K.Krasnykh, V.L.Lomidze, A.V.Novokhatsky, Yu.P.Popov, W.I.Furman. IREN Project, Intense Resonance Neutron Source. JINR, Dubna, 1994.

64. V.A.Khitrov, Yu.V.Kholnov, A.M.Sukhovoj, A.V.Vojnov. Possible Experimental Discovery of Multiplets of Low-Lying Levels. In: Specialists' Meeting on Measurement, Calculation and Evaluation of Photon Production Data, Bologna, November 9-11, 1994, Booklet of Abstracts, p.19.

65. V.A.Khitrov, Yu.V.Kholnov, O.D.Kjostarova, V.D.Kulik, Yu.P.Popov, V.N.Shilin, A.M.Sukhovoj, E.V.Vasilieva, A.V.Vojnov. Enhanced Cascades with Low Energy Primary Transition in ^{150}Sm, ^{156,158}Gd and ^{164}Dy. In: Capture Gamma-Ray Spectroscopy and Related Topics. Ed. J.Kern, Fribourg, 20-24 September 1993, p.600-602.

66. V.A.Khitrov, A.M.Sukhovoj. Principles and Possibilities of Determining the Main Parameters and Peculiaritis of Cascade γ-Decays of the Compound States of Heavy Nuclei. In: Capture Gamma-Ray Spectroscopy and Related Topics. Ed. J.Kern, Fribourg, 20-24 September 1993, p.596-599.

67. V.A.Khitrov, Yu.V.Kholnov, O.D.Kjostarova, V.D.Kulik, Yu.P.Popov, V.N.Shilin, A.M.Sukhovoj, E.V.Vasilieva, A.V.Vojnov. The Peculiarities of the 1^{+} States Excitation by Cascades of γ-Transitions in Deformed Nuclei. In: Capture Gamma-Ray Spectroscopy and Related Topics. Ed. J.Kern, Fribourg, 20-24 September 1993, p.603-604.

68. V.A.Khitrov, Yu.V.Kholnov, O.D.Kjostarova, V.D.Kulik, Yu.P.Popov, V.N.Shilin, A.M.Sukhovoj, E.V.Vasilieva, A.V.Voinov. The Peculiarities of the ^{196}Pt Compound-State Cascade γ-Decay. In: Capture Gamma-Ray Spectroscopy and Related Topics. Ed. J.Kern, Fribourg, 20-24 September 1993, p.605-607.

69. V.A.Khitrov, Yu.V.Kholnov, O.D.Kjostarova, V.D.Kulik, Yu.P.Popov, V.N.Shilin, A.M.Sukhovoj, E.V.Vasilieva, A.V.Voinov. Possible Equidistance of the Excitation Energies of Intermediate Levels of Intense Cascades. In: Capture Gamma-Ray Spectroscopy and Related Topics. Ed. J.Kern, Fribourg, 20-24 September 1993, p.608-610.

70. V.A.Khitrov. The Main Properties of γ-Decay Cascades in Heavy Nuclei and the Possibility of their Determination. In: Neutron Spectroscopy, Nuclear Structure, Related Topics, JINR, E3-94-113, Dubna, 1994, p.27.

71. V.A.Khitrov. Investigation of Main Parameters of Deformed Nuclei Compound-State Gamma-Decay. In: Proceedings of the Second International Symposium on Nuclear Excited States (Lodz, June 22-26, ed. L.Lason and M.Przitula) Lodz: Lodz University, 1993, p.190-195.

72. L.Koester, W.Waschkowski, L.V.Mitsyna, G.S.Samosvat, P.Prokofjevs, J.Tambergs. Neutron-Electron Scattering Length and Electric Polarizability of the Neutron Derived from Cross Sections of Bismuth and of Lead and its Isotopes. (Submitted to Phys.Rev.).

73. V.G.Nikolenko, A.B.Popov, G.S.Samosvat. Imaginary Experiment for Measuring the Scattering Cross Section Ratio of Noble Gases to Estimate the n,e- Amplitude. II International Seminar on Interaction of Neutrons with Nuclei, April 26-28, 1994, Dubna, Russia, JINR, E3-94-113, Dubna, 1994, p.48.

74. V.G.Nikolenko, A.B.Popov. Unmodel n,e-Amplitude Estimate on the Basis of Neutron Scattering Data. Proc. of the Symp. on Capture Gamma-Ray Spectroscopy. Fribourg, Sept. 20-24, 1993, p.812.

75. Yu.N.Pokotilovski. On the Experimental Verification of the Validity of the Weak Equivalence Principle for the Neutron. Yad. Fyz. 1994, 57, (3), pp.416-420 (in Russian).

76. S.J.Seestrom, D.Aldes, J.D.Bowman, B.F.Crawford, P.P.J.Delheij, C.M.Frankle, K.Fukuda, C.R.Gould, A.A.Green, D.G.Haase, M.Iinuma, J.N.Knudson, L.Y.Lowie, A.Masaike, Y.Masuda, G.E.Mitchell, S.Pentilla, S.Stephenson, Yu.P.Popov, H.Postma, N.R.Roberson, E.I.Sharapov, H.M.Shimizu, Y.-F.Yen, V.W.Yuan. New Results from Los Alamos in the Study of Parity Violation in Neutron p-Resonances. II International Seminar on Interaction of Neutrons with Nuclei, April 26-28, 1994, Dubna, Russia, JINR, E3-94-113, Dubna, 1994, p.55.

77. E.I.Sharapov, V.R.Skoy. Measurements of N-Odd, P-Even Effects in ^{113}Cd(n,γ) ^{114}Cd and ^{117}Sn(n,γ)^{118}Sn Reactions. Capture Gamma-Ray Spectroscopy and Related Topics, Fribourg, Switzerland, 20-24 Sept. 1993, World Scientific, Singapore, 1994, p.805.

78. E.I.Sharapov, V.R.Skoy. Measurement of T-Odd, P-Even Effect in ^{117}Sn(n,γ)^{118}Sn Reaction. Time Reversal Invariance and Parity Violation in Neutron Reactions, Dubna, Russia, 4-7 May 1993, Editors C.R.Gould, J.D.Bowman, Yu.P.Popov, World Scientific, Singapore, 1994, p.183.

79. E.I.Sharapov. Neutron Depolarization in Aligned Holmium and Time Reversal Invariance Test. ISINN-2: II International Seminar on Interaction of Neutrons with Nuclei, Dubna, Russia, 26-28 April 1994. JINR, E3-94-113 Dubna, p.16.

80. A.M.Sukhovoj. The Peculiarities of Transforming of the "Order" of Low-Lying Levels to the "Chaos" of Neutron Resonances. In: Specialists' Meeting on Measurement, Calculation and Evaluation of Photon Production Data, Bologna, November 9-11, 1994, Booklet of Abstracts, p.6.

81. A.M.Sukhovoj. From "Order" of Low-Lying Levels to the "Chaos" of Neutron Resonances. Experiment. In: Selected Topics in Nuclear Structure, Contributions, JINR, E4-94-168, Dubna, 1994, p.97.

82. D.I.Tambovtsev, W.I.Furman, A.A.Bogdzel, P.Geltenbort, N.N.Gonin, M.A.Gusseinov, J.Kliman, Yu.N.Kopach, L.K.Kozlovsky, L.V.Mikhailov, A.B.Popov, H.Postma, N.S.Rabotnov. New Results of Measurement of Fission Fragments Angular Anisotropy from Resonance Neutron Induced Fission of ^{235}U Aligned Target. Int. Conf. "Nuclear Fission & Fission Fragment Spectroscopy". Seyssyns, France, May 2-4, 1994.

Theory

A.L.Barabanov, W.I.Furman. New Theoretical Possibilities to Describe P-Even and P-Odd Angular Correlations of Fission Fragments from Resonance Neutron Induced Fission. Book of Abstracts of Int. Conf. on Nuclear Data for Science and Technology, May 9-13, 1994, Gatlinburg, USA.

2. G.G.Bunatian, J.Wambach. Temperature Dependence of the Chiral Condensate from an Interacting Pion Gas. Phys.Lett. B336, 290 (1994).

3. A.I.Frank, V.G.Nosov. Neutron Diffraction on a Moving Grating and Quasi-energy of Cold Neutrons. Physics Letters A, 1994, 188, 120-124.

4. A.I.Frank, V.G.Nosov. Quantum Modulation of Neutron Waves and a Time Interferometer. Yad.Fiz., 1994, 57, 1029-1035 (in Russian).

5. A.I.Frank, V.G.Nosov. Diffraction in Time and a New Type of Interferometry with Nonseparated Beams. Report on the conference: Fundamental Problems of Quantum Theory (Baltimore, MA, June 18-22, 1994). To be published in: Annals of New York Academy of Science, 1995.

6. A.I.Frank, V.G.Nosov. Quantum Effects Following Neutron Wave Modulation. In: Physics of Atomic Nucleus, Proceedings of the XXVII Winter School, PINP, St.Petersburg, 1993.

7. W.I.Furman, S.Kadmensky, Yu.Tchuvilsky. Some Predictions of New Spontaneous Cluster Emitters and Mechanism of Cluster Decay. Z. Phys., A349 (1994), pp.301-303.

8. V.K.Ignatovich. Semianalytical Approach to X-Ray and Neutron Reflection from Surface Films. Physical Review E 50 (5) 4231-4232 (1994).

9. V.K.Ignatovich. Classical Interpretation of Quantum Mechanics. in: Frontiers of Fundamental Physics. Eds. M.Barone and F.Selleri., Plenum Press, N.Y., 1994, p.493-501.

10. V.K.Ignatovich. How to Separate the Contribution of Substrate Scattering from Roughness Scattering of a Film (Comment). Physica B 198 (1) 40-41 (1994).

11. V.K.Ignatovich. Quantum Mechanics of Ultracold Neutrons. in: Waves and Particles in Light and Matter. Eds. A. van der Merve and A.Garuccio. Plenum Press, N.Y., 1994, pp.65-84.

12. V.K.Ignatovich. Time-of-Flight Fourier Spectroscopy with Polarized Neutron Beams. JINR, E3-93-65, Dubna, 1993, p.69-79.

13. V.G.Nosov, A.I.Frank. The Density Matrix and Slow Neutron Beam Transformation. JINR, P4-94-441, Dubna, 1994 (in Russian).

14. V.G.Nosov, A.I.Frank.. Long Wave-Length Neutron Dispersion Law and the Possibility of its Precise Experimental Test. JINR, P3-94-5, Dubna 1994 (Submitted to Yad.Fiz.) (in Russian).

15. V.G.Nosov, A.I.Frank. Superslow Neutrons and the Dispersion Law of Neutron Waves in Matter. JINR, P4-92-471, Dubna, 1992 (in Russian).

16. Yu.S.Zamyatnin, S.G.Kadmensky, W.I.Furman, Yu.M.Tchuvilsky, S.D.Kurgalin. Where are the New Examples of Cluster Decay to Be Found?. Yad.Fiz. (1994), v. 57, N11, p.1983 (in Russian).

APPLIED RESEARCH

1   N.G.Baboshin, M.V.Frontasyeva, P.A.Lavdansky, V.M.Nazarov, I.Stefanov. NAA for Optimization of Radiation Shielding of Nuclear Power Plants. Journal of Radioanal. and Nucl.Chem., 1994, v.180, No.1, p.83-95.

2.   S.B.Borzakov, V.M.Nazarov, L.S.Nefedyeva, T.M.Ostrovnaya, L.P.Strelkova. Software for INAA on the Basis of Relative and Absolute Methods Using Nuclear Data Base. In: Proc. of the Second Int. Workshop "Activation Analysis in Environment Protection". JINR, D14-03-325, Dubna, 1993, p.319.

3.   S.B.Borzakov, V.P.Chinaeva, M.V.Frontasyeva, V.M.Nazarov. NAA Biomonitoring of the Environment with Moss and Pine Tree Needles. In: Book of Abstracts of Int. Conf. on Nuclear Analytical Methods in the Life Sciences, Prague, Czech Republic, 13-17 September, 1993.

4.   T.E.Burkovskaya, M.V.Frontasyeva, S.F.Gundorina. Elemental Bone Composition of Rats Flown in American Space Scientific Laboratory SLS-1. In: Book of Abstracts. Int. Conf. on Methods and Applications of Radioanalytical Chemistry MARC-III, 10-16 April, 1994, Hawaii, USA.

     V.P.Chinaeva, M.V.Frontasyeva, V.M.Nazarov, V.V.Nikonov, V.F.Peresedov. Resonance Neutrons for Determination of Elemental Content of Moss, Lichens and Pine Needless in Atmospheric Deposition Monitoring. In: Book of Abstracts. Int. Conf. on Methods and Applications of Radioanalytical Chemistry MARC-III, 10-16 April, 1994, Hawaii, USA.

6.   R.Dybczynski, B.Danko, M.Wasek, K.Kulisa, M.V.Frontasyeva, V.M.Nazarov. Determination of Trace Amounts of Ni and Co in Biological Materials by Means of Non-Destructive Activation Analysis. In: Proc. Second Workshop "Activation Analysis in Environment Protection". JINR, D14-93-325, Dubna, 1993, p.376-386.

7.   M.V.Frontasyeva, V.M.Nazarov, E.Steinnes. Mosses as Monitors of Heavy Metal Depositions: Comparison of Different Multi-Element Analytical Technologies. Journ. of Radioanal. and Nucl. Chem., 1994, v.181, No.2, p.363-371.

8.   M.V.Frontasyeva, F.Grass, V.M.Nazarov, A.Ritschel, E.Steinnes. Intercomparison of Moss Reference Material by Different Multi-Element Techniques. In: Book of Abstracts. Int. Conf. on Methods and Applications of Radioanalytical Chemistry MARC-III, 10-16 April, 1994, Hawaii, USA.

     Ye.M.Grachevskaya, F.I.Tyutyunova, M.V.Frontasyeva, S.F.Gundorina. Assessment of Technological Constituent of Lowland River Chemical Runoff. In: Book of Abstracts. Int. Conf. on the Analysis of Geological and Environmental Materials GEOANALYSIS-94, 18-22 September, 1994, Ambleside, United Kingdom; Second Int. Symp. and Exhibition on Environmental Contamination in Central and Eastern Europe, 20-23 September, 1994, Budapest, Hungary.

10   V.N.Klochkov, V.M.Nazarov, V.F.Peresedov, V.P.Chinaeva. Activation Analysis of Super-Pure Aluminium. JINR, P3-94-453, Dubna, 1994 (in Russian).

11   V.S.Koryakin, M.P.Kuznetsov, V.M.Nazarov, L.R.Serebryanny, T.A.Vostokova. Snow Cover as Witness of Environmental Pollution from Norilsk Copper-Nickel Plant in the Taimyr Peninsula, Northern Siberia. In: Proc. of the 2nd. Int. Workshop "Activation Analysis in Environment". JINR, D14-93-325, Dubna, 1993.

12. V.M.Nazarov, V.V.Nikonov, E.Steinnes, N.V.Lukina, M.V.Frontasyeva. The Use of the Resonance Neutron Method in Biomonitoring Far North Forestry Ecosystems. In: Proc. of the All-Russian Scien-Techn. Conf. on the Problem: "Protection of Forestry Ecosystems and the Efficient Use of Timber Resources" 17-19 October, 1994, Moscow (in Russian).

14   S.P.Stanescu, O.M.Farcasiu, E.Gaspar, V.M.Nazarov, M.V.Frontasyeva. Activable Tracers as Ecological Tracers Used in Solving Environmental Problems. In: Proc. of the Second Workshop "Activation Analysis in

Environment Protection". JINR, D14-93-325, Dubna, 1993, p.407-410.

15. E.Steinnes, M.V.Frontasyeva. Epithermal Neutron Activation Analysis of Mosses Used to Monitor Heavy Metal Deposition Around an Iron Smelter Complex. In: Book of Abstracts. Int. Conf. on the Analysis of Geological and Environmental Materials GEOANALYSIS-94. 18-22 September, 1994, Ambleside, United Kingdom.

16. F.I.Tyutyunova, E.M.Grachevskaya, A.S.Savichev, S.B.Borzakov, V.P.Chinaeva, M.V.Frontasyeva, S.F.Gundorina, T.M.Ostrovnaya. Combined Nuclear-Related and Physical Chemical Methods in Monitoring Aquatic Ecosystems. In: Book of Abstracts. Int. Conf. on Methods and Applications of Radioanalytical Chemistry MARC-III, 10-16 April, 1994, Hawaii, USA.

NEUTRON SOURCES

S.V.Chuklyaev, Yu.N.Pepyolyshev. The KHK-21A Fission Ionization Chamber for Measuring the Flux and Temperature of Thermal Neutrons from Pulsed Sources. Atomnaja Energiya, v.76, issue 6, 1994 (in Russian).

2. A.A.Belyakov, V.G.Yermilov, V.V.Melikhov, et al. Solid Methane Moderator at the IBR-2: Test Operation at 2 MW. Int. Sem. PANS-2, Dubna, June 14-16, 1994.

3. A.A.Belyakov, V.G.Ermilov, V.L.Lomidze et al. The First Experience of a Cold Moderator and Solid Methane Irradiation at the IBR-2 Pulsed Reactor. Presented at the B6 Workshop Session of ICANS-XII, 1994.

4. A.D.Dementiev, V.G.Miroshnichenko, A.D.Rogov, et al. The Pulse Neutron Source for the Moscow Meson Factory on the Basis of Uranium Targets. Int. Sem. PANS-2, June 14-16, Dubna, 1994.

5. V.Dzwinel, Yu.N.Pepyolyshev. Clustering and Mapping of Patterns Methods for Presentation of Nuclear Reactor Noises. JINR, E10-94-61, Dubna, 1994.

6. V.V.Golikov, V.L.Kamionsky, E.N.Kulagin, V.I.Lushchikov, E.P.Shabalin. An Instrument for Industrial Doping Silicon with Thermal Neutrons on Beam 3 of the IBR-2 Reactor. JINR, P18-94-108, Dubna, 1994 (in Russian).

7. V.L.Lomidze, V.L.Kamionsky. The IBR-2 Reactor After Core Reloading. JINR, P13-94-215, Dubna, 1994 (in Russian).

8. V.L.Lomidze, Yu.P.Popov, A.D.Rogov, et al. Plutonium Booster IREN: Status of the Projects. Design Topics. Int. Sem. PANS-2, June 14-16, Dubna, 1994.

9. Yu.N.Pepyolyshev, A.B.Tulaev, V.F.Bobrakov et al. An Effective System for Measuring Thermal Neutron Spectra from Pulsed Sources. Atomnaja Energiya, v.76, issue 6, 1994 (in Russian).

10. Yu.N.Pepyolyshev, A.B.Tulaev. Experimental Study of Neutronic Performance of the IBR-2 Reactor Solid Methane Moderator. Int. Sem. PANS-2, June 14-16, Dubna, 1994.

11. Yu.N.Pepyolyshev, V.Dzwinel. Comparison of the Noise Diagnostic Systems Based on the Pattern Recognition and Discriminate Methods. JINR, E10-94-14, Dubna, 1994.

12. A.D.Rogov. An Experience of Distributed Monte Carlo Calculations for Pulsed Neutron-Neutron Interaction Problem. Int.b Workshop CONVEX - Metacomputing, Dubna, May 24-26, 1994.

COMPUTER CENTER

1. D.A.Balagurov, A.A.Bogdzel, G.F.Zhironkin, V.V.Zhuravlev, V.G.Muratov, V.E.Novozhilov, A.I.Ostrovnoy, V.E.Rezaev, V.V.Sikolenko, A.P.Sirotin, A.Tiitta, A.S.Trofimova, A.B.Tulaev. The System for Experiments Automation on High Resolution Fourier-Diffractometer. JINR, P10-94-91, Dubna, 1994 (in Russian).

2. V.A.Butenko, V.A.Drozdov, A.S.Kirilov, V.E.Novozhilov, A.I.Ostrovnoy, V.I.Prikhodko, V.E.Rezaev, Ya.Sudek, D.Krushinski. RTOF - Correlator Based on Digital Signal Processor TMS320C25 for the High Resolution Fourier Diffractometer. JINR, P10-94-87, Dubna, 1994 (in Russian).

3. V.A.Butenko, V.A.Drozdov, A.S.Kirilov, V.E.Novozhilov, A.I.Ostrovnoy, V.I.Prikhodko, V.E.Rezaev, Ja.Sudek, D.Krushinski. The DSP-Based RTOF-Correlator for High Resolution Fourier Diffractometers. Rep. to the JINR XVI Int. Symp. on Nuclear Electronics, September 12-19, Bulgaria, 1994.

4. D.Georgiev, V.V.Nietz, A.B.Roganov, A.P.Sirotin. The Control and Monitoring System of IMU-2 Pulse Magnetic Set-up of the SNIM-2 Spectrometer for Research with Rectangular Pulses of Magnetic Field. JINR, P13-94-77, Dubna, 1994 (in Russian).

5. E.I.Litvinenko, Yu.V.Obukhov. Program of Restoring of the Sample's Magnetic Moment at SQUID-Susceptometer Measurements. JINR, P10-94-44, Dubna, 1994 (in Russian).

6. V.E.Novozhilov, A.I.Ostrovnoy, V.E.Rezaev, A.P.Sirotin. Organization of the Distributed System in the VME Standard for Experiments Automation at the IBR-2 Reactor. JINR, P10-94-8, Dubna, 1994 (in Russian).

7. A.I.Ostrovnoy, T.B.Petukhova, A.B.Roganov, A.P.Sirotin. Programming CAMAC and VME Blocks for Control and Monitoring Parameters of Experimental Units at the Reactors IBR-30 and IBR-2. JINR, P13-94-76, Dubna, 1994 (in Russian).

8. A.B.Tulaev. Multi-Purpose Microcontroller. JINR, P10-94-379, Dubna, 1994 (in Russian).

9. Zen En Ken, N.N.Isakov, A.S.Kirilov, M.L.Korobchenko, A.I.Ostrovnoy, V.E.Rezaev, A.P.Sirotin, J.Heinitz. A VME Based Accumulation, Control and Supervising System for the NSHR Spectrometer. JINR, P13-94-73, Dubna, 1994 (in Russian).

4. PRIZES

Frank Prize:

Yu.G.Abov (ITEP), V.P.Alfimenkov (FLNP), L.B.Pikelner (FLNP). "For Fundamental Discoveries in the Field of Parity Violation in Neutron-Nuclear Interactions".

JINR Prizes:

For methodological and technical research:

Second Prize:

A.M.Balagurov, I.P.Barabash, G.M.Mironova, V.E.Novozhilov. "Real-Time Neutron Diffraction as a Tool for the Study of Transition Processes in Condensed Matter".

For applied research:

Second Prize:

I.V.Markichev, A.Yu.Muzychka, I.Natkaniec, E.V.Sheka, V.D.Khavryutchenko. "Investigation of the Vibrational States of Well Dispersed Materials with Inelastic Neutron Scattering".

FLNP Prizes:

In Nuclear Physics:

First Prize:

V.G.Nikolenko, A.B.Popov. "Analysis of Uncertainties in Experimental Estimates of n,e-Scattering Amplitudes and Neutron Polarizability Made on the Basis of Total Cross Sections".

Second Prize:

V.K.Ignatovich. "Classical Interpretation of Quantum Mechanics"

Third Prize:

1. A.V.Vojnov, Yu.P.Popov, A.M.Sukhovoj, V.A.Khitrov, Yu.V.Kholnov. "Analysis of Peculiarities of Two-Step Cascades in Nuclei";
2. Yu.M.Gledenov, Yu.P.Popov. "New Data from n,p and n,α Reaction Measurements on Radioactive and Small Samples for Nucleosynthesis".

In Condensed Matter Physics:

First Prize:

A.I.Beskrovnyi, S.Durchok, I.Heitmanek, Z.Jirak, M.Nevriva, I.G.Shelkova. "Structural Modulation, Oxygen Content and Superconducting Properties in Bi-HTSC".

Second Prize:

N.M.Blagoveshchenskii, I.V.Bogoyavlenskii, L.V.Karnatsevich, Zh.A.Kozlov, V.G.Kolobrodov, V.B.Priezzhev, A.V.Puchkov, A.N.Skomorokhov, V.S.Yarunin. "Excitation Spectrum Structure of Liquid Helium-4".

Third Prize:

L.S.Smirnov, I.Natkaniec, S.I.Bragin, Yu.A.Shadrin et al. "Neutron Scattering and Acoustic Investigations of Lattice and Dynamic Parameters and Phase Transitions in $K_{1-x}(NH_4)_xSCN$".

In Methodological and Applied Research:

First Prize:

V.A.Butenko, V.A.Drozdov, A.S.Kirilov, V.E.Novozhilov, A.I.Ostrovnoi, V.I.Prikhodko, V.E.Rezaev, Ya.Sudek, D.Krushinskii. "DSP-Based RTOF-Correlator for the High Resolution Fourier Diffractometer.

Third Prize:

K.Krezhev, V.Lilkov, P.Konstantinov, D.A.Korneev. "Domain Structure Study of Ferromagnetic Amorphous Alloys by Investigating the Wave Dependence of Neutron Depolarization".

5. NEUTRON SOURCES

5.1. THE IBR-2 PULSED REACTOR

Operation of the reactor. In 1994, the reactor operated, for physical experiments, for 720 hours in 3 scheduled cycles. In March, 1994 the reactor was shut down for a scheduled replacement of the movable reflector.

The reported year was the tenth year of IBR-2 operation for the rated power of 2 MW (started in February 1984). The International Seminar "Advanced Pulsed Neutron Sources" (June 1994, Dubna) was devoted to the main results of the past decade.

In the course of the reactor operating period the mean burning of fuel was 2.77%, and the achieved fluence in the jacket part subjected to the highest tension was 2.1×10^{22} n/cm^2. Careful investigations and calculations carried out together with NIKIET, Moscow, permitted the determination of the jacket (7 years) and sodium cooling system (20 years) residual resources. The results were approved by the General Constructor.

Movable reflector. Since October 1987, the reactor has operated with the second, PO-2, movable reflector. The total operation time was 19619 hours which corresponded to the operation resource determined by the General Constructor. In the first half of 1994 the new movable reflector PO-2R was manufactured. Its principal design repeated the PO-2 construction, but the new reflector was equipped with a more developed and updated system for dynamic control of rotor oscillations, displacements, and vibrations. In October, 1994 the PO-2R was assembled on a test stand, and after successful tests it was moved in December to its working site at the IBR-2 reactor. The PO-2 reflector was moved to the special storage room.

The automatic system for measuring reactor parameters (ASI IBR-2) was developed by the Regtron-KFKI firm (Hungary). Equipment delivery accomplished in the course of several years was completed in spring 1994. Tests of all systems are to be completed in 1995.

Cryogenic moderator (CM). In 1994 the test program for the CM prototype was completed with the following main results:

- the possibility of using solid methane at the reactor power of 2 MW was demonstrated;
- an increase in the cold neutron yield by 10-25 times (in dependence on the wavelength) in comparison with the water moderator was achieved (fig.10).

Design work on the new CM started (fig.11).
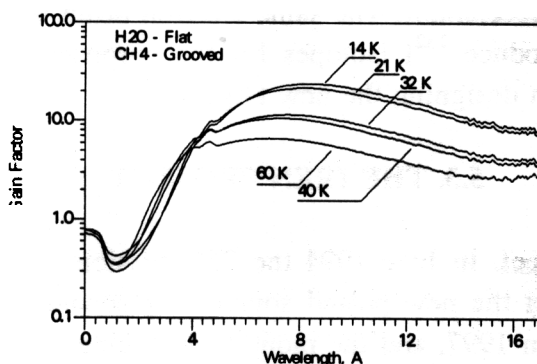
Fig.10. Ratio of the neutron yield from the cryogenic moderator surface for several values of mean methane temperature to the neutron yield from the moderator in a heated state (the plain water premoderator at 300 K). The x-axis is the neutron wavelength in angstroms.
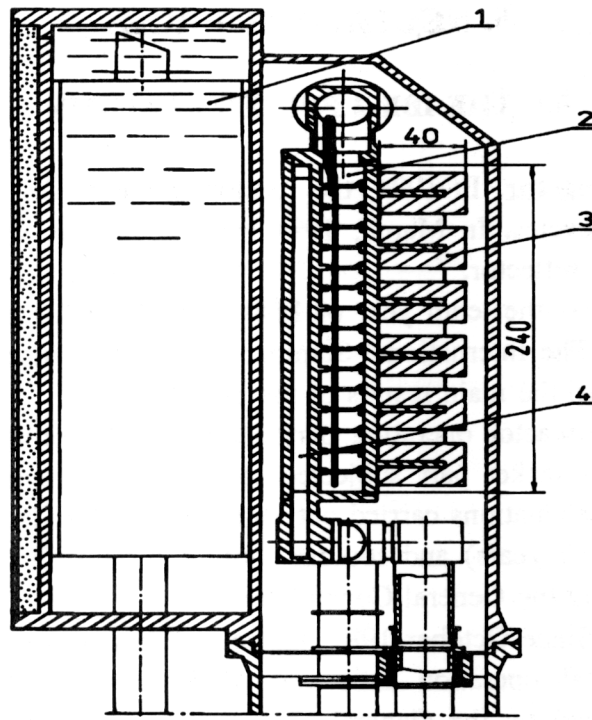
Fig.11. The cryogenic moderator for the IBR-2 reactor (vertical cross section): 1 - light water premoderator, 2 - solid methane, 3 - beryllium filter-reflector, 4 - helium-methane heat exchanger. The dimensions are given in mm.

5.2. THE IBR-30 BOOSTER

In 1994 the IBR-30 + LUE-40 complex operated for 2420 hours in ten scheduled cycles. Seven neutron beams were used to carry out experiments in nuclear physics and applied research.

In the reported year, a new system for electron beam control at the converter of the multiplying target was developed, constructed and tested. This system permitted increasing the power stability level of the neutron source. The new water moderator was installed on beams 3-5 of the booster to optimize the resonance neutron yield.

Tests of the principally new mono-crystal target of the converter were conducted on the electron beam of the LUE-40 accelerator. The same electron beam was used to test a xenon high pressure target intended to produce ^{132}I isotopes for the purposes of medical diagnostics. The obtained results will be used in designing the new target.

5.3. THE IREN PROJECT

The status of the project. In June 1994 the 76th session of the JINR Scientific Council adopted a decision to construct the new pulsed source of resonance neutrons, IREN. The work was decided to be completed in 1997, and the monthly financing scheme was determined by the JINR Directorate. The latter enabled JINR to not only pay debts to designing organizations but also start work on engineering design and manufacturing some systems of the source. The organization and financial rules for the work on the project carried out by other JINR laboratories were adopted by a special decision of the Institute Directorate.

Electron linear accelerator, LUE-200. In accordance with the JINR - DOE USA agreement for delivery of klystrons for the LUE-200, the first 5045 type klystron was shipped to Dubna and installed in bldg. 118 of FLNP in May 1994. By the end of the year, the first stage of the construction of a full-scale stand for the klystron modulator was completed.

In accordance with the approved working schedule a FLNP-LHE-LSHE collaboration carried out work on the creation of systems for synchronization and excitation of the klystron modulator. An agreement with RMIR (St.Petersburg), the leading organization in designing modulators, was signed. According to the agreement, equipment for the OLIVIN stations of these modulators will be delivered by ErPI as the contribution of Armenia to JINR.

MEPI in cooperation with the ISTOK industrial enterprise (Friazino) is designing and manufacturing HF fiders. Specifications for designing and manufacturing magnetic systems of the accelerator were agreed to with LNP JINR.

A contract with INP SB RAS (Novosibirsk), the top organization in constructing the LUE-200, for manufacturing and complex adjustment of the accelerating system before the end of 1997 was prepared for signing.

Multiplying target. NIKIET completed work on the engineering design of the first version of the target. Fuel element (TVEL) specifications were submitted for approval. A contract with the MAJAK industrial enterprise and the RF Ministry of Atomic Energy for renting feasible materials for TVELs was prepared.

Work on making the calendar plan and conditions of the agreement for developing a complex project of the IREN facility signed in 1993 more precise was carried out in collaboration with GSPI. A contract with the Obninsk Division of NIKIMT for the development of a project for disassembling the IBR-30 booster was prepared for signing. A working schedule for testing an electron-neutron converter for the multiplying target at the IBR-30 was adopted.

Participants of the International Seminar "Advanced Pulsed Neutron Sources" dedicated to the 10th anniversary of IBR-2 reactor operation (June 1994, Dubna).
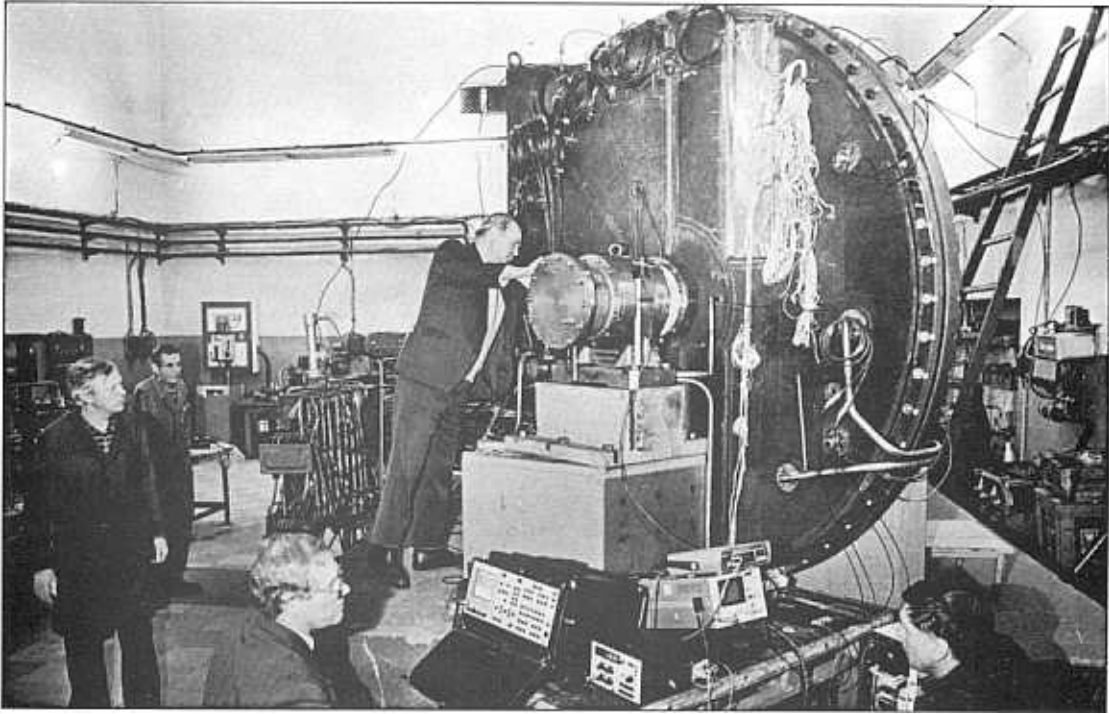
The testing   stand   the new movable
reflector PO-2RM (November 1994)
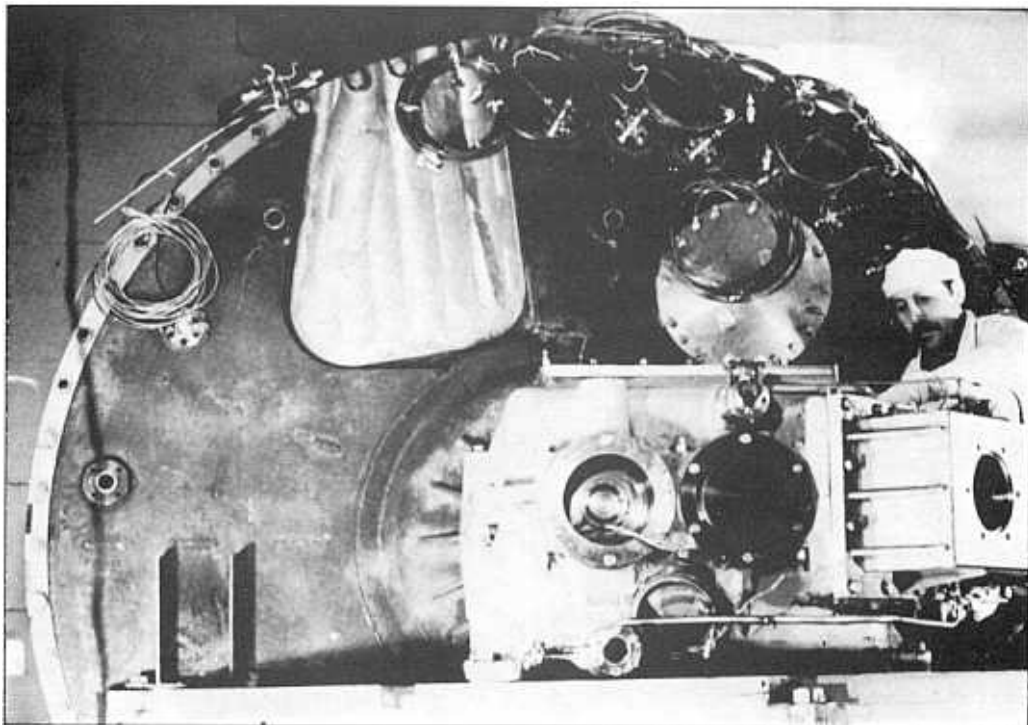
The final stage   installing the PO-2RM reflector   front of
the shielding gate   the IBR-2 reactor (December 1994).
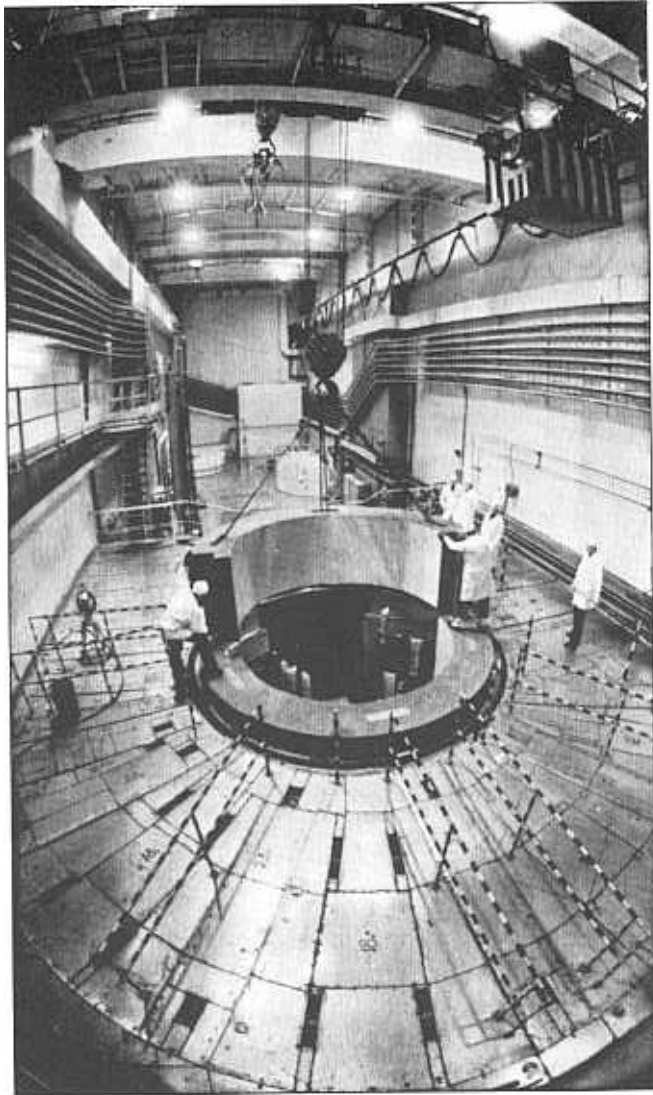
Assembly of the upper part of the ring shielding for the IBR-2 reactor jacket after completing maintenance work.
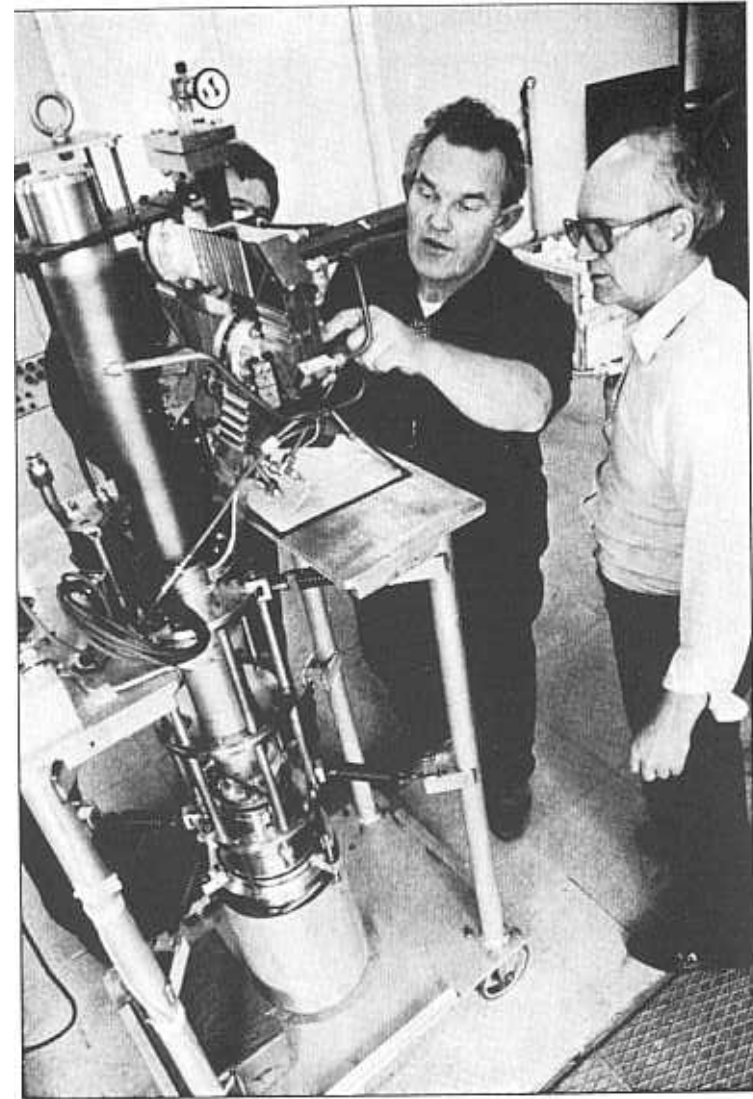
R.Koonz (SLAC) and A.K.Krasnykh are examining the 5045 klystron after its delivery from the USA.

6. COMPUTER CENTER

Network and computer infrastructure. The 1992-1993 experience in using the network resources which were implemented on the basis of SPARC workstations of the SUN firm and personal computers (PC), allowed us to start in 1994 the next stage of evolution of the network and computer infrastructure of FLNP (Fig.12). The network was reconfigured by involving new workstations (two SPARCStation 10 clone and one SPARCStation 2 clone) and additional hard disk devices with a total capacity of 16 Gb. The reconfiguration will be finalized at the end of 1995. In result, user access to the hard disks of the file servers and workstations will be optimized, and the stability of the network, file servers and workstation operation in the case of disk quota overflow will be improved. By the end of 1994, FLNP had 180 registered users of the Laboratory's network.

The distributed file system on several SPARCStations allows access to their data to users from any computer connected to the network. The new workstation console software presents the same desktop environment to users whether they enter the SUN-cluster from X-terminal, an X-terminal emulator on a PC or from the console of a workstation. Upon installation of the Mosaic user interface, the new information service World Wide Web (WWW) became accessible to users - it allows users to enter WWW-servers around the world and use the WWW data bases.

On the file servers of the network, a "pub" directory is installed with commonly used software for PCs, as well as descriptions and documentation of packages which may be used for novices on the workstations. The CERN library package was also installed. Although some SUN workstations are intended to perform special functions (e-mail service, entry to other networks, etc.) all workstations are accessible to users in the normal mode of operations.

Future development of the network assumes a replacement of some communications equipment, purchasing and installation of additional network bridges, laser printers, enlarging the disk capacity purchasing an archive system on the basis of JukeBox for long term data storing, etc.

Electronic equipment development. First and foremost, design and development of electronic equipment was aimed at utilization of the VME standard. A concept was elaborated for the development of electronic systems from the point of view of equipment unification and transition to the new VME technology. The main motive for introducing VME standard in place of the CAMAC standard was the necessity of supporting parallel processes of data acquisition, processing and viewing. In 1994, the first system in VME standard for data storing, monitoring and control was built for the NSVR texture spectrometer.

For investigations in nuclear physics, the new version of a mobile measuring module (MMM) was constructed. The new measuring module was made as a one-crate module that enabled its use in out-of-FLNP experiments. At the present time the MMM is used to perform experiments in the neutron beam of the proton accelerator at the meson factory of INP RAS (Troitsk). On the basis of the MMM, a stationary version of the measuring module was built for the spectrometer for (n,α) and (n,p) reactions at the IBR-30 reactor.

Work has been performed on the development of a computer and measurement module for the ROMASHKA multi-detector spectrometer operating in an IBR-30 reactor beam. The module permits performing three dimensional analysis by simultaneously measuring the time, amplitude, detector number or coincidence multiple. The measured spectra are accumulated in a

256 K 16-bit memory device. For information compression, two digital selection blocks are used. In addition to the main channel for accumulating three-dimensional information, there are two autonomous one-dimensional channels each consisting of a time coder and a 4K 16-bit memory, and one channel consisting of a time coder and a detector number coder for 8 detectors.

A large volume of work on the modernization of equipment and software for the other spectrometers at the IBR-2 and IBR-30 reactors has been done.

Software for data acquisition and control systems. The control software for the High Resolution Fourier Diffractometer (HRFD) consists of two programs - FDC and NDC. The FDC program allows users to check and setup parameters of the data acquisition electronics in BITBUS standard and Fourier chopper electronics, as well as to control them during experiments. FDC performs the experiments as a set of sweeps. The setup operation allows users to change the time of sweep, delay, speed of chopper rotation and type of frequency window. FDC allows users to start the measurement at a given time and to suspend measurement for a given time between two sweeps. This pause may be used to change the position of mechanical devices which are controlled by the NDC program on another computer. The NDC program is intended to control the mechanical devices, refrigerator and low resolution data acquisition systems, which are implemented in CAMAC standard. For synchronizing the work of both programs, the absolute time of the computer clocks is used. FD and NDVI routines are used for viewing high and low resolution spectra and for calculating parameters of marked interactive mode peaks (position, height and width at half height).

The new control software for the SNIM-2 spectrometer has been developed. It allows users to study the magnetic structures of single crystals as well as phase transitions which are induced by a pulsed magnetic field. The software controls the two data acquisition sets of electronics, mechanical devices, heater and magnetic field facility. The electronics of this system were implemented in CAMAC standard.

The software which was developed for the SPN-1, SPN-2 and REFLEX spectrometers allows the instruments to be controlled in the interactive and automatic modes and has some particular features. The control software reads out the large variety of experimental data during the experiments and stores it in a data base, which was specially designed for this system. In off-line mode the software allows users to browse the parameter list of the measurements, view the spectra and perform preliminary data analysis. One of the programs allows users to automatically search for the center of the neutron beam, measure the profile of the beam and move the detectors into a given position relative to the center of neutron beam.

The new generation of data acquisition and spectrometer control systems is being developed at FLNP on the basis of VME standard electronics, modern personal computers and workstations. The main principles for hardware and software organization of the distributed experiment automation system at the IBR-2 reactor have been defined. This organization will give us a maximum throughput for the data acquisition systems, allows us to implement complicated methods for experiment performance which need the simultaneous control of different devices and viewing parameters of the instruments, as well as of accumulated spectra, and allows users to remotely control an experiment via the ETHERNET network.
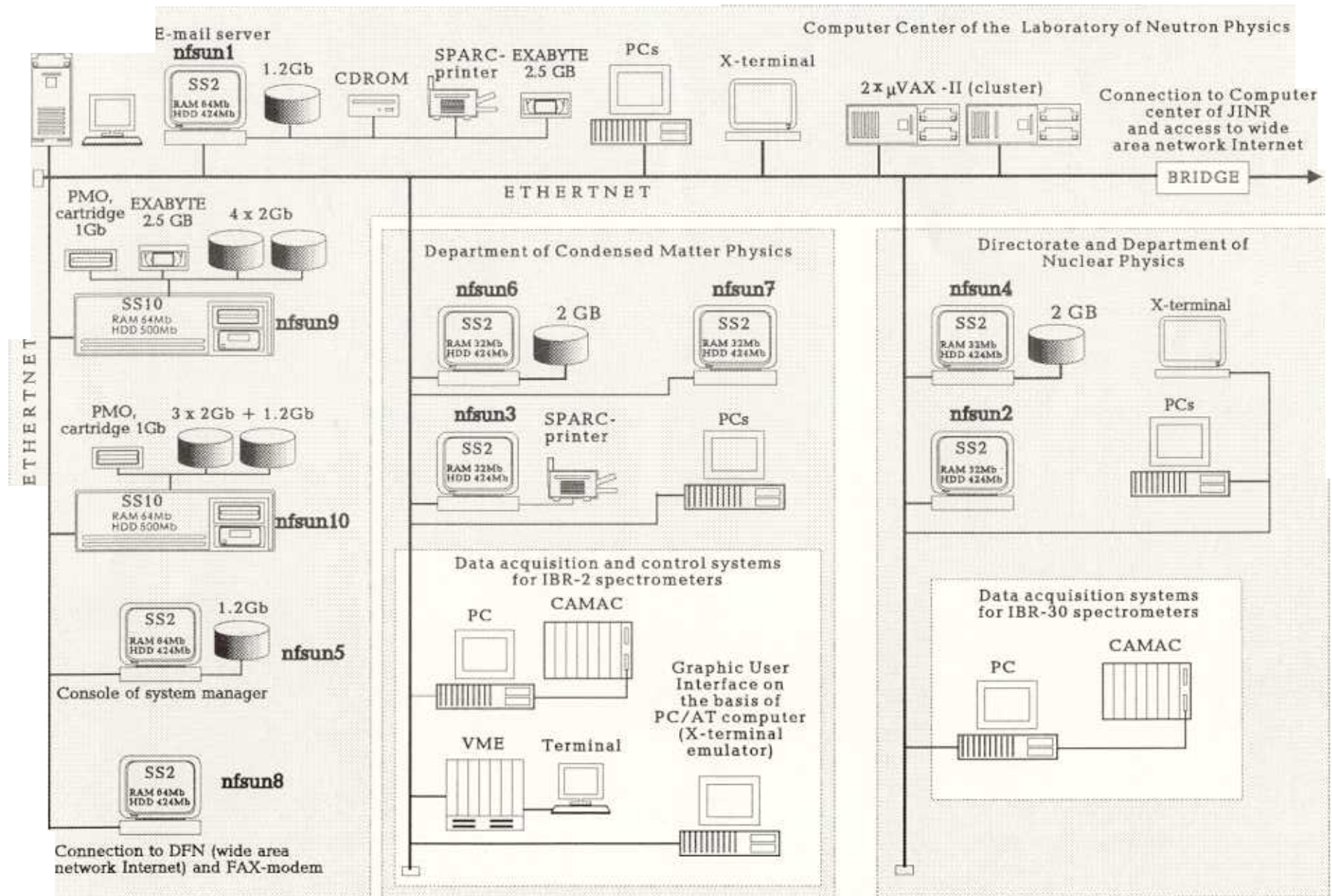
Fig.12. Configuration of the Frank Laboratory of Neutron Physics network resources.

7.1. STRUCTURE OF LABORATORY AND SCIENTIFIC DEPARTMENTS

Directorate:
Director:
V.L.Aksenov
Deputy Directors:
W.I.Furman
A.V.Belushkin
Scientific Secretary:
Yu.V.Taran

Reactor and Technical Departments
Chief engineer: V.D.Ananiev
Nuclear physics and pulsed neutron sources sector
Head: V.L.Lomidze
IBR-2 reactor
Chief engineer: A.V.Vinogradov
IBR-30 booster + LUE-40
Head: S.A.Kvasnikov
Mechanical maintenance division
Head: A.A.Belyakov
Electrical engineering department
Head: V.P.Popov
Design office
Head: B.I.Voronov
Construction
Head: A.N.Kuznetsov

Scientific Departments and Sectors
Condensed matter department
Head: A.M.Balagurov
Nuclear physics department
Head: V.N.Shvetsov
Department of electronics, computers and networks
Head: V.I.Prikhodko
Department of IREN
Head: A.K.Krasnykh
Activation analysis and radiation research sector
Head: V.A.Sarin
Applied research sector
Head: V.I.Lushchikov

Administrative Services
Deputy Director: S.V.Kozenkov
Secretariat
Finances
Personnel

Group of Scientific Secretary
Translation
Graphics
Photography
Painting

187

THE CONDENSED MATTER DEPARTMENT

Sub-division	Title	Head
Group No.1	HRFD	A.M.Balagurov
Group No.2	DN-2	A.I.Beskrovnyi
Group No.3	DN-12	B.N.Savenko
Group No.4	HRNS	K.Valter *Walther*
Group No.5	SNIM-2	V.V.Nietz
Group No.6	YUMO	M.A.Kiselev
Group No.7	Biomolecular neutron diffraction	I.N.Serdyuk
Group No.8	SPN-1	Yu.V.Nikitenko
Group No.9	REFLEX	D.A.Korneev
Group No.10	NERA-PR	I.Natkaniec
Group No.11	KDSOG	A.Yu.Muzychka
Group No.12	DIN-2	Zh.A.Kozlov
Group No.13	EG-5	A.P.Kobzev
Group No.14	Theoretical condensed matter physics	E.I.Kornilov
Group No.15	Technical support	V.V.Zhuravlev

THE NUCLEAR PHYSICS DEPARTMENT

Sub-division	Title	Head
Group No.1	Polarized neutrons and nuclei	V.P.Alfimenkov
Group No.1	Neutron spectroscopy	A.B.Popov
Group No.3	Nuclear reactions	Yu.S.Zamyatnin
Group No.4	Properties of the neutron	Yu.A.Alexandrov
Group No.5	Proton and α-decay	Yu.M.Gledenov
Group No.6	Properties of γ-quanta	A.M.Sukhovoy
Group No.7	Radiation capture of neutrons	G.P.Georgiev
Group No.8	Ultra-cold neutrons	V.N.Shvetsov
Group No.9	Neutron structure	G.S.Samosvat
Group No.10	Rare reactions	Yu.N.Pokotilovsky

7.2. USER POLICY

The IBR-2 reactor usually operates 10 cycles a year (2500 hrs. total) to serve the experimental program. A cycle has been established of 2 weeks of operation for users, each followed by a one week period for maintenance and machine development. There is a long shut down period between the end of June and the middle of October.

All experimental facilities of the IBR-2 are open to the general scientific community. The User Guide on neutron experimental facilities at FLNP is available by request from the Laboratory's Scientific Secretary.

Condensed matter studies at the IBR-2 facility have undergone some changes according to the experience gained during the last two years. It was found necessary to establish specialized selection committees formed of independent experts in their corresponding fields of scientific activities . The following 4 committees were organized:

1. Diffraction
   - V.A.Somenkov - Russia - chairman
   - V.A.Trounov - Russia
   - A.A.Loshmanov - Russia

2. Inelastic scattering
   - J.Janik - Poland - chairman
   - W.Gotze - Germany
   - V.Dimic - Slovenia
   - L.Bata - Hungary
   - A.V.Chalyi - Ukraine

3. Neutron optics
   - A.I.Okorokov - Russia - chairman
   - S.V.Maleyev - Russia
   - T.Rekveldt - The Netherlands
   - H.Lauter - France - Germany

4. Small angle scattering
   - L.Cser - Hungary - chairman
   - J.Plestil - Czech Republic
   - J.Teixeira - France
   - G.Zaccai - France
   - H.Stuhrmann - Germany

Dr. Vadim Sikolenko was appointed as the scientific coordinator of user policy at FLNP and Mr. Gizo Bokuchava as his deputy. Two deadlines for proposal submission were defined. For the experimental period from October through February the deadline is May 16 and for the period from February through June the deadline is November 16. The scientific coordinator and his deputy are responsible for organizing all necessary work for:

- distribution of "Application for Beam Time" forms to potential users;
- reception and registration of proposals;
- proposal review by instrument scientists to estimate their technical feasibility;
- sending the feasible proposals to members of the selection committees and reception of their comments and recommendations.

The IBR-2 beam schedules are drawn up by the head of the Condensed Matter Department together with the persons responsible for the instruments on the basis of the experts' recommendations. Schedules as adopted by the director or deputy director for condensed matter physics are sent to the chairmen of the selection committees. After performing an experiment the 'Experimental Report" form is filled out by the experimenter(s), which is then submitted to the scientific coordinator of user policy.

The first call for proposals resulted in 76 applications requesting 406 experimental days on 7 of the 12 IBR-2 spectrometers. The average overload factor for these instruments is 1.16, the largest being for the NERA-PR high resolution inelastic scattering spectrometer (2.4) and the YuMO small-angle scattering spectrometer (2.1).

Contact address:
Dr. V.Sikolenko or Mr. G.Bokuchava
Frank Laboratory of Neutron Physics
Joint Institute for Nuclear Research
141980 Dubna, Moscow region
Russia
Tel.: (+7)-095-924-39-14, (+7)-09621-63677
Fax: (+7)-09621-65803
E-mail: sikolenko@nfsun1.jinr.dubna.su,
gizo@nfsun1.jinr.dubna.su.

7.3. MEETINGS AND CONFERENCES

1. 2nd International Seminar on Interaction of Neutrons with Nuclei: "Neutron Spectroscopy, Nuclear Structure, Related Topics", April 26-28, Dubna.

The seminar was organized with the financial support of the Russian Fund for Fundamental research. The seminar continued the workshops on the investigation of atomic nuclei with neutrons which have been carried out in Dubna for a number of years. About 120 participants from more than 10 research institutes in Russia as well as participants from Belgium, Bulgaria, Germany, Holland, Italy, Latvia, Mexico, Poland, Slovakia, Slovenia, USA, Ukraine, Czechia, and Japan attended the Seminar.

The Seminar showed that the interest in neutron physics remains high. The spectrum of the considered problems was wide: from fundamental characteristics of the neutron to the structure of the nucleus and applied problems.

Reports by international scientific collaborations with FLNP participation (USA, Euratom, Germany, China, Latvia, Ukraine) were well represented at the Seminar, and the new joint works were discussed. The participants paid homage to the well known German nuclear physicist, an expert in nuclear fission and a great friend of our Laboratory, Professor Jurgen Theobald, who died just before the beginning of the Seminar.

2. International Seminar " Advanced Pulsed Neutron Sources", June 11-16, Dubna.

The Seminar was dedicated to the 10th anniversary of IBR-2 reactor operation. The Seminar was organized in conjunction with the Institute for Nuclear Research of the Russian Academy of Sciences, with the financial support of the Russian Fund for Fundamental Research.

The Seminar Program included:

- theoretical and experimental aspects of pulsed reactors;
- safety, reliability and diagnostics of pulsed reactors;
- alternative high flux pulsed sources;
- new proposals for creating high intensity neutron sources;
- unusual applications of pulsed sources;
- experimental techniques (moderators, choppers, etc.);
- prospects and trends of the IBR-2 reactor development;
- physical research program for neutron sources with a large pulse width.

3. 30th Conference on Low Temperature Physics, September 6-9, Dubna.

The Conference (formerly an all-union conference) was organized by the Scientific Council on the Physics of Low Temperatures of the Russian Academy of Sciences and the Joint Institute for Nuclear Research, with the financial support of the Russian Fund for Fundamental Research.

The Conference attended by 236 participants had the plenary and section sessions. The plenary sessions heard 11 invited talks, including one from FLNP. Over 150 reports, including posters, on fundamental problems of superconductivity, quantum liquids and crystals, low temperature physics of solid matter, and electron phenomena at low temperatures were contributed to the section sessions.

4. International Seminar "Neutron Investigations at High Pressures", October 5-7, Dubna.

New neutron instruments and techniques for creating high pressures, high pressure investigations of the atomic and magnetic structures of high temperature superconductors, alloys and hydrogen containing compounds, phase transitions and phase diagrams, lattice dynamics, geomaterials, as well as programs of future investigations and a number of other questions were included in the program of the Seminar.

Over 70 specialists from 9 member and non-member-states of JINR, including specialists from the leading neutron centers: Rutherford Appleton Laboratory (Great Britain), Leon Brillouin Laboratory (France) Los Alamos National Laboratory (USA), and Kurchatov Institute (Russia) attended the Seminar.

In 1995 the following meetings will be organized:

1	Workshop on Mathematical Methods of Texture Analysis	March 21-24	Dubna
2	Russian-French Seminar "Strongly Correlated Electronic Systems"	March 23-28	Grenoble
3	3rd International Seminar on Interaction of Neutrons with Nuclei	April 26-28	Dubna
4	3rd International Meeting "Nuclear Physics for Protection of the Environment"	May 23-28	Dubna
5	Russian-Japan Meeting on Synchrotron and Neutron Investigations	August 21-25	Dubna
6	VII International School on Neutron Physics	September 4-21	Dubna

7.4. COOPERATION

The FLNP Plan of Scientific Research and Scientific and Technical Cooperation reflects the whole diversity of links established by FLNP with many of the research centers in member- and non-member-states of JINR.

The many year cooperation of FLNP with leading neutron centers in Russia received an additional boost in connection with the establishment of the new National Scientific and Technical Program on Neutron Investigations of Matter, under the leadership of FLNP Director, V.L.Aksenov. The Scientific Council of the Program has created a plan for the development of a spectrometer structure at neutron sources in Russia, including the IBR-2 reactor, for users from research and higher education institutes.

Wide cooperation with many institutes in Germany was also established (Table 1). Agreements and protocols for cooperation with the ISIS Facility of the Rutherford Appleton Laboratory, the Imperial College Reactor Center (United Kingdom), and the Institute of Solid State Physics, HAS (Hungary) are in effect.

The collaboration of FLNP with scientific establishments in Europe received the support of the International Association for the Promotion of Cooperation with Scientists from the Independent States of the Former Soviet Union (INTAS). Four grants were given to FLNP scientists by INTAS (Table 2).

One of the indications of the extent of the cooperation is the number of visiting scientists from non-member-states, which was 43 people in 1994 (Table 3).

Table 1

Present status of collaborations between German Institutes and FLNP

Activity	Germany	FLNP
General Agreement on Scientific Co-operation	Hahn-Meitner Institute, Berlin, Prof.F.Mezei	Prof.V.L.Aksenov
Upgrading the spectrometer of polarized neutrons (SPN-2)	Prof.F.Mezei, Dr.H.J.Lauter	V.V.Pasiuk, A.V.Petrenko
Neutron diffraction studies of textures in materials	FZ Rossendorf Dr. K.Walther	Dr.J.Heinitz
Investigations of phase transitions in crystals with a partly disordered structure	Dr.F.Prokert	Dr. B.N.Savenko
Meson degree of freedom in nuclear matter	Dr.B.Kampfer	Dr.G.G.Bunatian
Use and development of the neutron spectrometer YuMO. Investigation of cement structures	FHIZP Saarbrucken/Dresden Prof.M.Kroning, Prof.H.Baumbach	Prof.I.N.Serdyuk, Dr.F.Hessler
Study of transfer processes in liquids and solids by radiography methods	Prof.M.Kroning, Prof.H.Baumbach	S.S.Pavlov
Precision investigation of the crystal structure of new materials and measurement of internal mechanical stresses by high-resolution neutron diffraction methods	Prof.M.Kroning, Prof.G.Dobmann, Prof.J.Schreiber	Prof.V.L.Aksenov, Dr.A.M.Balagurov, Dr.Yu.V.Taran

Safety and diagnostics improvement of the IBR-2 reactor	Prof.E.Pridoehl, Prof.J.Schreiber, Prof.K.-J.Froehlich	Prof.V.L.Aksenov, A.V.Vinogradov, Dr.Yu.N.Pepelyshev
Manufacture of the movable reflector for the IBR-2 reactor	Prof.M.Kroning, Prof.S.Kraus, Prof.J.Schreiber	Prof.V.L.Aksenov, V.D.Ananiev
Joint experiments on the High Resolution Fourier Diffractometer (HRFD)	GKSS Hamburg (Geesthacht) Dr.H.Priesmeyer	Dr.A.M.Balagurov
Investigation of ribosome structure by using triple isotopic substitution and spin dynamical polarization in neutron scattering	Prof.H.Stuhrmann	Prof. I.N.Serdyuk
Small angle scattering with polarized neutrons	Dr.R.Wagner	Prof.V.L.Aksenov, E.B.Dokukin
Investigation of transition phenomena in solids by the real-time method	TU Darmstadt Prof.H.Fuess	G.M.Mironova
Neutron induced fission	Prof.J.P.Theobald	Dr.W.I.Furman, Dr.E.Dermendjiev
Joint experiments on small angle neutron scattering	KFA Julich Prof.T.Springer	Prof.I.N.Serduyk
Investigation of surface dynamics and dynamics of adsorbed molecules by inelastic neutron scattering	Dr.E.Preuss	Dr.I.Natkaniec
Investigation of intermediate interactions in solutions of surface-active matter by SANS	Univ. Leipzig Prof.G.Klose	Prof.I.N.Serdyuk, Dr.N.I.Gorski
The influence of membrane surface properties on interactions between membranes	Prof.G.Klose	Dr.V.I.Gordeli, D.A.Korneev
Investigations of the influence of membrane lateral structures on inter-membrane interactions	RS Garching, TU Munchen Prof.Gr.Cevc	Dr.V.I.Gordeli
Investigation of atomic nuclei properties with the help of neutrons	Prof.T.von Edigy	Dr.A.M.Sukhovoy
New powerful ultracold neutron source	Prof.W.Glaser	Dr.W.I.Furman
Study of the electrical polarizability of the neutron	Dr.W.Waschkowski	Dr. G.S.Samosvat, Dr.Yu.A.Alexandrov
Wave optics with ultracold neutrons	Dr.R.Geller	Dr.A.I.Frank
Investigation of reactions on stable and radioactive nuclei	IK, Karlsruhe Prof.F.Kappeler	Dr.Yu.M.Gledenov
Investigation of magnetic structure of HTSC	TU Braunschweig Prof.J.Litterst	Dr.A.M.Balagurov
Investigation of the texture of geological samples	Univ. Gottingen Prof.Weber	Dr.J.Heinitz

IINS Studies of lattice dynamics and phase transitions in molecular crystals Investigation of intermediate interactions in solutions of surface-active matter by SANS	TU Bayreuth Prof. J.Kalus Prof.H.Hoffmann		Dr.I.Natkaniec Prof.I.N.Serdyuk, Dr.N.I.Gorski
Structural investigations of lipid and biological membranes by diffraction and SANS	Free Univ., Berlin Prof.G.Bueldt		Dr.V.I.Gordeli
Investigation of the spatial structure of the 16S ribosomal RNA of small ribosomesubunits	Institute of Molecular Genetics, Berlin Prof.K.Nierhaus		Prof.I.N.Serdyuk

Table 2.

INTAS

Project	Code	Leader
Polarized neutron reflectometry studies on high temperature superconducting films and ultrathin magnetic film sandwich structures	93-3617	V.L.Aksenov
Study of the chemical, structural and physical aspects for the new high T_c superconductors containing Cu oxide	93-2483	A.M.Balagurov
Improved measurements of the neutron β-decay lifetime	93-298	A.V.Strelkov
Calibration of volume residual stress measurements by neutron diffraction techniques and applications	94-3239	Yu.V.Taran

Table 3.

List of Visitors from Non-Member States of JINR in 1994

Name	Organization	Country	Dates
T.Strell	Fr. Inst. fur Mikroelektr. Schalt.+Sys.	Germany	09/01-16/01
W.Birkholz	Fr. Inst. fur Mikroelektr. Schalt.+Sys.	Germany	09/01-16/01
J.Schreiber	Fraunhof. Inst. fur Zerstror. Prufv., Dresden	Germany	31/01-11/02
P.Reichel	FZ Rossendorf	Germany	14/02-24/02
R.Jodicke	TU Chemnitz-Zwickau	Germany	14/02-25/03
N.El Sharouni	AEA Nuclear Research Center	Egypt	16/02-11/03
M.Alex	AEA Nuclear Research Center	Egypt	16/02-11/03
Young Nam Jang	KIGAM, Seoul	South Korea	18/02-18/02
W.H.Urbanus	Institute of Plasma Physics	The Netherlands	07/04-10/04
A.B.Sterk	Institute of Plasma Physics	The Netherlands	07/04-10/04
Refaat Maayouf	NRC-AEA-Cairo	Egypt	10/04-03/05

J.Schreiber	Fraunhof. Inst. fur Zerstror. Prufv., Dresden	Germany	21/04-24/04
William M.Sprague	Univ. of Washington, Seattle	USA	21/04-25/04
H.Lauter	ILL, Grenoble	France	22/04-04/05
Zhu Bin	Chalmers Univ. of Technology, Goteborg	Sweden	15/05-03/06
J.Schreiber	Fraunhof. Inst. fur Zerstror. Prufv., Dresden	Germany	26/05-04/06
R.F.Koontz	SLAC	USA	06/06-08/06
M.A.Kellett	Univ. of Birmingham	UK	18/06-06/07
H.Stuhrmann	GKSS, Geesthacht	Germany	24/06-05/07
K.Walther	FZ Rossendorf	Germany	24/06-24/06
K.L.Jager	GKSS, Geesthacht	Germany	24/06-05/07
Subramanian Raman	ORNL	USA	02/07-10/07
M.Van der Kaars	Institute of Plasma Physics	The Netherlands	10/08-14/08
A.B.Sterk	Institute of Plasma Physics	The Netherlands	10/08-14/08
T.Strell	Fr. Inst. fur Mikroelektr. Schalt.+Sys.	Germany	18/08-28/08
W.Birkholz	Fr. Inst. fur Mikroelektr. Schalt.+Sys.	Germany	18/08-28/08
J.J.Capponi	ILL, Grenoble	France	13/09-14/09
M.Marezio	ILL, Grenoble	France	13/09-14/09
B.Michaelis	Otto von Guericke Inst., Magdeburg	Germany	17/09-21/09
D.Mildner	NIST, Washington	USA	26/09-28/09
C.MacDonald	NIST, Washington	USA	26/09-28/09
H.Mayer	NIST, Washington	USA	26/09-28/09
R.Downing	NIST, Washington	USA	26/09-28/09
K.Walher	FZ Rossendorf	Germany	03/10-25/10
P.Reicher	FZ Rossendorf	Germany	03/10-25/10
W.Boede	FZ Rossendorf	Germany	03/10-25/10
G.Pepy	LLB, Saclay	France	05/10-08/10
M.Betzl	FZ Rossendorf	Germany	10/10-25/10
Refaat Maayouf	AEA Nuclear Research Center	Egypt	12/11-24/11
H.Lauter	ILL, Grenoble	France	12/11-19/11
J.Schreiber	Fraunhof. Inst. fur Zerstror. Prufv., Dresden	Germany	17/11-21/11
H.Ludwig	DaimlerBenz AG Tech. GUS	Germany	19/11-19/11

7.5. EDUCATION

The University Center (UC) affiliated with the Joint Institute for Nuclear Research and based on the faculties of the Moscow State University and Moscow Engineering Physics Institute admits, for continuation of studies, undergraduate students of the last two years of study in higher education institutions, who have attended introductory specialized courses of lectures in the following topics: particle physics, nuclear physics, investigation of condensed matter at nuclear reactors and accelerators, radiation biology. The second and third specializations are quite in line with research performed at FLNP, which has at its disposal, for both sectors, a good experimental base comprising the IBR-2 reactor and the IBR-30 booster pulsed neutron sources.

The education courses and practical training for the students affiliated with FLNP have been organized, to a large extent, to prepare specialists in neutron physics both for the Laboratory and for other Russian neutron centers.

As an example illustrating this aim we present the list of courses by lecturers of the Condensed Matter Physics Chair of the UC (Head: Prof.V.L.Aksenov):
- theoretical methods in condensed matter physics;
- methods of investigation of condensed matter at nuclear reactors and accelerators;
- fundamentals of neutron physics and neutron sources;
- methods for structure analysis of ideal and real crystals;
- synchrotron radiation spectroscopy of solid matter;
- influence of radiation on solid-state properties;
- methods of experimental data processing.

A number of leading FLNP scientists takes part in delivering these courses. Each student is allowed access to the Laboratory computer network. An obligatory condition for successful completion of the 4-th year is the capability of using modern personal computers. Earlier, students were included in the research groups led by their instructors from the FLNP scientists, which made it possible for under-graduate students working on their theses to take part in preparing or performing experiments.

In 1994 the teaching process of students of UC continued successfully. Ten students who had their UC training course at FLNP were employed by JINR or scientific centers in Russia.

The Condensed Matter Physics Chair gave graduation certificates to a third group of students in the reported year. This group had 7 students, making the total number of students who have graduated from the Chair 23. Nine of them were employed by FLNP, which has renewed the staff of the FLNP Scientific Department of Condensed Matter Physics to a noticeable degree. A somewhat smaller influx of graduates came from the Nuclear Physics Chair of the University Center. In the past three years only three of them have joined FLNP.

7.6. PERSONNEL

As of 31.12.1994, the staff of the Laboratory amounted to 511 employees. The staff can be divided into two categories: the main staff (455 people) and the directorate's staff (56 people). The main staff, in turn, is comprised of permanent and temporary members. The latter are the employees who work on a temporary contract basis.

The members of the directorate's staff work only on a temporary contract basis. This staff is mainly formed of specialists from 'bld" JINR member states. Recently, the number of specialists from "new" JINR member states has increased, however (table 1).

The processes of concluding contracts with the members of the main staff, which began in 1992, has practically been completed: the number of employees working on a temporary contract basis has reached 92.3%. The other process started at the same time and aimed at the reduction of the total number of employees continued, but at a slower pace: 4.5% for the reported year.

The distribution of the main staff personnel among Laboratory departments is illustrated in table 2.

Table 1.

Personnel of the Directorate as of 31.12.94

Country	People
"Old" member states	
Bulgaria	5
Czechia	2
KPDR	2
Mongolia	4
Poland	7
Romania	3
Slovakia	1
Vietnam	1
"New" member states	
Azerbaijan	1
Armenia	2
Georgia	1
Kazakhstan	2
Moldavia	1
Russia	16
Ukraine	1
Other country	
Germany	5
USA	2
TOTAL	**56**

Table 2.

Distribution of the Main Staff Personnel per Department as of 31.12.94

Departments	Permanent personnel			Contracts		
	S.	E. & T.	W.	S.	E. & T.	W.
Nuclear Physics Department	1	-	2	30.5	9.5	3
Condensed Matter Physics Department	4	1	-	27.5	10.5	6
Department of Electronics, Computers and Networks	-	-	-	18	26	9
Physical and Technical Research Sector Activation Analysis Sector	4	8	2	2	4.5	2.5
IREN Department	1	1	-	4.5	21	6
IBR-2 Department Nuclear Safety Sector	-	-	1	6	40	7
Technical and Administrative Service	1	6	7	3	52.5	127
	11	16	12	91.5	164	160.5
	39 (8.57%)			416 (91.4%)		
Total	455					

Comment: S. - Scientists, E. & T. - Engineers & Technicians, W. - Workers.

7.7. FINANCE

The financial situation in the Laboratory, though remaining strained, has somewhat improved in comparison with the previous year: the total income was 2626.5 th. $ in 1994 against 1584.4 th. $ in 1993 (table 1).

One of the reasons for the insufficiently improved financial situation is the systematic non-fulfillment of the decisions on the part of the JINR budget assigned to FLNP adopted by the Committee of Plenipotentiaries of JINR Member States (table 2).

Scientific investigations by FLNP are receiving increasing support from the Russian Fund for Fundamental Research. In 1994 the sum of 86.0 th $ was allocated to finance 13 FLNP projects (against 35.5 th. $ in 1993).

Financial support by the International Scientific Fund (ISF - Soros Fund) of the long-term projects and scientists of the Laboratory was the largest of external investments. In 1994, ISF was financing 8 projects, mainly, in nuclear physics.

Table 3 shows the distribution of the "pure" (the part alloted for the JINR infrastructure has been subtracted) financial support from the 1994 JINR budget among the IBR-2 basic facility and other departments which are carrying out and providing for scientific investigations in the Laboratory, as well as expenditures for equipment and materials.

FLNP budget in 1994

Income		Expenditure	
Source	th.dol.	Where to	th.dol.
1. Income from JINR	2530.1	1.1. Scientific research and infrastructure	2163.0
		1.2. Amount returned to JINR infrastructure	367.1
2. External investments	96.4	2. Scientific research and infrastructure	96.4
2.1. Russian fund for fundamental research	86.0		
2.2. Program of high temperature superconductivity	10.4		
Total	**2626.5**	**Total**	**2626.5**

Table 2.

The part of the JINR budget assigned to FLNP (%)

Year	Plan	Fact
1992	21.7	13.3
1993	16.7	14.7
1994	16.8	13.0

Table 3.

Expenditures for scientific research and FLNP infrastructure from the income supplied by JINR in 1994

Where to	th.dol.
1. Neutron source IBR-2:	273.5
1.1. Salary and accompanying expenses	145.1
1.2. Other expenses	128.4
2. Physics and Maintenance Departments	1889.5
2.1. Salary and accompanying expenses	533.2
2.2. Materials and equipment	458.1
2.3. Infrastructure	476.4
2.4. Other expenses	421.8
Total	**2163.0**